THE MECHANISM OF SYNAPTIC VESICLE RETRIEVAL IN EPILEPSY.

Emma Louise Clayton

Submitted for a PhD in Biomedical Sciences

The University of Edinburgh

March 2009

TABLE OF CONTENTS

TABLE OF FIGURES

ACKNOWLEDGEMENTS

"Ní neart go cur le chéile"

The most literal translation of this Irish seanfhocal would be "no strength without unity", but what it conveys here for me is simply that it would have been impossible for me to produce this work without the help of a number of different people.

First and foremost I would like to thank Dr Mike Cousin for being an excellent supervisor who was always available to answer questions.

Thanks to all the members of the Cousin lab, past and present. Thanks especially to all my friends and colleagues in the Hugh Robson Building who have helped; to those who have set a good example in their research and their interest in science. Particular thanks go to the support staff, without whom it would have been impossible to produce this work.

A huge thanks to my family; to Mum, Dad, Trish, Brian, Jane, Maeve and Ryan. Thanks for the phone calls, the chats and the visits, for the late night collections at the airport, and the early morning drop offs, and the occasional pretence at interest in my research topic.

Thanks to my extended family, all residents of 33/1 Montague Street, past, present, temporary and permanent. Antoine Ó'Súilleabháin, I don't know where else one would find a unicycling, beer making, chocolate providing Belgian; I fear you may be unique! Aoife, simply thanks for being such a great friend, there's loads more I could say but it's easier to take it for granted.

Last but far from the least, thanks John Denis for your support throughout, for weathering the highs and the lows. Mostly thanks for being you.

DECLARATION

I, Emma Louise Clayton, have composed this thesis myself. The work and the results reported herein are my own except where indicated, and have not been submitted for any other degree or professional qualification.

.....

ABSTRACT

Excessive release of neurotransmitter is a characteristic of epileptogenic cells. A number of lines of evidence implicate defects in the synaptic vesicle cycle as a cause of this excessive release. Synaptic vesicles are retrieved by more than one route in central nerve terminals. During mild stimulation the dominant synaptic vesicle retrieval pathway is classical clathrin mediated endocytosis. During elevated neuronal activity retrieval of synaptic vesicle membrane by bulk endocytosis is the predominant retrieval method. As it is triggered by strong stimulation, bulk endocytosis may be of importance in retrieval during epilepsy, however little is currently known about this pathway. In order to investigate the role of bulk endocytosis, we sought to establish a cell culture model of epilepsy, to develop an assay to distinguish retrieval by bulk endocytosis, and to use these tools to look at the molecular players controlling this form of endocytosis.

Characterisation of bulk endocytosis through the development of tailored assay systems has revealed that bulk endocytosis is a fast event that is triggered during strong stimulation. Bulk endocytosis provides the nerve terminal with an appropriate mechanism to meet the demands of synaptic vesicle retrieval during periods of intense synaptic vesicle exocytosis. Inhibition of a dephosphorylation specific dynamin I-syndapin I interaction by competitive peptides inhibits activity dependent bulk endocytosis, implicating this interaction in a role in this method of synaptic vesicle retrieval. Having characterised the strength of stimulation needed to activate bulk endocytosis, and the speed at which it occurs, we also investigated the effects of known anti-epileptogenic drugs on bulk endocytosis in our central nerve terminal model system.

PUBLICATIONS

The following papers were published during the course of this thesis;

Clayton, E. L. and M. A. Cousin (2008). "Differential labelling of bulk endocytosis in nerve terminals by FM dyes." Neurochem Int **53**(3-4): 51-5.

Clayton, E. L., G. J. Evans, et al. (2007). "Activity-dependent control of bulk endocytosis by protein dephosphorylation in central nerve terminals." J Physiol **585**(Pt 3): 687-91.

Clayton, E. L., G. J. Evans, et al. (2008). "Bulk synaptic vesicle endocytosis is rapidly triggered during strong stimulation." J Neurosci **28**(26): 6627-32.

List of Abbreviations

4-AP	4-Aminopyridine
ADBE	activity dependent bulk endocytosis
AED	antiepileptic drug
AP	action potential
AP180	adaptor protein 180
AP2	adaptor protein 2
AP3	adaptor protein 3
BAR	Bin/amphiphysin/Rvs
BPB	bromophenol blue
CaMK-II	calcium/calmodulin-dependent protein kinase II
C2	protein kinase C homologous
CCP	clathrin coated pit
CCV	clathrin coated vesicle
CDK5	cyclin dependent kinase 5
CGN	cerebellar granule neuron
chc	clathrin heavy chain
CLAP	clathrin/AP-2-binding
CME	clathrin-mediated endocytosis
DB	dbl homology
DPW	asparagine/proline/tryptophan
EH	eps15 homology
EM	electron microscopy
ENTH	epsin N-terminal homology domain

Eps15	epidermal growth factor pathway substrate 15
Epsin	Eps15 interacting protein
F-BAR	Fes-CIP homology and Bin-Amphiphysin-Rvs
FRAP	fluorescence recovery after photobleaching
GED	GTPase effector domain
GEF	guanine nucleotide exchange factor
Grb2	growth factor receptor-bound protein 2
HRP	horseradish peroxidase
Hsc70	70 kDa heat shock protein
KO	knockout
NMJ	neuromuscular junction
NPF	asparagines/proline/phenylalanine
NSF	N-ethylmalemide sensitive factor
N-WASP	neuronal Wiskott-aldrich syndrome protein
PH	pleckstrin homology
$PI(4,5)P_2$	PtdIns 4,5-bisphosphate
PKC	protein kinase C
PRD	proline rich domain
RP	reserve pool
RRP	readily releasable pool
SAC-1	suppressor of actin1
SH3	Src Homology 3
SM	sec1/p/Munc18-1
SNAP	soluble NSF attachment protein

SNARE	SNAP and NSF attachment receptors
SR	serum replacement
SV	synaptic vesicle
SVE	synaptic vesicle endocytosis
Syndapin	synaptic, dynamin-associated protein
TIRF	total internal reflection fluorescence
t-SNARE	target SNARE
SREDs	spontaneous recurrent epileptiform discharges
UIM	ubiquitin-interacting-motifs
VAMP	vesicle associated membrane protein
VGCC	voltage gated calcium channels
VGLUT	vesicular glutamate transporter
v-SNARE	vesicular SNARE
WT	wildtype

1. INTRODUCTION

1.1 INTRODUCTION

Communication between neurons occurs across the synapse. Neurotransmitters are packaged in membrane bound synaptic vesicles (SVs), which are located in pools near the active zone of the pre-synaptic neuron (Fig 1.1). Stimulation by an action potential (AP) causes an influx of Ca^{2+}, which triggers the fusion of the vesicle with the pre-synaptic membrane, and release of the vesicular content. Neurotransmitters are released from vesicles at the pre-synapse into the synaptic cleft, where the neurotransmitters can bind to post-synaptic receptors. The pre-synaptic cell must then retrieve and recycle the SV membrane and proteins in order to maintain a pool of vesicles sufficient for sustainable communication during periods of prolonged activity. The retrieved vesicles are re-filled with neurotransmitter, ready to repeat the cycle.

1.2 EXOCYTOSIS

Exocytosis is mediated by SNARE (soluble N-ethylmaleimide sensitive factor attachment protein) complexes, which are composed of plasma membrane SNARES (t-SNAREs) and vesicular SNARES (v-SNARE), in addition to NSF (N-ethylmalemide sensitive factor) and α-SNAP (α-soluble NSF attachment protein).

In neuronal and neuroendocrine cells exocytosis is mediated by the plasma membrane t-SNAREs syntaxin 1 and SNAP-25, and the v-SNARE vesicle associated membrane protein (VAMP 2, also known as synaptobrevin) (Burgoyne & Morgan, 2003). These neuronal SNAREs are the substrates for the metalloproteases botulinum neurotoxin and tetanus toxin (Schiavo *et al.*, 1992; Blasi *et al.*, 1993a; Blasi *et al.*, 1993b). The SNAREs are essential for SV exocytosis, as genetic ablation of the

Figure 1.1- Visualization of a synapse

Illustration of a synapse, showing the synaptic vesicle packaged neurotransmitters collected at the active zone ready to fuse and release neurotransmitter into the synaptic cleft in response to stimulation by an action potential (Adapted from the Science illustration visualization challenge, Johnson, 2005)

synaptic SNAREs in *C. elegans, S. cerevisiae, Drosophila* or mice abolished stimulated neurotransmission (Schulze *et al.*, 1995; Nonet *et al.*, 1998; Schoch *et al.*, 2001; Washbourne *et al.*, 2002).

The cytoplasmic regions of syntaxin, SNAP-25 and synaptobrevin interact to form a trimeric, four-helical complex, with syntaxin contributing 2 helices and the other proteins 1 helix each (Sutton *et al.*, 1998). After the SNARE complex assembles, the vesicular and plasma membranes fuse and release neurotransmitter (Hanson *et al.*, 1997). SNARE complexes are then recycled by NSF (an ATPase which breaks apart the SNARE complexes) and its adaptor protein α-SNAP (Sollner *et al.*, 1993; Mayer *et al.*, 1996)

The sec1/p/munc18-1 (SM) protein family modulate this process of SNARE complex formation, with munc-18 originally isolated through its ability to bind to monomeric syntaxin 1, which leaves syntaxin unable to form the ternary SNARE complex (Hata *et al.*, 1993; Pevsner *et al.*, 1994). SM proteins have been proposed to be important as trafficking chaperones of the closed form of syntaxin, ensuring it is trafficked correctly to the plasma membrane (Medine *et al.*, 2007). Recent work has shown that munc18-1 interacts with syntaxin 1a through two different modes of binding, which are spatially distinct. A closed form of syntaxin-munc18-1 binding exhibits high affinity and occurs primarily on intracellular membranes, whilst an alternative mode of binding is mediated by interaction of munc18-1 with the N terminus of syntaxin (Rickman et al., 2007). This suggests there may be distinct spatial and functional interactions of munc-18-1 with syntaxin 1a.

1.2.1 SYNAPTOTAGMIN

Synaptotagmin is composed of 5 protein domains; an N-terminal intravesicular sequence, a transmembrane domain, a linker sequence and 2 protein kinase C (PKC) homologous C_2 domains (C_2A and C_2B) (Perin *et al.*, 1991), a structure which is conserved across all 15 members of the synaptotagmin family (Südhof, 2002). Most neurons coexpress either synaptotagmin I or II with synaptotagmin III, all of which bind to the clathrin adaptor protein AP2 with high affinity, and have distinct but overlapping functions (Ullrich *et al.*, 1994).

Synaptotagmin I interacts with syntaxin (Bennett *et al.*, 1992) and also with phospholipids, and has been proposed as the Ca^{2+} sensor in SV exocytosis. Binding of synaptotagmin to phospholipid membrane is mediated by basic residues at the tip of C_2A and C_2B, and this interaction is critical for the coupling of Ca^{2+} influx and vesicle fusion (Martens *et al.*, 2007). The C_2A domain of synaptotagmin binds three Ca^{2+} ions, and all three ions are needed for the interaction with syntaxin and phospholipids (Ubach *et al.*, 1998), whilst the C_2B domain binds 2 Ca^{2+} ions (Fernandez *et al.*, 2001). The synaptotagmin C_2B domain has been shown to be sufficient to facilitate the simultaneous binding of 2 membranes by synaptotagmin (Arac *et al.*, 2006). The Ca^{2+} dependent membrane insertion of synaptotagmin I and SNARE binding have both been found to be important in driving the size of the fusion pore during exocytosis (Lynch *et al.*, 2008).

Functional studies have confirmed the importance of synaptotagmin I in the SV cycle. Synaptotagmin I KO mice display impaired synaptic transmission, although interestingly spontaneous and asynchronous release appears to be

unaffected (Geppert *et al.*, 1994). This evidence indicates that synaptotagmin I may be the Ca^{2+} sensor for synchronous Ca^{2+} evoked neurotransmitter release.

1.3 Endocytosis Pathways

The number of SVs within a nerve terminal is limited (typically 100 to 200 in central nerve terminals), therefore the SV membrane and associated proteins need to be recycled in order to avoid depletion of the vesicle pool. The first evidence for the recycling of SVs came from seminal work on the frog neuromuscular junction (NMJ). In these studies vesicles were found to fuse with the nerve terminal membrane, and then re-form to accumulate neurotransmitter (Ceccarelli *et al.*, 1973; Heuser & Reese 1973). Heuser and Reese found that stimulating cultures at 10 Hz for 15 minutes led to a 60 % depletion in SV membrane, concurrent with the appearance of numerous cisternae. Following a 15 minute rest, these cisternae disappeared and SVs re-appeared (Heuser & Reese, 1973). Ceccarelli *et al.* on the other hand found in the same preparation that vesicles were retrieved directly from the axolemma. Since then a number of different mechanisms for the endocytosis of SV membrane have been described. Clathrin-mediated endocytosis (CME), kiss-and-run and bulk endocytosis have all been proposed to function as endocytic mechanisms in the SV cycle (Fig 1.2).

1.4 Methods for monitoring the SV cycle

Several tools are available for the investigation of synaptic vesicle endocytosis (SVE) at the nerve terminal. Capacitance measurements of large synapses, electron microscopy (EM) or fluorescent imaging techniques monitoring

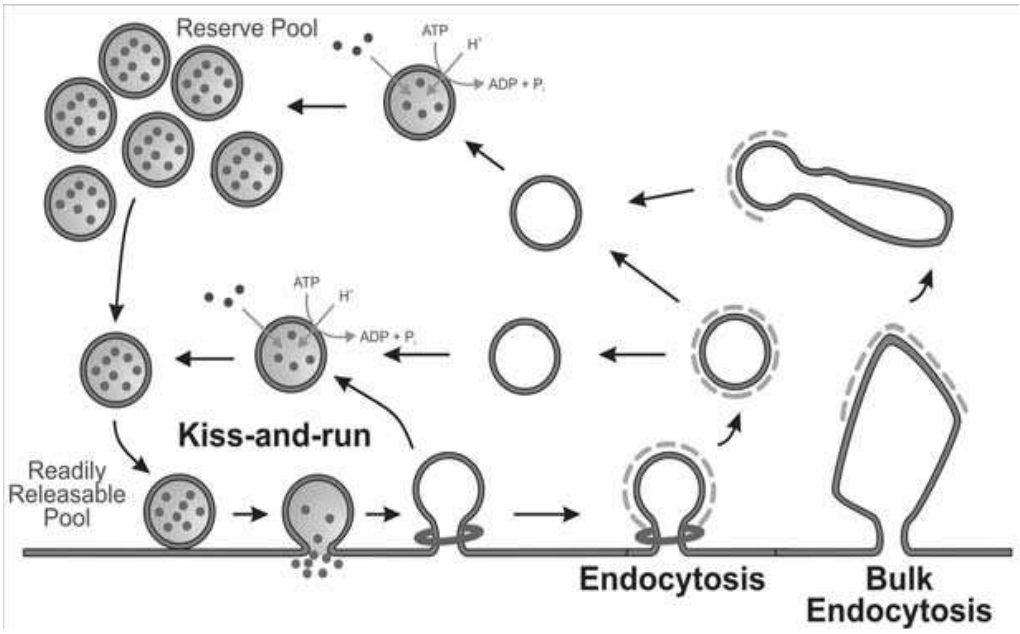

Figure 1.2 - Multiple synaptic vesicle retrieval pathways in central nerve terminals

Three different mechanisms are proposed to retrieve synaptic vesicle (SV) membrane after exocytosis in nerve terminals. Kiss-and-run is a mechanism where the SV never fully fuses with the plasma membrane and retrieves intact. Classical clathrin-dependent endocytosis involves the invagination of a single clathrin-coated bud from the plasma membrane before its fission and uncoating. Bulk endocytosis is the process where large areas of nerve terminal membrane are invaginated to produce endosomes from which SVs can bud (Clayton et al, 2007).

FM dyes, dextran internalisation or pHluorin assays have all been used in various studies of endocytosis at model synapses.

1.4.1 FM DYES

Styryl (FM) dyes posses a number of properties which make them a useful tool for tracking SV exocytosis and endocytosis in living cells. These FM dyes are amphiphilic molecules that posses a hydrophilic head group and a hydrophobic tail; this allows them to reversibly partition into membranes without passing through the membrane. These dyes only fluoresce when they have partitioned into membrane and do not fluoresce in solution. The length of the lipophilic tail determines the departition rate of the dye, and also the staining intensity of the dye; those with shorter tails are less lipophilic and stain less brightly (for example FM2-10 with two carbon atoms in the tail), whilst conversely those with longer tails are more lipophilic and stain more brightly (for example FM1-43, which has a four carbon tail) (Betz et al, 1996). When these dyes are incubated with neuronal cultures, following stimulation either by elevated K^+ or APs, the dye will label all vesicles which are turned over as a result of the stimulus. The remaining dye in solution can then be washed away, leaving an FM dye-labelled synapse. Since these dyes can departition from the membrane, a further stimulus can release the SV packaged dyes. The amount of dye released as a result of this unloading stimulus can provide information on the turnover of SVs (Cousin & Robinson, 1999).

Another useful feature of FM dyes is the ability to photoconvert the dye to an electron dense marker, which can then be imaged by EM (Harata *et al.*, 2001). This

allows investigation of labelling at the level of the individual synapse, allowing clarification of the endocytosis route active at the synapse.

1.4.2 pHluorins

The reacidification of SVs following their retrieval and re-filling with neurotransmitter is a property which has enabled the development of a further set of fluorescent tools for investigation of the SV cycle. Fusion of a pH sensitive green fluorescent protein (GFP) protein, pHluorin, to SV related proteins has enabled the study of kinetics of vesicle reacidification and other aspects of SV trafficking. pHluorins are a pH sensitive version of GFP, which fluoresce in the pH of the extracellular environment (pH of ~ 7.4), but are quenched following reacidification of the vesicle contents (pH of ~ 5.6) (Miesenböck *et al.*, 1998; Sankarnarayanan *et al.*, 2000). As vesicle reacidification occurs rapidly after internalisation, pHluorin fluorescence and quenching can be used as a measure of exocytosis at a synaptic terminal. Prevention of the reacidification of the vesicle (for example by application of bafilomycin) can then be used to derive information about endocytosis at the terminal (Ryan, 2001). Several different vesicle protein-pHluorin constructs are commonly used; synaptopHluorin is a conjugate of pHluorin to VAMP2 (Sankarnarayanan *et al.*, 2000), synaptotagmin-pHluorin is pHluorin tagged synaptotagmin I (Wienisch & Klingauf, 2006), VGLUT1 has been tagged with pHluorin (Voglmaier *et al.*, 2006), and sypHy is a construct of pHluorin conjugated to synaptophysin (Granseth *et al.*, 2006).

1.4.3 DEXTRANS

Dextrans are inert polysaccharides which, when conjugated to fluorescent dyes, have been used to monitor a number of different cellular processes. Dextran conjugates are membrane impermeant, and, depending on the size of dextran used, they are excluded from single recycling vesicles, and thus can be used as a selective marker of large fluid phase bulk endocytic events. Large fluorescent dextrans have been used at both the goldfish retinal bipolar cell (Holt *et al.*, 2003) and the snake motor bouton (Teng *et al.*, 2007) to investigate retrieval of bulk endosomes.

1.4.4 HRP/EM

Uptake of horseradish peroxidase (HRP) has frequently been used to visualise mechanisms of endocytosis in neurons. HRP is a fluid phase marker, and therefore will non-selectively label active endocytosis processes. Use of EM to study the uptake of HRP after conversion to an electron dense marker is extremely useful as morphological changes can be detected at the level of the individual synapse (Marxen *et al.*, 1999; Leenders *et al.*, 2002; de Lange *et al.*, 2003; Di Paolo *et al.*, 2002; Evans & Cousin, 2007).

1.4.5 CAPACITANCE MEASUREMENTS

Large synapses such as the calyx of held are amenable to the study of endocytic events by whole-cell capacitance measurement. As biological membranes behave like electrical capacitors, measurement of the membrane capacitance can detect changes that reflect the insertion or removal of membrane at the nerve

terminal which occurs due to exocytosis or endocytosis (Neher & Marty, 1982). This method can be applied to large synapses, such as retinal bipolar cells and the calyx of held. Although a very useful method of analysis, capacitance recordings reflect the sum of the total changes in surface membrane, and thus can lack specificity. Typical small central nerve terminals are too small for capacitance measurements.

1.4.6 AMPEROMETRY

Amperometric detection of secretory events of oxidizable substrate using carbon fibre microelectrodes can be used to analyse secretory events that occur in close proximity to the surface of the electrochemical detector (Leszczyszyn *et al.*, 1991). Amperometry has provided much evidence on the release of catecholamines from secretory granules in neuroendocrine cells (Burgoyne & Morgan, 2003). However as this technique is only applicable for the measurement of oxidizable substrates (such as dopamine), the use of amperometry at small central nerve terminals is limited.

1.5 "KISS-AND-RUN"

Perhaps the most controversial method of endocytosis, kiss-and-run has been proposed to facilitate rapid neurotransmitter release and recycling of the vesicle membrane. This method of recycling takes place *in situ* at the plasma membrane, where vesicles fuse and form a transient fusion pore sufficient for release of neurotransmitters (Fesce *et al.*, 1994). Full collapse of the vesicle does not occur with this method of endocytosis, and the vesicle is retrieved by closure of the fusion pore. Kiss-and-run has been firmly established as a mechanism of vesicle retrieval in

neuroendocrine cells using capacitance, amperometry and fluorescence measurements (Spruce *et al.*, 1990; Alvarez de Toledo *et al.*, 1993; Tsuboi & Rutter, 2003). Capacitance measurements of dense core granule secretion in mast cells have tracked the opening and dilation of a fusion pore, leading to a capacitance "flicker" which can be equated to kiss-and-run (Spruce *et al.*, 1990). Amperometric analysis of release from murine mast cells combined with patch clamp measurements show a release of serotonin during transient fusion events (Alvarez de Toledo *et al.*, 1993). Dopamine release from midbrain neurons has also been shown to occur via a flickering fusion pore (Staal *et al.*, 2004). Kiss-and-run events in pancreatic β-islets can be detected through use of synaptopHluorin, where the formation of a fusion pore can result in transient increases in synaptopHluorin fluorescence with no lateral diffusion detected (Tsuboi & Rutter, 2003). Combinational capacitance and amperometric measurements in chromaffin cells indicate that an increase in calcium concentration leads to a shift in exocytic mechanisms towards that of kiss-and-run (Alés *et al.*, 1999),

Despite the obvious importance of kiss-and-run in neuroendocrine cells, the evidence for this method of SV recycling is still controversial in central neurons.

1.5.1 Evidence supporting a model of kiss-and-run;

The techniques used to study kiss-and-run in neuroendocrine cells (primarily capacitance and amperometry) cannot be used on central synapses due to their small size. Therefore the field has had to rely on indirect, generally fluorescence based methods of analysis to investigate kiss-and-run at these synapses.

In 2000 the lab of Stevens and Williams stimulated hippocampal neurons using hypertonic solutions. This resulted in normal glutamate release from the readily releasable pool (RRP) of SVs, but there was partial prevention of FM1-43 dye unloading from cells. The authors attributed this discrepancy to the formation of a fusion pore sufficiently large to allow escape of glutamate, but not the 4 times larger FM1-43 (Stevens & Williams 2000). In similar studies, using both a burst of APs or hypertonic solutions, it was observed that less of the slowly dissociating FM1-43 was released from hippocampal preparations than the more rapidly dissociating FM2-10 (Pyle *et al.*, 2000), which the authors suggested was due to the formation of a fusion pore limiting the time available for the dyes to escape. Both studies can now be explained by the observation that the RRP is selectively labelled by FM2-10, whilst FM1-43 labels both the RP and the RRP (Richards *et al.*, 2000). As hypertonic stimulation will only turn over the RRP, this disproportionate amount of dye labelling means that only a partial loss of FM1-43 will be observed. Therefore FM dyes are not an accurate marker of kiss-and-run events.

Gandhi and Stevens (2003) proposed a fast mode (400-860 ms) of exocytosis which utilized a fusion pore, resolved through use of single-vesicle imaging techniques using synaptopHluorin. They proposed that this mode of “kiss-and-run” is used by synapses with a low release probability. However it was subsequently shown that diffusion of synaptopHluorin in the plane of the plasma membrane accounted for the perceived fast mode of exocytosis (Granseth *et al.*, 2006).

In *Drosophila* synaptojanin and endophilin null mutants, neurotransmitter release exhibited depression at strong stimulation, however a component of release was still observed. It was postulated that this sustained release may be occurring by a

"kiss-and-run" mechanism, an idea which is supported by the observation of small clusters of SVs at the active zone (Verstreken *et al.*, 2003). However this was refuted by Dickman *et al.* (2005), who analysed the quantal size and FM1-43 loading of these mutants, and concluded that even in the synaptojanin and endophilin null *Drosophila* mutants, vesicles undergo full fusion and not kiss-and-run.

Perhaps the strongest evidence which supports a mechanism of kiss-and-run in neurons again comes from studies of hippocampal neurons. Intravesicular fluorescence (either FM1-43 or VAMP-EGFP) can be quenched through use of a hydrophilic quencher bromophenol blue (BPB, the longest dimension of which is 1.5 nm; glutamate is 1 nm). Through the reversible quenching of both FM1-43 and VAMP-EGFP by BPB, the authors argued that the recycling pool of vesicles engaged in kiss-and-run events, and that variations in stimulation modify both the balance between kiss-and run events versus full fusion events, and also the kinetics of vesicle re-use (Harata *et al.*, 2006). Interestingly, it was noted that the lower the stimulation rate the higher the number of incidences of kiss-and-run, which concurs with the observations made by Gandhi and Stevens (2003).

Most recently quantum dots have been used to probe the incidences of kiss-and-run in hippocampal neuronal cultures. Quantum dots are proposed to be useful for this purpose, as they are small enough to fit within vesicles (24 nm), but too large to pass through fusion pores (1-5 nm), and the emission from quantum dots is pH dependent. By sparsely loading the synapses with quantum dots to trace individual vesicles, the authors found that kiss-and-run dominated at the beginning of a stimulus, and also that the incidence of kiss-and-run increased during rapid firing (Zhang et al, 2009).

1.5.2 Evidence opposing a role of kiss-and-run;

It is known that under physiological conditions, endocytosis occurs at a rate sufficient to maintain the vesicle pool required for exocytosis (Ceccarelli *et al.*, 1973). During turnover evoked by continuous stimulation at 10 Hz at physiological temperature in hippocampal neurons, using styryl dye imaging techniques, escape of the hydrophobic FM4-64 was observed, indicating that only full fusion events were occurring (Fernández-Alfonso & Ryan, 2004). In sparse cultures of hippocampal neurons loaded with FM1-43 by incubating with the dye for 1 minute in the absence of stimulation (where loading can only occur by spontaneous turnover) it was found that these vesicles that spontaneously turned over during loading released dye in a quantal "all or nothing" fashion, which would negate a function for kiss-and-run (Chen *et al.*, 2008). In addition, in hippocampal cultures imaged using pHluorin tagged synaptophysin, only a slow (an approximate time course of 15 seconds), mode of endocytosis occured in response to a single or short burst of APs (Granseth *et al.*, 2006). CME was responsible for this mode of endocytosis, since either silencing of clathrin expression by siRNA or overexpression of dominant negative mutants blocked the sypHy response.

It is not only the hippocampal synapse where evidence against kiss-and-run as a mechanism of vesicle retrieval can be seen. Studies of the frog NMJ found that after 30 Hz stimulation for 0.5 s in the presence of FM1-43, labelled vesicles were observed at the surface membrane outside the active zone, and also scattered within the vesicle pool, indicating that these vesicles had not undergone kiss-and-run events, as such kiss-and-run events by their nature would have resulted in a build-up of vesicles at the active zone (Rizzoli & Betz, 2004). The observation that the SV

proteins which are associated with the exocytosing vesicle are not the same as those which are subsequently retrieved (Fernandez-Alfonso *et al.*, 2006; Wienisch & Klingauf, 2006) also provided evidence against an in situ mechanism of neurotransmitter release and immediate vesicle retrieval, as is implied by kiss-and-run.

The above evidence both for and against this mechanism of endocytosis shows that kiss-and-run is still a controversial mechanism of SVE.

1.6 CLATHRIN MEDIATED ENDOCYTOSIS.

CME of single vesicles is the best characterised method of endocytosis in neurons. Receptor-mediated endocytosis is the mechanism which non-neuronal eukaryotic cells use to internalize ligands, and it is modulated by clathrin-coated pits and vesicles. This internalization can occur either constitutively or in response to stimuli. Whilst many of the features of CME at the synapse are the same as in other cell types, some of the components are unique to nerve terminals.

1.7 THE KEY PROTEINS INVOLVED IN SYNAPTIC VESICLE ENDOCYTOSIS

CME of SVs occurs in a number of stages; nucleation, invagination, fission and uncoating (Fig 1.3). A number of different coat components, membrane factors and accessory proteins function as part of the endocytic machinery.

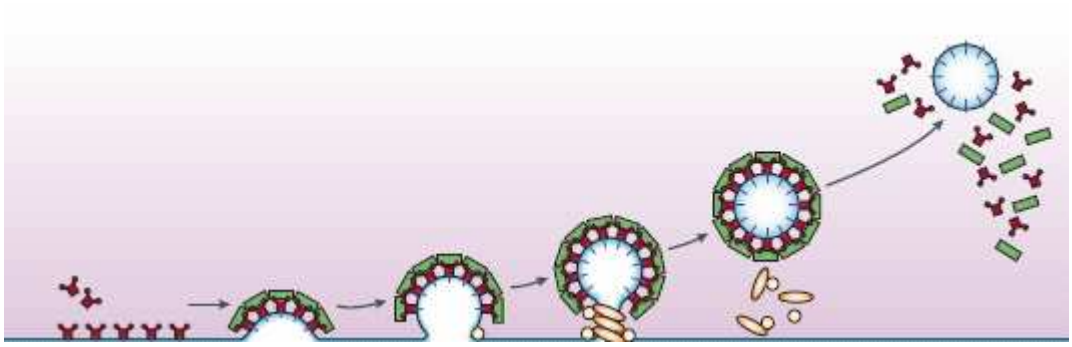

Figure 1.3 - Clathrin mediated endocytosis of a synaptic vesicle.

Clathrin-mediated endocytosis progresses through several stages of nucleation, invagination, fission and uncoating mediated by components of the endocytic machinery. Adapted from Lopez, 2004.

1.7.1 INITIATION OF ENDOCYTOSIS

The endocytosis of SV membrane is though to be initiated by the binding of AP2 to vesicle membrane proteins (Fig 1.4). This binding may be mediated by the action of synaptotagmin, which bind at its C2B domain to AP2 (Jorgensen *et al.*, 1995). The recruitment of AP2 to synaptotagmin is mediated by a tyrosine endocytoic motif, YxxØ, where Ø represents a bulky hydrophobic residue. The binding of AP2 to this endocytic motif enhances the interaction between AP2 and other SV proteins containing this motif (Haucke & De Camilli, 1999).

1.7.1.1 AP2

AP2 is a tetramer, composed of two large subunits (α and β2), one medium subunit (μ2) and a small subunit (σ2). The α and β2 subunit of AP2 can be divided into an N terminal trunk and a C terminal "head" or "ear", which are joined by a linker region of about 100 amino acids that is proline/glycine/alanine-rich, and is protease sensitive (Schröder & Ungewickell 1991). The β2 subunit alone is sufficient for driving formation of the clathrin coat (Shih *et al.*, 1995). The N terminal of the α subunit of AP-2 binds to $PI(4,5)P_2$, anchoring AP-2 at the membrane (Gaidarov & Keen, 1999). The hinge and ear region of the β2 subunit is then responsible for the recruitment of clathrin (Shih *et al.*, 1995). AP-2 binds to the C terminus of eps15, in an area of eps15 which contains 4 of the characteristic 15 DPF repeats of eps15 (Benmerah *et al.*, 1996). AP-2 is also known to bind to the central region of epsin (Chen *et al.*, 1998), and can also interact directly with AP180, auxilin and amphiphysin (Hao *et al.*, 1999).

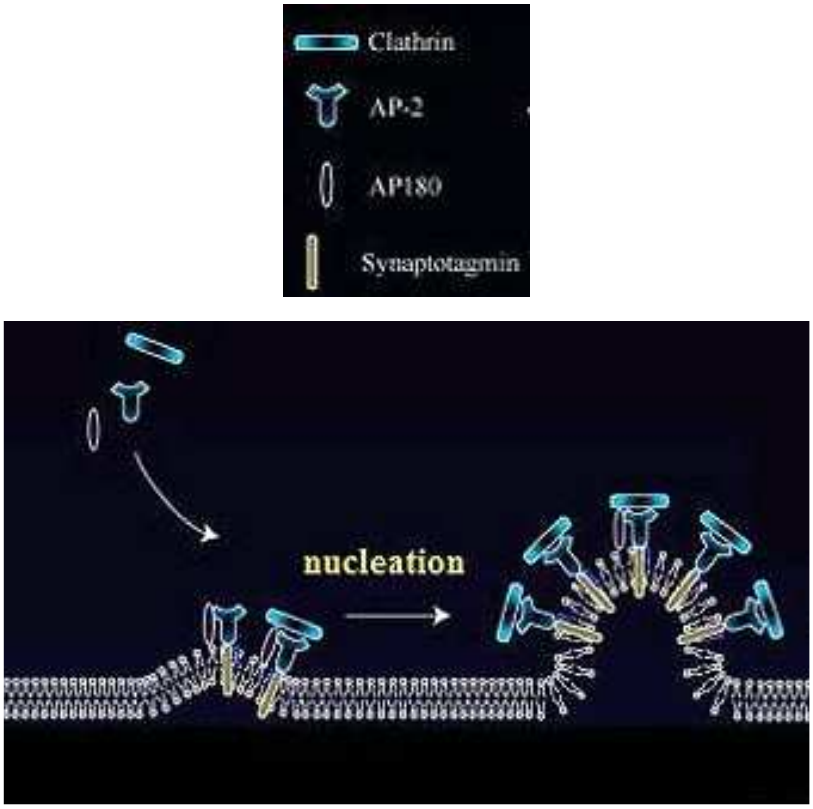

Figure 1.4 - Nucleation of a synaptic vesicle

The endocytosis of synaptic vesicle membrane is though to be initiated by the binding of AP2 to synaptotagmin. The N terminal of the α subunit of AP2 binds to $PI(4,5)P_2$, anchoring AP-2 at the membrane. The hinge and ear region of the β2 subunit of AP2 is then responsible for the recruitment of clathrin. AP180 promotes the polymerization of clathrin through its interaction with clathrin heavy chains.

(From seiri1.med.okayama-u.ac.jp/research_activities/research_contents/index003wuhtml.html)

1.7.1.2 AP180

AP180 was first characterized following its purification from coated vesicles of bovine brain (Ahle & Ungewickell, 1986). AP180 promotes the polymerization of clathrin through its interaction with clathrin heavy chains (Prasad & Lippoldt, 1988; Lindner & Ungewickell, 1991), thereby inducing the assembly of clathrin triskelia into 60-70 nm coats (Morris *et al.*, 1993).

The essential role of AP180 in SVE was first shown in *Drosophila.* In lap (AP180 null) *Drosophila*, SVE efficiency is severely compromised, and clathrin is mislocalised (Zhang *et al.*, 1998). The size of both SVs and quanta are significantly increased, suggesting a regulatory role of AP180 in control of SV size. The lap mutation also disrupts calcium coupling to exocytosis (Bao *et al.*, 2005).

There is a direct and synergistic clathrin-independent interaction between AP180 and AP-2; this AP180-AP-2 complex is more efficient at assembling clathrin under physiological conditions than either protein alone (Hao *et al.*, 1999). Injection of a peptide corresponding to the C-terminal domain of squid AP180 which disrupts clathrin assembly completely blocked synaptic transmission; analysis of terminals revealed a reduction in the number of SVs, with both the remaining SVs and the plasma membrane showing an increase in size (Morgan *et al.*, 1999), showing that the interaction between AP180 and clathrin is important in maintaining a pool of vesicles for release.

Ford *et al.* in 2001 found that AP180 can bind to PtdIns(4,5)P2 and clathrin simultaneously, which may serve to tether clathrin to the membrane. In support of this the presence of AP180 led to the formation of clathrin lattices, in the presence of AP2 these progressed to coated pits (Ford *et al.*, 2001). PI(4,5)P_2 is a

phosphoinositide concentrated in the plasma membrane that binds endocytic clathrin adaptors. In support, $PI(4,5)P_2$ depletion results in a reduction in clathrin puncta (Zoncu *et al.*, 2007).

It has been established that eps15 is also essential for coated pit formation, since inhibition of the binding between eps15 and AP180 inhibits the formation of both CCPs and coated vesicles (Morgan *et al.*, 2003).

1.7.1.3 CLATHRIN

Clathrin was first described in fibroblasts, where pentagonal and hexagonal shapes were seen to form the spherical baskets which coated and enclosed vesicles (Heuser, 1980). The clathrin triskelion is composed of three heavy and three light chains, with each heavy chain in contact with a light chain, and can assemble into cages without the assistance of any other proteins (Kirchhausen & Harrison, 1981). Removal of the light chain does not abolish the ability to form coats, suggesting the heavy chain is responsible for coat formation (Schmid *et al.*, 1982). Although the C terminal region of the clathrin heavy chain is not required for formation of trimers, it may be important for normal clathrin coated vesicle (CCV) structure and function (Lemmon *et al.*, 1991). Each clathrin triskelion contributes to two connecting edges of the polyhedral cage (Smith *et al.*, 1998). The assembly of clathrin into coats is driven by the adaptor protein complexes AP2 and AP180 (Hao *et al.*, 1999).

1.7.2 PROGRESSION OF ENDOCYTOSIS BY INVAGINATION

The progression of endocytosis from nucleation to internalisation of a coated vesicle then progresses by the action of a set of proteins that can facilitate membrane curvature and recruitment of further protein interaction partners (Fig 1.5).

1.7.2.1 EPSIN

Epsin (Eps15 interacting protein), was initially discovered through its binding to the auxiliary protein Eps15 (Chen *et al.*, 1998). Epsin I is ubiquitously expressed but is found to be enriched in the brain (Rosenthal *et al.*, 1999).

The structure of the epsin N-terminal has led to the description of another protein domain, the epsin N-terminal homology domain (ENTH) domain, identified in yeast homologs of epsin (Wendland *et al.*, 1999). ENTH domains interact with tubulin (Hussain *et al.*, 2003), and bind the membrane lipid $PI(4,5)P_2$, where epsin directly induces membrane curvature, binding to $PI(4,5)P_2$ in conjunction with clathrin (Ford *et al.*, 2002). Epsin induction of membrane curvature may be driven by the formation of an amphipathic alpha helix in epsin upon binding to $PI(4,5)P_2$, and the insertion of this helix into one leaflet of the lipid bilayer (Ford *et al.*, 2002).

Adjacent to the ENTH domain are the ubiquitin-interacting-motifs (UIMs), which interact with polyubiquitin chains (Hawryluk *et al.*, 2006). The asparagine/proline/tryptophan (DPW) central domain of epsin binds to the heterotetrameric AP-2 adaptor complex, and the central portion of epsin also interacts directly with clathrin (Drake *et al.*, 2000). The three C terminal asparagine/proline/phenylalanine (NPF) repeats of epsin are important for binding of epsin to both eps15 and intersectin (Chen *et al.*, 1998; Yamabhai *et al.*, 1998).

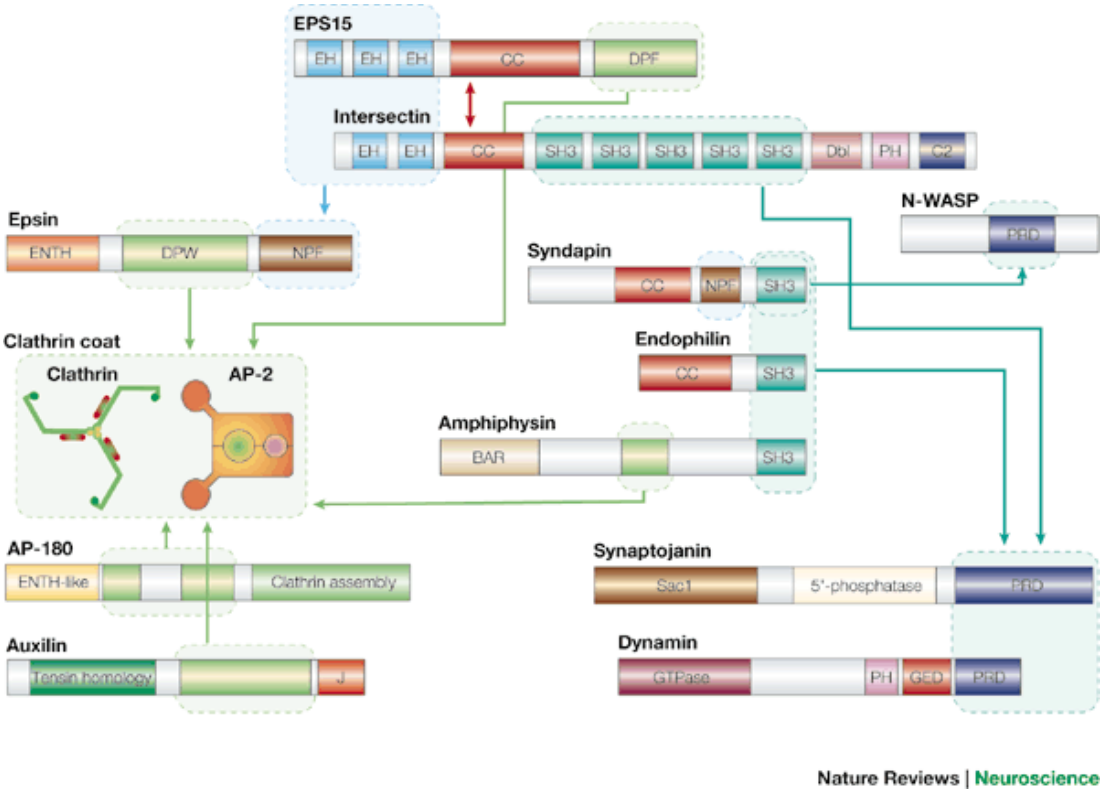

Figure 1.5 - Interactions of the coat components and accessory proteins in SVE

The domains of key synaptic endocytic proteins, and their interacting partners are shown (adapted from Slepnev and Di Camilli 2000).

Epsin I and epsin II are both similar in their ENTH domain, however the multiple DPW motifs which are typical of the central region of epsin I are only partially conserved in epsin II although both proteins interact via this region with clathrin (Rosenthal *et al.*, 1999).

Microinjection of antibodies to either the ENTH or (clathrin/AP-2-binding) CLAP binding region of the lamprey ortholog of epsin resulted in the accumulation of coated structures that showed a bias of early endocytic intermediates of shallow coated pits (Jakobsson *et al.*, 2008). This functional study indicated a role for epsin in coordination of curvature generation, and also generation of uniformly sized vesicles.

1.7.2.2 EPS15

Eps15 (epidermal growth factor pathway substrate 15) was a novel tyrosine kinase substrate discovered in a study of the epidermal growth factor receptor-signalling pathway (Fazioli *et al.*, 1993). A domain in eps15 was found to be highly conserved across several heterogeneous yeast and nematode proteins; this domain was designated eps15 homology (EH) domain (Wong *et al.*, 1995). EH domains bind to NPF motifs (Salcini *et al.*, 1997) this interaction of the EH domain of eps15 with the NPF motifs of syndapin is crucial in endocytic internalisation (Braun *et al.*, 2005). Synaptojanin-170, an alternatively spliced isoform of synaptojanin 1, binds Eps15; binding is mediated by the three NPF motifs at the N-terminal of synaptojanin-170 (Haffner *et al.*, 1997). Eps15 can oligomerise, mediated by its

coiled-coil region and can be found in complexes as covalent dimers or multimers (Tebar *et al.*, 1997).

A role in SVE was suggested when it was determined that eps15 is constitutively associated with the adaptor protein AP2, an interaction mediated by the C-terminal of eps15 (Benmerah *et al.*, 1995; Benmerah *et al.*, 1996), and also the observation that eps15 is located at the rim of coated pits (Tebar *et al.*, 1996) strengthened this hypothesis. Implications for the function of eps15 in SVE can be seen in a number of functional studies. In an eps15 mutant lacking EH domains, the plasma membrane punctate distribution of both AP-2 and clathrin was lost, implying the absence of coated pits (Benmerah *et al.*, 1999). Ehs-1 (the C. elegans orthologue of Eps15)-impaired worms showed temperature-dependent depletion of synaptic vesicles. Ehs-1 acts in synaptic vesicle recycling and its function may be linked to that of dynamin (Salcini *et al.*, 2001). Eps15 stimulates the ability of the clathrin adaptor protein, AP180, to assemble clathrin, and perturbation of the binding between eps15 and AP180 inhibits the formation of clathrin coated pits (CCPs) and coated vesicles (Morgan *et al.*, 2003). Temperature sensitive eps15 *Drosophila* mutant shows reversible paralysis at the restrictive temperature (Majumdar *et al.*, 2006) and *Drosophila* eps15-null mutants show that eps15 is required for both proper synaptic bouton development and normal levels of SVE (Koh *et al.*, 2007). Thus multiple studies have shown the key role of eps15 in SVE.

1.7.2.3 AMPHIPHYSIN

In 1992 a screen for novel neuronal proteins using antisera against synaptic plasma membrane proteins led to the discovery of a novel 75 kDa protein, termed

amphiphysin (Lichte *et al.*, 1992). Amphiphysin has 3 distinct domains; an N-terminal BAR (Bin/amphiphysin/Rvs) (Elliott *et al.*, 1999) domain, a variable central domain and a C terminal src homology 3 (SH3) domain. The amphiphysin BAR domain can sense membrane curvature, bind membrane and mediate lipid tubulation (Takei *et al.*, 1999; Peter *et al.*, 2004), and also mediates the dimerization of amphiphysin (Ramjaun *et al.*, 1999). The variable central CLAP region of amphiphysin mediates interactions with the α_c subunit of AP2 adaptin, and with clathrin (David *et al.*, 1996; Evergren *et al.*, 2004). Distinct regions of the C terminal SH3 domain of amphiphysin mediate interactions with the proline rich domains (PRDs) of dynamin, (David *et al.*, 1996) and synaptojanin (McPherson *et al.*, 1996). The amphiphysin isoform, amphiphysin II, also binds to dynamin and synaptojanin through its SH3 domain (Ramjaun *et al.*, 1997). Amphiphysin II splice variants bind clathrin at two distinct clathrin-binding sites (Ramjaun & McPherson 1998). Both amphiphysin I and II undergo constitutive rephosphorylation and Ca^{2+} dependent dephosphorylation, mediated by calcinuerin (Bauerfeind *et al.*, 1997).

A number of lines of evidence implicate amphiphysin in a role in the fission of recycling vesicles. The structure of the *Drosophila* amphiphysin BAR domain has been determined to be a crescent-shaped dimer that binds to highly negatively charged membranes (Peter *et al.*, 2004). Amphiphysin I can tubulate lipids, and assembles with dynamin I into ring like structures around the tubules (Takei *et al.*, 1999). This interaction of dynamin I with amphiphysin I prevents dynamin I self assembly into rings (Owen *et al.*, 1998).

Studies of amphiphysin I knock out (KO) mice have aided in the study of the role of amphiphysin I in the SV cycle. Amphiphysin I KO mice have defective SV

recycling, which became apparent following stimulation. The KO mice exhibit major learning defects, and show increased mortality as a result of rare irreversible seizures. Interestingly there is a concurrent lack of amphiphysin II in amphyphisin I deficient mice (Di Paolo *et al.*, 2002). Amphiphysin II KO mice die at birth as a result of severe cardiomyopathy, indicating a crucial role of amphiphysin II in the development of cardiac muscle (Muller *et al.*, 2003). Studies at the large lamprey reticulospinal synapse have also enabled a closer study of the stage of endocytosis at which amphiphysin functions. Microinjection of ampiphysin SH3 domains at the lamprey reticulospinal synapse arrests SVE at the stage of invaginated CCPs (Shupliakov *et al.*, 1997), whilst microinjection of antibodies against the central CLAP region inhibited recycling of SVs and caused accumulation of various clathrin-coated intermediates (Evergren *et al.*, 2004). The presence of these clathrin-coated intermediates suggests that the dynamin I-amphiphysin I interaction is necessary for fission of the SV.

Conversely, studies in *Drosophila* have shown that amphiphysin I is not necessary for SVE. Amphiphysin I is localised postsynaptically in *Drosophila*, and amphiphysin mutants are viable but flightless. The sarcoplasmic reticulum is disorganised in these mutants, indicating a role in muscle organisation, but SVE is unaffected (Razzaq *et al.*, 2001; Zelhof *et al.*, 2001).

1.7.2.4 ENDOPHILIN

Like amphiphysin, the SH3 domain of endophilin binds to the PRDs of both synaptojanin and dynamin I (Micheva *et al.*, 1997; Cestra *et al.*, 1999). Endophilin

binds to the PRD of synaptojanin at a single binding site, which is distinct from the 2 binding sites of amphiphysin (Cestra *et al.*, 1999).

Purified endophilin I can bind and tubulate lipid bilayers, a property mediated by its N terminal BAR domain (Farsad *et al.*, 2001). The BAR domain of endophilin has several distinct features, driving positive membrane curvature through use of both its crescent-shaped BAR domain and a pair of helices which extend from the crescent and penetrate into the membrane bilayer (Masuda *et al.*, 2006). The endophilin N-BAR domains function as low affinity dimers, and serve to recruit binding partners to areas of high membrane curvature (Gallop *et al.*, 2006).

The endophilin I binding site within synaptojanin also binds endophilin II; the distribution of endophilins I and II in central synapses does not usually overlap. Both endophilins I and II are found as stable dimers, dimerising via their N terminal domain (Ringstad *et al.*, 2001), which may allow for interaction with a number of different binding partners.

Studies of interference of endophilin in several model systems have served to illustrate the function of endophilin in SVE. Microinjection of antibodies disrupting endophilin function results in a block in the invagination of CCPs in lamprey, and specific perturbation of endophilin SH3 interactions results in a block of CME at two distinct stages; free CCVs and invaginated CCPs (Ringstad *et al.*, 1999; Gad *et al.*, 2000). *Drosophila* endophilin A null mutants show severe mobility defects, and do not progress to adulthood. Reduction in the level of *Drosophila* endophilin A results in an accumulation of endocytic intermediates, many of which are arrested at early-stage invagination (Guichet *et al.*, 2002). Interestingly, *Drosophila* endophilin mutant larva are still able to sustain a small proportion of release, about 20% of

normal rate at high frequency stimulation (Verstreken *et al.*, 2002). *Drosophila* synaptojanin null and double synaptojanin/endophilin mutants are found to be electrophysiologically and ultrastructurally similar to endophilin null mutants, with synaptojanin mislocalised at endophilin null synapses (Verstreken *et al.*, 2003). This finding is supported by studies in *C. elegans*, where unc-57 (ortholog of endophilin A) defects resemble those in synaptojanin mutants, with the electrophysiological phenotype of double mutants also identical to that of the single mutants. Endophilin stabilizes expression of synaptojanin at this synapse (Schuske *et al.*, 2003). Thus endophilin recruits and stabilizes synaptojanin on invaginating vesicles, and promotes vesicle uncoating.

An interaction between voltage gated calcium channels (VGCCs) and endophilin in endocytosis has also been observed, as expression of a dominant negative endophilin contruct that constitutively binds Ca^{2+} reduces endocytosis of FM4-64 but does not abolish exocytosis (Chen *et al.*, 2003).

Several observations indicate functions of endophilin which are mechanistically different from other SH3 domain containing proteins. Both endophilin and syndapin bind the same region of dynamin I, but they do so in a mutually exclusive fashion (Anggono & Robinson, 2007). *Drosophila* endophilin mutant larva are still able to sustain a small proportion of release, about 20% of normal rate at high frequency stimulation (Verstreken *et al.*, 2002), indicating that a pool of vesicles is possibly undergoing a form of endophilin independent recycling. This could possibly be explained if endophilin functions at distinct spatial/temporal/mechanistically different stages of SVE. Endophilin is also a binding partner for vesicular glutamate transporter 1 (VGLUT1), suggesting a

possible mechanism for functional differences between VGLUT1 and VGLUT2 terminals in replenishment of SV pools (De Gois *et al.*, 2006; Vinatier *et al.*, 2006).

1.7.2.5 SYNDAPIN

Syndapin (synaptic,dyamin-associated protein I) was discovered through its' ability to bind to the PRDs of dynamin I, synaptojanin I and synapsin I (Qualmann *et al.*, 1999). Syndapin I is neuronally expressed whilst syndapin II is ubiquitously expressed, (Qualmann & Kelly , 2000). Syndapin also associates with neuronal Wiskott-aldrich syndrome protein (N-WASP, a potent activator of the Arp2/3 complex which is a critical part of the actin polymerisation machinery), suggesting a link between cytoskeletal dynamics and SV recycling (Qualmann *et al.*, 1999). Because of this, syndapins were proposed to coordinate N-WASP and dynamin I at different steps of receptor mediated endocytosis (Kessels & Qualmann, 2002). The removal of NMDA receptors containing NR3A is regulated by syndapin in an activity dependent manner, where syndapin binds via its NPF motifs to the carboxy terminal of the NMDAR NR3A subunit, and recruits dynamin and clathrin (Pérez-Otaño *et al.*, 2006). EHD proteins can interact with syndapin by direct EH domain/NPF motif interactions (Braun *et al.*, 2005).

The N-terminal Fes-CIP homology and Bin-Amphiphysin-Rvs (F-BAR) domain of syndapin self polymerises forming tetrameric structures (Halbach *et al.*, 2007). Self association of F-BAR domains leaves the SH3 domain and NPF motifs available, allowing their simultaneous interactions with more than one other binding partner (Kessels & Qualmann, 2006). F-BAR domains differ from N-BAR domains in the length of their helices, which are longer and shallower for F-BAR domains

(Itoh *et al.*, 2005; Frost *et al.*, 2007). F-BAR domains can bend liposome into tubules of a maximum diameter of 130 nm, whilst N-BAR domains generally induce tubules of a smaller diameter (Henne *et al.*, 2007). It is possible that N-BAR and F-BAR domains mediate tubulation of membranes of different curvature, or perhaps at a distinct stage in the increasing curvature of an invaginating vesicle.

Stimulus-dependent dephosphorylation of dynamin I recruits syndapin I for SVE, but does not control amphiphysin I nor endophilin I binding (Anggono *et al.*, 2006). The binding sites for syndapin I and endophilin I on dynamin I are within the same region of the PRD, and as these binding sites overlap they are mutually exclusive (Anggono & Robinson, 2007). Taken together this indicates that these interactions with dynamin I may function at different stages or in different forms of SVE.

Presynaptic microinjection of syndapin I antibodies inhibit vesicle recycling evoked by intense stimulation, but have no effect on light stimulation (Andersson *et al.*, 2008). This is in contrast to perturbation of amphiphysin I which disrupts SV recycling at light stimulation (Shupliakov *et al.*, 1997). This indicates that syndapin I may play a role in endocytosis during increased activity. Interestingly though, studies of syndapin in *Drosophila* have found that the *Drosophila* syndapin isoform, which is found post synaptically, is dispensable for SVE (Kumar *et al.*, 2008), indicating that the function of syndapin may not be evolutionarily conserved and may only play a role in higher organisms.

1.7.2.6 INTERSECTIN

A screen of a *xenopus laevis* cDNA library with an SH3 peptide resulted in the discovery of intersectin, a protein which contains 2 EH domains and 5 SH3 domains (Yamabhai *et al.*, 1998). Hippocampal immunofluoresence analysis subsequently revealed that intersectin co-localises at the plasma membrane with clathrin (Hussain *et al.*, 1999), and this coupled with its ability to interact with both dynamin and synaptojanin (Yamabhai *et al.*, 1998) identified intersectin as a protein putatively involved in endocytosis. Intersectin has also been proposed to putatively couple exocytosis and endocytosis, as its central domain can bind to both SNAP-25 and SNAP-23 (Okamoto *et al.*, 1999).

Intersectin can be alternatively spliced to produce a longer neuronally expressed isoform, containing additional C-terminal dbl homology (DB), pleckstrin homology (PH), and C2 domains (Hussain *et al.*, 1999). Intersectin facilitates interactions with the actin cytoskeleton, through the action of the DH domain. The DH domain of intersectin is a guanine nucleotide exchange factor (GEF) for Cdc-42, an interaction which promotes actin assembly via N-WASP and the Arp2/3 complex (Hussain *et al.*, 2001).

Drosophila mutants of intersectin (dap160) have shown an insight into the function of intersectin at the synapse. Loss of function mutants show decreased levels of dynamin, endophilin, synaptojanin and AP180 (Marie *et al.*, 2004). EM analysis shows that the synapses are smaller, have fewer vesicles, and show an accumulation of endocytic intermediates (Koh *et al.*, 2004). Synapses are unable to sustain release during high frequency stimulation, and FM4-64 loading is severely reduced, illustrating severe defects in the SV cycle (Marie *et al.*, 2004). *Drosophila*

double mutants of intersectin and eps15 indicate that the proteins function in conjunction with each other in endocytosis, supported by the observation that both single mutants are phenotypically similar (Koh *et al.*, 2007). Intersectin has also been proposed to function as a negative regulator of dynamin I recruitment, as microinjection of either intersectin antibodies or SH3 homology domains result in a dramatic decrease in the amount of dynamin I at the constricted neck of invaginated vesicles (Evergren *et al.*, 2007).

1.7.2.7 SYNAPTOJANIN

Synaptojanin is a phosphatidylinositol phosphate (PIP) 5-phosphatase, responsible for the dephosphorylation of $PI(4,5)P_2$. Synaptojanin is composed of an N terminal suppressor of actin1 (SAC-1)-like phosphatase domain, a central inositol 5-phosphatase domain, and a C-terminal PRD (McPherson *et al.*, 1994; McPherson *et al.*, 1996). Originally identified via it's binding to the SH3 domain of Grb2 (growth factor receptor-bound protein 2), binding that occurred concurrent with dynamin binding, it was originally thought to function in conjunction with dynamin (McPherson *et al.*, 1994).

Both amphiphysin and endophilin bind to the PRD of synaptojanin via their SH3 domains, at distinct sites (de Heuvel *et al.*, 1997; Micheva *et al.*, 1997), indicating a possible spatial/temporal/functional difference of these interactions in SVE. Amphiphysin binds to 2 sites in synaptojanin, whilst endophilin has a single distinct binding site (Cestra *et al.*, 1999).

Two isoforms of synaptojanin are reported, termed synaptojanin I and synaptojanin II. The isoforms differ at their non-homologous C terminals, the mRNA

of which can be alternatively spliced in both isoforms to produce a shorter neuronal specific variant and a longer ubiquitously expressed variant (Khvotchev & Südhof, 1997). The alternative splice variants of synaptojanin I produce proteins of 145 kDa and 170 kDa, which differ in their membrane affinity, with the 170 kDa isoform remaining membrane associated even in the presence of 1 M salt whilst the 145 kDa version can be removed from the membrane by a low salt wash (Ramjaun & McPhearson, 1996). The use of TIRFM to look at the spatial-temporal recruitment of synaptojanin I and its binding partners to CCPs found that the 145 kDa isoform was rapidly recruited, along with endophilin, in a "burst" at a relatively late stage of formation of the CCP, whilst the ubiquitously expressed 170 kDa isoform was found to be present at all stages of CCP formation (Perera *et al.*, 2006). This suggested that endophilin mediates recruitment of synaptojanin-145 to the plasma membrane.

Studies in synaptojanin KO neurons confirmed that the dual action of both phosphatase domains is necessary for SV cycling, as although the defects associated with the KO phenotype could be rescued by expression of wild type synaptojanin, abolishing the catalytic function of either phosphatase domain by mutation meant that the phenotype could no longer be rescued (Mani *et al.*, 2007).

Synaptojanin I deficient mice have elevated levels of $PI(4,5)P_2$, and exhibit an accumulation of CCVs (Cremona *et al.*, 1999). FM dye imaging illustrates that this accumulation of coated vesicles occurs following stimulation, and that these coated vesicles are unable to progress to the functioning synaptic vesicle pool (Kim *et al.*, 2002). This finding was corroborated in studies of mutations in the unc-26 *C. elegans* ortholog of synaptojanin, where defects are observed at several stages of the SV cycle, from budding to uncoating and the recovery of vesicles from endosomes

(Harris *et al.*, 2000). Antibodies to the PRD of synaptojanin resulted in the accumulation of free clathrin coated vesicles in the lamprey reticulospinal synapse (Gad *et al.*, 2000). Taken together, these studies implicate synaptojanin in a function in the uncoating of clathrin from fissioned clathrin-coated vesicles.

1.7.3 FISSION OF CLATHRIN COATED VESICLES

The fission of the invaginated synaptic vesicle is mediated by the large GTPase dynamin I.

1.7.3.1 DYNAMIN I

To date three isoforms of dynamin have been reported, encoded for by separate genes with numerous splice variants. Differently spliced dynamin proteins have been observed to associate with distinct membrane compartments of the plamsa membrane, golgi apparatus and vesicles (Cao *et al.*, 1998). Dynamin I is neuronally expressed, and as mentioned is important in the fission of SVs during endocytosis. Dynamin II is ubiquitously expressed (Cook *et al.*, 1994; Diatloff-Zito *et al.*, 1995), and has been shown to be important in a number of different functions. For example dynamin II is necessary for the coat-independent micropinocytosis of fluid in epithelial cells (Cao *et al.*, 2007), and secretion of hormones from neuroendocrine cells (Yang *et al.*, 2001). Less is known about the functional role of dynamin III, although it is known to interact with mGluR5 and Homer at the post synapse (Gray *et al.*, 2003), and localises to dendritic spine tips where it may modulate the actin dependent morphogenesis of dendritic spines (Gray *et al.*, 2005).

Dynamin I is composed of a GTPase domain, a PH domain, a GTPase effector domain (GED) and a PRD (Sweitzer & Hinshaw, 1998; Cousin & Robinson 2001) (Fig 1.6). The GED domain of dynamin stimulates the GTPase activity, and also mediates oligomerisation of dynamin; these oligomers can exist in equilibrium with the monomer (Chugh *et al.*, 2006).

Dynamin I, like the other dephospins, is constitutively phosphorylated and undergoes activity-dependent dephosphorylation. The major phosphorylation sites for dynamin I are found in the PRD, where serines 774 and 778 of the phosphobox are phosphorylated by cyclin dependent kinase 5 (cdk5) (Tan *et al.*, 2003), and dephosphorylated by calcinuerin (Liu *et al.*, 1994). In addition to these major phosphorylation sites of dynamin (up to 69 % of the total), three more sites of the PRD have also been shown to undergo phosphorylation to a lesser extent; serines 851 and 857 (12%), and serine 822 (5%) (Graham *et al.*, 2007). Dynamin III is phosphorylated on serines 759, 763 and 853, where serine 853 of dynamin II is homologous to serine 851 of dynamin I, whilst dynamin II is not phosphorylated (Graham *et al.*, 2007). The PRD of dynamin I mediates the interaction of dynamin I with the SH3 domains of a number of effector proteins during SVE. The SH3 domains of both endophilin I and syndapin I bind the PRD of dynamin I in the same region, and do so in a mutually exclusive fashion (Anggono & Robinson, 2007). The phosphorylation status of the phospho-box of the PRD is also important, as stimulus dependent dephosphorylation of dynamin I has been shown to recruit syndapin for SVE, but does not control amphiphysin I or endophilin I binding (Anggono *et al.*, 2006). The mutually exclusive way in which endophilin I and syndapin I bind dynamin I, coupled with the dephosphorylation-dependent interaction of dynamin I

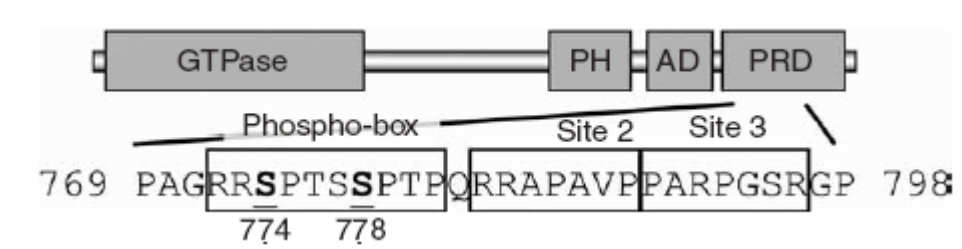

Figure 1.6 - Dynamin I The 4 distinct domains of dynamin I; GTPase domain, PH domain, assembly domain and the proline rich domain. The major phosphorylation sites of dynamin I, serines 774 and 778 are highlighted in the phospho-box. (Adapted from Anggono et al, 2006).

with syndapin I, hints at a possible mechanism by which dynamin could function in distinct spatial/temporal/mechanistically different forms of SVE.

The PH domain was originally identified in platelets, where pleckstrin is a major substrate of PKC (Sano *et al.*, 1983). The PH domain of dynamin I, which binds to $PI(4,5)P_2$, is important for the membrane localisation of dynamin I, and this binding of dynamin I to $PI(4,5)P_2$ increases the GTPase activity of dynamin I (Salim *et al.*, 1996). Oligomerisation of the PH domain of dynamin I into tetramers strengthens the lipid binding properties of dynamin I (Klein *et al.*, 1998).

The GTPase activity of dynamin I is known to be responsible for fission of vesicles (Sweitzer & Hinshaw, 1998). However the exact mechanism by which the GTPase domain mediates vesicle fission is still under debate, with a number of slightly mechanistically different models proposed. The mechanism of fission by pinching the neck of the vesicle and constricting refers to dynamin I as a “pinchase” (McNiven, 2000). Alternatively dynamin I may serve to “pop” the vesicle free from the plasma membrane, via a spring-like extension of the helix after hydrolysis (Stowell *et al.*, 1999). A corkscrew model of dynamin I constriction has also been proposed, based on X-ray crystallography and cryo-electron microscopy (Mears *et al.*, 2007). A GTP dependent “twisting” of dynamin I has been observed when GTP is added to lipid tubules coated in dynamin I; this model proposes that GTP hydrolysis induces a twisting action, inducing a tension that is released when the tubule breaks (Roux *et al.*, 2006). Real time visualisation of dynamin showed recently that assemblies of dynamin catalysed membrane fission in the presence of GTP, showing the importance of GTP for the fission of vesicles (Pucadyil & Schmid, 2008).

The function of dynamin I in endocytosis was originally seen in the temperature sensitive *Drosophila* mutant *shibire*, which cannot hydrolyse GTP. At the permissive temperature of 19 ºC SVE is normal, however after 8 minutes at the restrictive temperature of 29 ºC the vesicle pool is completely depleted, where SVs had formed but were unable to fission from the plasma membrane. Dynamin rings could be seen formed at the neck of these arrested vesicles. Within 2-3 minutes of returning to the permissive temperature, uncoated invaginations can be seen, which by 10 minutes have pinched off to form large cisternae. These cisternae in turn are decreased in number after 20 minutes, concurrent with the reappearance of SVs (Koenig & Ikeda, 1989; van der Bliek & Meyerowitz, 1991).

Another striking tool for functional dynamin analysis came with the report of the generation of a dynamin I KO mouse. Surprisingly, these mice actually form functional synapses, but they show little postnatal viability. Striking features of the cultured synapses of these KO mice are the extensively branched, tubular membrane invaginations, which are capped by clathrin. Vesicles could effectively recycle during mild stimulation, but were severely impaired during stronger stimulus (Ferguson *et al.*, 2007). Hayashi *et al.* (2008), used electron tomography to characterise these tubular membrane invaginations, and concluded that these endosome-like intermediates originate by a dynamin I independent form of endocytosis. However studies in the calyx of these dynamin I KOs have found that the response of the synapse to mild stimuli is no different to wildtype; however in response to stronger stimuli the speed of slow endocytosis fails to compensate for the increased endocytoic load (Lou *et al.*, 2008).As defects in SVE at dynamin I KO synapses manifest during conditions of strong stimulation, this indicates that the

dynamin I may play a role in the response of the synapse to increased stimulus intensity.

1.7.4 UNCOATING

Following the internalisation of the CCV, the clathrin coat must be removed from the internalised vesicle.

1.7.4.1 HSC70 AND AUXILIN

The dissociation of clathrin from CCVs is mediated by the 70 kDa heat shock protein, hsc70 (Ungewickell, 1985; Chappell *et al.*, 1986). This process is ATP dependent, as ATP greatly increases the rate of formation of this clathrin/hsc70 complex whilst ADP has an inhibitory effect (Prasad *et al.*, 1994). This ATPase activity can be greatly increased by the presence of auxilin (Jiang *et al.*, 1997), a cofactor in the uncoating of CCVs. Auxilin is a DnaJ protein as it has a J domain at its carboxyl terminal, the deletion of which results in the loss of cofactor activity (Ungewickell *et al.*, 1995). The interaction of auxilin, hsc70 and clathrin is highly specific, with auxilin initially binding to a clathrin triskelion, and hsc70 then is recruited to this complex (Barouch *et al.*, 1997). Auxilin binding induces a change in the contacts between the heavy chains of the clathrin triskelia, thereby destabilising the clathrin structure and facilitating the uncoating of the vesicle (Fotin *et al.*, 2004)

Drosophila hsc70 mutants (Hsc4) have developmental defects that are ultimately lethal (Elefant & Palter, 1999). However these mutants show an impairment in neurotransmitter release caused by a reduction in the Ca^{2+} sensitivity

of exocytosis, but not SV recycling (Bronk *et al.*, 2001). Evidence for the importance of auxilin *in vivo* comes from studies in both *S. cerevisiae,* where aux I is required for the uncoating of CCVs (Pishvaee *et al.*, 2000), and from the nematode, where *C. elegans* auxilin is essential for CME in vivo (Greener *et al.*, 2001). The role of hsc70 and auxilin in CCV uncoating at the presynapse was shown in the squid giant synapse, where a point mutation of the histidine/proline/ aspartate (HPD) motif in the J domain of auxilin prevented auxilin binding to hsc70 and inhibited CCV uncoating *in vivo* (Morgan *et al.*, 2001).

1.8 DEPHOSPHINS

Some of the above SVE proteins display certain homology in their protein interaction domains; however the key overlap between these proteins is the nature of their phosphorylation/dephosphorylation and how this affects and controls the endocytosis of synaptic membrane.

The importance of the proteins involved in SVE has been demonstrated in model systems, where the ablation of their function either leads to an inhibition or complete termination of SVE. A number of structural domain similarities exist between subgroups of these protein, for example the presence of a BAR domain in amphiphysin, endophilin and syndapin, or the ENTH domains of eps15 and epsin. However there is a more striking similarity which defines and unifies a subset of these proteins, which is their status as dephosphins. Dynamin I was the first of these dephosphins identified, it was found to be rapidly dephosphorylated (in approximately 2 s) following depolarization (Robinson *et al.*, 1994). Subsequently several more proteins were found to be dephosphorylated in nerve terminals

following stimulation, and the full set of dephosphins includes dynamin I, amphiphysins I and II, PIPKIγ, synaptojanin, AP180, epsin and eps15, which are all co-ordinately and rapidly dephosphorylated by calcineurin following nerve terminal stimulation (Cousin & Robinson, 2001). Ca^{2+} initiates SVE by binding to a Ca^{2+} sensor, calcineurin (Cousin, 2000). Calcineruin was identified as the calcium sensor for endocytosis through inhibition by cyclosporin A and FK506 (Marks & McMahon, 1998; Cousin *et al.*, 2001). Both the dephosporylation and the rephosphorylation of the dephosphins are essential for progressive cycles of SVE. Cdk5 rephosphorylates at least three of the dephosphins *in vivo*: dynamin I, PIPKIγ, and synaptojanin (Tan *et al.*, 2003; Lee *et al.*, 2004; Lee *et al.*, 2005). No evidence is available to show which SVE pathway requires which dephosphin, however it is known that cdk5-dependent protein rephosphorylation is necessary for bulk endocytosis (Evans & Cousin, 2007), suggesting that one of the cdk5 dephosphin substrates may be essential for this process.

1.9 Bulk Endocytosis

A large number of model synapse systems have shown evidence for the use of bulk retrieval as a method to retrieve large amounts (greater than is sufficient for one vesicle) of SV membrane during endocytosis. Most clearly pictured in EM, the resultant endocytic structures are significantly larger than SVs, and seem to occur in response to elevated stimuli. Exocytic load scales in response to increases in stimulus strength. This greatly increases the amount of membrane at the presynaptic terminal, and in order to maintain both the integrity of the synapse and a functional pool of vesicles, large amounts of membrane must be recovered. Bulk endocytosis has been

proposed to function in response to this elevated stimulus, to effectively counteract the increase in membrane surface area by retrieving a large amount of synaptic vesicle membrane in one “bite”. Evidence for the bulk endocytosis of SV membrane has been observed in a number of different synapses.

1.9.1 Frog Neuromuscular Junction

The first evidence for endosomal intermediates in the SV cycle came from Heuser and Reese, in 1973 (Fig 1.7 **A**). Terminals of the frog NMJ were stimulated at 10 Hz for 15 minutes, which resulted in the depletion of the SV pool, and the appearance of large cisternae and coated vesicles. After a 30 minute rest period at 10 ºC, the cisternae disappeared, and the SV pool was observed to partially recover. Complete reversal of the observed changes was achieved with a 60 minute rest at room temperature (Heuser & Reese, 1973). Application of an electrical stimulus in the presence of 4-aminopyridine (4-AP**)** showed that within a couple of seconds after stimulation large vacuoles pinch off from the plasma membrane. A slower clathrin mediated form of endocytosis was also observed, however the invagination of the large vacuoles was notably not mediated by uncoated pits (Heuser & Reese, 1981). Treatment of these synapses with latrunculin A (which disrupts the actin cytoskeleton by binding to actin monomers), and wortmannin (an inhibitor of PI-3-kinase) hints at the molecular mechanisms which may be involved in this form of endocytosis. Treatment with both drugs disrupted the pattern of presynaptic β-actin staining, but not the appearance of vesicle clusters in resting cells, however they did inhibit FM1-43 uptake (driven by 30 Hz stimulation for 1 min) (Rizzoli & Betz, 2004). Interestingly EM pictures in stimulated treated cultures show no

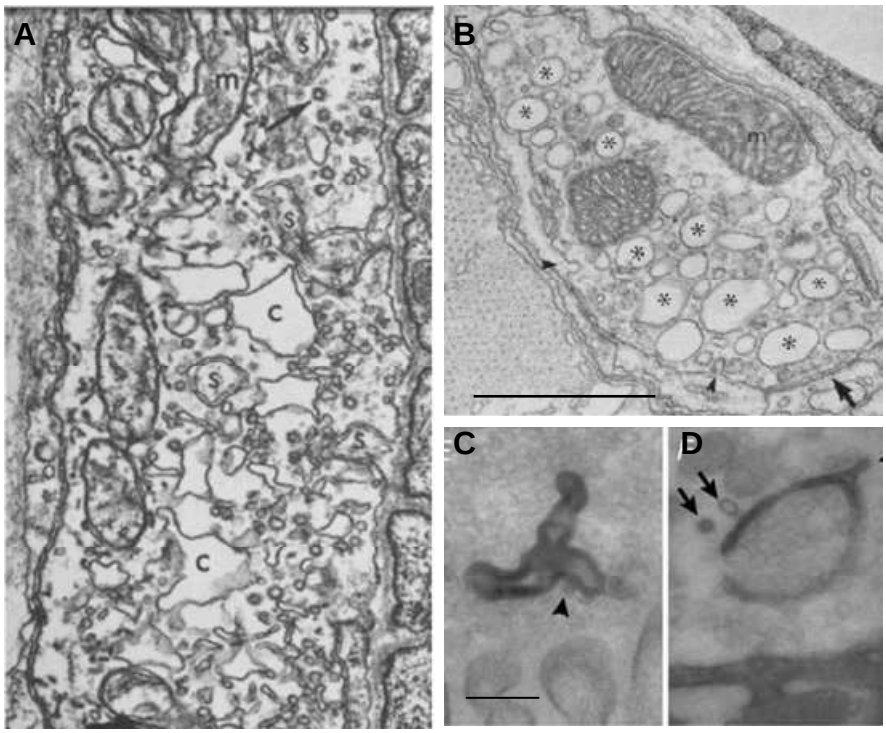

Figure 1.7 - Bulk endocytosis at neuromuscular junctions.

A, Frog NMJ after 15 minutes of stimulation at 10 Hz. Annotated in the terminal are cisternae (c), coated vesicles (arrow), mitochondria (m) and enlarged Schwann processes (s). Magnification x 30,000. **B,** *Shibire* NMJ after 8 minutes recovery from complete vesicle depletion at 29 ºC. Large cisternae are marked by asterisks, arrowhead indicates small pits, arrow indicates release site, m = mitochondria. Scale bar 1 µM. **C+D,** Snake NMJ, loaded with HRP during 90 stimuli. Arrowhead indicates possible budding vesicle, arrows indicate CCVs. Scale bar 200 nM. (Adapted from; **A**, Heuser and Reese, 1973, **B**, Koenig and Ikeda, 1989, **C+D**, Teng et al, 2007.)

cisternae compared to controls, indicating a possible role for PI-3-kinase and the actin cytoskeleton in bulk endocytosis at the frog NMJ.

1.9.2 *Drosophila* Neuromuscular Junction

The temperature sensitive *Drosophila shibire* mutant is an extremely useful tool for imaging of the synaptic vesicle cycle, as endocytosis can be reversibly blocked at 29ºC. The synapse of the *Drosophila* NMJ can be completely exhausted of SVs by stimulation at this temperature, and endocytosis can then be resumed at the permissive temperature, 19ºC. Under these conditions, gradually enlarging invaginations at the plasma membrane were observed, which pinched off to form large cisternae (Fig 1.7 **B**). Over a time frame of approximately 30 minutes SVs then began to appear, apparently at the expense of the cisternae (Koenig & Ikeda, 1989). This indicates that bulk endocytosis compensates for the increase in size at the pre-synaptic membrane caused by complete depletion of the SV pool, and also that vesicles are re-formed from these bulk endosomes.

Budding from these endosomal structures may be clathrin dependent, as clathrin heavy chain (chc) mutants of *Drosophila* allow massive internalisation of membrane in bulk endosomes, as determined by FM dye uptake and EM. However the membrane is not able to re-release, and because of this the synapses fail to maintain neurotransmission (Kasprowicz *et al.,* 2008). In agreement with this, perturbation of the clathrin light chain (clc) by photoinactivation does not impair vesicle fusion, but in response to stimulus membrane is retrieved into large endosomes, which are unable to generate functional vesicles (Heerssen *et al.*, 2008). Thus it would appear that in the *Drosophila* NMJ, the absence of functional clathrin

causes retrieval to be facilitated by bulk endosomes from which SVs are unable to bud.

1.9.3 Snake Motor Boutons

Bulk endocytosis has been termed "macro-endocytosis" in the snake NMJ, as originally the retrieval of large amounts of membrane was equated to macropinocytosis (Wilkinson & Teng, 2003). Bulk membrane retrieval was characterised over a range of stimulation frequencies in this system through use of a combination of fluorescent dyes and HRP EM (Fig 1.7, **C** & **D**). Endosomes were found to form rapidly at all stimulation frequencies (1-2s), and the endosomal structures dissipated rapidly into vesicles (~10s) (Teng *et al*, 2007). Interestingly, in these preparations there was no evidence for a stimulation dependency for employment of this macroendocytosis.

1.9.4 Rat Calyx of Held

Depolarization of the rat calyx of held with high K^+ resulted in the appearance of large HRP labelled endosome-like structures from which SVs appeared to form (Fig 1.8 **A**). These structures were observed after 3 minutes of stimulation, and the progression of the bulk retrieval process was referred to as very slow (de Lange *et al.*, 2003).

Due to the large size of this synapse, it is a good model for the study of endocytosis events using capacitance methods. In this same system, infrequent occurrence of downward capacitance shifts were recorded, peaking at less than 10

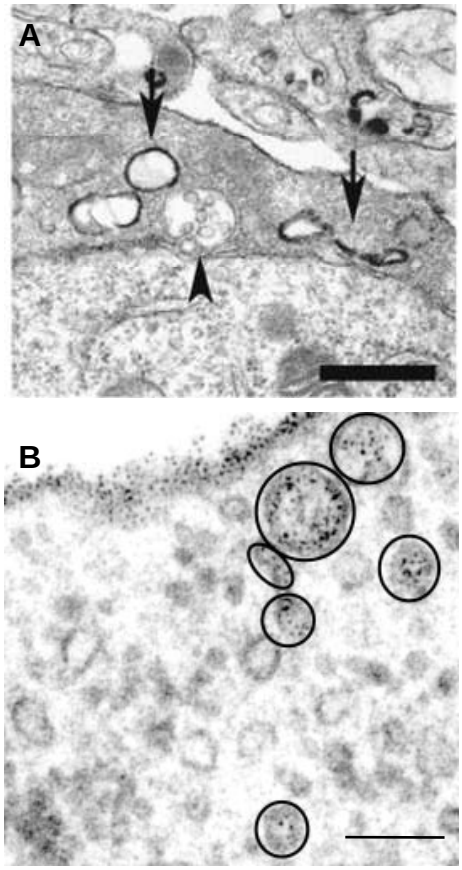

Figure 1.8 - Bulk endocytosis at large central synapses.

A, Endosomes at the rat calyx of held, labelled with HRP during 3 minutes of high K^+ stimulation. Arrowhead indicates a multivesicular body, arrows indicate endosomes (note the difference in appearance at the same synapse). Scale bar 1µM. **B,** Goldfish retinal bipolar cell labelled with cationic ferritin during 8 minutes of spontaneous activity. Ferritin labelled endosomes are encircled, scale bar 100 nM. (Adapted from; **A**, de Lange et al, 2003, **B**, Paillart et al, 2003.)

seconds after stimulation, with approximately 10 % of vesicles retrieved this way (Wu & Wu, 2007). These large downward shifts indicate rapid retrieval of a large chunk of membrane. Reducing or buffering intracellular Ca^{2+} with EGTA has been seen to inhibit rapid endocytosis at the calyx of held, indicating that Ca^{2+} concentration may play a role in the rapid retrieval of vesicles (Wu *et al.*, 2005). If, as is suggested by the capacitance measurements, bulk endocytosis is a rapid method of retrieval, then the action of Ca^{2+} concentration in facilitating this rapid retrieval may implicate Ca^{2+} concentration in a role in this form of endocytosis.

Capacitance measurements of both WT and dynamin 1 KO calyces of held show that with weak stimuli there is no impairment of endocytosis, however with stronger stimuli the "slow" phase of endocytosis is impaired (Lou *et al.*, 2008). As bulk endocytosis is seen in response to strong stimuli (for example high K^+, as shown by de Lange *et al.*, 2003), and the dynamin I KO shows impairment once the strength of stimulus is increase, dynamin I may be important for the bulk endocytosis pathway.

1.9.5 Goldfish Retinal Bipolar Cells

EM analysis of cationized ferritin labelling in goldfish retinal bipolar cells showed that retrieved membrane is endocytosed in large "bites" (endosomes of 60-200 nM in size), which then give rise to SVs that enter the RP (Paillart *et al.*, 2003). This occurred very rapidly, as stimulation was through application of 80mM KCl by pipette, typically for only 1 s, then samples were fixed 15 to 45 seconds afterward stimulation (Paillart *et al.*, 2003) (Fig 1.8 **B**). This supports the observations made in

previous systems, where retrieval of large amounts of membrane occurs in response to strong stimulation, and functional vesicles are re-formed from these endosomes.

The most comprehensive study of bulk endocytosis in the retinal bipolar cell utilised the retrieval of a 40kDa dextran. Dextran internalisation occurred predominantly during the initial stages of a prolonged stimulation, whereas in the later stages retrieval into single vesicles accounted for a larger fraction of the retrieved membrane. As was found in the frog NMJ, cytochalasin D and latrunculin B inhibited formation of vacuoles, and the formation of large compartments (Holt *et al.*, 2003), indicating that the formation of these endosomes is dependent on both PI-3-kinase and the actin cytoskeleton.

Total internal fluorescence microscopy (TIRF) and fluorescence recovery after photobleaching (FRAP) imaging showed that a 1 minute depolarisation, releasing 500-1000 vesicles, caused 80-90% of the subsequently recycled membrane to be taken up into cisternae that pinched off from the surface (Holt *et al.*, 2004). This, coupled with the observation of internalisation of large dextrans, indicates that vacuoles observed in the terminal of bipolar cells were formed by bulk retrieval of surface membrane rather than by the fusion of a number of small vesicles within the terminals. Also of interest in this system is the fact that some of these retrieved endosomes are capable of undergoing stimulated exocytosis. This phenomenon was observed when using evanescent field fluorescence microscopy, and although the occurrence of such exocytosis events was extremely rare, it is possible for endosomes to undergo stimulated exocytosis (Coggins *et al.*, 2007).

1.9.6 Cultured Hippocampal Neurons

Bulk endocytosis was originally observed in small central synapses in 1996. In a study of cultured hippocampal neurons, it was found that exposure to high K^+ stimulation resulted in the appearance of endosome-like vacuoles (Fig 1.9, **A**). Using serial sectioning, narrow necks could be visualised connecting the membranes of the endosomes and the plasmalemma, indicating that the vacuoles originate from deep invaginations, and are not pre-existing internal structures acting as processing intermediates for plasma-membrane derived endocytic vesicles (Takei *et al.*, 1996). CM budding takes place concurrently from both these endosomes and the plasma membrane.

1.9.7 Rat Cerebellar Granule Neurons

Retrieval of SV membrane by bulk endocytosis has also been documented in primary cultures of rat cerebellar granule neurons (CGNs), where stimulation with 50 mM KCl in the presence of HRP results in accumulation of HRP in both endosomal structures and single SVs (Fig 1.9 **B**) (Marxen *et al.*, 1999). Preincubation with roscovitine, an inhibitor of cdk5, significantly reduces the number of these endosomes formed, but does not affect the generation of single SVs, indicating that cdk5 may play a role in the bulk endocytosis of SV membrane following strong stimulation (Evans & Cousin, 2007). Interestingly roscovitine only blocks a second round of endocytosis. This is explained by the nature of cdk5 rephosphorylation, where it rephosphorylates at least three of the dephosphins important for SVE only after stimulation. This block is only seen following strong stimulation of CGN cultures (Evans & Cousin, 2007).

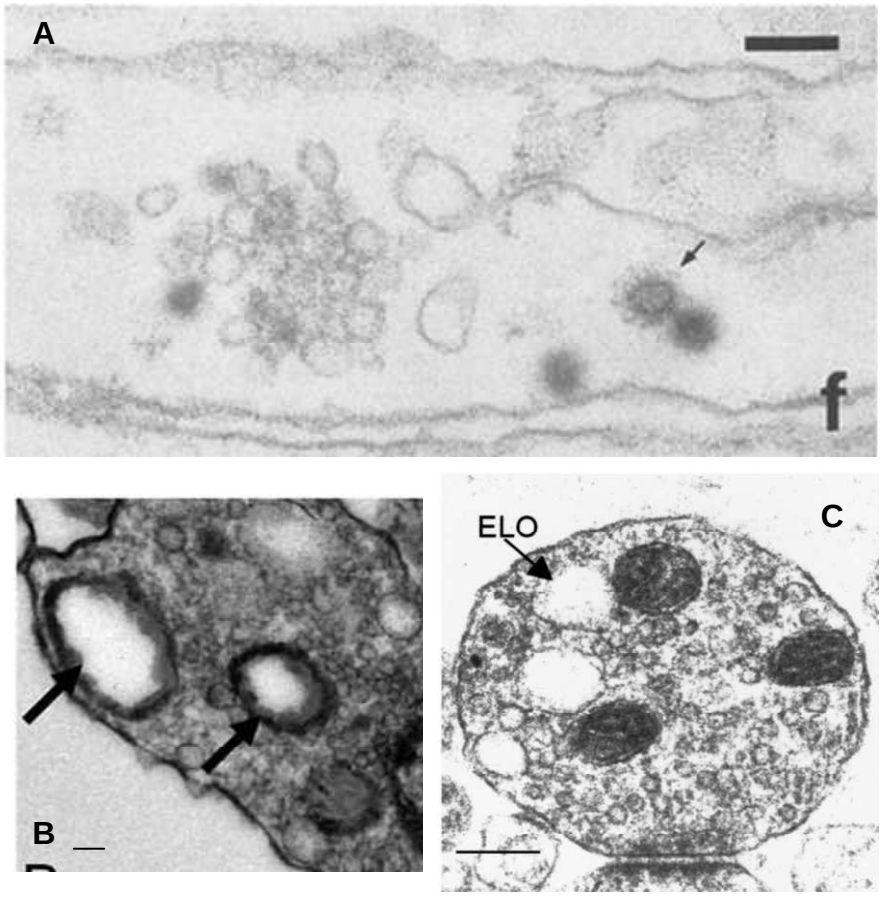

Figure 1.9 - Bulk endocytosis at small central synapses.

A, Hippocampal neuron labelled with HRP-Syt_{lum}-Ab during 10 minutes of stimulation in depolarizing medium. Arrow indicates vesicle cluster, or buds. Scale bar 100 nM.

B, Cerebellar granule neurons incubated with HRP during 1 minute of 50 mM KCl stimulation. Arrows indicate HRP labelled endosomes, scale bar 100nM. **C,** Synaptosomal preparation after 15 seconds depolarisation. ELO = endosome like organelle, scale bar 200 nM. (Adapted from; **A,** Takei et al, 1996, **B**, Evans and Cousin, 2007, **C**, Leenders et al, 2002.)

1.9.8 Rat Synaptosomes

Stimulation of synaptosomes with 50 mM KCl for either 15 s or 3 minutes led to an accumulation of HRP labelled endosomes as detected by EM (Fig 1.9 **C**). These endosomes disappeared after repolarisation, whilst the number of SVs was restored to control levels, indicating that the re-formation of SVs may be at the expense of the endosomes (Takei *et al.*, 1996, Leenders *et al.*, 2002).

1.10 Kinetics of Endocytosis

Membrane capacitance measurements of goldfish retinal bipolar cells indicate that following long depolarizations 2 rates of endocytosis occur; a fast rate with a constant of 0.8 vesicles s^{-1} and a slow one of 0.1 vesicles s^{-1} (Neves & Lagnado, 1999). Ca^{2+} influx may be the trigger for this fast endocytosis, as BAPTA or EGTA incubation results in membrane retrieval with slower kinetics (Neves *et al.*, 2001). The slow mode of endocytosis (with a time constant of approximately 15 seconds) is clathrin dependent, as it can be blocked either by overexpression of the C-terminal fragment of AP180, or by RNAi knockdown of clathrin (Granseth *et al.*, 2006).

1.11 Vesicle Pools

Two SV pools exist at the synapse; the RRP and the reserve pool (RP). Characterisation of SV pools at the frog NMJ shows that at rest, 20 % of the vesicles are in the RRP, which is depleted by strong stimulation (of 30 Hz) in about 10 s. Following depletion, the RRP refills in approximately one minute, but interestingly it refills with recycling vesicles and not by recruitment from the RP. At lower

frequency stimulation (2-5 Hz), vesicle supply is maintained entirely by RRP recycling (Richards *et al.*, 2003).

Photoconversion of FM dyes shows preferential staining of cisternae by FM1-43 compared to FM2-10. This was interpreted at the time to represent retention of hydrophobic FM1-43 in slowly retrieving structures in contrast to the more hydrophilic FM2-10. Depletion of the RP at 30 Hz took approximately 40 seconds, and recycling to this pool was mediated by vesicles which budded from cisternae and membrane infoldings (Richards *et al.*, 2003). Recycling of this much slower pathway which is mediated by infoldings and cisternae delivered vesicles to the RP with a half time of about 8 minutes (Richards *et al.*, 2000). Thus bulk endocytosis replenishes the RP.

Further evidence for replenishment of the RP by bulk endocytosis came from treatment of these synapses with latrunculin A (which disrupts the actin cytoskeleton by binding to actin monomers), and wortmannin (an inhibitor of PI-3-kinase). Both drugs affected traffic to the RP (80%), whilst the RRP (remaining 20 %) was apparently unaffected (Richards *et al.*, 2004).

The vesicle pools of the frog NMJ were further characterised by Rizzoli and Betz, who in agreement with the previous work found that the RRP comprises approximately 12 – 17 % of the total vesicle pool. They further characterized the structure of these pools, and found by analysis of photoconverted FM1-43 that vesicles endocytosed at sites distinct from active zone, and that the labelled vesicles were distributed seemingly randomly throughout the nerve terminal (Rizzoli & Betz, 2004; Rizzoli & Betz, 2005). The RRP and RP are not spatially distinct within the

synapse, and thus cannot be classified based on compartmentalisation or distance from active zone, as has previously been attempted.

This supports a model in the frog NMJ whereby during mild stimulation the RRP can cycle. However stronger stimulation results in the recruitment of bulk endocytosis of large amounts of SV membrane, from which vesicles can bud to slowly fill the RP.

Two distinct pools of vesicles can also be distinguished in *shibire* mutants. By completely depleting the SVs of *shibire* nerve terminals at 34 ºC and labelling the reforming vesicles at 22 ºC with FM1-43, then comparing the labelling of the depletion-reformation loading to high K^+ stimulation loading, separate vesicle pools could be dissected. The first pool cycled and was seen at the periphery of the bouton, whilst the RP existed at the centre of the bouton. Treatment with cytochalasin D, an inhibitor of actin polymerisation, eliminated the RP, resulting in reduced transmission during strong stimulation (Kuromi & Kidokoro, 1998). As cytochalasin D has also been shown to inhibit bulk endosome formation, this is a further indication that bulk endocytosis may serve to re-populate the RP of vesicles.

Finally, studies in primary neurons have shown that inhibition of bulk endocytosis via a block of cdk5 activity arrests a late phase of subsequent FM1-43 unloading thought to be part of the RP (Evans & Cousin, 2007).

1.12 The relevance of bulk endocytosis.

All of the above examples establish that bulk endocytosis is an important mechanism in the recycling of SVs, as it has been observed in various model synapses from neuromuscular junctions through to large and small central synapses,

and is likely to facilitate vesicle replenishment of the RP. However there remain questions as to the relevance of, and reasons for, this particular form of membrane recovery.

Is this method of endocytosis stimulus dependent? It would appear that a relatively strong stimulus is need to recruit this method of endocytosis in conjunction with CME at the synapse. Stimulation with KCl induces the appearance of endosomes in many of the above systems; however this is not a relevant form of physiological stimulation. Dissection of the strength of physiological stimulus at which bulk retrieval is recruited in addition to CME would aid the characterisation and understanding of this endocytosis pathway.

Could the recruitment of this method of endocytosis differ according to developmental stages? At early developmental stages, bulk endocytosis has been found to be the primary endocytic pathway for rapid retrieval of growth cone plasma membrane, whilst later stages downregulate basal bulk endocytosis. In growth cones the pathway is mediated by PI-3-kinase, the small GTPase Rac1 and the pinocytic chaperone Pincher (Bonanomi *et al.*, 2008).

What are the key molecular players for bulk endocytosis? Not much is known about the signalling which results in retrieval of membrane by bulk invaginations. As disruption of the actin cytoskeleton by treatment with cytochalasin D (Kuromi & Kidokoro, 1998) and latrunculin A (Holt *et al.*, 2003; Richards *et al.*, 2004) affects the bulk endocytosis pathway, the actin cytoskeleton is likely important for this form of retrieval. Bulk endocytosis may also be dependent on PI-3-kinase activity, as inhibition of this kinase also inhibits bulk endocytosis (Holt *et al.*, 2003, Richards *et al.*, 2004). Budding of SVs from these endosomes seems to be clathrin heavy chain

dependent, as *Drosophila* chc mutants retrieve membrane in bulk chunks but are then subsequently unable to maintain neurotransmission (Kasprowicz *et al.*, 2008). Recycling evoked by intense stimulation can be inhibited by the presynaptic microinjection of syndapin antibodies. As strong stimulation evokes retrieval by bulk endocytosis, syndapin may possibly play a role in the progression of bulk endocytosis (Andersson *et al.*, 2008). AP3 (AP180) has been implicated in a role in endosomal budding in neuroendocrine PC12 cells (Faúndez *et al.*, 1998), which may have relevance for the budding of SVs from endosomes in neuronal synapses. The *Drosophila* EFR3 integral membrane lipase temperature sensitive mutant rolling blackout, which displays a synergistic interaction with syntaxin-1a, is necessary for bulk endocytosis in both garland cells and neuronal cells (Vijayakrishnan *et al.*, 2008). Thus a number of molecules are postulated to be important for retrieval of SV membrane by bulk endocytosis, however no clear signal pathway has yet been identified.

What is the rate of progression of this process? There is controversy over the time constant of bulk retrieval of SV membrane. Bulk endosomal structures were observed after 3 minutes of stimulation in the rat calyx of held, and the progression of the bulk retrieval process was equated to “slow endocytosis” (de Lange *et al.*, 2003). Conversely however, endosomes were found to form rapidly (1-2s), and also to dissipate rapidly into vesicles (approximately 10s) at the snake motor bouton (Teng *et al.*, 2007). Controversy exists even between studies of the same model synapse. Applications of an electrical stimulation at the frog NMJ (in the presence of 4-AP) resulted in the appearance of cisternae within a couple of seconds (Heuser & Reese, 1981), however at the same terminal a time constant with a half life of 8

minutes was estimated for the recycling by infoldings and cisternae of vesicles to the RP (Richards *et al.*, 2000).

Thus the strength of stimulation which triggers bulk endocytosis, the rate at which this process progresses and the key players involved in this process are all in need of further characterisation and clarification.

1.13 Evidence of a role for Synaptic Vesicle Recycling in Epilepsy

In cells in an epileptic state excessive neurotransmitter is released which facilitates the spread of the seizure and also causes neuronal damage. Several lines of evidence exist to implicate a link between epilepsy and defects in the SV cycle.

1.13.1 Transgenic Animals and Gene Linkage

Transgenic animals deficient in proteins involved in the synaptic vesicle cycle have impairments in synaptic vesicle recycling, and a number of these SVE protein deficient models exhibit increased propensity for seizures. For example synapsin I deficient mice show marked impairment in the organisation of vesicles at the presynaptic terminal, and enhancement of stimulation evoked epileptic seizures (Li *et al.*, 1995). Generation of amphyphysin I KO mice produces a model with rare irreversible seizures, and defects in multiple stages of the vesicle cycle (Di Paolo *et al.*, 2002). SNAP-25b KO mice (which retain the SNAP25-a isoform) display learning defects, and develop seizures (Johansson *et al.*, 2008). VGLUT3 deficient mice, which are deaf, exhibit primary, generalised epilepsy but do not manifest any other serious motor impairments (Seal *et al.*, 2008)

Defects in SV proteins have also been implicated by studies of a family with a genetic susceptibility for epilepsy. A nonsense mutation in the gene for synapsin I was determined by linkage and microsatellite analysis as the likely cause of the epilepsy phenotype in a four generation family studied (Garcia *et al.*, 2004).

1.13.2 Synaptic Vesicle Protein Expression Levels in Epilepsy

It is also known that seizures upregulate the expression of synaptotagmin IV (Babity *et al.*, 1997), a protein which has been proposed to control the transition between "kiss-and-run" endocytosis and full fusion (Wang *et al.*, 2003). Both clathrin and amphyphisin I expression levels are increased in the hippocampus of phenytoin-resistant kindled rats compared to non-phenytoin resistant kindled rats (Zeng *et al.*, 2008), suggesting that SV trafficking may be altered/upregulated in this form of epilepsy which is resistant to intervention with the antiepileptic drug (AED) phenytoin.

1.13.3 Antiepileptogenic Drugs and Synaptic Vesicle Proteins

A link between epilepsy and proteins connected to SVs is also evident in the current treatment available for epilepsy. A mechanism of action for AEDs at the synaptic vesicle level is suggested by two different lines of evidence. The AED levetiracetam binds to the SV protein SV2A, which suggests that levetiracetam somehow acts via modulation of SV2A (Lynch *et al.*, 2004). AEDs also alter the glutamate release probability of excitatory synapses (Prakriya & Mennerick, 2000).

The mechanisms which lead to the changes in neuronal plasticity of epileptic cells are undefined. As increased proliferation of neurotransmitter release is characteristic of epileptogenic cells, and bulk retrieval as a mechanism for SV recycling is induced by strong stimulation, then there may well be a correlation between epileptogentic cells and the employment of bulk endocytosis. Investigation into the method of endocytosis employed by cells in this excitable state could potentially identify novel proteins as targets for treatment in the management of epilepsy.

1.14 Hypothesis of the Project

That the mechanism of synaptic vesicle recycling in epileptic neurons is different from that of normal neurons.

1.15 Project Aims

To establish a cell culture model for epilepsy.

To establish an assay for bulk endocytosis.

To characterise the bulk endocytosis pathway.

To identify molecular players involved in bulk endocytosis.

2. MATERIALS AND METHODS

2.1 MATERIALS

10 kDa tetramethylrhodamine dextran, 40 kDa tetramethylrhodamine dextran, D-PBS, EBSS, MEM Earles w/o L-Glut, and penicillin/streptomycin were from Invitrogen (Paisley, UK).

BSA, $CaCl_2$, cytosine arabinosidase, diaminobenzidine, DNase, glucose, glycine, HRP, KCl, KH_2PO_4, L-glutamine, $MgCl_2.6H_2O$, $MgSO_4.7H_2O$, Na_2SO_4, NaCl, $NaHCO_3$, Poly-d-lysine, SBTI, serum replacement medium 2, silicone grease, TES, trypsin and uranyl acetate were purchased from Sigma-Aldrich (Poole, UK).

Cyclosporin A was purchased from CN Biosciences (Nottingham, UK)

Glutaraldehyde and osmium tetroxide were from Agar Scientific (Essex, UK).

FM1-43, FM2-10 and Fura-2AM were from Cambridge Bioscience (Cambridge, UK)

CT99021 and AR-AO14418 were gifts from Dr. Calum Sutherland (University of Dundee, Dundee).

Dynamin peptides were synthesized by Genemed Synthesis (San Antonio, Texas, USA).

Dynasore and Dyngo4-a were gifts from Dr. A McClusky (University of Newcastle, Australia) and Dr. Phil Robinson (The University of Sydney, Australia).

Levetiracetam, UCB22060 and UCB106758-1 were gifts from UCB.

2.2 METHODS

2.2.1 CELL CULTURE

Cerebellar granule neuron (CGN) cultures were prepared by dissociation of cerebella from 6-8 day old Sprague-Dawley rat pups. Cerebella were dissected from pups immediately after a schedule 1 procedure. Cerebella were cut at 375 μm intervals by passing twice through a McIlwain tissue chopper. The cells were then dispersed by incubation at 37 ºC for approximately 10 minutes in buffer (153 mM Na^+, 4 mM K^+, 1.5 mM Mg^{2+}, 139 mM Cl^-, 10 mM PO_4^{2-}, 1.5 mM SO_4^{2-}, 14 mM glucose, and 50 μM BSA) supplemented with 0.25 mg/ml trypsin. Trypsinisation was terminated by the addition of buffer containing 8 μg/ml soybean trypsin inhibitor and 8 U/ml DNase. Cells were pelleted by centrifugation at 1000 g for 1 minute. The supernatant was discarded and the cells were triturated in 1.5 mls buffer (containing 3 mM $MgSO_4$, 50 μg/ml soybean trypsin inhibitor and 50 U/ml DNAase) using a series of flame polished pasteur pipette with progressively narrowed ends to generate a single cell suspension. After this thorough trituration the cells were layered onto 4 % BSA Earle's Balanced Salt Solution and pelleted by centrifugation at 1500 g for 5 minutes. The resulting pellet was then resuspended in 2 mls of culture medium. The dissociated cells were plated onto round coverslips, pre-treated with poly-d-lysine, at a density of 250,000 per cm^2. Cells were left to settle for 30-60 minutes before addition of 2 mls culture medium. Cell culture medium consisted of Eagle's modified minimum essential medium containing 10 % foetal calf serum, 33 mM glucose, 2 mM glutamine, 25 mM KCl, 100 U/ml penicillin and 100 μg/ml streptomycin. After twenty-four hours 10 μM cytosine arabinosidase was added to the media. Cultures

were maintained in a 5 % CO_2 37 ºC humidified incubator for up to 10 days, and were typically imaged at days 8 to 10.

2.2.1.1 SR Cell Culture

The preparation of the CGNs was performed identically until just after the point of plating the cells. After the cells were plated, cell culture medium was replaced by a serum replacement medium (SR), which contained Eagle's modified minimum essential medium with 1x SR medium 2, and 2 mM glutamine. The cells were cultured in this medium in a 5 % CO_2 37 ºC humidified incubator for up to 10 days, and were typically imaged at days 8 to 10.

2.2.2 FM Dye Imaging (S1 S2 Assay)

Cells were removed from culture medium and repolarized in incubation buffer for 10 minutes. Cultures were then mounted in a Warner imaging chamber and attached to a perfusion system through which incubation medium, high potassium medium, FM dye solution, or drug containing medium could be perfused.

Cells were loaded with FM dye by stimulating synaptic vesicle turnover either via application of high (50 mM) KCl or trains of action potentials (APs). FM dyes insert into the invaginating synaptic vesicle (SV) membrane as it is retrieved from the plasma membrane, thereby labelling the retrieved vesicles with fluorescent dye. Excess dye solution was washed from the cultures with incubation medium immediately after termination of stimulation (Fig 2.1 **A a**). Cells were left to rest for 10 minutes.

After 10 minutes of rest the dye accumulated during the load was unloaded from the cultures. Dye was unloaded through stimulation of SV exocytosis by two sequential stimuli of either action potentials or 30 seconds of 50 mM KCl at 20 and 120 seconds (Fig 2.1 **A b**). Cells were then left to rest for 20 minutes.

After a 20 minute rest the loading and unloading of cells is repeated as per S1 (Fig 2.1 **A c**&**d**), with variations either in the pre S2 incubation period or the duration of the S2 loading. All deviations from the normal S1/S2 assay are described within the results of the experiments. Dye unloading was visualised at excitation of 480 nm and greater then 510 nm emission using a Nikon epifluorescence microscope and x 20 air objective. Fluorescent images were visualised using a Hamamatsu (Hamamatsu City, Japan) Orca-ER CCD digital camera and offline imaging software (Simple PCI, Compix Imaging Systems, USA).

2.2.2.1 S1 S2 Assay Analysis

Cloned regions of interest were placed around putative nerve terminals to measure the fluorescence loss resulting from stimulation of the cultures (Fig 2.1 **B**). In this way the fluorescence loss for S1 and S2 for each independent nerve terminal was calculated. In the event of the field of view moving slightly between the imaging of S1 and S2 unloads, the ROIs were moved correspondingly, to ensure they were still reporting the same nerve terminal. Puncta which did not respond to stimulation either during S1 or S2 were discounted from the analysis, so that only nerve terminals that responded during both S1 and S2 were included in the analysis.

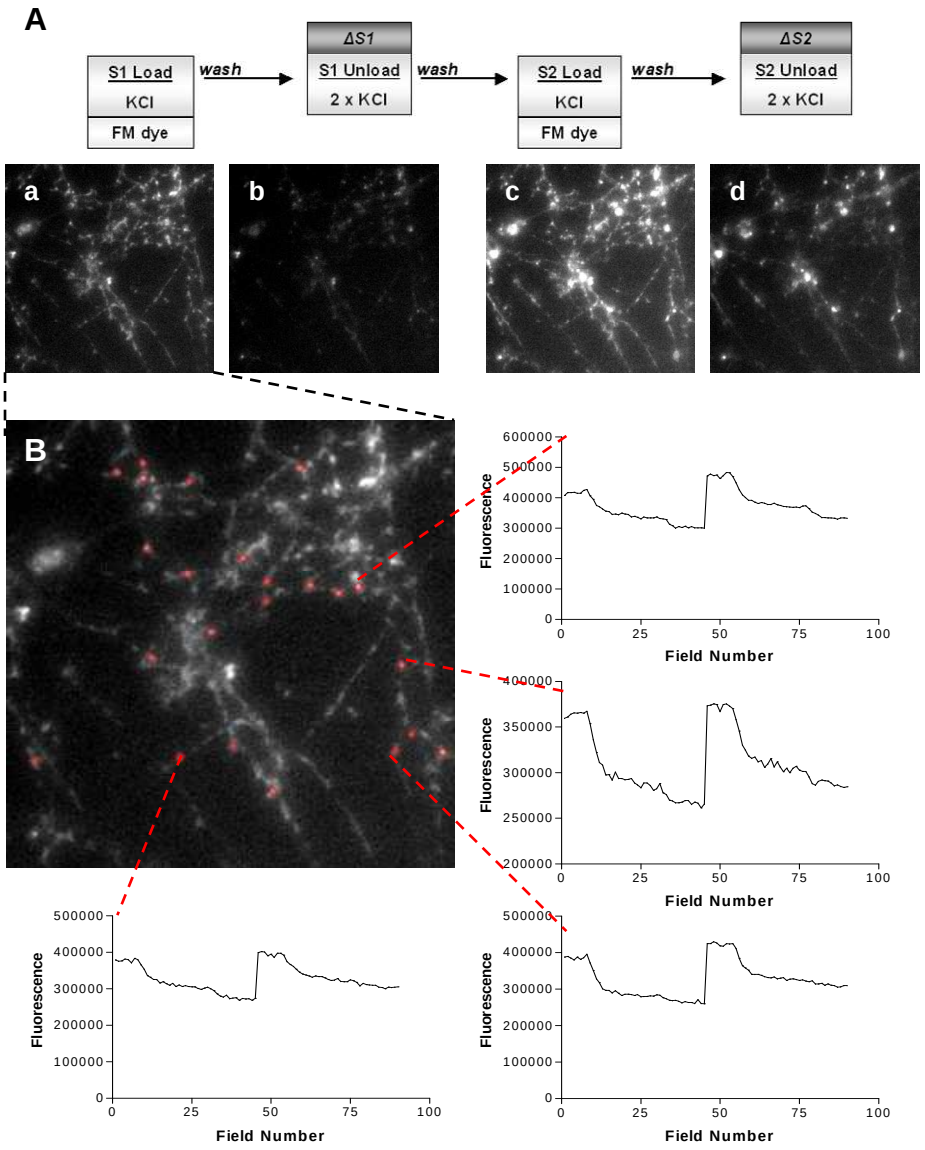

Figure 2.1 - Example of the S1 S2 FM dye assay. **A,** Cultures are loaded and unloaded with FM dye by KCl stimulation; representative images show the cultures following the S1 load (**a**), S1 unload (**b**), S2 load (**c**) and S2 unload (**d**). **B,** ROIs are placed at putative nerve terminals to determine the fluorescence loss as a result of KCl stimulation. Representative traces are shown from several ROIs, typically up to 90 ROIs are analysed per experiment.

Generally a total of 90 ROIs were taken from each experiment, except for stimulation of 200 APs where the number of responding nerve terminals was typically lower.

With 90 traces corresponding to the fluorescence loss for S1 (ΔS1) and S2 (ΔS2) available, the traces must then be normalised relative to each other in order to quantify the ratio of loss between S1 and S2. Traces were normalised at the time point directly before fluorescence loss began. To account for the inherent decay of fluorescence due to light exposure, a line of best fit was applied to each fluorescence drop (corresponding to each stimulation pulse) to subtract the inherent decay (Fig 2.2 **A**). This decay was tailored within each separate analysis, as the decay varied across and within experiments.

Once the traces have been normalised and corrected for fluorescent decay, the ΔS2/ΔS1 ratio can be calculated for each individual nerve terminal (Fig 2.2 **B**). The ΔS2/ΔS1 ratio can then be pooled across each experiment for each of the various conditions, and an average obtained for each condition.

2.2.2.2 SR FM IMAGING

Cells were removed from culture medium and repolarized in incubation buffer for 10 minutes. Cultures were then mounted in a Warner imaging chamber and attached to a perfusion system. Cells were then labelled with FM dye in an identical manner to the S1 loading protocol previously described. 50 mM KCl was used as the loading stimulus for the S1 load and unload. Following the 20 minute rest period after S1 unload, the cells were then loaded for S2. The cells were loaded with 50 mM

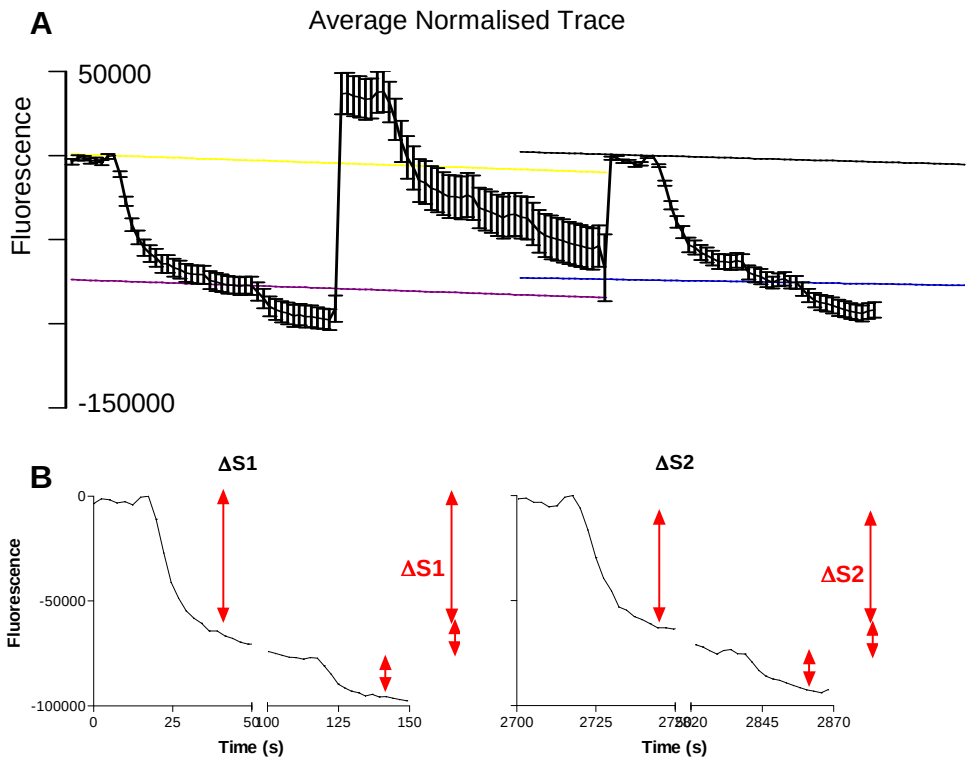

Figure 2.2 - Analysis of the drop in fluorescence at S1 and S2 for the FM dye assay. **A,** Fluorescence drop of all traces are normalised to 0 at the time point preceding the fluorescence drops for both S1 and S2 separately. The inherent decay caused by bleaching of the fluorescent dye is accounted for by fitting a trace to each of the slopes just before KCl stimulation (coloured lines), and subtracting the decay trace. **B,** The fluorescence drop for S1 and S2 is calculated by taking the average normalised corrected traces and averaging the drop across all ROIs for each experiment.

KCl for 2 minutes, left for 10 minutes and then unloaded by perfusion with the $-Mg^{2+}$ buffer. This was done to look at the effect of inducing excitability on the unloading of FM dye from the cultures. Alternatively the cells were loaded for S2 by loading the FM dye in $-Mg^{2+}$ buffer, and then unloaded with 50 mM KCl.

Analysis was performed in an identical manner to the usual S1 S2 FM dye assay analysis.

2.2.3 FURA 2-AM IMAGING

Cells were incubated in a 1 μM solution of the Ca^{2+} sensitive dye Fura 2-AM (an acetoxymethyl ester derivative of Fura 2) for 30 minutes at room temperature. Dye loading and initial subsequent perfusion was performed in basic buffer (170 mM NaCl, 3.5 mM KCl, 0.4 mM KH_2PO_4, 20 mM Tes, 5 mM $NaHCO_3$, 5 mM glucose, 1.2 mM Na_2SO_4, 1.2 mM $MgCl_2$, 1.3 mM $CaCl_2$, pH 7.4). After 10 seconds of perfusion with regular basic medium, perfusion was changed to a minus $MgCl_2$ medium, containing 0.01 mM glycine. Alternate images of 340 and 380 nm excitation were captured every 0.8 s at emission of greater than 475 nm.

2.2.4. DEXTRAN IMAGING

Cells were removed from culture medium and repolarized in incubation buffer for 10 minutes before imaging. A number of different loading conditions were used to observe the uptake of 40 kDa tetramethylrhodamine-dextran.

A time course of dextran loading was conducted by applying 50 μM 40 kDa tetramethylrhodamine-dextran to the cells in the presence of 50 mM KCl for either

two minutes, 60 seconds, 30 seconds or 10 seconds only. The cells were then extensively washed by perfusion of incubation buffer.

Post stimulation uptake of dextran was investigated by applying 50 μM dextran in incubation buffer to the cells for 2 minutes immediately following a stimulation with 50 mM KCl for either 2 minutes, 60 seconds, 30 seconds or 10 seconds. Cells were washed extensively by perfusion with incubation buffer following termination of labelling

Dextran labelling during trains of action potentials was observed by application of dextran in incubation buffer for the duration of a stimulation of 800 APs (80 Hz for 10 seconds), 400 APs (40 Hz for 10 seconds) or 200 APs (10 Hz for 20 seconds). The dextran solution was washed from the cultures immediately following termination of stimulation.

Extent of dextran labelling of cultures post physiological stimulation was identified through application of dextran to the cells immediately following termination of the train of APs. Dextran in incubation buffer solution was extensively washed from the cells following 2 minutes of immediately post-stimulation incubation.

Dextran loaded cells were imaged immediately after termination of perfusion. For all dextran experiments the cells were excited at 550 nm, with a gain of 6.5 and exposure of 1.55 s. All dextran images were captured at emission greater than 575 nm using a Nikon epifluorescence microscope and x 20 air objective. Fluorescent images were visualised using a Hamamatsu (Hamamatsu City, Japan) Orca-ER CCD digital camera and offline imaging software (Simple PCI, Compix Imaging Systems, USA).

Controls to quantify the extent of background fluorescence were performed by mirroring the experimental procedure for each loading condition but without the use of dextran.

Extent of dextran loading was quantified by post hoc analysis. Controls were subjected to an identical post-hoc analysis as the experiments which incorporated dextran. This gave a measure of the extent of background fluorescence generated by the cells at the excitation and emission spectra used for the experimental procedures.

All experimental conditions were repeated with a 10 kDa tetramethylrhodamine-dextran exactly as described for the 40 kDa dextran.

2.2.4.1 Co-localisation of Dextran with FM1-43

Cells were removed from culture medium and repolarized in incubation buffer for 10 minutes, before being loaded with dextran during 2 minutes of 50 mM KCl stimulation. Cells were imaged by excitation at 550 nm and imaged at emission of greater than 575 nm with a x 20 air objective. Cells were left to rest for 10 minutes, and then loaded with FM1-43 during 2 minutes of KCl stimulation. To determine the localisation of the FM dye the same field was imaged by excitation of 480 nm, with emission of greater then 510 nm captured. Co-localisation was determined in photoshop, by overlaying layers from the dextran and FM captured images. Extent of co-localisation was analysed by determining the number of dextran labelled ROIs in a set area, and the percentage of those dextran ROIs which corresponded to a FM labelled synapse was calculated and averaged across 3 fields.

2.2.5 Dextran Analysis

2.2.5.1 Quantification of Fluorescence

Initially quantification of the amount of fluorescence per labelled bouton was determined in an attempt to observe any differences between the various loading conditions. This was done by cloning a region of interest and manually affixing this ROI to all labelled boutons per field. The fluorescent intensity per bouton was measured, and averaged per coverslip for each loading condition. The average fluorescent intensity per bouton per coverslip was averaged across all coverslips for all conditions to calculate the average fluorescence for each loading condition.

2.2.5.2 Quantification of Extent of Dextran Loading

Dextran loading was ultimately determined as the number of labelled puncta observed in a defined region of the captured field, rather than the quantification of the amount of fluorescence per puncta. For each captured field, a 130 μm x 130 μm square field of view was chosen. A thresholding limit was applied to this selected field, to discount all fluorescence emanating from structures which were too large to be considered individual nerve terminals (diameter greater than 2 μm). Once the thresholding limit had been applied, all structures of between 7 and 50 pixels were selected as representative of individual nerve terminals labelled with dextran dye (Fig 2.3). The average fluorescence intensity of individual puncta was measured, but found not to differ between stimulation conditions. The number of labelled puncta

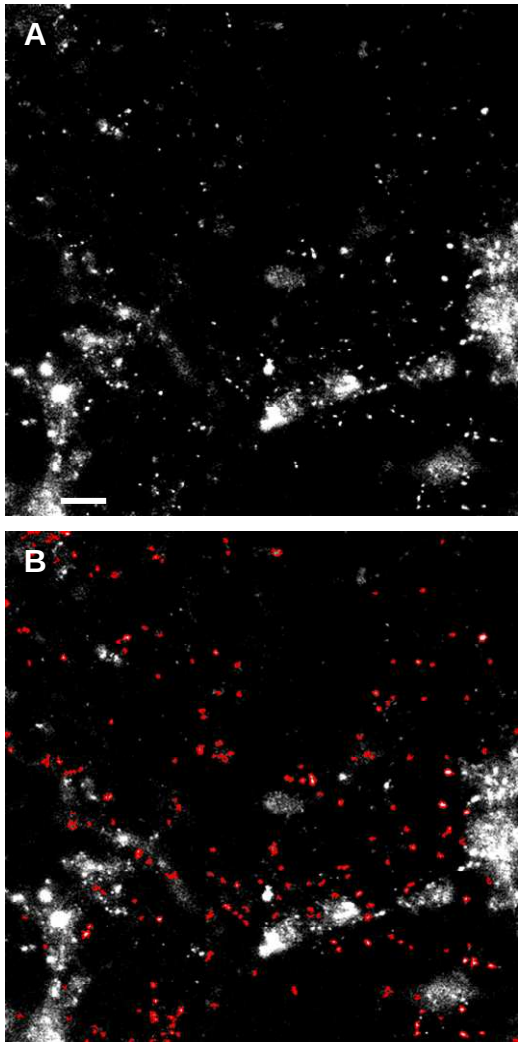

Figure 2.3 - Analysis of dextran loading. **A,** Representative image of CGNs loaded with 40 kDa dextran during a 2 minute 50 mM KCl stimulation. **B,** Example of analysis ROIs of between 7 and 50 pixels generated following fluorescence thresholding of the image. Scale bar 80 µM

per selected field was used as a measure of the extent of detran labelling for each of the stimulation conditions. At least 3 independent experiments were imaged for each stimulation condition, with an average of 10 fields recorded and analysed per coverslip. The number of labelled puncta for each condition was averaged across all fields for each experimental condition.

2.2.6 Electron Microscopy

Cell cultures for electron microscopy were plated at twice the normal culture density. Cells were removed from culture medium and repolarized in incubation buffer for 10 minutes. Cells were then incubated with horse radish peroxide (HRP, 10 mg/ml) either during or for 5 minutes immediately after stimulation. Stimulation was either via application of 50 mM KCl or trains of APs (800, 400 or 200 APs at 80, 40 and 10 Hz respectively).

After washing away the HRP solution, the cells were then fixed in a 2 % solution of glutaraldehyde in PBS at 37 ºC for 30 minutes. Cells were then washed twice with 100 mM Tris buffer (pH 7.4). After washing the cells were incubated for 15 minutes in Tris buffer containing 0.1 % diaminobenzidine (DAB) in the presence of 0.2 % H_2O_2. Once the colour had developed cells were again washed twice with 100 mM Tris. Cells were then incubated in a 1 % osmium tetroxide in H_2O solution for 30 minutes at room temperature. After washing the cells twice with distilled water, a 2% aqueous uranyl acetate solution was used to stain the cells. After 15 minutes of staining, the cells were again rinsed in distilled water, and sent to Dundee for processing.

3. Development of an Assay for Bulk Endocytosis

3.1 INTRODUCTION

To study the effects of epileptogenesis on synaptic vesicle (SV) turnover necessitates the development of tailored assay systems.

One method of studying epilepsy in vitro would be to establish a cell culture model system of epileptogenic neurons, which would allow the use of imaging assays to determine the effect (if any) on SV turnover. As the effects of epileptogenesis are characterised by the proliferation of excessive neurotransmitter release, it is possible that this excessive release occurs through modification of the SV cycle. In order to investigate any alterations to the SV cycle, it is necessary to use assay systems that can differentiate between different types of endocytosis.

3.1.2 CELL CULTURE MODEL OF EPILEPTOGENIC CELLS

In order to study alterations to the SV cycle in epileptogenic neurons, a reliable culture system of excitable cells is necessary. Neuronal culture models of spontaneous synaptic activity due to endogenous NMDA receptor activation are well established in hippocampal cell culture systems (Forsythe & Westbook, 1988; Abele *et al*., 1990; McLeod *et al*., 1998; Shanley *et al*., 2002). This effect is induced by the removal of Mg^{2+} from the perfusion medium, which has been supplemented with the NMDA receptor co-agonist glycine. The removal of Mg^{2+} from the perfusion medium removes the block from Mg^{2+} gated synaptic NMDA receptors (Abele *et al*., 1990), whilst the addition of glycine facilitates an allosteric activation of the NMDA receptor (Johnson & Ascher, 1987). This results in fluctuations in intracellular calcium levels, detectable by Ca^{2+} imaging. The resulting rapid spontaneous firing observed in these neuronal cultures mimics that which is seen in epileptogenic cells.

Whilst a number of groups have reported in hippocampal cultures that the spikes were synchronised for all the neurons in an imaged field (McLeod *et al*., 1998), it has been noted in cerebellar granule neurons (CGNs) that the first few Ca^{2+} spikes are not well synchronised, and in fact do not become so until after a few spikes (Lawrie *et al*., 1993).

In order for this model system to be a reliable tool for investigating the effects of epilepsy on SV turnover, it is necessary to know that these oscillations are due to synaptic activity. Intracellular Ca^{2+} concentration fluctuations have been blocked by tetanus toxin and the NMDA receptor antagonist APV (Lawrie *et al*.; 1993; Abele *et al*., 1990), showing that these effects are definitely synaptically mediated. It has also been observed that these aberrant patterns of glutamatergic activity are highly neurotoxic, with 30% cell death observed in cultures 24 hours after $-Mg^{2+}$ (glycine supplemented) treatment (Abele *et al*., 1990). This fits with the model of excitotoxicity caused by excess endogenous glutamate in status epilepticus. The recurrent discharges from these cells are treatable with anticonvulsant drugs (Sombati & Delorenzo, 1995), as are used to treat epilepsy.

This low Mg^{2+} induced model of spontaneous recurrent epileptiform discharges (SREDs) has previously been used to study alterations in $GABA_A$ receptor endocytosis (Blair *et al*., 2004), and calcium/calmodulin-dependent protein kinase II (CaMK-II) activity levels (Carter *et al*., 2006) in epileptiform activity.

The synaptically mediated release of excess glutamate in these excitable cells, which is sensitive to treatment with anticonvulsant drugs, makes them a good culture model system in which to study the synaptic effects of epilepsy.

3.1.3 Assays for investigation of SV turnover.

In order to investigate the effects of epilepsy on SV turnover it is necessary to use assays which will differentiate between the different forms of endocytosis. At least 2 different forms of endocytosis are used to retrieve SV membrane, dependant on the stimulus received. Mild stimulation results in the clathrin-mediated retrieval of single SVs (Granseth *et al*., 2006). Stronger stimulation activates the bulk endocytosis pathway in addition to the single SV pathway (Rizzoli & Betz, 2005; Royle & Lagnado, 2003). FM dyes are a useful tool in the study of SV turnover, as variations in dye uptake report differences in SV turnover. Studies have shown that FM2-10 does not label the bulk endocytosis pathway, whereas FM1-43 labels all endocytic structures (Richards *et al*., 2000; Virmani *et al*., 2003). This property could be used to assess differences in SV turnover.

Strong stimulation is representative of the type of stimulation delivered in epilepsy. Bulk endocytosis is recruited under conditions of strong stimulation, and is therefore a likely candidate if epilepsy mediates its effects via changes in SV endocytosis (SVE). Clathrin-mediated endocytosis (CME) is an extremely well characterised method of endocytosis (Granseth *et al*., 2007), however much less is understood about the bulk membrane retrieval method of endocytosis. Therefore a more direct assay of bulk endocytosis than FM dye imaging would be a valuable tool in the study of epileptogenic cells. Establishing an assay to specifically detect this type of endocytosis in the CGN culture could prove to be useful in the understanding of the molecular and physiological mechanisms underlying this form of endocytosis.

3.1.4 LABELLING OF BULK ENDOSOMES.

Holt *et al*. (2003) reported using tetramethylrhodamine labelled 40 kDa dextrans to selectively label large endocytic compartments in retinal bipolar cells. Dextrans are inert polysaccharides which, when conjugated to fluorescent dyes, have been used to monitor a number of different cellular processes. Fluorescently conjugated dextrans have been used as both retrograde and anterograde neuronal tracers (Vercelli *et al*., 2000), and as tracers to determine cell lineages during development (Raible & Eisen, 1994). Dextran conjugates are membrane impermeant, and thus if they label the cells they have been internalised by an endocytic mechanism. Due to their size they will be excluded from recycling single vesicles, and thus could be used as a selective marker of bulk endocytic events. If these dextrans can be shown to be localised to synapses, then they could potentially be used as a measure of bulk endocytosis.

Bulk endocytosis is likely to play a role in the endocytosis of SVs in epileptic cells as this is the prevalent method of endocytosis following a strong stimulus. Developing an assay for bulk endocytosis, which is currently poorly understood, would allow this form of endocytosis to be characterised. Characterisation of bulk endocytosis would allow greater understanding of the molecular mechanisms and physiological relevance of this form of SV endocytosis, which in turn could explain its role in pathological conditions such as epilepsy.

3.2 Results

3.2.1 Cell Development

The development of the serum replacement (SR) cells (medium supplemented with SR instead of FCS) was compared to that of the normal CGN cell culture. Images were taken from cultures prepared on the same day, one set cultured in normal cell culture medium (Fig 3.1 **A**), and the other in SR medium (Fig 3.1 **B**). The SR cells were plated at twice the normal density of the regular cells, to allow for the high degree of cell death prevalent in the SR culture medium. By day 6 it is possible to see how the cells bodies of the SR cells have aggregated much more so than the regular cell culture (Fig 3.1 **B d**). A high number of crenulated dead cells are also visible. The processes from the regular cell culture have formed regular networks of connections by day 6 (Fig 3.1 **A d**). At day 7 in the SR cell cultures (Fig 3.1 **B e**) it is obvious that the processes are poorly formed, that there is a high degree of cell death (considering the double density of cells to begin with), and that there are a number of astrocytes contaminating the cultures (due to the absence of astrocyte suppression by cytosine arabinosidase).

3.2.2 Excitable Cells

Fura-2am was incubated with the SR cells in order to look at differences in intracellular Ca^{2+} levels in response to perfusion of the cells with $–Mg^{2+}$ buffer medium. Fura-2am is a ratiometric indicator of intracellular Ca^{2+} levels, where the

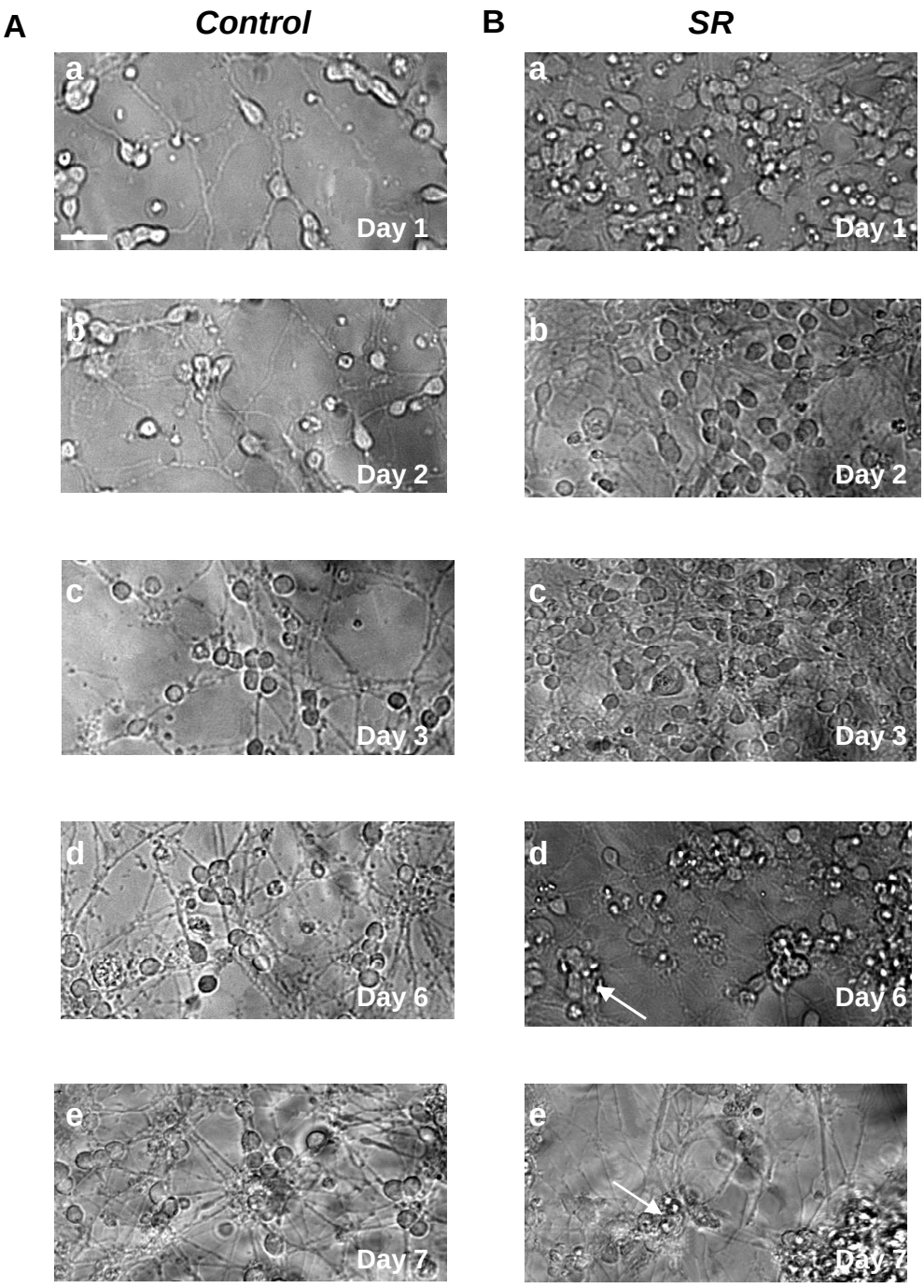

Figure 3.1 - Cell culture development. **A**, Representative images of cerebellar granule neurons (CGN) and **B**, serum replacement (SR) cultures at 1 (**a**), 2 (**b**), 3 (**c**), 6 (**d**) and 7 (**e**) days post preparation (as labelled). Arrows indicate dead cells in SR culture. Scale bar 20 µm.

emitted fluorescence depends on the wavelength of light used to excite the dye. When intracellular Ca^{2+} increases, excitation at 340 nm results in an increase in fluorescent emission whilst excitation at 380 nm results in a converse decrease in emission. The ratio between these emissions is a reliable indicator of intracellular Ca^{2+}, as it negates any effects caused by differences in dye concentration or photobleaching. Perfusion of $-Mg^{2+}$ buffer was initiated 10 seconds into the recording. By 20s (Fig 3.2 **B**) the ratio of red to green can be seen to alter, showing that the cells are beginning to fire spontaneously in response to the perfusion medium (Fig 3.3). The spontaneous firing of the cells persists for at least 3 minutes after initial $-Mg^{2+}$ perfusion. Therefore it is possible to induce spontaneous and rapid firing from epileptogenic cells in the cell culture model system of SR cells.

3.2.3 FM Assay of Excitable Cells.

In order to determine if these epileptogenic cells can be used in an FM dye assay system they must be reliably loadable with FM dye in the S1 S2 assay model. To determine this SR cells were loaded and unloaded with KCl at S1. At S2 the cells were loaded with KCl and then unloaded with $-Mg^{2+}$ (Fig 3.4 **A**) The cells could be loaded and unloaded with KCl at S1, but as is shown in the trace of S1 unload (Fig 3.4 **C a**) the fluorescence drop was not as pronounced as it would be with the regular cell culture system (Fig 2.2). However when the cells were loaded with KCl at S2, and then unloaded by perfusion of $-Mg^{2+}$ buffer, it wasn't possible to identify a discernable unload (Fig 3.4 **D**). The average normalised fluorescence trace seems to decay without obvious simultaneous stimulation evoked unloads. This could possibly

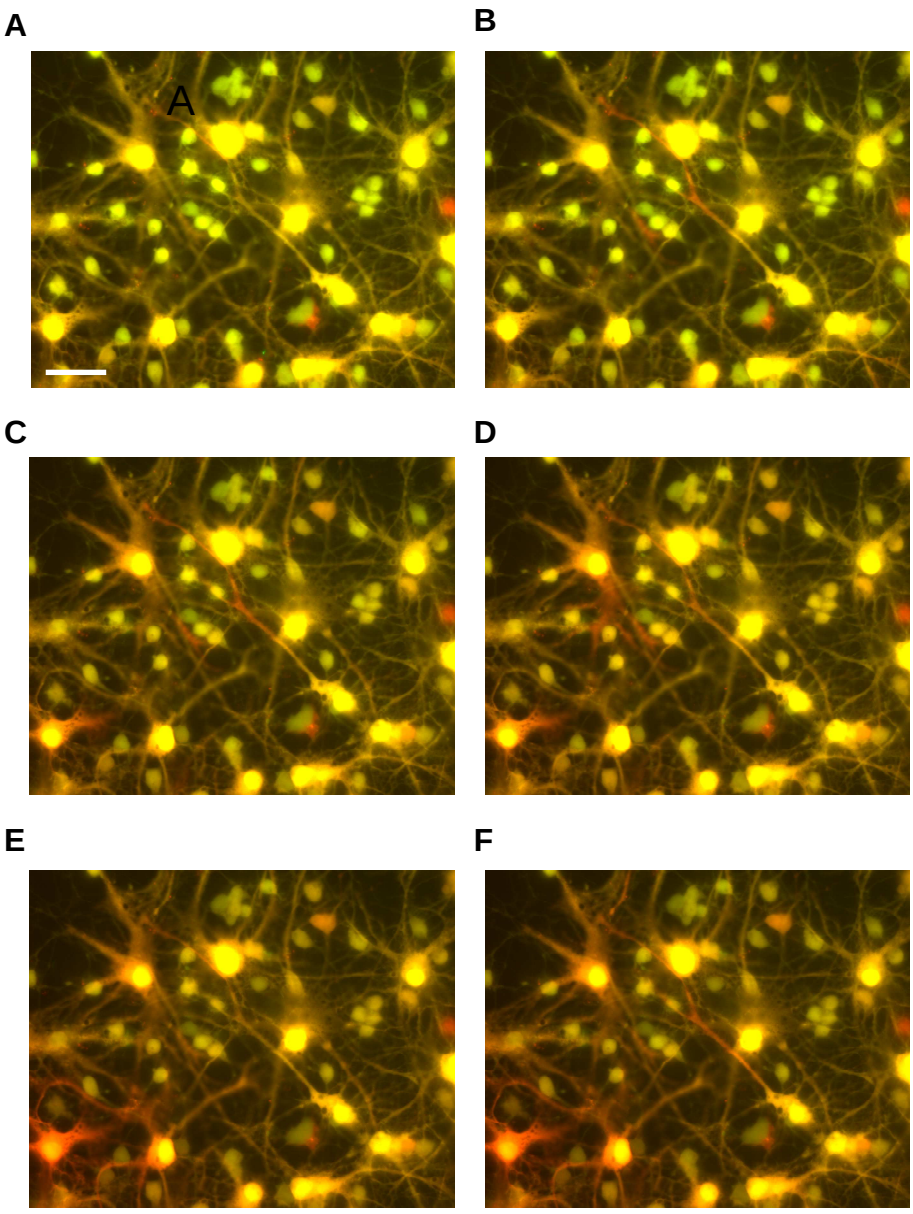

Figure 3.2 - Excitable cells loaded with Fura 2-AM. Differences in the levels of intracellular Ca^{2+} can be seen as the emission alters throughout the stills at 340 nm and 380 nm excitation during $-Mg^{2+}$ perfusion of the excitable cells. **A**, 00:00 **B**, 00:20 **C**, 01:23 **D**, 01:28 **E**, 02:35 **F**, 02:46. Scale bar 30 µm

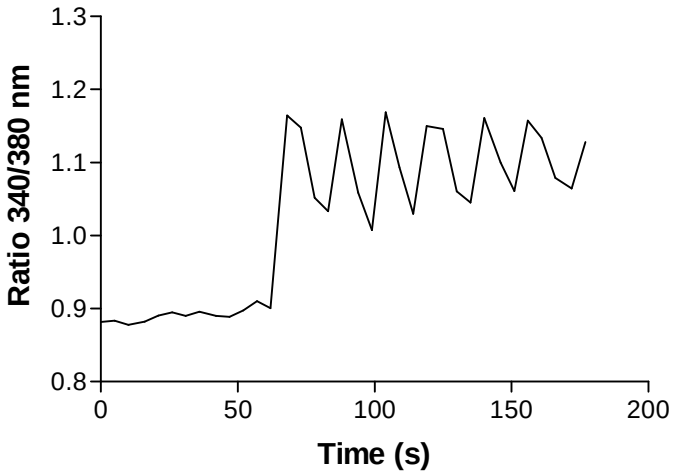

Figure 3.3 – Ratiometric analysis of SR cells loaded with Fura 2-AM. An example trace from one ROI, showing the differences in the levels of intracellular Ca^{2+}, as seen by the alteration in the ratio of 340/380nm over time. Perfusion of $–Mg^{2+}$ buffer was initiated 10 seconds after beginning of the recording.

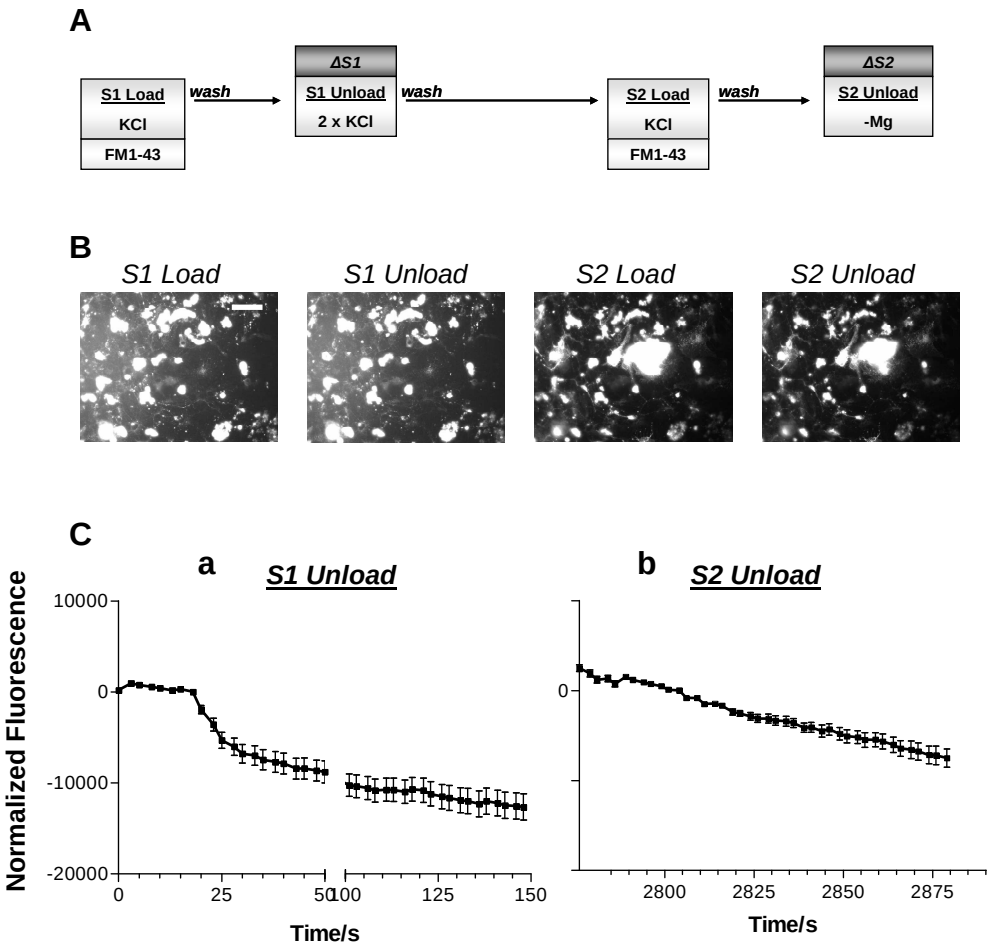

Figure 3.4 - FM Assay with excitable cells. S1 S2 assay performed on SR cells. **A**, Cells were loaded and unloaded with KCl at S1. Cells were then loaded with KCl at S2, and unloaded with perfusion of –Mg2+ buffer. **B**, Representative images showing the FM staining after loading and unloading of S1 and S2. **C**, Graphs showing the average fluorescence drop during S1 (a) and S2 (b) unloads (normalised to 0). Scale bar 20 μm.

be due to the disjointed and random nature of the $-Mg^{2+}$ evoked spontaneous firing. If the cells are not releasing the endocytosed dye simultaneously then the unloading

traces cannot be normalised to a synchronised starting time point, resulting in a lack of discernable unload in the S2 normalised trace.

As the lack of an obvious unload could be due to the nature of the firing of the epileptogenic cells, the converse experiment was performed. At S2 the cells were loaded with $-Mg^{2+}$ buffer, and then unloaded with KCl (Fig 3.5 **A**). The cells loaded and unloaded successfully with KCl at S1 again (Fig 3.5 **C**), however loading with 2 minutes of $-Mg^{2+}$ incubation, and then unloading with KCl again produced a trace which gave the appearance of a decay rather then a FM dye unload. Due to the inability of the –Mg model to reproducibly load and unload FM dye this model system was discarded.

3.2.4 40 kDa Dextran Internalisation

Since the SR system model did not turn over vesicles at sufficient levels for observation with FM dyes, a different system was employed using the control CGN cultures. A 40 kDa fluorescently tagged tetramethylrhodamine dextran was used to develop a potential assay for bulk endocytosis in the cerebellar granule cell culture system. Stimulation with 50 mM KCl in the presence of dextran for 2 minutes led to the accumulation of fluorescent puncta (Fig 3.6 **A**). Incubating cells at rest with the same concentration of dextran resulted in only a few fluorescent puncta being internalised (Fig 3.6 **B**). This suggests dextran uptake is stimulation dependent.

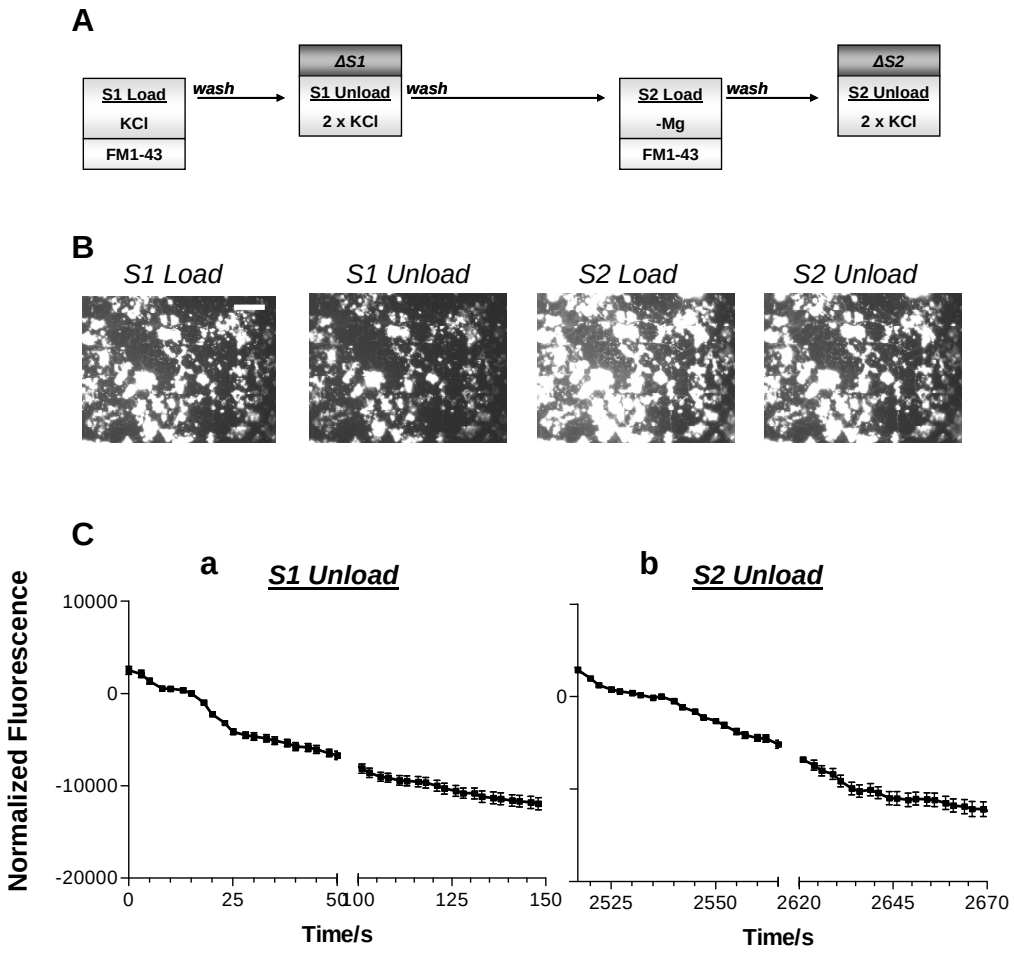

Figure 3.5 - FM Assay with excitable cells. S1 S2 assay performed on SR cells. **A**, Cells were loaded and unloaded with KCl at S1. Cells were then loaded with by incubation with –Mg2+ buffer at S2, and unloaded with KCl. **B**, Representative images showing the FM staining after loading and unloading of S1 and S2. **C**, Graphs showing the fluorescence drop during S1 (a) and S2 (b) unloads (normalised to 0). Scale bar 20 µm.

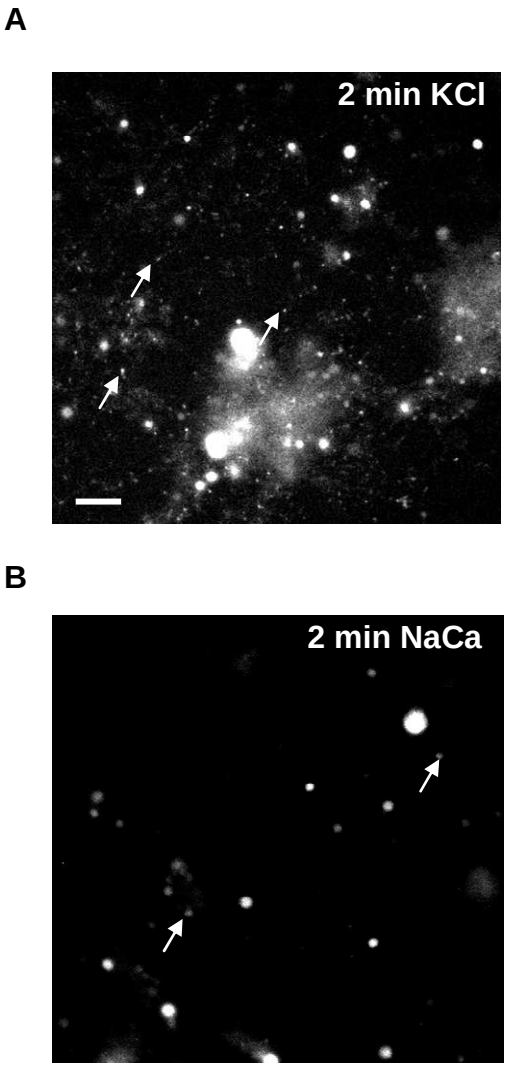

Figure 3.6 - 40 kDa loading of CGNs **A**, Representative field of CGNs labelled with 40 kDa dextran by stimulating with 50 mM KCl for 2 minutes. **B**, Corresponding image of cells labelled with 40 kDa dextran in the absence of stimulation. White arrows indicate examples of dextran loaded puncta. Scale bar 30 μm.

3.2.5 Co-Localisation with FM1-43

The dextran loaded fields (Fig 3.7 **A**) were overlaid with the corresponding bright field image (Fig 3.7 **B**) to show the neurite localisation of the loaded puncta (Fig 3.7 **C**). In order to then prove that the puncta were synaptically localised within the neurites, the cells were loaded with FM1-43 (Fig 3.8 **B**) following dextran loading (Fig 3.8 **A**). The resulting fluorescence patterns were overlaid to see any regions of co-localisation (Fig 3.8 **C**). To quantify the co-localisation, 5 regions were chosen from each of 3 separate experiments. The percentage of dextran puncta that co-localised with FM labelling was determined. The percentage of dextran co-localisation per field for 40 kDa dextran averaged 87.8 ± 13.6%, suggesting that the vast majority of dextran uptake was synaptic.

The preliminary experiments show that internalisation of the 40 kDa dextran was stimulation dependant, localised to the synapse, and occurred within 2 minutes.

3.2.6 Unloading of internalised 40 kDa dextran.

To assess whether it was possible to release these internalised 40 kDa dextrans, the cells were perfused with 50 mM KCl 30 minutes after the initial dextran loading. Representative fields were imaged before (Fig 3.9 **A**) and after KCl unload (Fig 3.9 **B***)* to see if any of the dextran puncta could be released from the cells. The dextran images taken before and after unloading were then overlaid (Fig 3.9 **C**). Dextran puncta release was determined by averaging the percentage of unloaded puncta per field. The average dextran loss per field was found to be 11.2 ± 2.3%.

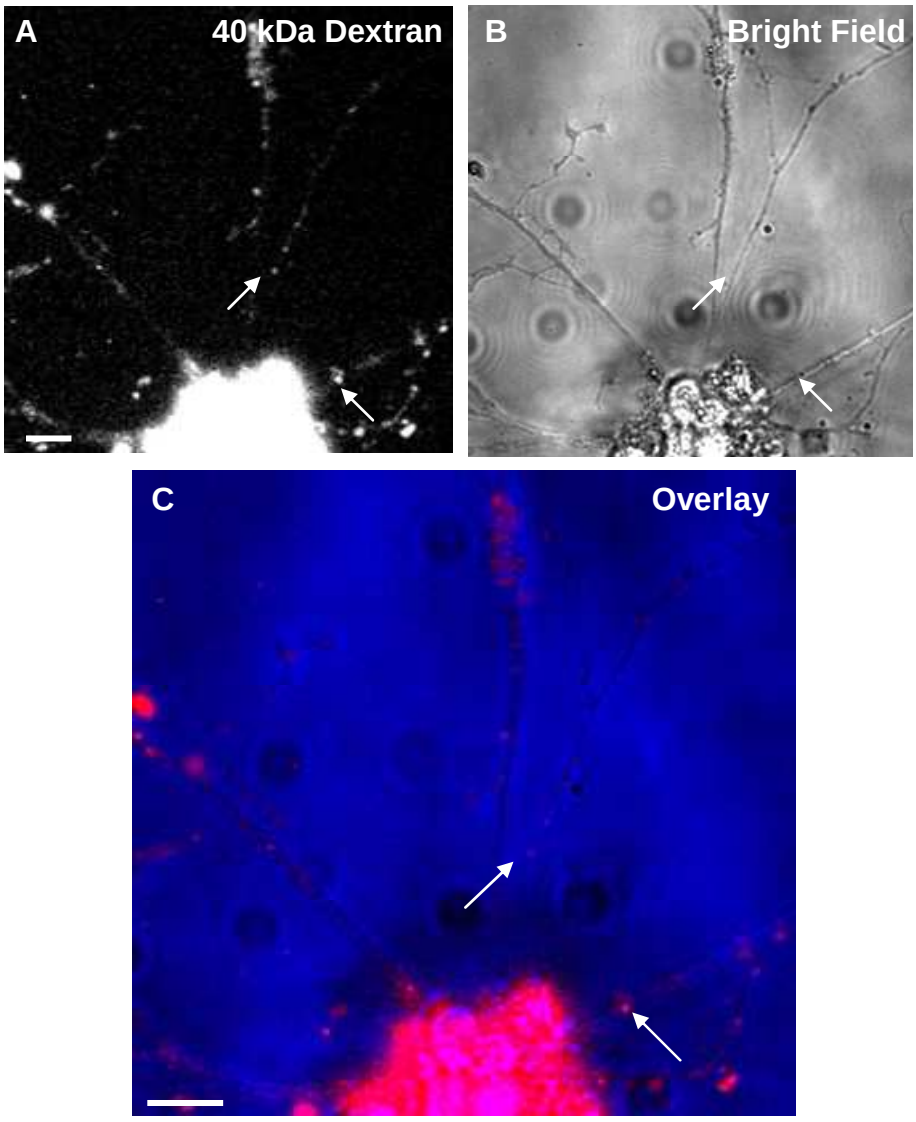

Figure 3.7 - Synaptic Localisation of 40 kDa dextran. **A**, Cells were loaded with 40 kDa dextran by stimulating with 50 mM KCl for 2 minutes. **B**, The corresponding bright field image. **C**, Overlay of dextran loaded cells (red) with the bright field image (blue). White arrows indicate the synaptic localisation of dextran loaded puncta. Scale bar 10 µm.

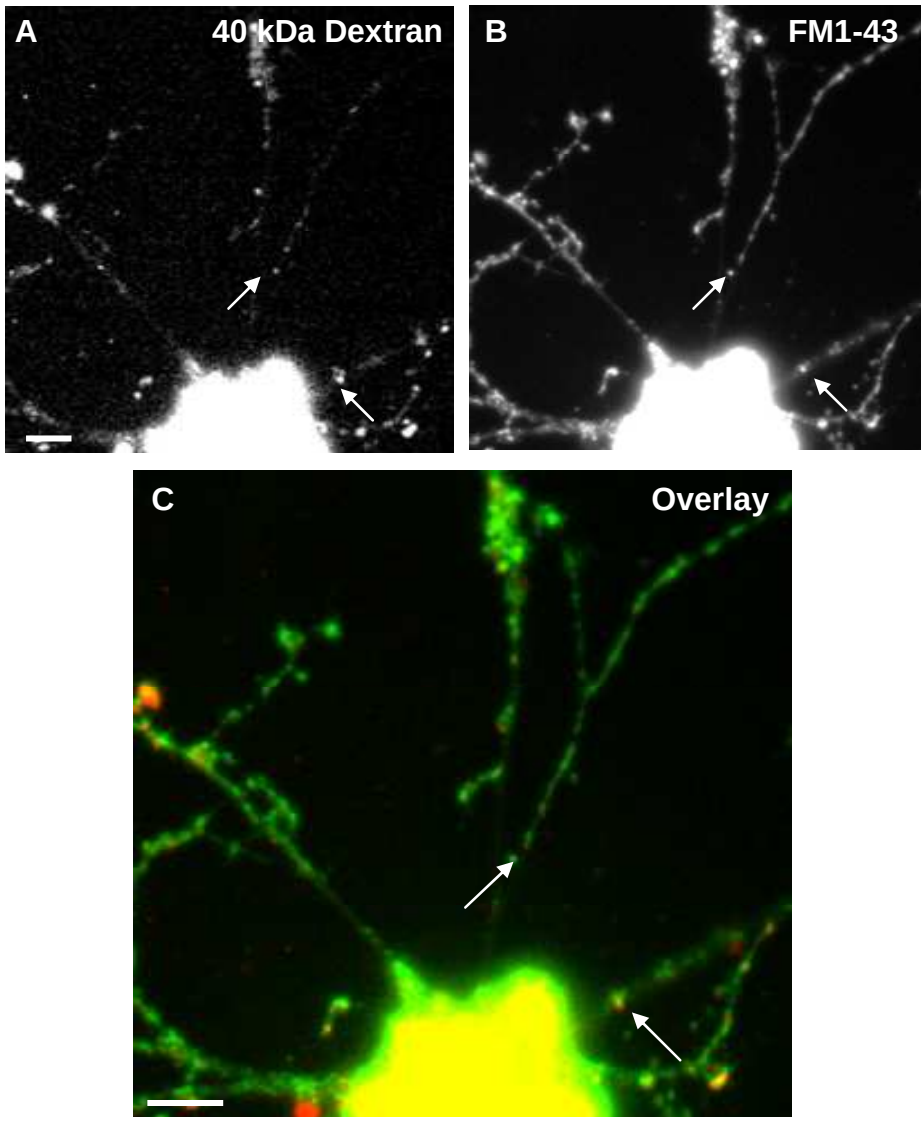

Figure 3.8 - Co-localisation of 40 kDa dextran with FM1-43. **A**, CGNs were loaded with 40 kDa dextran by stimulating with 50 mM KCl for 2 minutes. **B**, The corresponding FM1-43 loaded field of cells. **C**, Overlay of dextran loaded cells (red) with FM loaded cells (green). White arrows indicate the co-localisation of dextran loaded puncta with FM1-43 loaded synapses. Scale bar 10 μm.

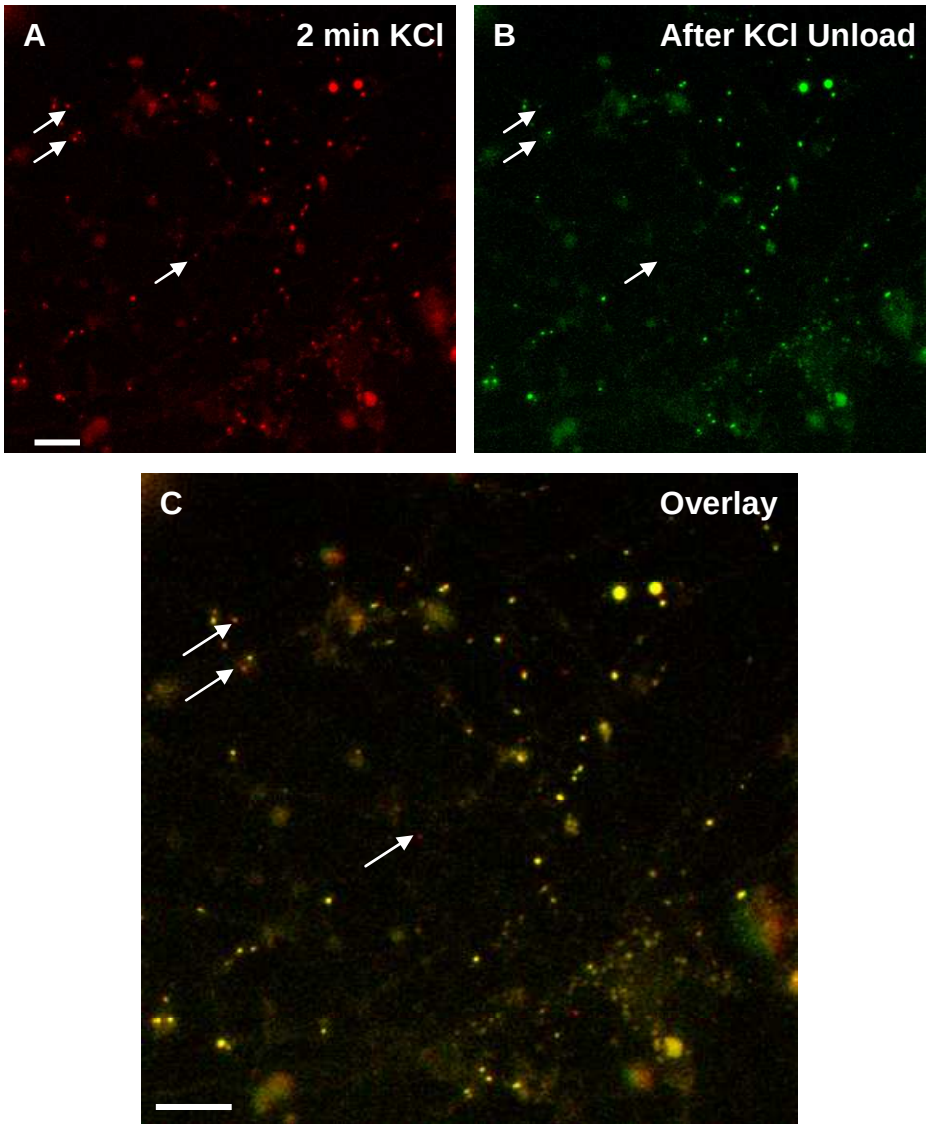

Figure 3.9 - Unload of 40 kDa dextran. **A**, Cells were loaded with 40 kDa dextran by stimulating with 50 mM KCl for 2 minutes. **B**, After a 30 minute rest the cells were unloaded by stimulation with 50 mM KCl. **C**, Overlay of dextran loaded cells before (red) and after unloading (green). Red puncta indicates a loss of dextran loaded puncta. White arrows indicate these lost puncta before and after stimulation. Scale bars 30 μm.

(N=2, 3 regions per experiment). Therefore the proportion of dextran labelled structures that could be unloaded is small.

3.2.7 Time Course of 40 kDa Dextran Loading

It was thought that slow endocytosis equated to bulk endocytosis, as the invagination of large in-foldings of membrane was thought to take longer then single synaptic vesicle endocytosis (Rizzoli & Betz, 2005). To investigate this we used different time points of KCl mediated dextran loading in our CGN culture system. Cells were stimulated with KCl and dextran for 2 minutes, 30 seconds or 15 seconds (Fig 3.10). Representative stills taken from 30 second (Fig 3.10 **A**) or 15 second (Fig 3.10 **B**) KCl stimulation experiments show that dextran is already internalised at these shorter time points, suggesting that bulk endocytosis is in fact a relatively rapid process.

3.2.8 Quantification of dextran loading by measuring fluorescence intensities.

In order to identify any differences between the different stimulation time points we quantified the amount of fluorescence from the internalised puncta. To do this a cloned region of interest was placed on the puncta in each of the field images captured. 5 images were taken for every coverslip used for each condition. The total amount of fluorescence for each region of interest was measured. Although the gain and exposure times were identical for image capture for every dextran experiment, the background fluorescence for each field was seen to vary. This is likely due to the

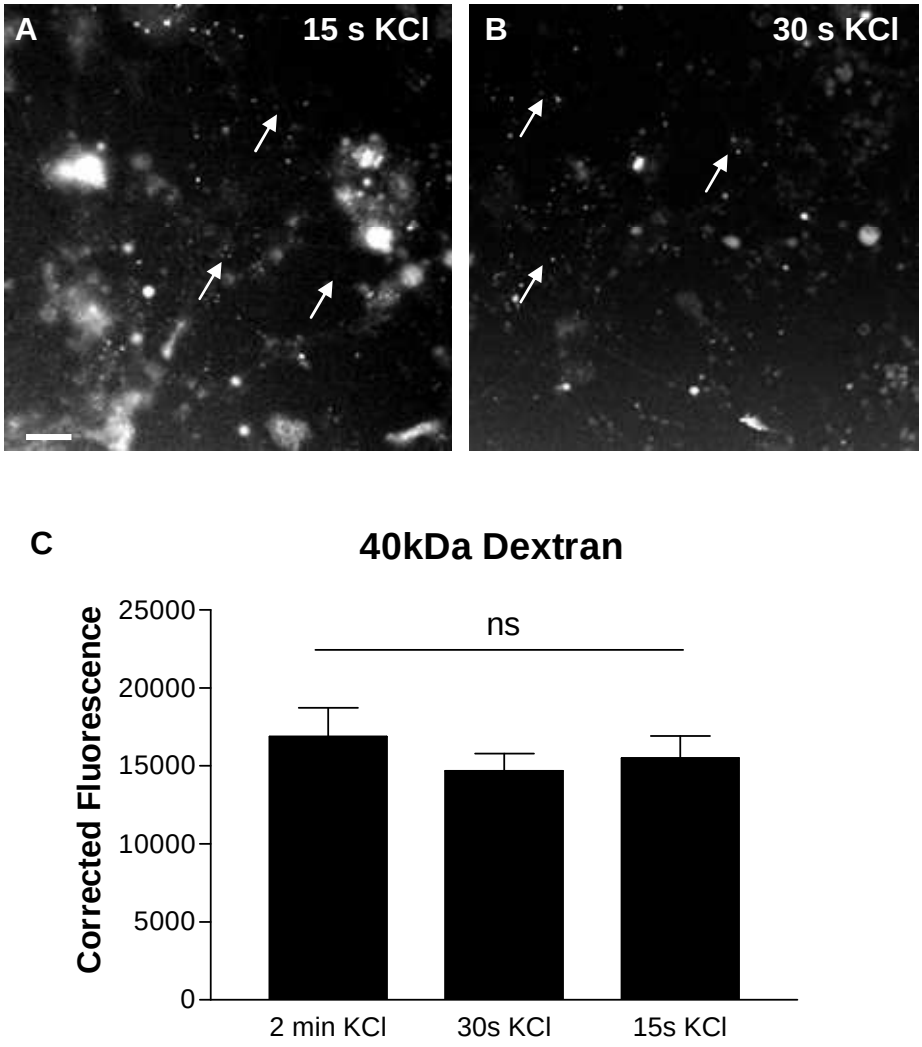

Figure 3.10 - Time course of 40 kDa dextran loading. 40 kDa dextran loaded with KCl for 15 (**A**) and 30 (**B**) seconds. White arrows indicate examples of dextran loaded puncta. **C**, Bar chart showing no significant difference (one-way ANOVA) between average fluorescence per puncta (corrected for background) for different loading times. N=3 for all experiments, with at least 5 fields per experiment. Scale bar 30 μm.

large amount of fluorescence seen to occur at groups of cell bodies, probably caused by accumulations of dextran stuck at these areas. This caused uneven distribution of fluorescence between different images. In order to alleviate any bias this could introduce to a quantification based on fluorescent intensity, identical regions of interest were displaced a short distance from each fluorescent punctum to measure the background fluorescence. The paired background fluorescence measurements were then subtracted from the fluorescence reading for each punctum, so each measurement was internally corrected for. The total amount of corrected fluorescence per puncta was then averaged across each field (5 in total) for every condition. The average fluorescence per coverslip was then averaged across all coverslips for each condition, resulting in a corrected average fluorescence value for each condition. However this corrected average showed no difference between the various time conditions (Fig 3.10 **C**). This suggests that bulk endocytosis is either complete by 15 seconds, or alternatively fluorescence intensity is not a reliable method of quantification of bulk endocytosis.

3.2.9 10 kDa Dextran Internalisation

As no difference could be detected between the various time points for 40 kDa dextran loading in the presence of KCl stimulation, it was decided to utilise a smaller dextran to see if this could be used to detect differences.

Firstly the 10 kDa dextran was used to label the cells with 2 minute KCl stimulation (Fig 3.11 **A**). This labelled the cells in a punctate manner similar to the 40 kDa dextran loading. When cells at rest were incubated for 2 minutes in the absence of any stimulation, a vastly greater amount of fluorescence was visible

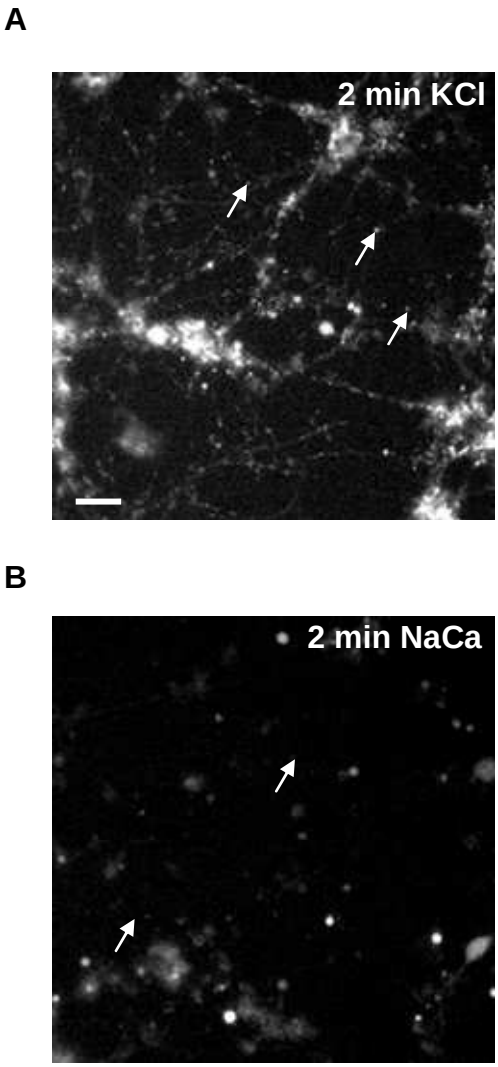

Figure 3.11 - 10 kDa loading of CGNs **A**, Representative field of CGNs labelled with 10 kDa dextran by stimulating with 50mM KCl for 2 minutes. **B**, Corresponding image of cells labelled with 10kDa dextran in the absence of stimulation. White arrows indicate examples of dextran loaded puncta. Scale bar 30 μm.

(Fig 3.11 **B**). Uptake of the 10 kDa dextran, like that of the 40 kDa, is stimulation dependent.

3.2.10 Co-Localisation with FM1-43

The 10 kDa dextran loaded fields were overlaid with the corresponding bright field image to show the neurite localisation of the loaded puncta (Fig 3.12). To show that the puncta were synaptically localised, the cells were loaded with FM1-43 following dextran loading and the resulting fluorescence patterns were overlaid to see any regions of co-localisation (Fig 3.13). To quantify the co-localisation, 5 regions were chosen from each of 3 separate experiments. The percentage of dextran puncta which co-localised with FM labelling was determined. The percentage of dextran co-localisation per field averaged 96.4 ± 3.2%.

This showed that the internalisation of 10 kDa dextran was largely stimulation dependant, was localised to the synapse, and occurred within 2 minutes (as is the case with the 40 kDa dextran).

3.2.11 Time Course of 10 kDa Dextran Loading

In order to see any detectable changes in fluorescence dependant on incubation times, the amount of fluorescence per puncta for each condition of loading time was performed for the 10 kDa dextran (Fig 3.14). The experiments and analysis were performed in an identical way to those conducted for the 40 kDa dextran. Representative images for the 30 second (Fig 3.14 **A**) and 15 second

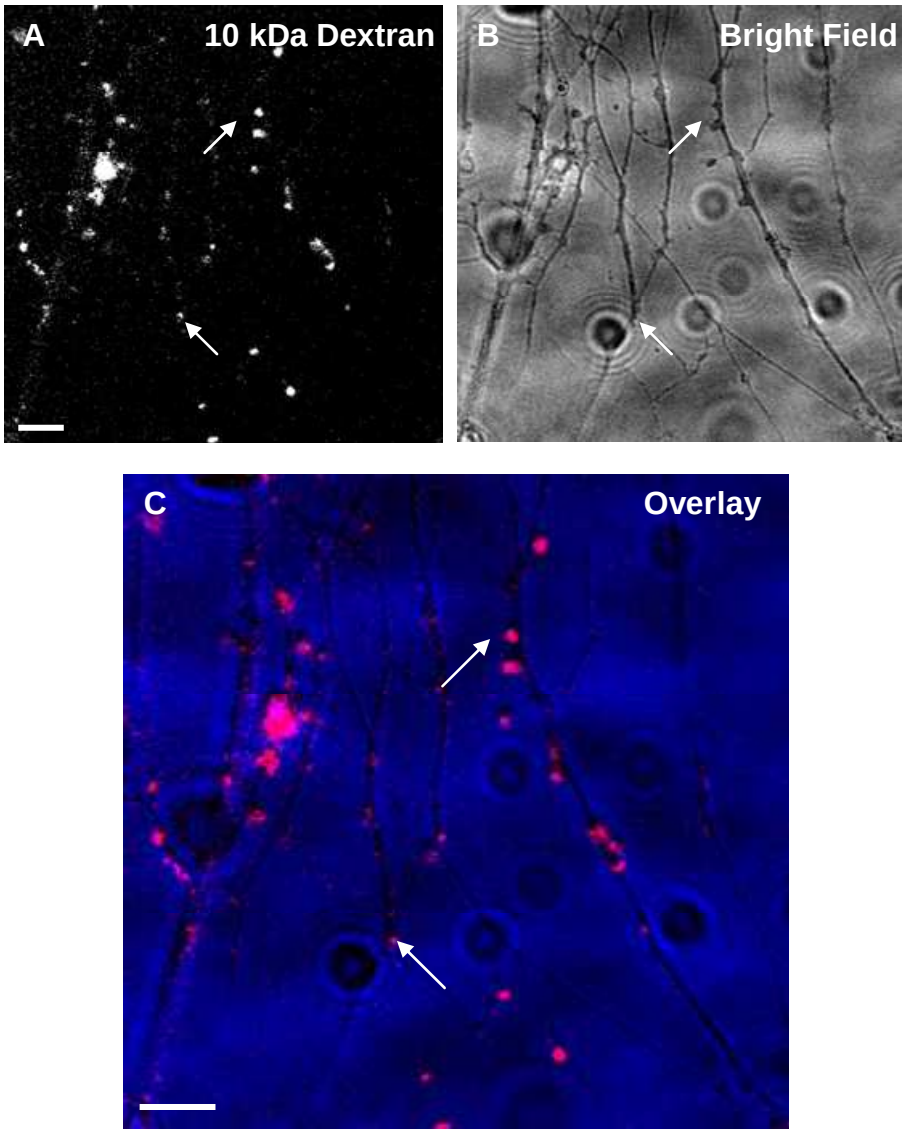

Figure 3.12 - Synaptic Localisation of 10 kDa dextran. **A**, Cells were loaded with 10 kDa dextran by stimulating with 50 mM KCl for 2 minutes. **B**, The corresponding bright field image. **C**, Overlay of dextran loaded cells (red) with the bright field image (blue). White arrows indicate the synaptic localisation of dextran loaded puncta. Scale bar 10 µm.

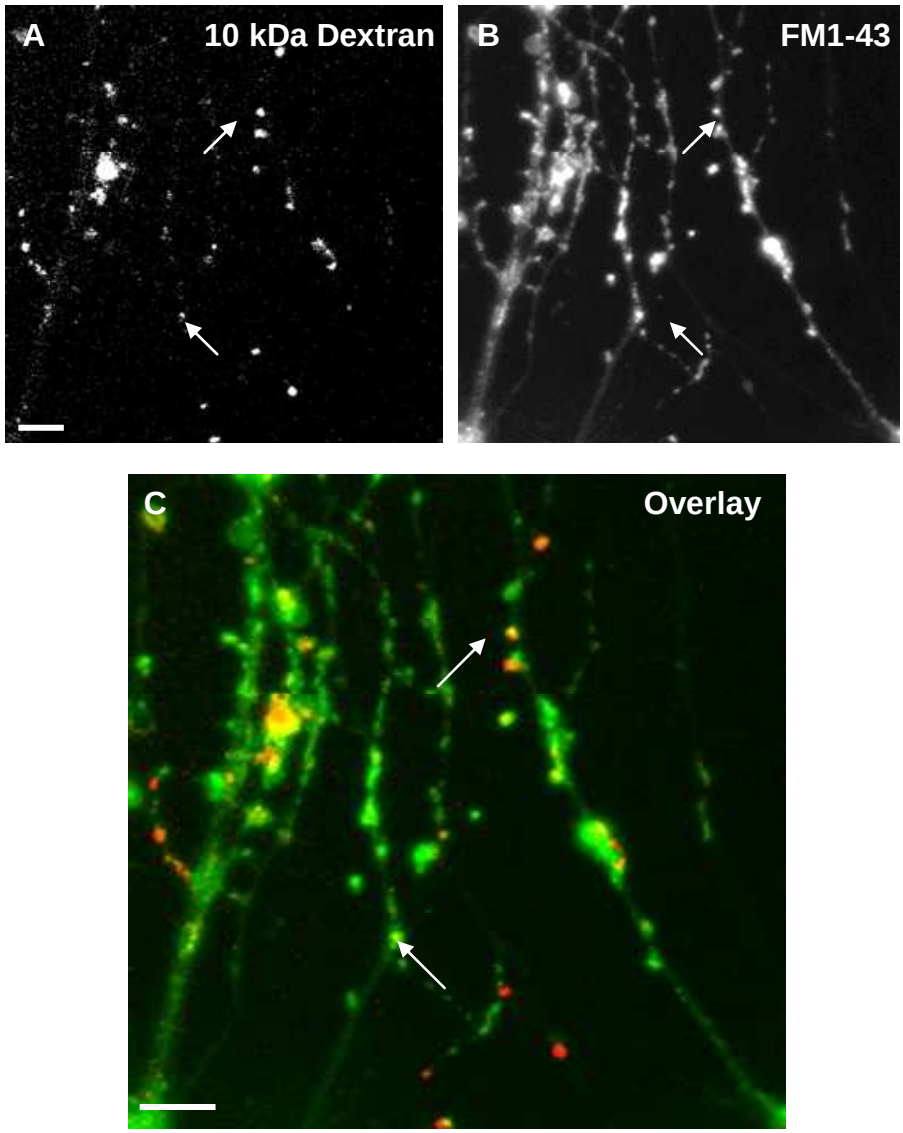

Figure 3.13 - Co-localisation of 10 kDa dextran with FM1-43. **A**, CGNs were loaded with 10 kDa dextran by stimulating with 50 mM KCl for 2 minutes. **B**, The corresponding FM1-43 loaded field of cells. **C**, Overlay of dextran loaded (red) cells with FM loaded cells (green). White arrows indicate the co-localisation of dextran loaded puncta with FM1-43 loaded synapses. Scale bar 10 μm.

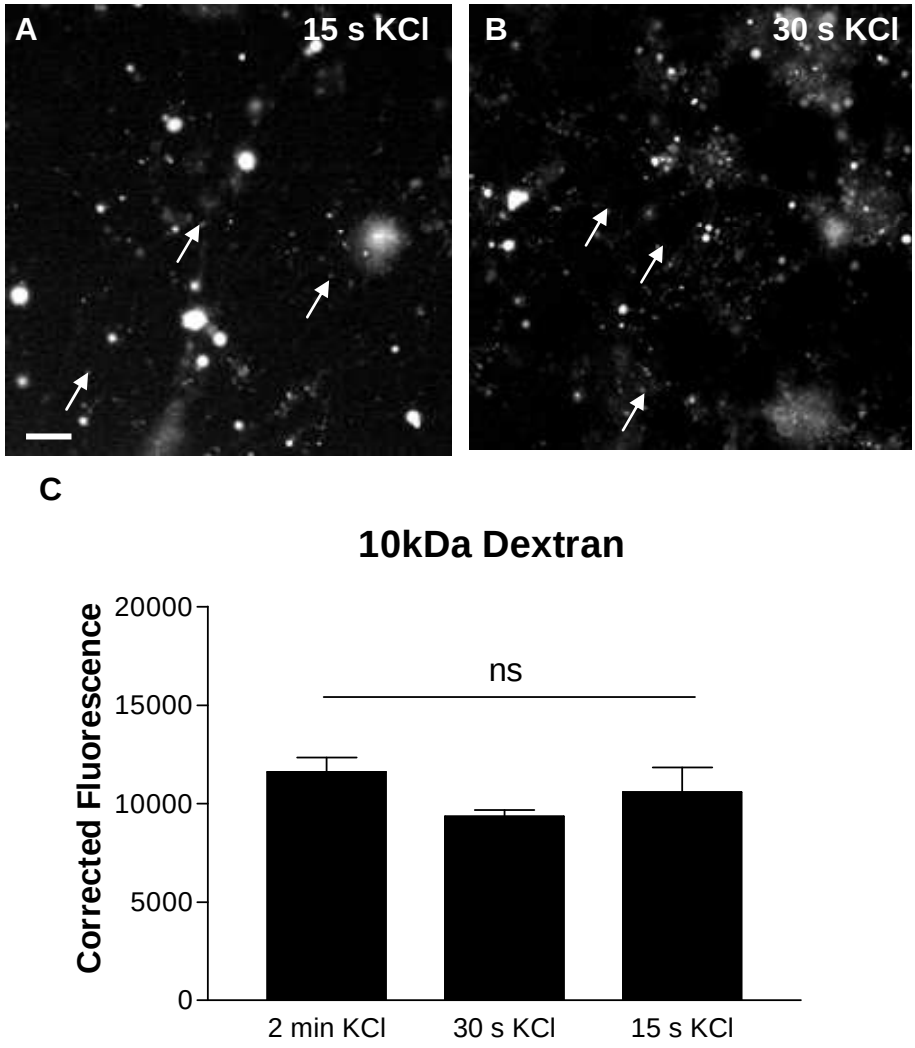

Figure 3.14 - Time course of 10 kDa dextran loading. 10kDa dextran loaded with KCl for 15 (**A**) and 30 (**B**) seconds. White arrows indicate examples of dextran loaded puncta. **C**, Bar chart showing no significant difference (one-way ANOVA) between average fluorescence per puncta (corrected for background) for different loading times. N=3 for all experiments, with at least 5 fields per experiment. Scale bar 30 μm.

(Fig 3.14 **B**) time points are shown. The amount of loading between time points again was very similar. When the average amount of corrected fluorescence was quantified (in an identical manner to the 40 kDa analysis), again no difference was seen between the different times points of loading (Fig 3.14 **C**).

3.2.12 Delayed 10 kDa Dextran Loading

In order to further investigate the speed of dextran loading, loading of 10 kDa dextran was delayed after different time-points of stimulation with KCl. Following the stimulation with KCl, dextran was added to the cultures for 2 minutes, to assess the amount of dextran loading occurring immediately after cessation of stimulation. Images of the dextran internalised during the 2 min and 30 second KCl stimulation are shown (Fig 3.15 **A** and **C**). Representative images of loading following the delayed addition of dextran show greatly reduced loading of the cultures after stimulation with both 2 minutes (Fig 3.15 **B**) and 30 seconds KCl (Fig 3.15 **D**), suggesting that bulk endocytosis terminates after stimulation.

However quantification of the amount of corrected fluorescence per puncta again revealed no difference between amounts of fluorescence for immediate (Fig 3.16 **A**) versus delayed (Fig 3.16 **B**) loading conditions for any time point. Clearly despite the difference in the extent of loading between immediate and delayed loading being visually very obvious, using quantification of fluorescence as a measure of dextran loading is not informative as to differences between loading conditions. Thus a different means of determining differences between culture conditions was necessary.

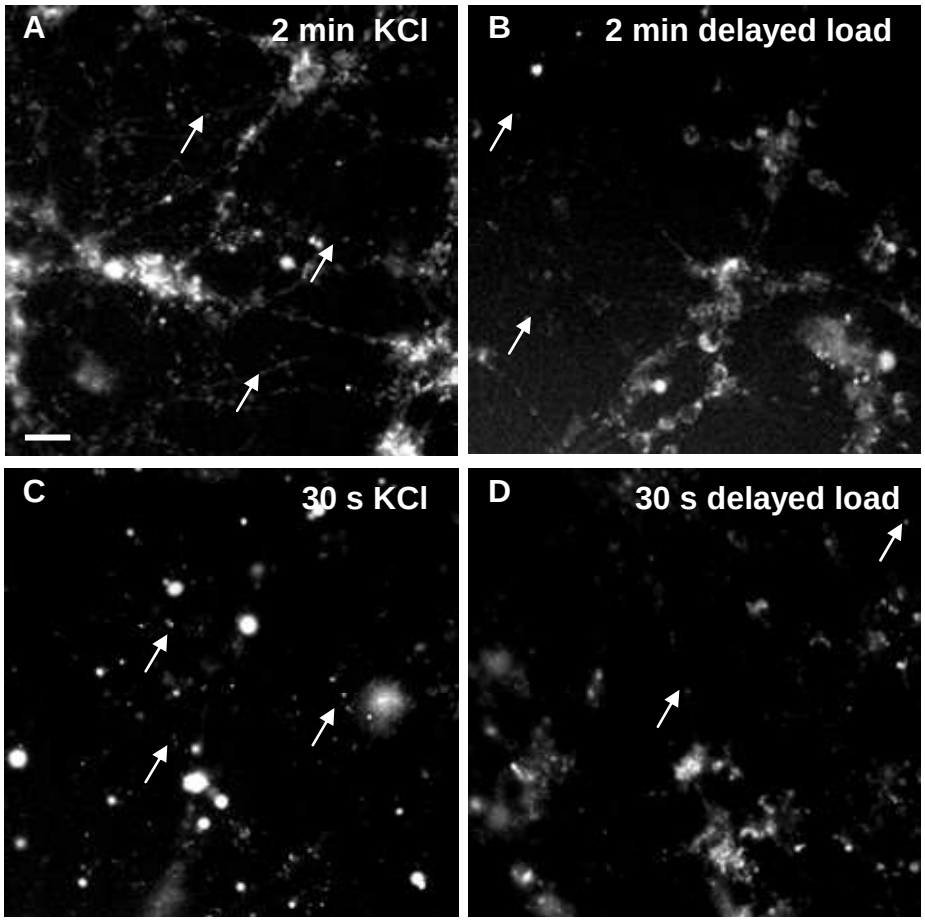

Figure 3.15 - Immediate and delayed loading of 10 kDa dextran. **A,** Cells were loaded during 2 minutes KCl stimulation. **B**, Cells incubated with dextran for 2 minutes directly after KCl stimulation. **C**, Cells loaded during 30 s KCl stimulation, **D**, Cells incubated with dextran for 2 minutes immediately after 30 s KCl stimulation. White arrows indicate examples of dextran loaded puncta. Scale bar 30 μm.

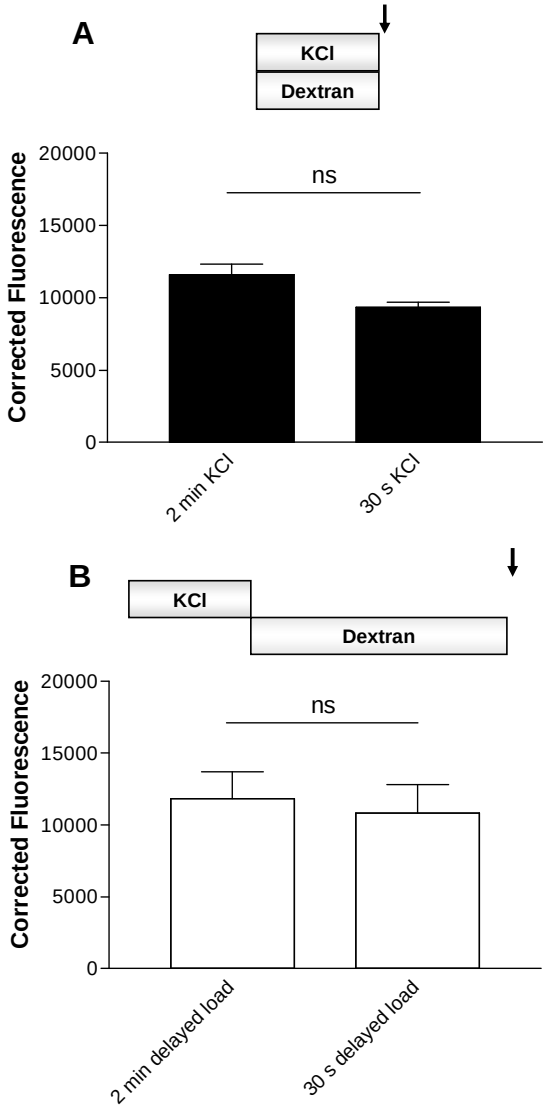

Figure 3.16 - Fluorescent intensities of immediate and delayed 10 kDa loading. Bar chart of average fluorescence per puncta (corrected for background) for immediate (**A**) and delayed loading (**B**) of 10 kDa dextran. No significant difference in intensity of fluorescence between immediate or delayed loading conditions (unpaired t-test). N=3 for all experiments, with at least 5 fields for each experiment. No difference between any of the immediate and delayed loading values (one-way ANOVA).

3.2.13 Count of Loaded Puncta

Visually the difference between the immediate versus delayed loading is very obvious; therefore a way to quantify the number of puncta visible between different conditions has to be developed in order give a definitive answer as to any effects on dextran loading. In order to do this, we applied a thresholding limit to the images, discounting the majority of the background fluorescence immediately. The thresholded images were then filtered so that only areas of fluorescence between 7 and 50 pixels in size were highlighted. The numbers of resulting regions of interest highlighted were counted for each experimental condition.

Although the majority of the background fluorescence is discounted by the application of a thresholding limit to the image, some background fluorescence remains that is occasionally picked up erroneously by the analysis parameters of the experiments. In order to discount this fluorescence, 2 negative controls were performed. To discount any intrinsic fluorescence caused by the autofluorescence of the cells, cells were stimulated but no dextran was included in the medium. Fields were captured at the normal gain and exposure used, and the resulting images were subjected to the thresholding analysis as described. This gave a baseline reading of the number of puncta that would be erroneously reported by the analysis method. Dextran was also applied to the cells in the absence of any stimulation, to measure the amount of spontaneous uptake of dextran. Both of these measurements allowed a calculation of the proportion of the reported puncta that have been included in the count that can be discounted due to background fluorescence.

3.2.14 Quantification of internalisation by counting of 40 kDa dextran loaded puncta.

The 40 kDa dextran was again applied to cultures in a time course of KCl stimulation. This time the time points chosen were 2 minutes, 60 seconds, 30 seconds and 10 seconds, to more closely resemble time points of stimulation for which the bulk endocytosis assay could potentially be used. Representative images for loading at 60 seconds (Fig 3.17 **A**) and 10 seconds KCl load (Fig 3.17 **C**) are shown. Again, as with the 10 kDa dextran, dextran loading was also delayed. The 40 kDa dextran was applied for 2 minutes directly following cessation of the KCl stimulation for each of the time points of the time course of loading. Representative images from 60 seconds KCl delayed dextran load (Fig 3.17 **B**) and 10 seconds delayed dextran load (Fig 3.17 **D**) are shown.

The average number of puncta for each coverslip was then averaged across all coverslips for the experimental condition, and the resulting average number of puncta compared across time conditions. For these experiments 10 fields were normally chosen from each coverslip.

Implementing the new method of dextran analysis by thresholding and puncta count, no significant difference can be seen between the 2 min, 60 s, or 10 s time points (Fig 3.18 **A,** Fig 3.19). However a large difference is evident between the immediate versus delayed load for each of the time points of loading (Fig 3.18 **B,** Fig 3.19). This indicates that the majority of 40 kDa dextran loading occurs within the first 10 seconds of stimulation, and that the majority of the dextran loading is complete during stimulation.

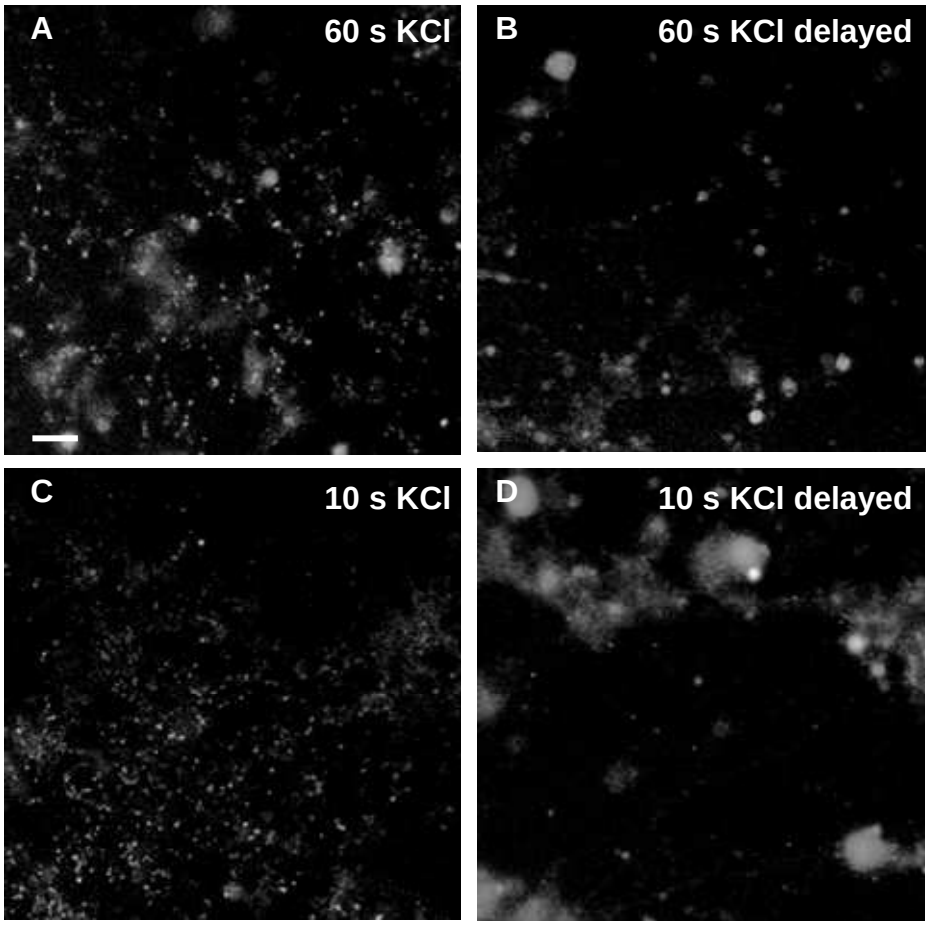

Figure 3.17 - Immediate and delayed loading of 40 kDa dextran. **A,** Cells loaded with dextran during 60 seconds KCl stimulation. **B**, Cells incubated with dextran for 2 minutes directly after KCl stimulation. **C**, Cells loaded with dextran during 10 seconds KCl stimulation, **D**, Cells incubated with dextran for 2 minutes immediately after 10 seconds KCl stimulation. White arrows indicate examples of dextran loaded puncta. Scale bar 30 µm.

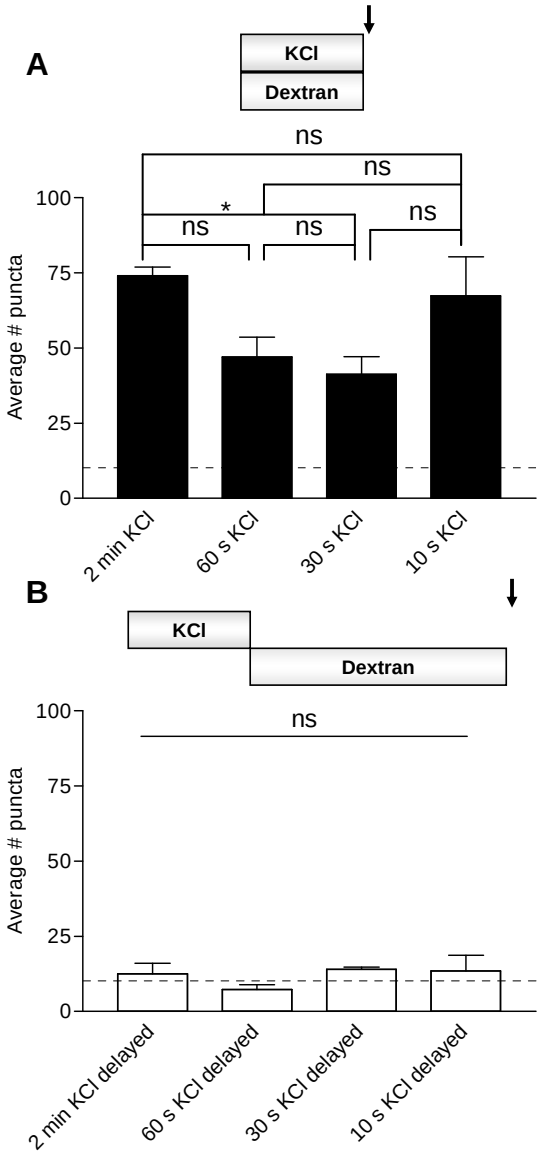

Figure 3.18 - Average number of dextran puncta loaded. Bar chart of average puncta count for immediate (**A**) and delayed loading (**B**) of 40 kDa dextran. Quantification of the amount of dextran internalisation by counting the number of fluorescent puncta shows a large increase in dextran loading in cells labelled during stimulation as opposed to those labelled after stimulation. N=3, with at least 5 fields for each experiment. One way ANOVA, ns = $p>0.05$, * = $p<0.05$

	10 s Delayed	30 s Delayed	60 s Delayed	2 min Delayed	10 s KCl	30 s KCl	60 s KCl
2 min KCl	***	***	***	***	*ns*	*	*ns*
60 s KCl	*	*	**	*	*ns*	*ns*	
30 s KCl	*ns*	*ns*	*	*ns*	*ns*		
10 s KCl	***	***	***	***			
2 min Delayed	*ns*	*ns*	*ns*				
60 s Delayed	*ns*	*ns*					
30 s Delayed	*ns*						

ns = p > 0.05

* = p < 0.05

** = p < 0.01

*** = p < 0.001

Figure 3.19 - One-way ANOVA analysis of dextran loaded puncta count. Dextran loaded puncta count of all immediate and delayed loads analysed by one-way ANOVA, with a post-hoc Tukey test.

The mean fluorescence from each of these ROIs was calculated to see if this method of analysis could detect any difference in immediate versus delayed loads. Again, no significant difference could be detected with any duration of stimulation between immediate versus delayed load (Fig 3.20). Therefore the extent of bulk endocytosis can be quantified by counting the number of dextran puncta, and not their intensity.

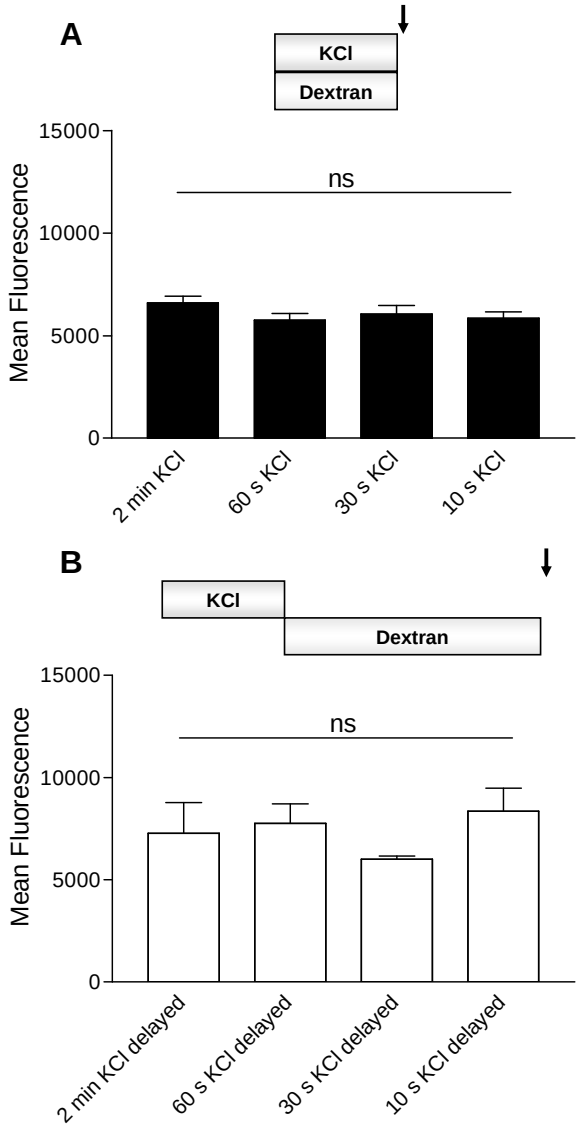

Figure 3.20 - Mean fluorescence per dextran loaded puncta . Bar chart of mean fluorescence intensity per ROI for immediate (**A**) and delayed loading (**B**) of 40 kDa dextran. No significant difference was observed between any duration of stimulation for immediate or delayed load, nor was there any difference when all values for immediate and delayed loading were compared together (one-way ANOVA). N=3, with at least 5 fields for each experiment.

3.3 DISCUSSION

3.3.1 SR CELLS AS A MODEL OF EPILEPTOGENESIS.

The SR cell cultures can be loaded and unloaded with KCl at S1, albeit not as cleanly or with as definite a drop in the fluorescence as would normally be seen in the regular cell culture. This reflects the fact that the cultures are not particularly healthy, as is evidenced by the appearance of the cells in culture, with a high degree of cell death and aggregates of cell bodies.

At S2 loading was initially attempted with KCl, followed by an S2 unload mediated by perfusion of – Mg^{2+} buffer. Stimulation with KCl at S2 allowed FM1-43 to label the granule cells. However when –Mg^{2+} buffer was perfused onto the cells, no discernable synchronous unload was detectable in the cells. A gradual decay could be seen, which is moderately steeper than the usual fluorescence decay caused by bleaching of the fluorophore. It's probable that the cells are not firing synchronously, which would mean it's not possible to normalise the fluorescence drop to a starting time point. Ca^{2+} oscillations in both cortical and hippocampal neurons in a –Mg^{2+} buffer are reported to be spontaneously synchronous (Murphy *et al*., 1992; McLeod *et al*., 1998; Shanley *et al*., 2002). However when the oscillations are activated by removal of Mg^{2+} (as is the case in our system), it has been observed in cerebellar granule cell cultures that the first few spikes of the oscillations are not well synchronized (Lawrie *et al*., 1993). This could explain the disparity seen in our SR cultures unloads at S2.

The converse S2 load (–Mg^{2+}) and unload (KCl) was also performed. Again, this did not allow a detectable drop in fluorescence when normalised to a starting

time point. Without being able to normalise the S2 unload to a start point, it's not possible to use the S1 S2 assay system to look at SV turnover in the SR cells. It has been proposed that SVs which release and recycle spontaneously represent a subpopulation of vesicles, distinct from the general vesicle population (Sara *et al*., 2005). It's possible that the activity induced by superfusion with $-Mg^{2+}$ is turning over a distinct subpopulation of vesicles. This could explain the lack of a clear drop in FM dye, if some or all of the vesicles turned over by KCl stimulation are distinct from those turned over with $-Mg^{2+}$ perfusion. To address this possibility, loading and loading at S2 could be stimulated with $-Mg^{2+}$ perfusion. However we opted not to pursue this possibility, as the concept was refuted by Groemer & Klingauf in 2007, who showed that SVs released spontaneously and during activity belonged to the same pool.

It was therefore necessary to develop another method for investigating SV turnover as it relates to epileptogenic cells. Dextrans have previously been reported as markers of endocytosis of large vacuoles in retinal bipolar cells (Holt *et al*., 2003), and in snake motor boutons (Teng *et al*., 2007), so it was decided to further investigate these properties with a view to developing and characterising an assay for bulk endocytosis in our culture system.

3.3.2 SYNAPTIC LOCALISATION OF INTERNALISED DEXTRAN PUNCTA.

As expected, when the dextran loaded images were overlaid with their corresponding FM loaded image, the vast majority of dextran loaded puncta co-localise with FM1-43, showing that the internalised dextrans are synaptically localised, and thus are being internalised during SV membrane retrieval.

Interestingly, occasionally the dextran seems to be surrounded by FM dye, rather than the 2 labelling the exact same location. This is probably due to the size of the internalised dextran, as the bulk endosomes are likely to physically displace the FM labelled SVs occasionally. This fits with the observation made in the retinal bipolar cell, where FM1-43 taken up into small vesicles did not appear in the large vacuoles labelled with dextran (Holt *et al*., 2003). Observing this in our culture system provides additional proof that the dextran endocytosed compartments are separate from the FM dye as they cannot be accessed by the single vesicle loaded FM dye.

For the co-localisation images, the contrast levels have been enhanced to provide the strongest signal of both labels to show the extent of the co-localisation levels. An alternative method to show this co-localisation would be to transfect cultures with GFP/mCER tagged synaptic proteins such as sypHy, or synaptopHluorin (labelling all synaptic terminals) and then loading these transfected cultures with dextran. This would negate the necessary enhancement of FM1-43 levels, as the slightly weak FM signal is most likely caused by the physical displacement of the FM labelled SVs by the large endosomes in the relevant plane of focus. However, as a primary neuronal cell line, the CGN cultures have very low transfection efficiency. The co-localisation of FM1-43 with dextran indicates that not all synapses internalise dextran. This, combined with the low transfection efficiency, would mean that it could be extremely difficult to accrue relevant N numbers to statistically analyse this method.

3.3.3 Are the internalised dextrans able to exocytose?

When cells were stimulated 30 minutes after dextran loading, the disappearance of some puncta was noted. The puncta that disappeared did not display unload kinetics, but rather the puncta disappeared asynchronously between recording frames of 0.4 seconds duration. This fits with the observation of Coggins *et al*., who used a combination of evanescent field microscopy and membrane capacitance to study exocytosis of endosomes in retinal bipolar cells. They reported that some endosomes are capable of stimulated exocytosis, however they did not quantify what proportion of the endosome pool this represented (Coggins *et al*., 2007). This property may be due to the localisation within the synapse of the endosomes. If the endosome has been recycled to a region close to the plasma membrane, then because of proximity it may be able to utilise the exocytosis scaffolding proteins present at the membrane, allowing exocytosis of the endosome. However endosomes recycled to a region distal from the plasma membrane may be unable to do this. Measurement of the distance from the plasma membrane in electron microscopy samples of endosomes in cells loaded with HRP with identical stimulation protocols might allow investigation of this possibility.

An alternative possibility is that this releasable 10% actually represents the release of SVs that have been labelled with dextran. Heterogeneity in SV size can be quite varied, so it is possible that some of the larger vesicles are able to internalise these large dextrans. Preliminary results with 10 kDa unloading (data not shown) indicate that the percentage of dextran which is unloadable is the same for this smaller dextran as it is for the 40 kDa size dextran, indicating that this proportion of

unloadable puncta, whether they are endosomes or are large vesicles, is a consistent proportion of the total internalised pool.

3.3.4 Quantification of dextran labelling

A time course of 40 kDa dextran loading shows no obvious difference between 15 seconds, 30 seconds or 2 minutes of KCl stimulation when the mean amount of fluorescence per ROI is measured. It is possible that the size of the dextran is such that only 1 to 2 dextran molecules are internalised per bulk endocytosis event. If this were the case, then it would explain how an identical amount of fluorescence is observed between the stimulated and control conditions, as each region of interest measured is indicative of the fluorescence emitted from a similar amount of internalised dextran. However loading with the smaller 10 kDa dextran, which should allow a greater number of dextran molecules to be internalised per endocytosis event, again shows no difference between the various time points of loading. There are several possible explanations for this observation. It is possible that the 10 kDa dextran is simply no more informative than the 40 kDa dextran, and that bulk endocytosis is activated and largely complete after 15 seconds stimulation with KCl. Alternatively (or possibly in conjunction with the former reason), using the measurement of fluorescence intensity as an analysis tool is not informative enough, and another method of data analysis is necessary.

3.3.5 Immediate versus delayed application of dextran

If fission of bulk endosomes is complete during stimulation then loading of the cells with dextran following termination of stimulation should result in far fewer internalisation events, as was observed. However when quantifying this difference, using the same method of fluorescence intensity measurement showed no significant difference between cultures loaded during stimulation versus cultures loaded post stimulation, despite a visually striking difference in number of dextran puncta. This highlighted the necessity of a tailored method of analysis to assess this difference in puncta number which is not quantifiable through fluorescent intensity measurement.

3.3.6 Analysis of dextran loading by puncta count

Quantification of the average number of dextran loaded puncta per field per stimulation condition highlights significant differences between immediate versus delayed load. In order to validate this method of analysis, the mean amount of fluorescence from the ROI detected by use of thresholding was calculated for each condition. As no significant difference could be detected between immediate versus delayed load for any duration of stimulation with KCl, this proves that the most informative method of quantification of dextran internalisation is to count the internalised fluorescent puncta. Internalisation does indeed occur rapidly, which fits with the observation made in snake motor boutons, where endosomes formed rapidly, within 1-2 seconds (Teng *et al.*, 2007).

In conclusion, use of 40 kDa tetramethylrhodamine dextran is an effective assay for investigation of bulk endocytosis in CGN cultures. Strongly stimulating CGNs in the presence of 40 kDa dextran results in the internalisation of synaptically

localised, largely inert, fluorescent puncta. These internalisation events happen rapidly (within 10 seconds), and do not persist after cessation of stimulation. Although these dextrans have been used to report bulk endocytosis in several systems, no previous publications have characterised dextran internalisation as an assay for bulk endocytosis in a central nerve terminal.

4. CHARACTERISATION OF BULK ENDOCYTOSIS

4.1 INTRODUCTION

In order to maintain a pool of synaptic vesicles sufficient for neurotransmission, following exocytic collapse into the plasma membrane, synaptic vesicle (SV) membrane must be retrieved and recycled ready for another round of transmission. At least two mechanisms of endocytosis are known to occur in the synapses of central nerve terminals; clathrin-mediated endocytosis (CME) of single vesicles, and bulk endocytic retrieval of membrane sufficient for several vesicles. CME of single SVs is the dominant mechanism of vesicle retrieval following mild stimulation. A single nerve impulse triggers slow (~ 15 s) clathrin-mediated retrieval in the hippocampus (Granseth *et al*., 2006). The molecular mechanisms and accessory proteins that are involved in CME are relatively well understood, however the molecular players and triggers controlling the alternate form of endocytosis of large amounts of membrane are less well understood.

4.1.1 SPEED OF BULK ENDOCYTOSIS

Originally identified by Heuser & Reese in 1973 in the frog neuromuscular junction (NMJ), formation of endosomes was observed within 1 second of stimulation. Further studies of bulk endocytosis in the frog NMJ determined a time course in the order of several minutes (Richards *et al*., 2000), thus bulk endocytosis has traditionally been thought to equate to a slow form of SV recycling. Some studies in other model synapses support this slow time course of bulk membrane retrieval. For example the appearance of endosomes was observed in the calyx of held after 3 minutes of high potassium stimulation (de Lange *et al*., 2003). Conversely, rapid kinetics of bulk endocytosis have also been observed, which agree with the initial

observations on the speed of bulk retrieval. In snake NMJs, large fluorescent dextrans are accumulated into nerve terminals within a few second after stimulation (Teng *et al*., 2007), whilst in retinal bipolar cells the accumulation of ferritin into nerve terminals was observed within seconds of stimulation by action potentials (APs) (Paillart *et al*., 2003).

Relatively little is known about the molecular mechanisms that underlie the bulk endocytosis retrieval pathway. However it is known that the phosphatase calcineurin and the protein kinase cdk5 are required. These control the dephosphorylation and rephosphorylation respectively of the group of proteins known as the dephosphins (Evans & Cousin, 2007).

4.1.2 Possible functions of bulk endocytosis

Bulk endocytosis has been observed to occur in response to strong stimulation (Royle & Lagnado, 2003; Holt *et al*., 2003). Periods of strong stimulation increase the rate of vesicle exocytosis, which will result in the insertion of a large amount of membrane at the synaptic terminal. In order to avoid destabilizing the synapse due to this large increase in surface area, and also in order to maintain a healthy pool size of releaseable vesicles, a large and rapid amount of compensatory vesicle membrane endocytosis must occur. The time constant of CME, which has been calculated by a number of different groups to be in the order of 15 seconds (Sankaranarayanan & Ryan, 2000; Granseth *et al*., 2006; Balaji & Ryan, 2007), would not be sufficient to sustain neurotransmission during intense periods of synaptic activity. Bulk endocytosis would be a likely candidate to facilitate this compensatory endocytosis of excess SV membrane, as it would retrieve the large

amounts of membrane needed to maintain high rates of SV turnover. Capacitance measurements in the rat calyx of held have recently shown the infrequent occurrence of downward capacitance shifts after strong stimulation. This large shift in capacitance indicates the retrieval of a large chunk of membrane, and occurs rapidly after strong stimulation (Wu & Wu, 2007). This indicates that bulk endocytosis is occurring at a faster time constant then previously thought, strengthening the hypothesis that bulk endocytosis is activated rapidly in response to strong stimulation. In order to investigate this possibility, we have used a combination of imaging techniques to characterise bulk endocytosis in a central nerve terminal of the cerebellar granule neuron (CGN).

4.1.3 Visualisation of bulk endocytosis in central nerve terminals

There are several different methods used to visualise bulk endocytosis in central nerve terminals. Uptake of the fluid phase marker horseradish peroxidase (HRP) can be analysed using EM (Evans & Cousin, 2007), tetramethylrhodamine labelled dextran uptake can be used to label bulk endosomes in nerve terminals (Holt *et al*., 2003; Teng *et al*., 2007), and FM dyes can also be used to visualise bulk endocytosis events (Richards *et al*., 2000; Virmani *et al*., 2003).

Photoconversion of FM dyes has shown that FM2-10 does not label bulk endocytic structures, whereas FM1-43 labels both single synaptic vesicles and bulk endosomes (Richards *et al*., 2000). Disparities in the labelling of SV turnover at different strengths of stimulation could be used to further dissect the bulk endocytosis pathway in CGNs. Studies have used the internalisation of large tetramethylrhodamine tagged dextrans to visualise bulk endocytosis events in

goldfish retinal bipolar cells (Holt *et al*., 2003) and snake motor boutons (Teng *et al*., 2007), but not in a central nerve terminal model. We have established that these dextrans report bulk endocytosis events in CGNs (Chapter 3), and recognise the capacity of dextran assays to further analyse dissect the bulk endocytosis pathway. The strength of stimulation that activates these bulk endocytosis events, and the rate at which these events occur, is unknown. Characterisation of the physiological strength of stimulus and rate at which bulk endocytosis is activated will facilitate the further study of the molecular players and accessory proteins responsible for this form of endocytosis.

4.2 RESULTS

4.2.1 THERE IS NO DIFFERENCE BETWEEN FM1-43 AND FM2-10 LABELLING AFTER DELAYED WASHOUT AT ANY STIMULATION PARADIGM

Richards *et al*. in 2000 observed a disparity between endocytic structures labelled by FM1-43 and those labelled by FM2-10 at the frog NMJ. Photoconversion of the dyes showed that FM2-10 does not label bulk endosomes during stimulation, whereas the more "sticky" FM1-43 labels both SVs and bulk endosomes. The proposed reason is that the relative hydrophobicity of FM2-10 may be responsible for the inability of the dye to label these bulk invaginations, as FM2-10 departitions more rapidly from membranes. The rapid washout of dye from cultures after stimulation may mean that FM2-10 is washed from these bulk invaginations before they have time to fission from the plasma membrane.

In order to investigate bulk endocytosis in our culture system, we used 2 rounds of SV loading and unloading (S1 and S2) with both FM1-43 and FM2-10 (Fig 2.1). Dye was washed out from the cultures immediately after stimulation at S1, but washout was delayed for 5 minutes at S2. Dye washout was delayed in order to allow the labelling of bulk invaginations by FM2-10, as bulk endocytosis was thought to be a relatively slow process. SV turnover was quantified by measuring the fluorescence drop during the unloading stimuli (ΔS1 and ΔS2). Loading was performed at several different strengths of stimulation, in order to visualise the strength of stimulation at which bulk endocytosis is activated.

Mild stimulation does not activate the bulk endocytosis pathway (Evans & Cousin, 2007), so we began by looking at FM dye labelling of CGNs by stimulating

with 200 APs at 10Hz (Fig 4.1 **A**). Delayed washout at S2 results in twice as much dye being unloaded for both FM1-43 and FM2-10 (Fig 4.5 **A**). This additional proportion of dye uptake represents the membrane retrieval that persists after termination of stimulation. As expected no difference was seen between FM1-43 and FM2-10 labelled turnover (Fig 4.1 **B**), as SV endocytosis at this mild stimulation is only through the single SV CME route.

Next, to look at the effects of strong stimulation on SV turnover, we used a maximal loading stimulation. Stimulation with 50 mM KCl activates the maximum amount of vesicle turnover. After this strong stimulation SV membrane should now also be retrieved through bulk endosomes. Cultures were stimulated with KCl for 2 minutes to maximally label all synapses. Dye washout at S1 was immediate, whilst dye washout was again delayed at S2 to allow FM2-10 to label invaginating bulk endosomes (Fig 4.2 **A**). It was expected that a large increase would be seen in FM2-10 labelling at S2, as it would now be able to label bulk endosomes as well as the post-stimulation retrieved single vesicles. However, converse to predictions, there is no difference between labelling with FM2-10 and FM1-43 after 2 minutes stimulation with KCl (Fig 4.2 **B**). Thus there is no additional increase in loading with delayed FM2-10 washout following KCl stimulation.

There seemed to be little additional uptake of either FM1-43 or FM2-10 using a 2 minute stimulation. This suggests that most endocytosis may be complete by this stage and we were missing kinetic differences between bulk endocytosis and CME. As this strong stimulation with elevated KCl is not a physiologically relevant method of stimulation, the identical procedure was repeated using stimulation with physiologically relevant short trains of action potentials, and there is now a much

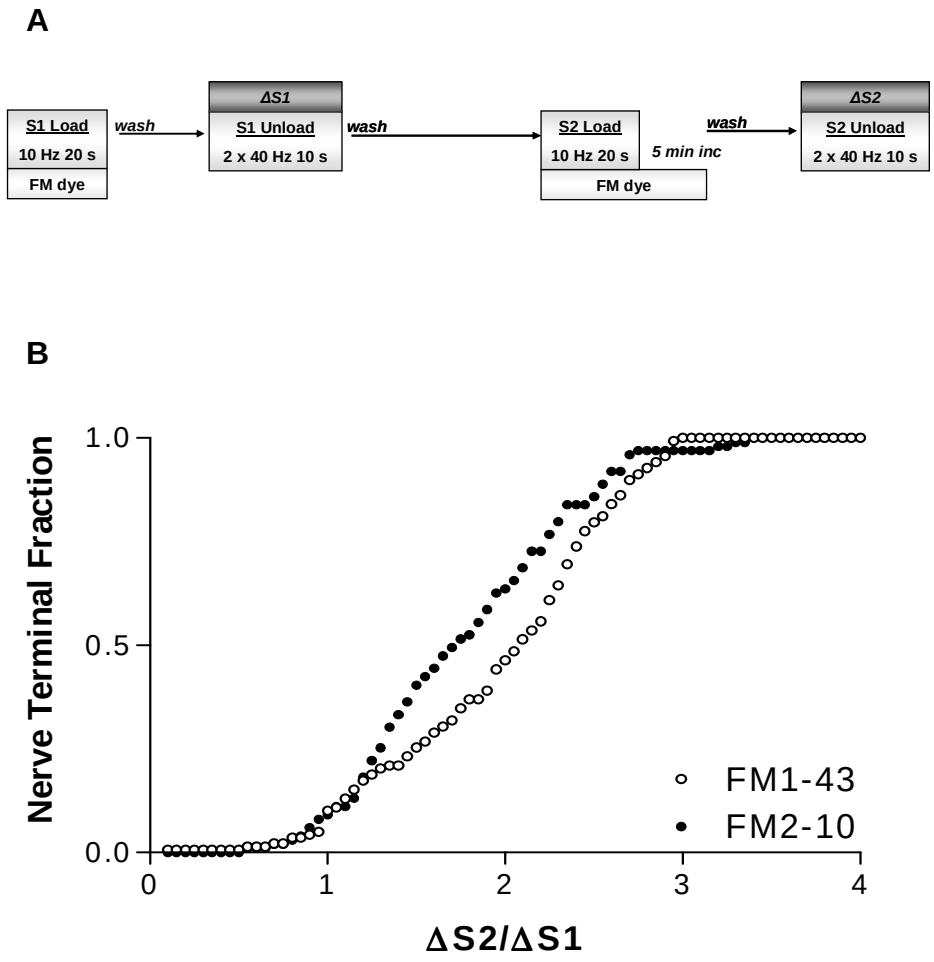

Figure 4.1 - No difference between 200 action potential evoked post-stimulation loading for FM1-43 and FM2-10. **A,** Cerebellar granule cultures were loaded with either FM1-43 or FM2-10 using stimulation with 200 action potentials delivered at 10 Hz. Dye was rinsed immediately following stimulation at S1, but dye washout was delayed for 5 minutes at S2. Dye was unloaded with two trains of 400 APs (at 40 Hz). **B**, Cumulative histogram of the effect of delayed washout on SV turnover in individual nerve terminals (ΔS2/ΔS1, 1-43 N=138, 2-10 N=99). Open symbols = FM1-43, solid =FM2-10.

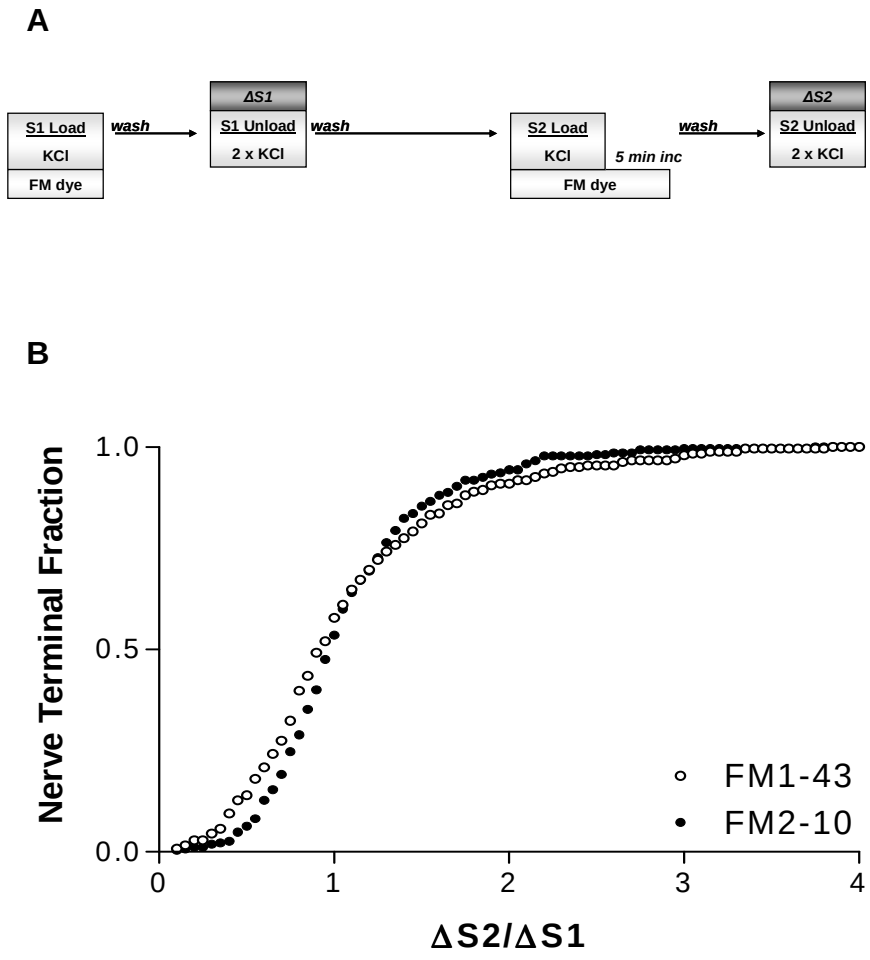

Figure 4.2 - No difference between KCl evoked post-stimulation loading for FM1-43 and FM2-10. **A,** Cerebellar granule cultures were loaded with either FM1-43 or FM2-10 using KCl stimulation. Dye was rinsed immediately following stimulation at S1, but dye washout was delayed for 5 minutes at S2. Dye was unloaded with two 30 s 50 mM KCl stimuli. **B**, Cumulative histogram of the effect of delayed washout on SV turnover in individual nerve terminals (ΔS2/ΔS1, 1-43 N=244, 2-10 N=267). Open symbols = FM1-43, solid =FM2-10.

greater component of post-stimulation uptake when 5 minutes dye incubation post-stimulation before washout was allowed. However, there is still no additional component of FM2-10 loading seen with either stimulation at 800 APs (Fig 4.3 **B)** or 400 APs (Fig 4.4 **B).**

There are several possible explanations for this observation. Firstly FM2-10 may actually in fact be labelling bulk endocytosis, contrary to previous observations. Secondly bulk endocytosis may not be activated by strong stimulation. Alternatively, bulk endocytosis may be occurring at a much more rapid rate then previously thought, with the fission of bulk endosomes complete during the period of stimulation, and all additional post-stimulation observed is occurring through the single vesicle pathway which is equally well labelled by both FM dyes. We sought to rectify which of these explanations is correct by looking at different more selective assays for bulk endocytosis.

4.2.2 Bulk endocytosis occurs rapidly, and predominantly occurs during stimulation.

Internalisation of large 40 kDa dextrans is a more direct way of visualising bulk endocytosis events. These dextrans are too large to be incorporated into single SVs, and thus selectively label bulk endosomes. We have established that dextran internalisation is stimulation dependent, and synaptically localised, and is a marker of bulk endocytosis (Chapter 3). We sought to use this dextran internalisation assay to characterise the speed of bulk endocytosis. Cultures were stimulated with action potentials, and dextran was applied either during the stimulation or for 2 minutes immediately after the stimulation (Fig 4.6). Incubation of dextran during stimulation

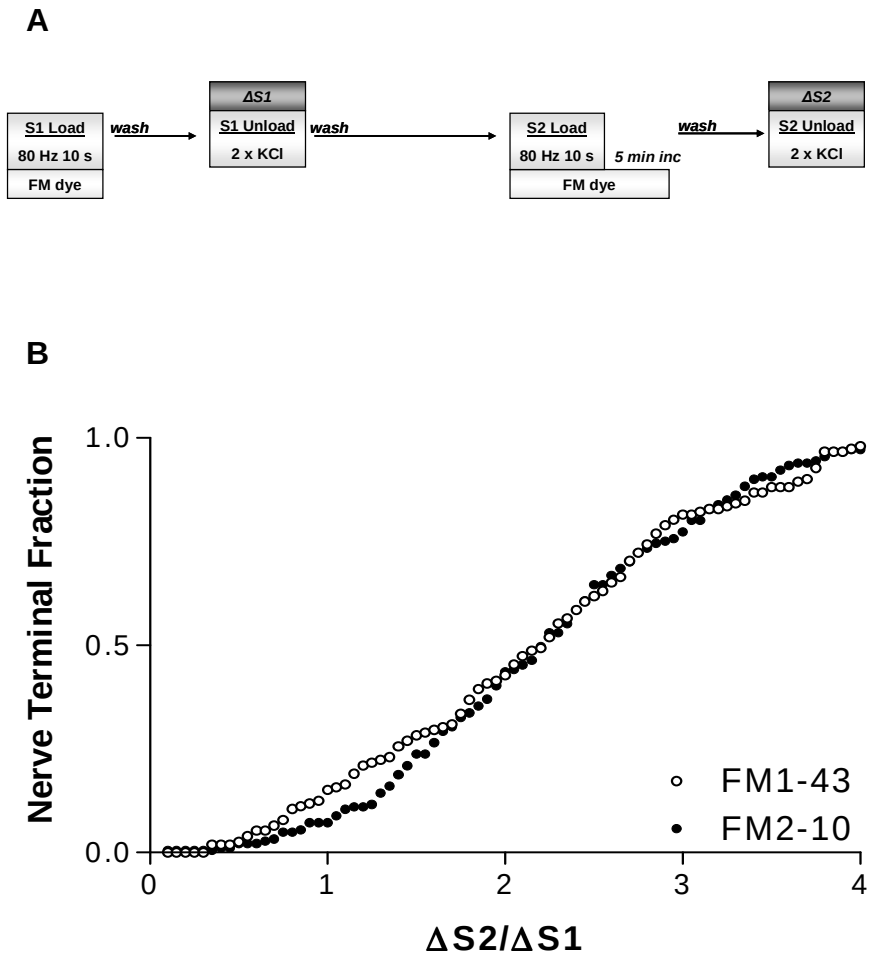

Figure 4.3 - No difference between 800 action potential evoked post-stimulation loading for FM1-43 and FM2-10. **A**, Cerebellar granule cultures were loaded with either FM1-43 or FM2-10 using stimulation with 800 APs at 80 Hz. Dye was rinsed immediately following stimulation at S1, but dye washout was delayed for 5 minutes at S2. Dye was unloaded with two 30 s 50 mM KCl stimuli. **B**, Cumulative histogram of the effect of delayed washout on SV turnover in individual nerve terminals (ΔS2/ΔS1, 1-43 N=113, 2-10 N=181). Open symbols = FM1-43, solid =FM2-10.

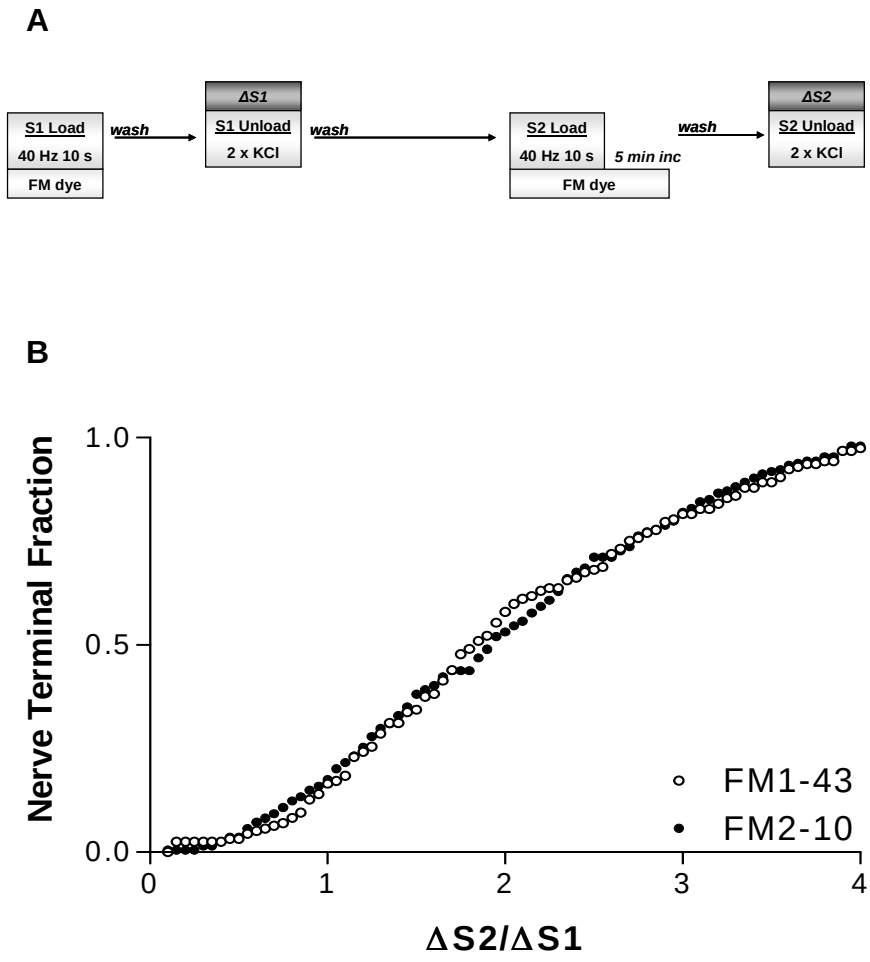

Figure 4.4 - No difference between 400 action potential evoked post-stimulation loading for FM1-43 and FM2-10. **A**, Cerebellar granule cultures were loaded with either FM1-43 or FM2-10 using stimulation with 400 action potentials at 40 Hz. Dye was rinsed immediately following stimulation at S1, but dye washout was delayed for 5 minutes at S2. Dye was unloaded with two 30 s 50 mM KCl stimuli. **B**, Cumulative histogram of the effect of delayed washout on SV turnover in individual nerve terminals (ΔS2/ΔS1, 1-43 N=145, 2-10 N=191). Open symbols = FM1-43, solid =FM2-10.

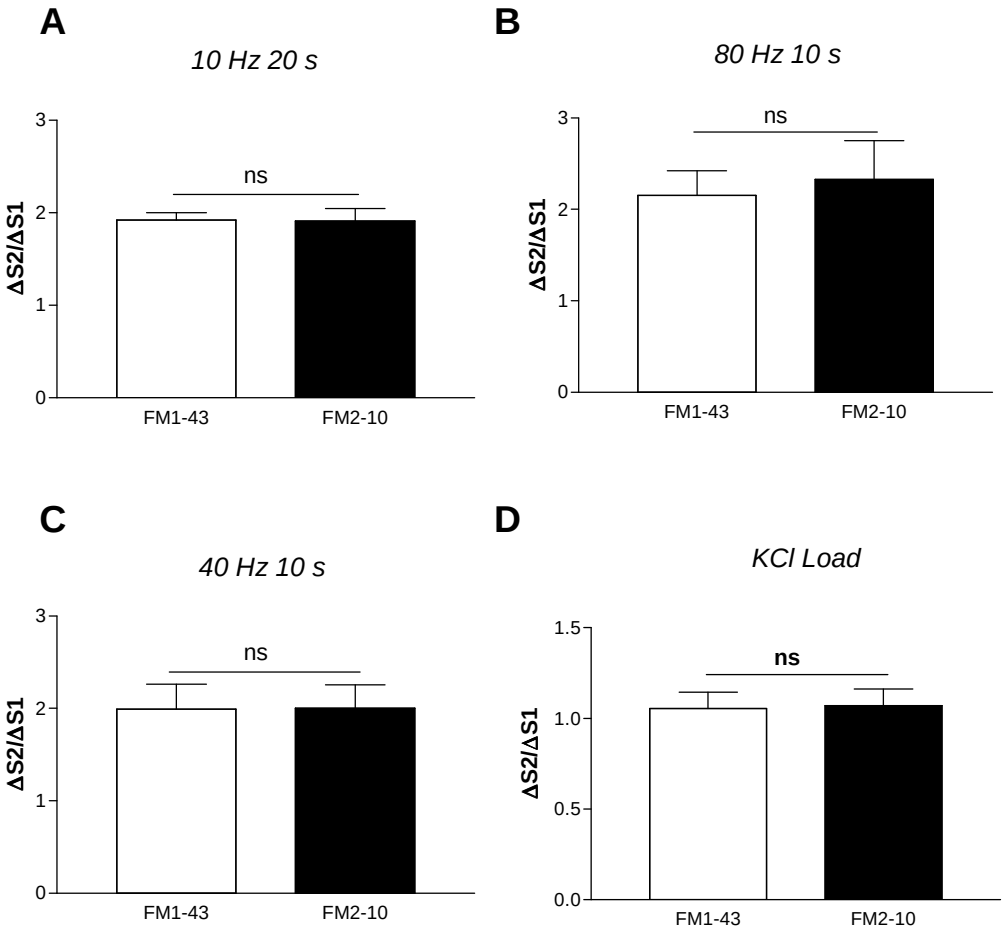

Figure 4.5 - No difference between post-stimulation loading for FM1-43 and FM2-10 with any stimulation paradigm. Bar charts represent the mean proportion of SV turnover (mean ΔS2/ΔS1 ± SEM) for FM1-43 and FM2-10 labelled cultures. For all graphs data was collated from the experiments described in previous figures. **A**, 10 Hz 20 s loaded cultures. (FM1-43 N=3, FM2-10 N=3). **B**, 80 Hz 10 s loaded cultures. (FM1-43 N=4, FM2-10 N=4). **C**, 40 Hz 10 s loaded cultures. (FM1-43 N=3, FM2-10 N=3). **D**, KCl loaded cultures. (FM1-43 N=3, FM2-10 N=3). All experiments analysed with unpaired T test.

of 200 APs at 10 Hz results in no dextran loading (Fig 4.6 **A**), confirming that bulk endocytosis does not occur as a response to this mild stimulation. However when the cultures were challenged with stimuli of 400 APs (at 40 Hz) (Fig 4.6 **C**) and 800 APs (at 80Hz) (Fig 4.6 **E**) a large increase in the number of internalised puncta was observed (Fig 4.7 **A**). This showed that bulk endocytosis is activated by strong physiological stimulation. Delayed addition of dextran, for the 2 minutes directly after stimulation, did not result in a significant labelling with dextran at any of the stimulation frequencies (Fig 4.7 **B**). Thus bulk endocytosis does not persist after termination of stimulation. The mean fluorescence intensity per ROI was also compared, in order to confirm that the method of analysis by puncta count is the correct way to approach the analysis. As when previously analysed, no difference in mean amount of fluorescence were detected between cultures loaded with dextran either during or after stimulation at any of the stimulation frequencies used (Fig 4.8).

As was seen with the 40 kDa dextran, stimulation with 200 APs results in very little internalisation of 10 kDa dextran, indicating that bulk endocytosis is not active following this mild stimulation (Fig 4.9 **A**). A significant increase in the number of internalised puncta is observed when 10 kDa dextran is applied during stimulation of the cells with either 400 or 800 APs (Fig 4.9 **C** & **E,** Fig 4.10 **A**). Again, incubation of the cultures with dextran post-stimulation results in internalisation of very few dextran puncta (Fig 4.10 **B**). We also again looked at the mean amount of fluorescence from each ROI, in order to provide the final definite proof that puncta count is the best way to analyse the quantity of dextran loading. There is no significant difference between the mean amount of fluorescence per ROI

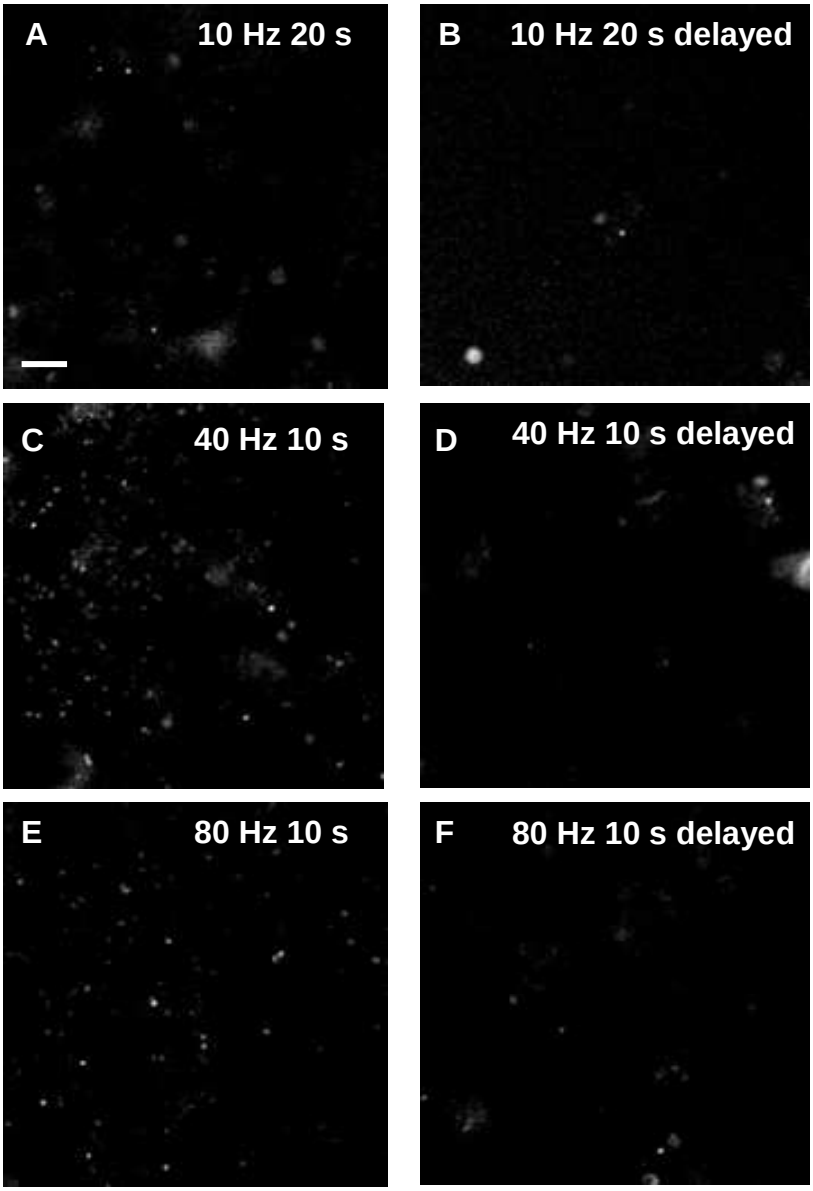

Figure 4.6 - Immediate and delayed loading of 40 kDa dextran evoked by action potential stimulation. Representative pictures of culture labelled with 40 kDa dextran loaded either during stimulation or for 2 minutes post-stimulation. Loading with 200 APs during (**A**) or post-stimulation (**B**), 400 APs during (**C**) or post-stimulation (**D**), or 800 APs during (**E**) or post-stimulation (**F**). Scale bar 25 µm.

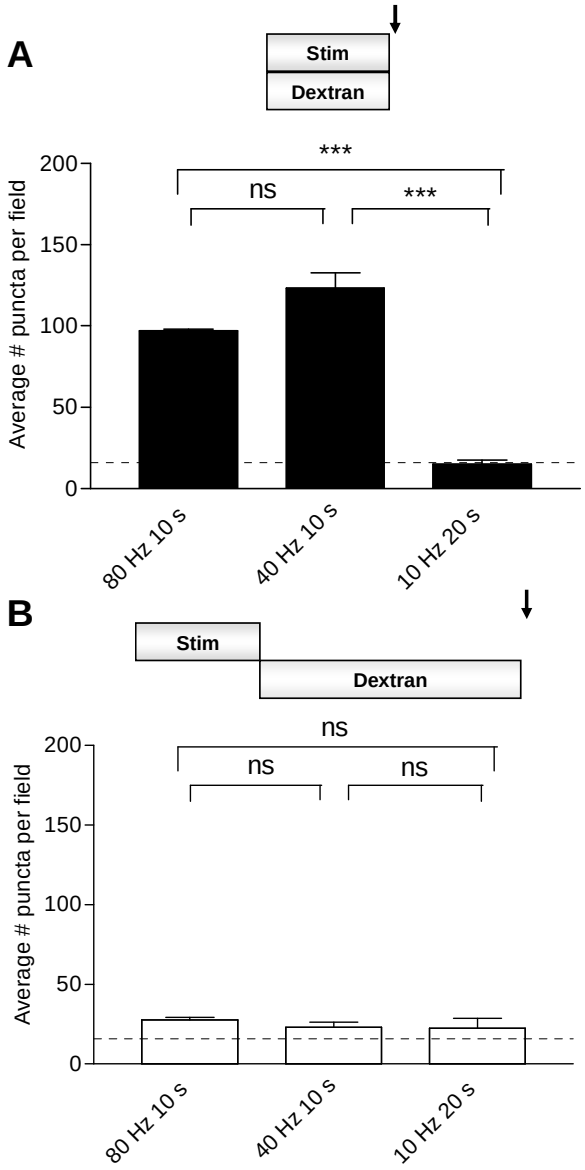

Figure 4.7 - Quantification of immediate and delayed loading of 40 kDa dextran evoked by action potential stimulation. The average number of puncta loaded per field ± SEM is shown for cultures loaded both during (**A**, closed bars) or after (**B**, open bars) stimulation. The hatched line represents the puncta count attributable to intrinsic fluorescence in the absence of dextran. For all experiments N=3, with at least 5 fields per experiment. One-way ANOVA, ns = $p>0.05$, *** $p = < 0.001$.

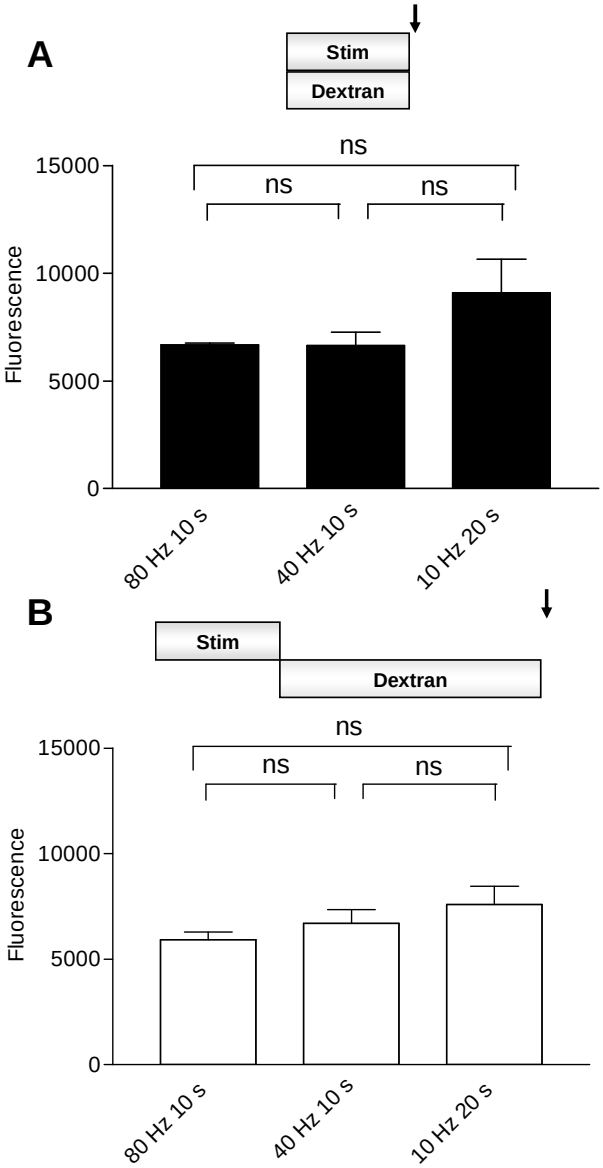

Figure 4.8 - Quantification of immediate and delayed loading of 40 kDa dextran evoked by action potential stimulation. The average fluorescence of dextran-loaded puncta per field ± SEM is shown for cultures loaded both during (**A**, closed bars) or after (**B**, open bars) stimulation. For all experiments N=3 with at least 5 fields per experiment. Experiments were analysed with a one-way ANOVA.

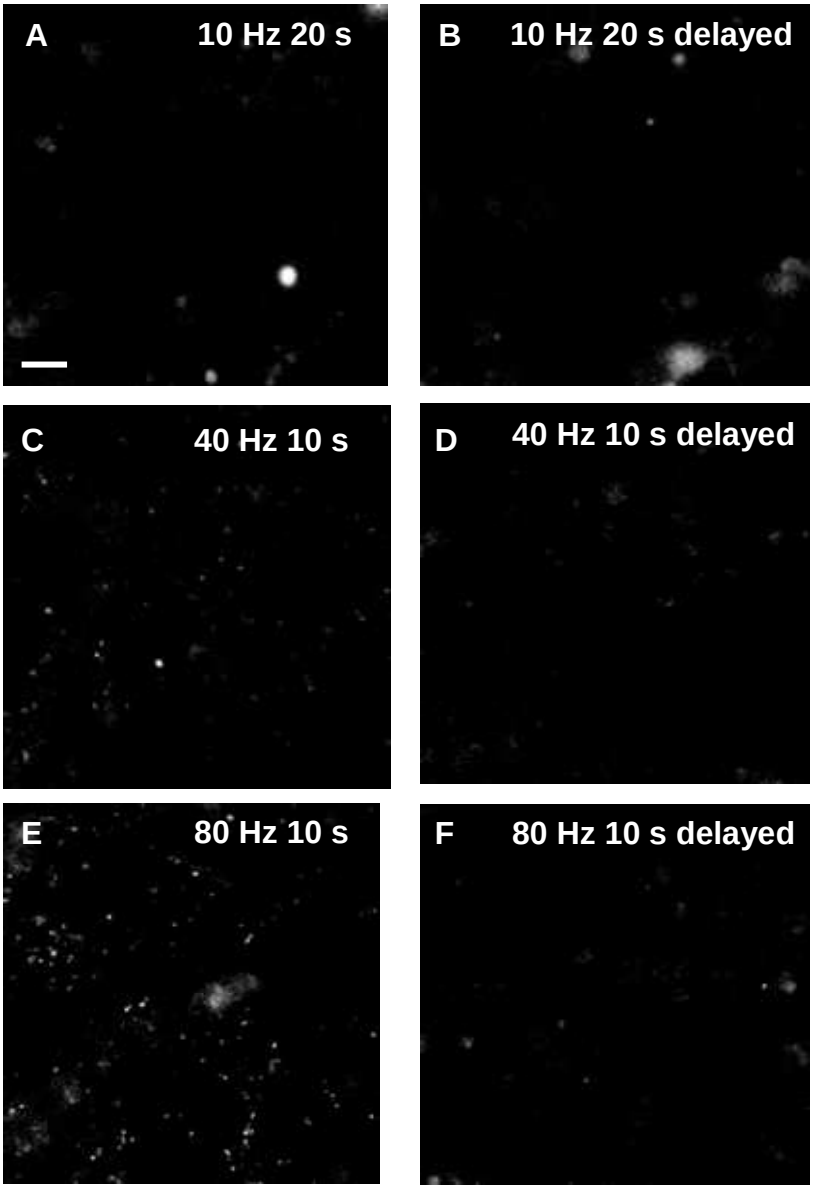

Figure 4.9 - Immediate and delayed loading of 10 kDa dextran evoked by action potential stimulation. Representative pictures of culture labelled with 10 kDa dextran loaded either during stimulation or for 2 minutes post-stimulation. Loading with 200 APs during (**A**) or post-stimulation (**B**), 400 APs during (**C**) or post-stimulation (**D**), or 800 APs during (**E**) or post-stimulation (**F**). Scale bar 25 µm.

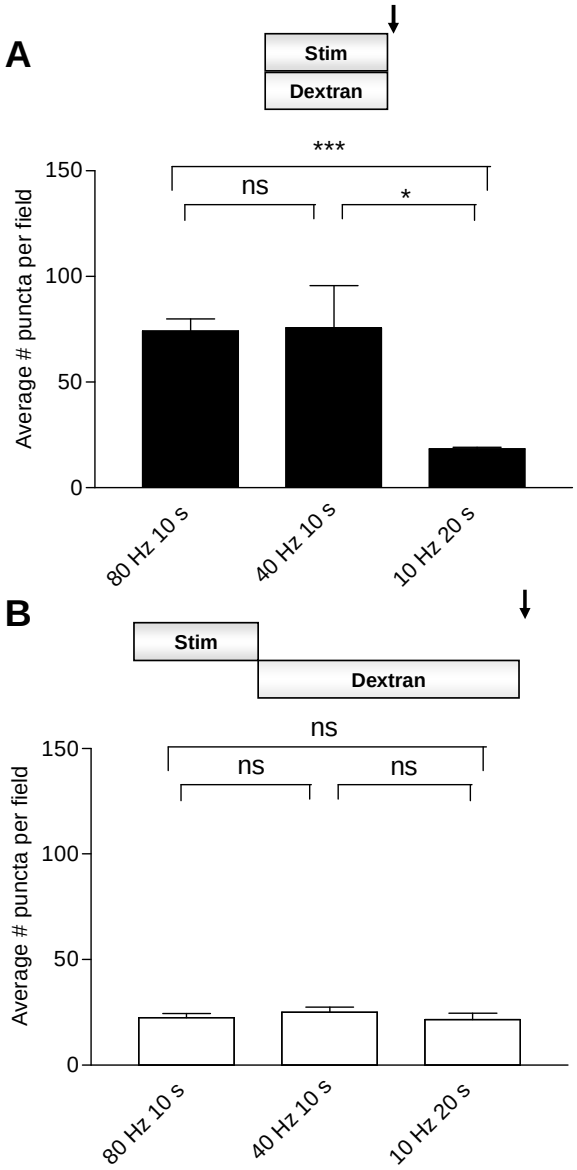

Figure 4.10 - Quantification of immediate and delayed loading of 10 kDa dextran evoked by action potential stimulation. The average number of puncta loaded per field ± SEM is shown for cultures loaded both during (**A**, closed bars) or after (**B**, open bars) stimulation. For all experiments N=3 with at least 5 fields per experiment. One-way ANOVA, ns = p>0.05, *** p = < 0.001, * p = < 0.05.

in cultures loaded during stimulation compared to cultures loaded after stimulation, at any stimulation frequency (Fig 4.11).

The quantification of dextran internalisation during stimulation compared to after stimulation suggests that bulk endocytosis occurs much more rapidly then previously thought, and that bulk endocytosis as a mechanism of SV membrane retrieval does not persist to any degree after the termination of stimulation.

This observation is supported by analysis of cultures labelled with the fluid phase marker HRP, which enables analysis of cultures at the level of the individual nerve terminal. Mild stimulation with 200 APs resulted in the formation of very few HRP labelled endosomes (Fig 4.12 **A**) whilst stronger stimulation with 400 (Fig 4.12 **C**) or 800 (Fig 4.12 **E**) APs resulted in the appearance of large numbers of endosomes (Fig 4.13 **A**). Application of HRP post-stimulation with any of the different strengths of stimulation (Fig 4.12 **B, D, F**) resulted in the labelling of very few endosomes (Fig 4.13 **B**), again indicating that endosomes are formed during periods of strong stimulation, and that retrieval by bulk endocytosis is largely complete during the stimulation.

Retrieval by single SV is the predominant method of retrieval during mild stimulation; however the number of SVs being retrieved during stimulation does not significantly increase as the strength of stimulation increases (Fig 4.13 **C**). This indicates that this pathway may rapidly become saturated (Sankaranarayanan & Ryan, 2000). When the number of single SVs being retrieved following stimulation is investigated a large number of HRP labelled vesicles are observed (Fig 4.13 **D**). Thus the main pathway of retrieval post-stimulation is the single SV pathway, whilst bulk endocytosis is the predominant method of retrieval during strong stimulation.

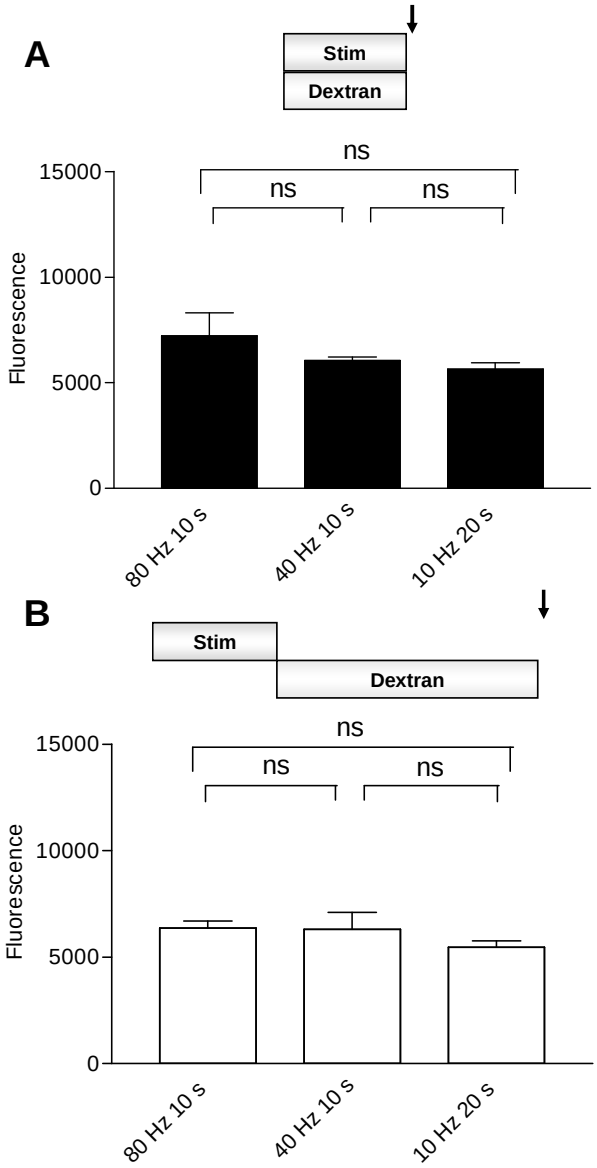

Figure 4.11 - Quantification of immediate and delayed loading of 10 kDa dextran evoked by action potential stimulation. The average fluorescence of dextran-loaded puncta per field ± SEM is shown for cultures loaded both during (**A**, closed bars) or after (**B**, open bars) stimulation. For all experiments N=3 with at least 5 fields per experiment. Experiments were analysed with a one-way ANOVA.

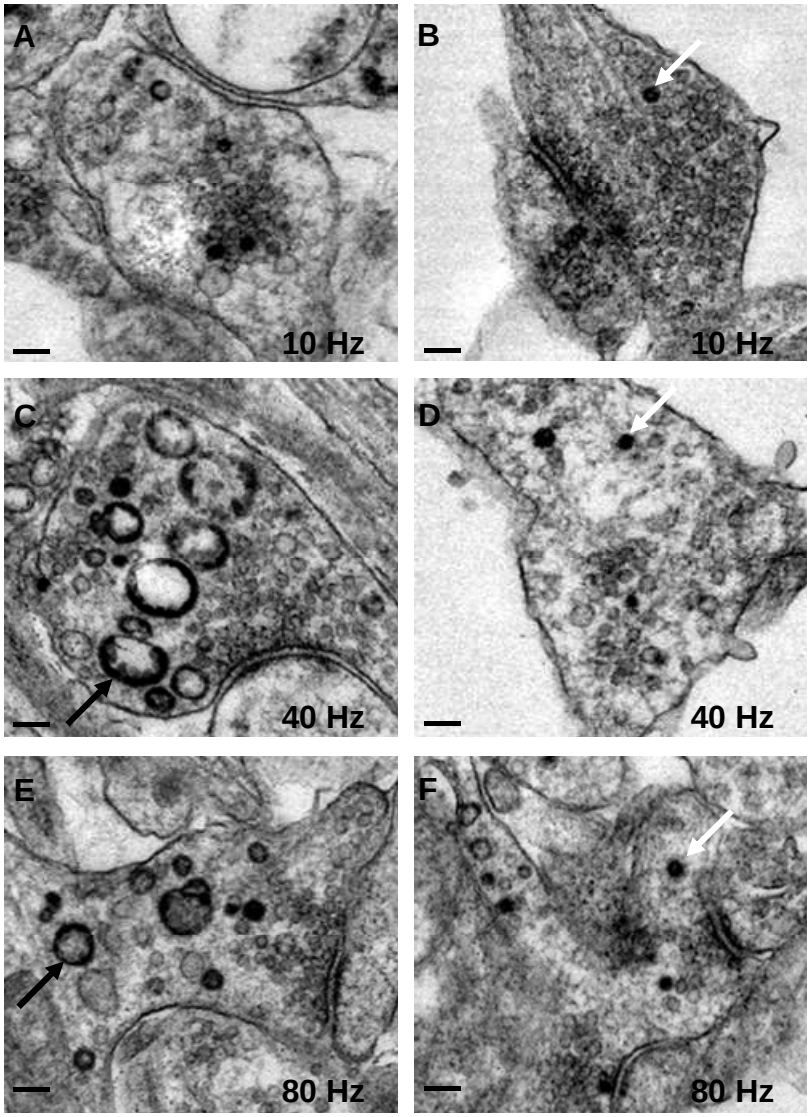

Figure 4.12 - Representative EM pictures of HRP labelled nerve terminal during and after stimulation. HRP was applied to cultures during trains of 200 (**A**; 10 Hz), 400 (**C**; 40 Hz), or 800 (**E**; 80Hz) APs and then immediately fixed. Alternatively, HRP was applied to cultures for 5 min immediately after trains of 200 (**B**; 10 Hz), 400 (**D**; 40 Hz), or 800 (**F**; 80 Hz) APs and then fixed. Black arrows indicate HRP-labelled endosomal structures, white arrows indicate HRP-labelled SVs. Scale bars, 100 nm.

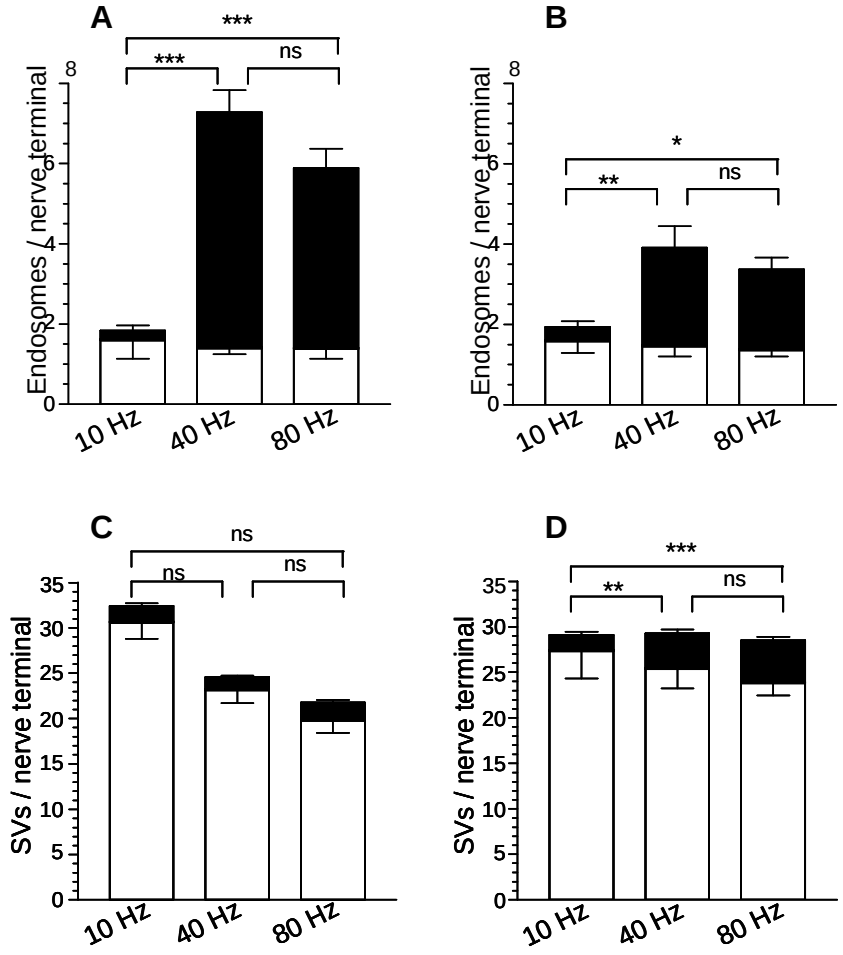

Figure 4.13 - Quantification of HRP labelled SVs and endosomes labelled both during and after stimulation. Mean number ± SEM of either HRP-labelled (solid bars) or clear (open bars) endosomes (**A**) or SVs (**B**) generated during stimulation is displayed (200 action potentials, *n*=17 nerve terminals; 400, *n*= 26; 800, *n*=53). Mean number ± SEM of either HRP-labelled (solid bars) or clear (open bars) endosomes (**C**) or SVs (**D**) generated after stimulation is displayed per nerve terminal (200 action potentials, *n*=18 nerve terminals; 400, *n*=39; 800, *n*=38). * = $p<0.05$, ** = $p<0.01$, *** = $p<0.001$, one-way ANOVA for HRP structures.

4.2.3 FM2-10 DOES NOT LABEL THE BULK ENDOCYTOSIS PATHWAY

Since FM labelling is an indirect method of examining bulk endocytosis, we next sought to determine whether FM1-43 and not FM2-10 could label the endocytosis pathway activated by 400 APs. In order to confirm the selectivity of bulk endosome labelling by FM dyes, we loaded our cultures first with mild stimulation at S1 (200 APs at 10 Hz to label the single SV route of retrieval), and then with a stronger stimulus at S2 (400 APs at 40 Hz to activate retrieval by bulk endocytosis) (Fig 4.14 **A**). Dye was immediately washed out after both S1 and S2 loading stimuli, and SV turnover as reported by both FM1-43 and FM2-10 was then compared. As expected, at S2 a large increase in turnover is seen when FM1-43 is used to label the cultures, compared to FM2-10 (Fig 4.14 **B**). This reflects the ability of FM1-43 to label the bulk pathway activated due to stronger stimulation. No additional dye unloading at S2 is observed when the cultures are labelled with FM2-10, indicating that FM2-10 is not labelling any extra SVs, despite the increased stimulus. We know that this stronger stimulus actives the bulk pathway immediately (Fig 4.6 **C**, Fig 4.7 **A**, Fig 4.9 **C**, Fig 4.10 **A**). Thus FM2-10 is not reporting the extra amount of membrane retrieval, which is mediated by bulk endocytosis. Dye turnover is equivalent for FM2-10 at S1 and S2 as the dye is only labelling the single vesicle pathway, which is retrieving comparable amounts of SV membrane via the single SV route during mild or stronger stimulation. Thus in agreement with the EM data, FM2-10 definitively does not label bulk endosomes in CGN cultures meaning this assay is a useful assay to determine the extent of bulk endocytosis.

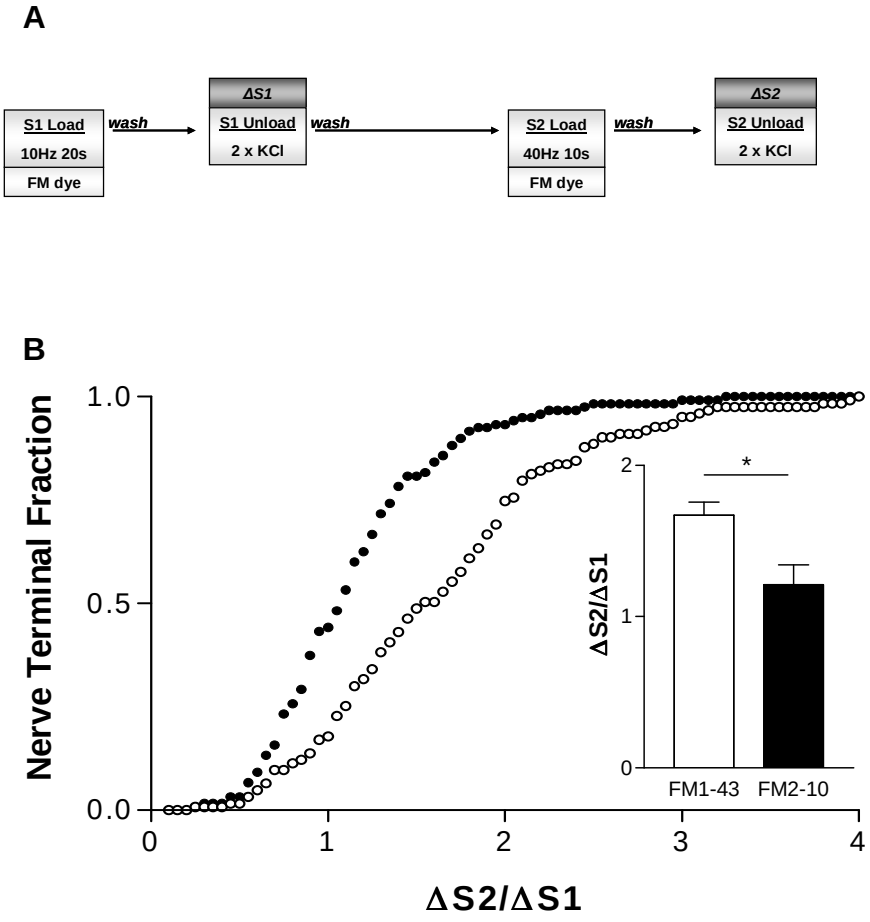

Figure 4.14 - FM1-43 selectively labels an additional endocytosis pathway during strong stimulation. **A**, Cultures were incubated with FM dyes during mild stimulation of 200 APs at 10Hz for S1, and with a stronger stimulation of 400 APs at 40 Hz at S2. Dye was washed from the cells immediately after stimulation. Unloading was stimulated with 2 sequential 30 s stimuli of 50 mM KCl. **B**, Cumulative histogram of the ratio of dye turnover (ΔS2/ΔS1). Open symbols = FM1-43, N=125. Closed symbols = FM2-10, N=121. Inset is the bar chart of proportion of dye turnover (unpaired t-test, $p < 0.05$).

4.2.4 DYE CONCENTRATION DEPENDENT LABELLING OF BULK ENDOSOMES.

As delayed washout is not the reason for the inability of FM2-10 to label bulk endosomes, what is the reason for this disparity in FM dye loading? One possibility is that FM1-43 has a higher affinity for bulk endosome membrane then FM2-10. If this were true then varying the concentrations of the dyes should change their ability to label the bulk retrieval pathway. Labelling of the bulk endocytosis pathway was investigated through treatment of the cultures with the calcineurin antagonist cyclosporin A (CsA) which is known to inhibit bulk endocytosis in this culture system (Evans & Cousin, 2007). Firstly the inhibition of the bulk endocytosis pathway was confirmed by repeating the observations made by Evans & Cousin in 2007, showing inhibition of the bulk endocytosis pathway when labelling with FM1-43 (Fig 4.15 **B**), but no inhibition when FM2-10 is used to label the cultures (Fig 4.16 **B**). Then the concentration of FM2-10 was increased 10 fold, in order to try and shift the probability that enough of the dye would internalise into bulk endosomes to result in a sufficient labelling of the resultant SVs which would be derived from labelled bulk endosomes. SV turnover with 10-fold FM2-10 was examined by loading with strong stimulation at S1 and S2, with the calcineurin antagonist CsA present prior to and during the S2 load (Fig 4.17 **A**). CsA inhibits the bulk endocytosis pathway, so cultures stimulated in the presence of CsA will not undergo any bulk retrieval despite being challenged with strong stimuli. When loading with 1mM FM2-10 was compared in the presence and absence of CsA, it can be seen that SV turnover is decreased when compared to the control conditions (Fig 4.17 **B**). This suggests that the control conditions are turning over more vesicles. This extra retrieval must be through the bulk pathway, which has been inhibited in the CsA

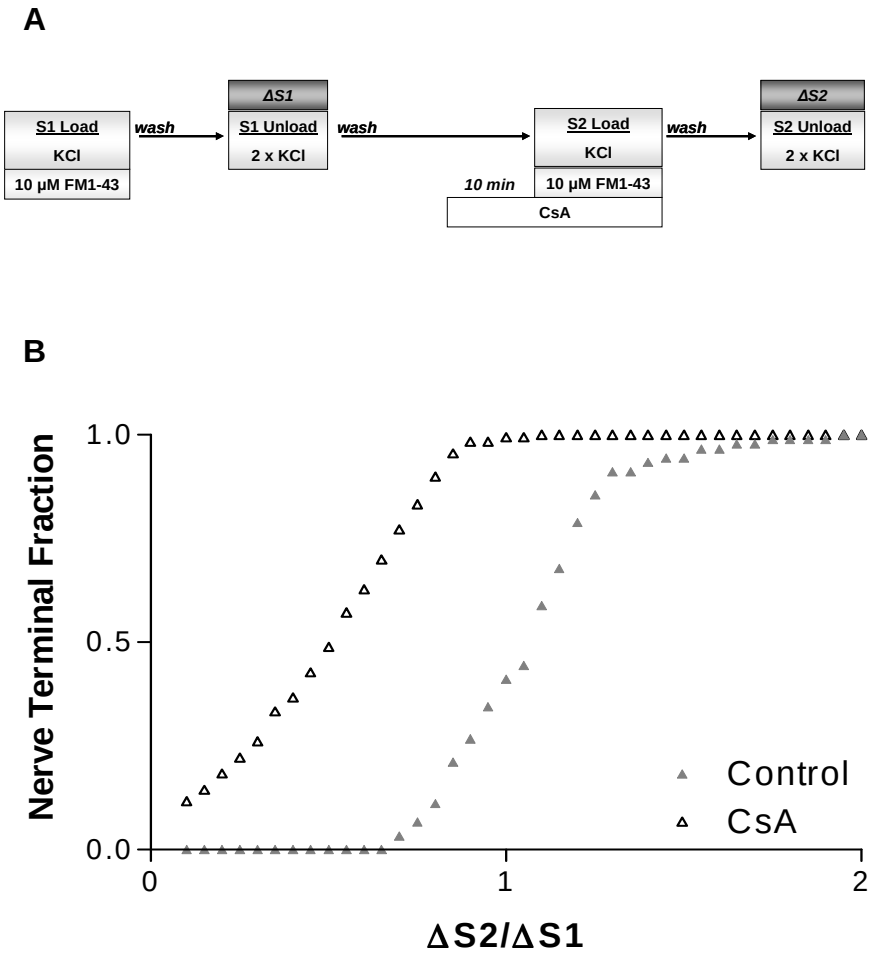

Figure 4.15 - Incubation with CsA inhibits FM1-43 uptake. **A**, Cultures were loaded with 10 µM FM1-43 during 2 minutes of stimulation with 50 mM KCl. Cultures were incubated with CsA prior to and during S2 loading. Unloading was stimulated with 2 sequential 30 s stimuli of KCl. **B**, Cumulative histogram of the ratio of dye turnover (ΔS2/ΔS1) in the presence and absence of CsA. Grey triangles = control, N=90, open triangles = CsA, N=180.

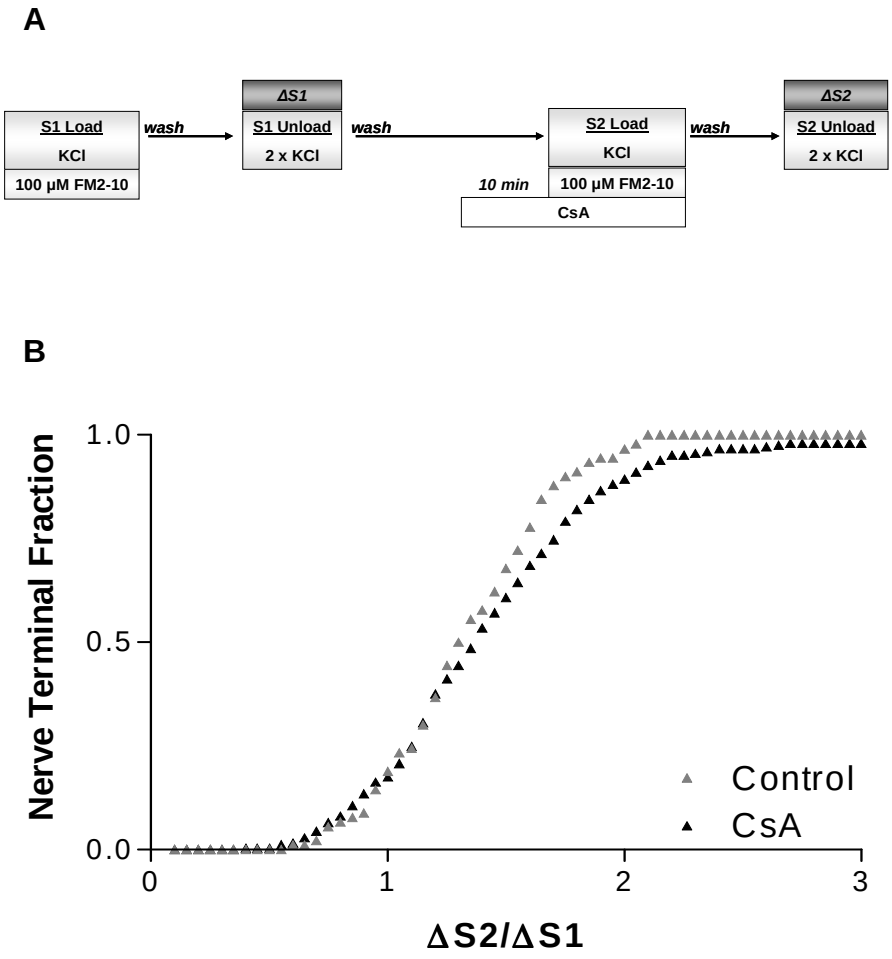

Figure 4.16 - Incubation with CsA does not inhibit FM2-10 uptake. **A**, Cultures were loaded with 100 µM FM2-10 during 2 minutes of stimulation with 50 mM KCl. Cultures were incubated with CsA prior to and during S2 loading. Unloading was stimulated with 2 sequential 30 s stimuli of KCl. **B**, Cumulative histogram of the ratio of dye turnover (ΔS2/ΔS1) in the presence and absence of CsA. Grey triangles = control, N=90, open triangles = CsA, N=245.

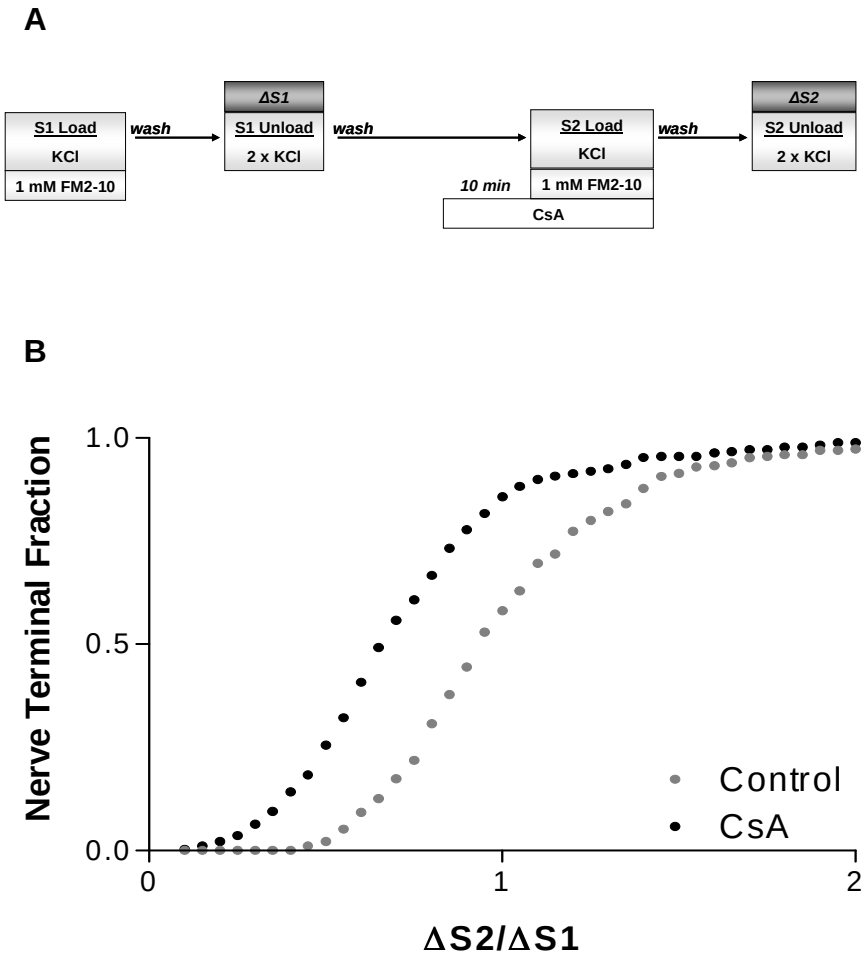

Figure 4.17 - Labelling of bulk endocytosis by FM2-10 is dependent on its loading concentration. **A**, Cultures were loaded with 1 mM FM2-10, 10 times the normal loading concentration, during 2 min 50 mM KCl. Cultures were incubated with CsA prior to and during S2 loading. Unloading was stimulated with 2 sequential 30 s stimuli of KCl. **B**, Cumulative histogram of the ratio of dye turnover (ΔS2/ΔS1) in the presence and absence of CsA. Grey symbols = control, N=270, closed symbols = CsA, N=360.

treated cultures. Thus by greatly increasing the concentration of dye used for loading the cultures it is possible to label bulk endosomes with FM2-10.

If increasing the concentration of FM2-10 10 fold allows the dye to label bulk endosome, can the converse be true for FM1-43? Does reducing the amount of dye loaded 10-fold result in a loss in ability to label the bulk endocytosis pathway for FM1-43? We used the same protocol, loading with strong stimuli, washing immediately at S1 and S2, and including a bulk endocytosis inhibitor CsA prior to and during the S2 load (Fig 4.18 **A**). As expected, reducing the amount of FM1-43 resulted in no inhibition of labelling by CsA (Fig 4.18 **B**). In fact the amount of loading appears to be slightly increased in the CsA treated cultures compared to control. Thus the ability of FM dyes to label bulk endocytosis is due to their affinity and not to their washout properties. Furthermore the concentration of dye used when looking at the labelling of the bulk endocytosis pathway is critically important to the interpretation of the imaging data.

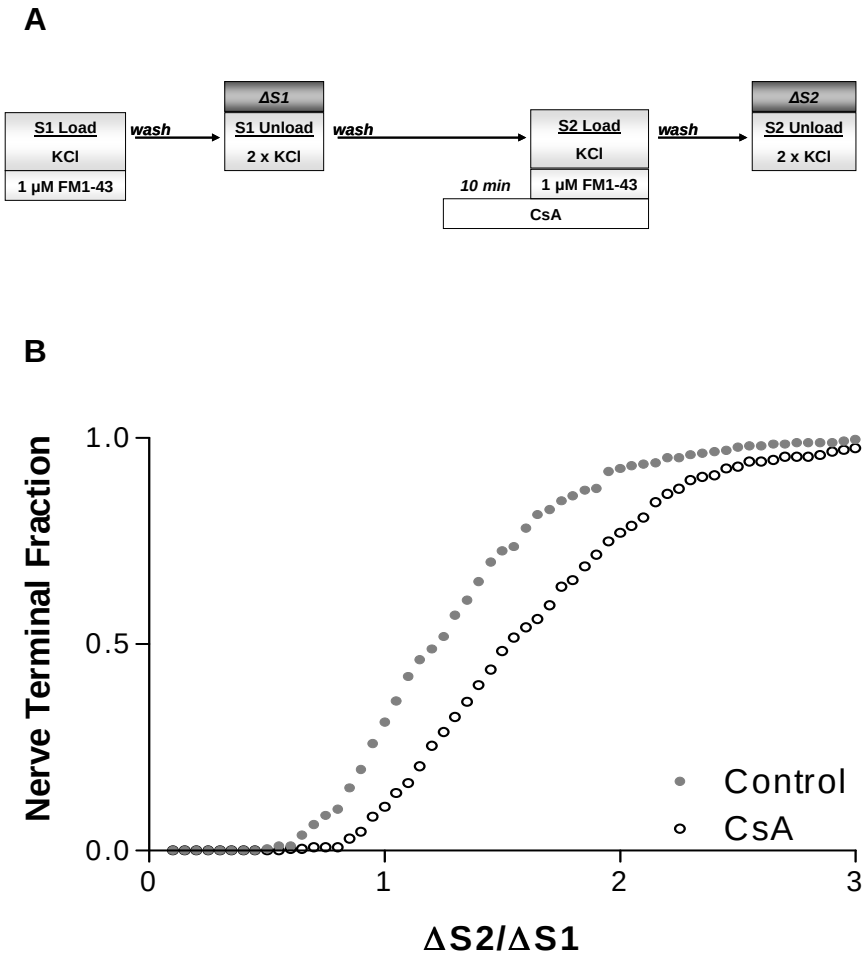

Figure 4.18 - Labelling of bulk endocytosis by FM1-43 is dependent on its loading concentration. **A,** Cultures were loaded with 1 µM FM1-43, one-tenth the normal loading concentration, during 2 min 50 mM KCl. Cultures were incubated with CsA prior to and during S2 loading. Unloading was stimulated with 2 sequential 30 s stimuli of KCl. **B**, Cumulative histogram of the ratio of dye turnover (ΔS2/ΔS1) in the presence and absence of CsA. Grey symbols = control, N=270, open symbols = CsA, N=244.

4.3 Discussion

Using several different approached we have shown that bulk endocytosis is triggered immediately during strong stimulation, and does not persist after termination of stimulation. Stimulation with APs and labelling with FM dyes has shown no disparity between FM1-43 and FM2-10 in the post-stimulation phase, labelling with dextrans resulted in internalisation only during stimulation, and labelling with HRP shows formation of endosomes during stimulation, whilst the major post-stimulation retrieval pathway was the single SV route. The major retrieval pathway during stimulation is bulk endocytosis, whilst CME is the major post-stimulation retrieval pathway.

4.3.1 No disparity is observed between FM1-43 and FM2-10 labelling with delayed wash-out.

Bulk endocytosis is known to occur in response to strong stimulation, but the process of bulk membrane invagination was thought to progress with a slow time constant. Surprisingly, no difference was seen between FM2-10 and FM1-43 at any of the stimulation strengths used when extra labelling time to allow FM2-10 internalisation is allowed. Bulk endocytosis in our culture system actually progresses at a much faster rate than previously thought. This agrees with the original observations about the rate of bulk endocytosis, which was seen to occur rapidly in the frog NMJ (Miller & Heuser, 1984). Other model systems have also shown a fast rate of bulk endocytosis, with dextran internalisation in retinal bipolar cells showing the formation of vacuoles within the first minute of stimulation (Holt *et al*., 2003), whilst similar studies at the snake motor bouton found that endosomes also formed

rapidly, within 1 to 2 seconds of stimulation (Teng *et al*., 2007). In CGN cultures and in isolated nerve terminals bulk endosomes were observed within 5 to 15 seconds of elevated KCl (Marxen *et al*., 1999; Leenders *et al*., 2002). Capacitance measurements in the calyx of held have shown rapid downward shifts in capacitance, correlating to rapid bulk endocytosis (Wu & Wu, 2007). Thus bulk endocytosis is activity dependent, and is rapidly triggered by this activity.

4.3.2 Bulk endocytosis is the major retrieval pathway during stimulation; single clathrin-coated SV endocytosis mediates post-stimulation retrieval.

In some cultures the bulk invaginations seen after stimulation are still connected to the plasma membrane by a thin neck (Koenig & Ikeda, 1996; Gad *et al*., 1998), or the appearance of the endosomes is that of flattened cisternae (de Lange *et al*., 2003). Although we have never seen structures of either shape in our cultures, we investigated the internalisation of 2 different sizes of dextran in case that the size of the larger dextran was restricting access through the neck of the bulk invagination. The same result was observed with both sizes of dextran, with no post-stimulation internalisation, indicating that the size or shape of the endosomes is not influencing the results.

Analyses of EM samples correlates with the dextran analysis, as very few bulk endosomes are observed when the HRP is applied post stimulation. The major pathway of retrieval is the single SV route as the number of HRP labelled SVs increases almost threefold after stimulation, with a corresponding decrease in the number of endosomes observed. This pathway can be labelled by FM dyes but not

dextrans when both are applied post-stimulation, indicating that single SVs are being retrieved.

Bulk endocytosis thus does not correspond to “slow endocytosis”, as it is rapidly activated and completed during 10 s of stimulation in our cultures. The predominant method of “slow-endocytosis” is most likely via the single SV clathrin-mediated pathway, which persists for a length of time after termination of stimulation. CME has been seen to act as the slow phase of membrane retrieval in retinal bipolar neurons, with a time constant similar to that observed in small central nerve terminals (Jockusch *et al*., 2005).

Interestingly the number of dextran loaded puncta internalised during stimulation with 400 APs appears greater than the number internalised following 800 APs stimulation (despite not being statistically significant). This is also true of the HRP labelled cultures, with more endosomes observed after 400 APs than with 800 APs. The GTPase activity of dynamin is inhibited at high concentrations of Ca^{2+} (Cousin & Robinson, 2000), within the range of Ca^{2+} concentrations found at the active zone (Liu *et al*., 1994). It is possible that the increased Ca^{2+} concentration caused by more intense stimulation results in a block in dynamin GTPase activity which results in fewer endosomes being formed at 800 APs than at 400 APs.

4.3.3 Labelling of bulk endosomes by FM dyes is dye-concentration dependent.

We have shown that FM2-10 does not label bulk endosomes either during or after strong stimulation. It was previously thought that the lack of ability of FM2-10 to label these bulk endocytic structures was due to the slow speed at which this

process occurs. It was hypothesized that FM2-10, which is more hydrophilic than FM1-43, would be washed from these structures before the fission of the invaginating neck due to its quicker rate of departitioning (Richards *et al*., 2000). However we have just shown that bulk endocytosis occurs rapidly, and that the process is predominantly complete during strong stimulation of only 10 seconds duration. What then is the real reason for this disparity in dye labelling?

To resolve this question we looked at the concentrations of FM dyes used in conjunction with a treatment known to block bulk endocytosis, to see if the concentration of the dye being used could possibly be responsible for this disparity. Our results show that FM2-10 can label the bulk endocytosis pathway when the concentration of dye used is increased ten-fold. Conversely, we have also shown that when the concentration of FM1-43 is reduced ten-fold, it loses the ability to report the bulk endocytosis pathway. Thus labelling of the bulk endocytosis pathway is not dependent on FM dye type, but rather the concentration of dye used.

What could cause this concentration-dependent labelling? The ability of FM dyes to label the bulk endocytosis pathway may be dependent on the membrane affinity of the dye. As FM2-10 departitions more rapidly from membranes, it is feasible that higher concentrations of the dye will shift the equilibrium to favour insertion in the membrane, allowing labelling of the endosomes. This difference between labelling of SV membrane and bulk endosome membrane may be due to intrinsic properties of bulk endosomes, for example lipid composition or pH. Further experiments are needed to examine the properties of the dye with differing lipid compositions and varying pHs in vitro should address this question.

Concentration of internalised dye has been shown to influence the fluorescent emission wavelength of the dye. Recently pituitary lactotroph staining with FM1-43 has shown a 25 nm range of fluorescence emission, with emission ranging from 470 – 495 nm (Johnson & Betz, 2008). However as emission from our cultures is captured with a long pass filter (>510 nm), any of this reported deviation in fluorescence wavelength will be captured, so will not interfere with the results we have observed.

These findings highlight the importance of dye concentration chosen when using FM dyes. A range of dye concentrations have been used for both dyes, ranging from 3.2 – 15 μM for FM 1-43 (Richards *et al*., 2000; Waters & Smith 2002), and 24μM to 200 μM for FM 2-10 (Richards *et al*., 2003; Klingauf *et al*., 1998). The differential labelling of cultures by these FM dyes is not dependent on their post-stimulation washout, but rather on the loading concentration used, and the relevant affinity of the dye for bulk endosome membrane after internalisation. The concentration of FM dye used should be taken into account when interpreting FM dye labelling, as the amount of dye used may have an effect on the results.

4.3.4 Bulk endocytosis is stimulation dependent and occurs rapidly

As bulk endocytosis occurs in response to elevated stimuli, a slow progression of the membrane retrieval mechanism activated at this stronger stimulation does not make sense. Strong stimulation results in large amounts of vesicle membrane being added to the synapse, greatly increasing the surface area which would be likely to destabilise the synapse. For bulk endocytosis to proceed at a slow pace would mean that this rapid increase in surface area would be slowly

countered by a retrieval of excess membrane, an inefficient method of re-stabilising the integrity of the synapse. However as we have determined, bulk endocytosis occurs rapidly, and is activity-dependent. It occurs in response to strong stimuli, where it functions in conjunction with CME. As elevated stimulation intensity triggers the bulk retrieval mechanism, and reduction of synaptic Ca^{2+} concentration inhibits rapid endocytosis (Wu *et al*., 2005), it's likely that elevated Ca^{2+} is the switch which initiates activation of the bulk retrieval pathway.

5. The Role of Dynamin I in Bulk Endocytosis

5.1 INTRODUCTION

The previous chapter establishes that bulk endocytosis is activity dependent, occurs rapidly and is largely complete during stimulation. However there is still very little known about the molecular players which are involved in this process. Clathrin-mediated endocytosis (CME) and activity dependent bulk endocytosis (ADBE) probably utilise the same endocytic proteins, however it is likely that they are regulated by different signal pathways. We used a number of different approaches to target certain interactions which could potentially be playing a role in the control of ADBE. In order to begin to understand the key proteins which regulate this process and the signals which control the switch between different forms of endocytosis, we combined bulk endocytosis assays with several interference techniques. Obvious targets for manipulation were the proteins already known to be essential for synaptic vesicle endocytosis (SVE), thus we looked at the effects of interfering with these proteins by several different methods including penetratin peptides and pharmacological inhibition.

Arguably the most important protein in SVE is the large GTPase dynamin 1. Identification of dynamin was facilitated through studies of the *Drosophila* temperature sensitive mutant *shibire*, in which endocytosis occurs normally at 19 ºC, but is reversibly blocked once the temperature is raised to 29 ºC (Koenig & Ikeda, 1989). The ability of dynamin to fission the neck of invaginating vesicles via its GTPase activity was thought to be an essential process in all forms of SVE, until the publication of recent studies in dynamin I knockout (KO) mice. Surprisingly, the KO mouse still supported minimal SVE at mild stimulation, and impairment is only seen during periods of elevated stimulation (Ferguson *et al*., 2007).

ADBE is regulated by the calcium dependent protein phosphatase calcineurin (Evans & Cousin, 2007). In synaptic terminals the rapid coordinated dephosphorylation of at least eight proteins, mediated by calcineurin in response to Ca^{2+} influx, is essential for SVE. Dynamin is constitutively phosphorylated in terminals at rest, and is rapidly dephosphorylated in response to stimuli. Following de-phosphorylation, dynamin must then be re-phosphorylated to enable further rounds of endocytosis. The major phosphorylation sites in dynamin are on serine residues 774 and 778 of the dynamin proline rich domain (PRD). Site mutagenesis of these serines has revealed that syndapin I is the phosphorylation regulated dynamin I partner for SVE (Anggono *et al*., 2006).

5.1.2 PENETRATIN PEPTIDES

The PRD of dynamin binds to the src homology 3 (SH3) domains of several proteins that function as membrane curving facilitators. Syndapin is one of three major SH3 domain containing binding partners of the dynamin PRD (the others being amphiphysin I and endophilin I). Both endophilin I and syndapin I bind the same region of the dynamin PRD, but do so in a mutually exclusive manner, indicating that the function of these proteins in SVE may differ (Anggono & Robinson, 2007). This suggests that the specific phosphorylation regulated dynamin-syndapin interaction may either be important in a particular type, or alternatively at a distinct stage, of endocytosis. Inhibition of syndapin results in a reduction in SVE induced by strong stimulation in lamprey reticulospinal synapse (Andersson *et al*., 2008). We have shown that strong stimulation rapidly activates the bulk endocytosis pathway in cerebellar granule neurons (CGNs). We therefore sought to characterise

the response of our cell culture system to strong stimuli in the presence of phospho-mimetic and phospho-null dynamin penetratin peptides which target the site of interaction between dynamin and syndapin (Anggono *et al*., 2006). Penetratin peptides are highly cationic cell-penetrating peptides, derived from the homeodomain of the *Drosophila* trans-activating factor Antennapedia. The third helix of this homeoprotein was found to be sufficient for internalisation (Derossi *et al*., 1994). These peptides translocate in an energy independent manner, as they can internalise at 4 ºC. The exact mechanism by which this translocation occurs is still unknown, however it is proposed to occur via a form of endocytosis (Lundin *et al*., 2008), as incubation of penetratin with various lipid phases can induce negative fluid membrane curvature (Lamaziere *et al*., 2008). The highly efficient translocation of peptides incorporating this penetratin sequence allows internalisation of specific peptide or oligonucleotide sequences, facilitating the study of their effects in cells.

5.1.3 Pharmacological Inhibition

As phosphorylation is an essential process in SVE, the identification of kinases novel to the SVE pathway, or specific parts thereof, would be extremely beneficial to the study of the pathway. The neuronal kinase cdk5 is known to mediate the phosphorylation of at least 3 of the de-phosphins, dynamin I, PIPKIγ and synaptojanin I (Tan *et al*., 2003; Lee *et al*., 2004; Lee *et al*., 2005); however little is known about alternative kinases involved in the re-phosphorylation of the dephosphins.

Glycogen synthase kinase 3 (GSK3) is a serine/threonine kinase which was originally characterised as the enzyme responsible for the phosphorylation and

resultant inactivation of glycogen synthase (Embi *et al*., 1980). It has subsequently been shown to function in numerous different pathways, and due to this property it has been identified as a potential therapeutic target in a hugely diverse number of diseases, such as diabetes, Alzheimer's, AIDs and schizophrenia (Bostik et al., 2001; Jope & Roth, 2006; Jope et al., 2007; Jolivalt et al, 2008) . GSK3 has 2 isoforms, GSK3α and GSK3β, which are encoded by 2 separate genes (Woodgett, 1990).

GSK3 exhibits a requisite for phosphorylation-primed substrates, recognising the primed sequence –S/TXXXS/T(P) (Fiol *et al.*, 1987). Interestingly, the phospho-box of dynamin I (which contains the major phosphorylation sites) contains the sequence S(774)PTSS(778), corresponding to the recognition sequence for GSK3. GSK3 has been implicated in the regulation of synaptic plasticity. In rat hippocampal slices, GSK3β activity is enhanced during NMDA receptor-dependent LTD, and inhibited following the induction of LTP, indicating a mechanism of action of GSK3β in mediating synaptic plasticity (Hooper *et al.*, 2007). The role of GSK3β in plasticity at the post-synaptic level indicates that the enzyme may also be of importance at the pre-synapse. GSK3 β is known to be expressed in rat cerebellum (Leroy & Brion, 1999). We opted to look at the effects of GSK3β inhibition on endocytosis in our cell culture system to see if inhibiting the action of the kinase would have any effect on SVE.

5.1.4 Small molecule cell permeable dynamin I inhibitors.

A recent development in the study of SVE was the discovery of the cell-permeable dynamin I inhibitor, dynasore, by a high throughput screen of a Chembridge library (Macia *et al.*, 2006). Treatment with dynasore results in the

accumulation of 2 different types of coated endocytic structures, both early stage U-shaped and late stage arrested O-shaped pits, suggesting that dynamin I functions at 2 distinct steps in clathrin-coat formation (Macia *et al.*, 2006). Dynasore has been reported to block endocytosis at both strong and mild stimulation in hippocampal cultures, without having any effect on exocytosis (Newton *et al.*, 2006).

Hydroxyl substitution has been used to create an analogue variant of dynasore, termed dyngo 4-a (Phil Robinson, personal communication). We investigated the effects of dynasore, plus this new dynamin I inhibitor dyngo4-a, on ADBE in our CGN culture system to determine the requirements for dynamin I GTPase activity.

By combining 3 methods of perturbation of dynamin I-mediated functions in a neuronal cell culture system; 1, Inhibition of essential interactions with penetratin-peptides, 2, inhibition of rephosphorylation by GSK3 β inhibition and 3, inhibition of dynamin I GTPase activity by small molecule cell permeable inhibitors, we sought to further elucidate some of the mechanisms controlling the switch between different forms of SVE in response to differing stimuli.

5.2 RESULTS

5.2.1 DYNAMIN PEPTIDES

In order to investigate if the phosphorylation-regulated interaction of dynamin I with syndapin I has any effect on different forms of SVE, peptide sequences specific for the phospho-box of dynamin were incubated with cells prior to and during the S2 load. These penetratin tagged peptides specifically interfere with the dynamin I-syndapin I interaction, but not that of dynamin I with either endophilin I or amphiphysin I (Anggono *et al.*, 2006). The peptide sequence incorporates the serines 774 and 778, which are the major phosphorylation sites on dynamin I. Phospho-null mutation peptides of these residues (serines 774 and 778 to alanine, $dynI_{769\text{-}784}AA$) bind to syndapin I, and interrupt the dynamin I-syndapin I interaction in vivo, whilst the corresponding phospho-mimetic mutations (serines 774 and 778 to glutamate, $dynI_{769\text{-}784}EE$) have no effect as they do not bind syndapin (Anggono *et al.*, 2006).

To determine the effect of the dynamin I-syndapin I interaction on ADBE, cultures were labelled with FM dyes during strong physiological stimulation of 800 action potentials (APs) at 80 Hz (Fig 5.1 **A**). Incubation of $dynI_{769\text{-}784}AA$ peptides prior to and during the S2 load resulted in a block in SV turnover in cultures labelled with FM1-43 during strong physiological AP stimulation (Fig 5.1 **B**). The effects of the phospho-null peptides on FM1-43 labelling were not due to non-specific effects on exocytosis, as incubation with $dynI_{769\text{-}784}AA$ during the S2 unload (Fig 5.3 **A**) had no effect on unloading (Fig 5.3 **B**). To determine whether the block was due to residues 774/778 regulating the interaction with syndapin, the same experiment was

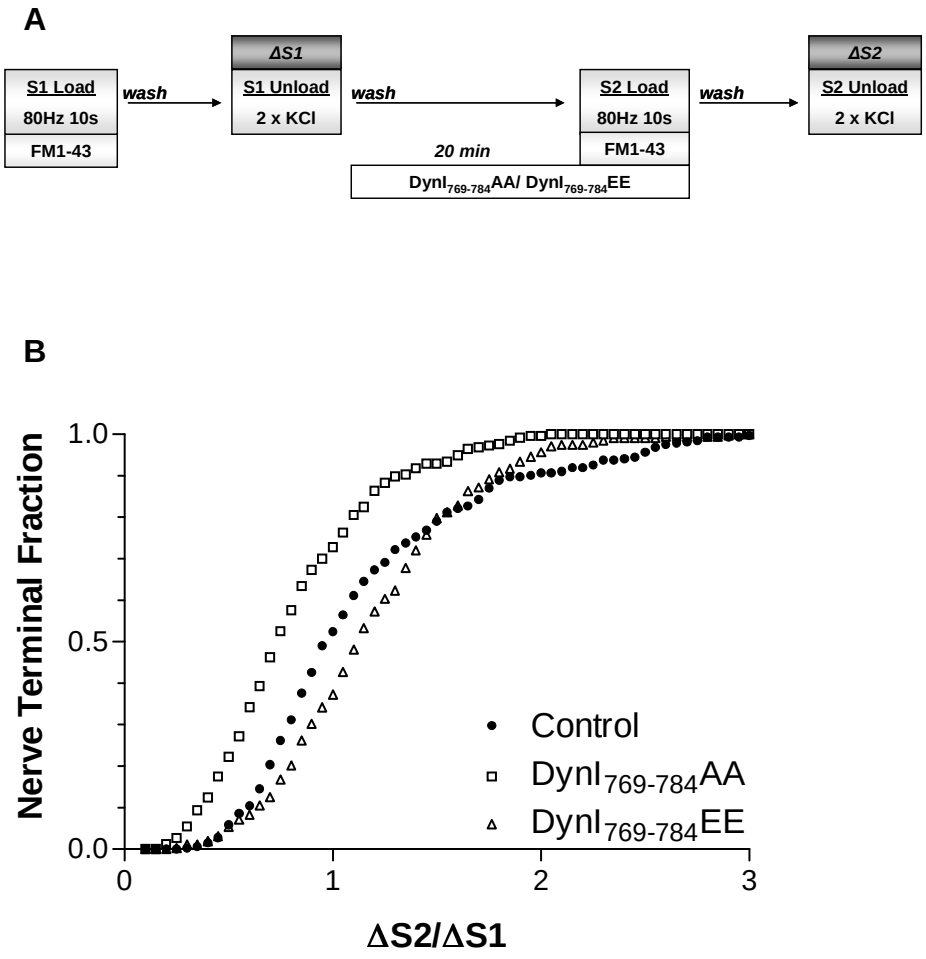

Figure 5.1- Dynl$_{769-784}$AA, but not Dynl$_{769-784}$EE, peptides block FM1-43 uptake during strong stimulation. **A,** CGNs were labelled with FM1-43 during stimulation with 800 APs (at 80 Hz) at S1 and S2. Cultures were incubated with 30 μM Dynl$_{769-784}$AA or Dynl$_{769-784}$EE for 20 minutes prior to and during the S2 load. Cells were unloaded with 2 sequential 30 s perfusions of KCl. **B.** Cumulative histogram of the extent of FM dye unloading (ΔS2/ΔS1) in individual nerve terminals. Closed circles = control, N=268, open squares = Dynl$_{769-784}$AA, N = 256, open triangles = Dynl$_{769-784}$EE, N = 351.

repeated using the dynI$_{769\text{-}784}$EE peptides. DynI$_{769\text{-}784}$EE had no effect on the amount of SV turnover with the same strength of stimulation (Fig 5.2 **B**), suggesting a selective role for the dynamin/syndapin interaction in SVE. However when the same experiments were conducted with FM2-10 instead of FM1-43, no effect was seen when cells were pre-incubated with either the dynI$_{769\text{-}784}$AA or the dynI$_{769\text{-}784}$EE peptides (Fig 5.4 **B,** Fig 5.5 **B**). Since FM2-10 does not report the bulk endocytosis pathway (Richards *et al.*, 2000), this then indicates that the phospho-null peptides are modulating the ADBE pathway. The lack of effect of the dynI$_{769\text{-}784}$AA peptides on FM2-10 uptake evoked by 800 APs suggests no role for the dynamin I-syndapin I interaction in CME.

To confirm this, cultures were mildly stimulated with 200 APs at 10 Hz (Fig 5.6 **A**), as this strength of stimulation only activates single SV retrieval by CME. Preincubation with either the dynI$_{769\text{-}784}$AA or dynI$_{769\text{-}784}$EE peptides at this strength of stimulation had no effect on SV turnover measured with FM1-43 (Fig 5.6 **B**, Fig 5.7 **B**). Thus inhibition of the dynamin I-syndapin I interaction has no effect on CME, indicating a specific function of the interaction in ADBE.

To confirm the role of the dynamin I-syndapin I interaction in ADBE, the effects of pre-incubation with the peptides on dextran uptake was examined. In agreement with the FM data, pre-incubation of cultures with the dynI$_{769\text{-}784}$AA peptide results in a significant block in the average number of dextran labelled puncta per field of view, whilst pre-incubation with the dynI$_{769\text{-}784}$EE peptide has no significant effect on dextran uptake (Fig 5.8 **C**). As dextran internalisation is a selective marker of ADBE, this provides further evidence that disruption of the dynamin I-syndapin I interaction arrests this pathway.

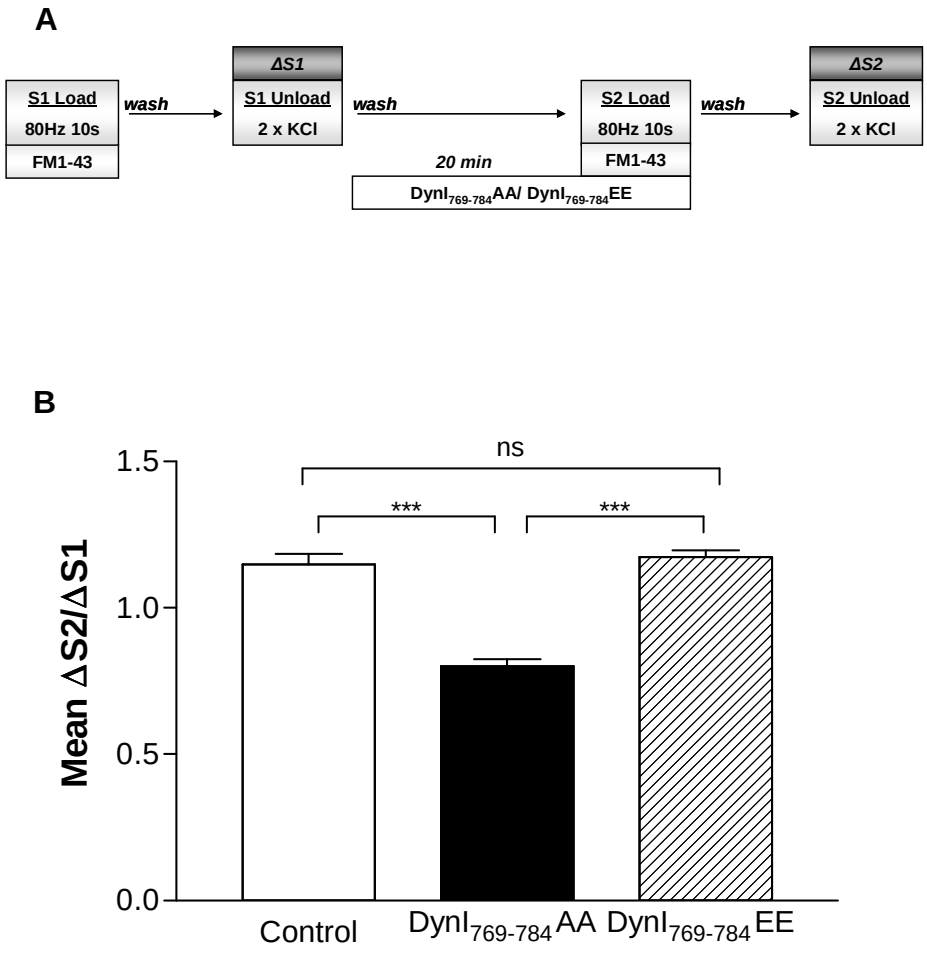

Figure 5.2 - Extent of FM1-43 dye unloading following incubation with DynI$_{769-784}$AA or DynI$_{769-784}$EE. **A,** CGNs were labelled with FM1-43 during stimulation with 800 APs (at 80 Hz) at S1 and S2. Cultures were incubated with 30 μM DynI$_{769-784}$AA or DynI$_{769-784}$EE for 20 minutes prior to and during the S2 load. Cells were unloaded with 2 sequential 30 s perfusions of KCl. **B,** Bar chart of the extent of FM dye unloading (ΔS2/ΔS1). For all N=3 ± SEM. One way ANOVA, ns = p>0.05, *** = p<0.001.

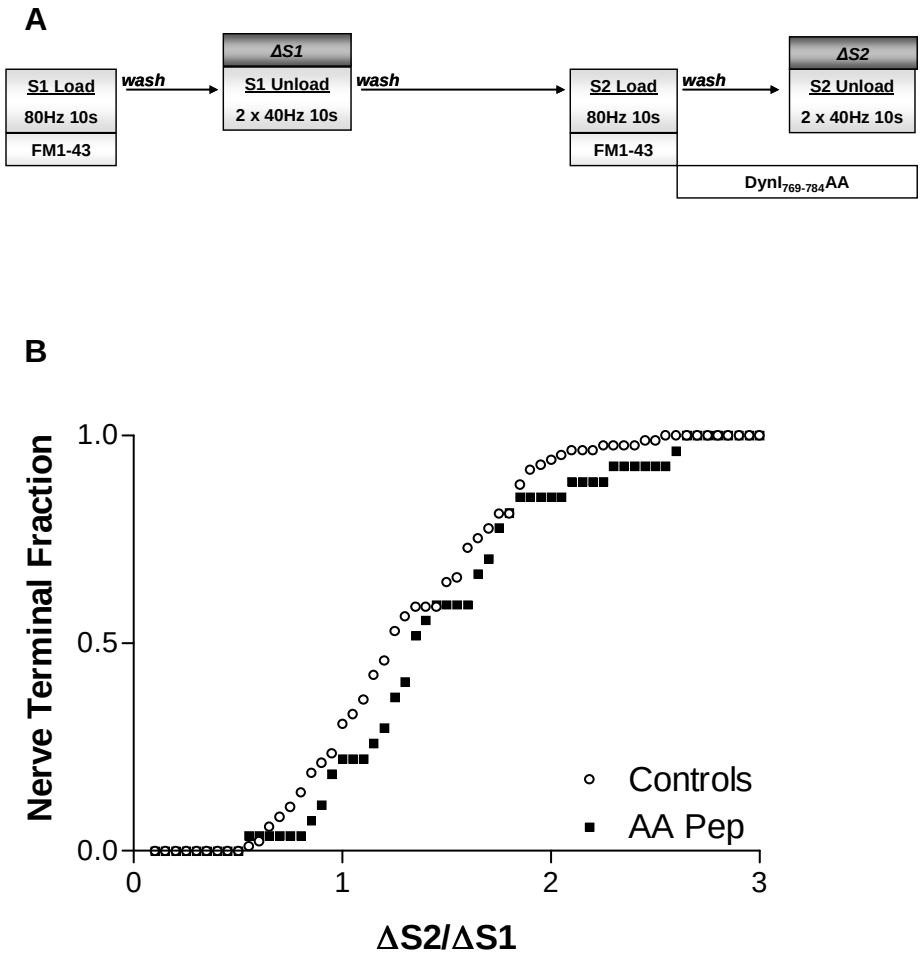

Figure 5.3 - DynI$_{769-784}$AA has no effect on FM1-43 unloading during strong stimulation. **A,** CGNs were labelled with FM1-43 during stimulation with 800 APs (at 80 Hz) at S1 and S2. Cultures were incubated with 30 μM DynI$_{769-784}$AA for 10 minutes prior to and during the S2 unload. Cells were unloaded by stimulation with 2 sequential 400 APs (at 40 Hz). **B.** Cumulative histogram of the extent of FM dye unloading (ΔS2/ΔS1) in individual nerve terminals. Open circles = control, N = 85, closed squares = DynI$_{769-784}$AA, N = 80.

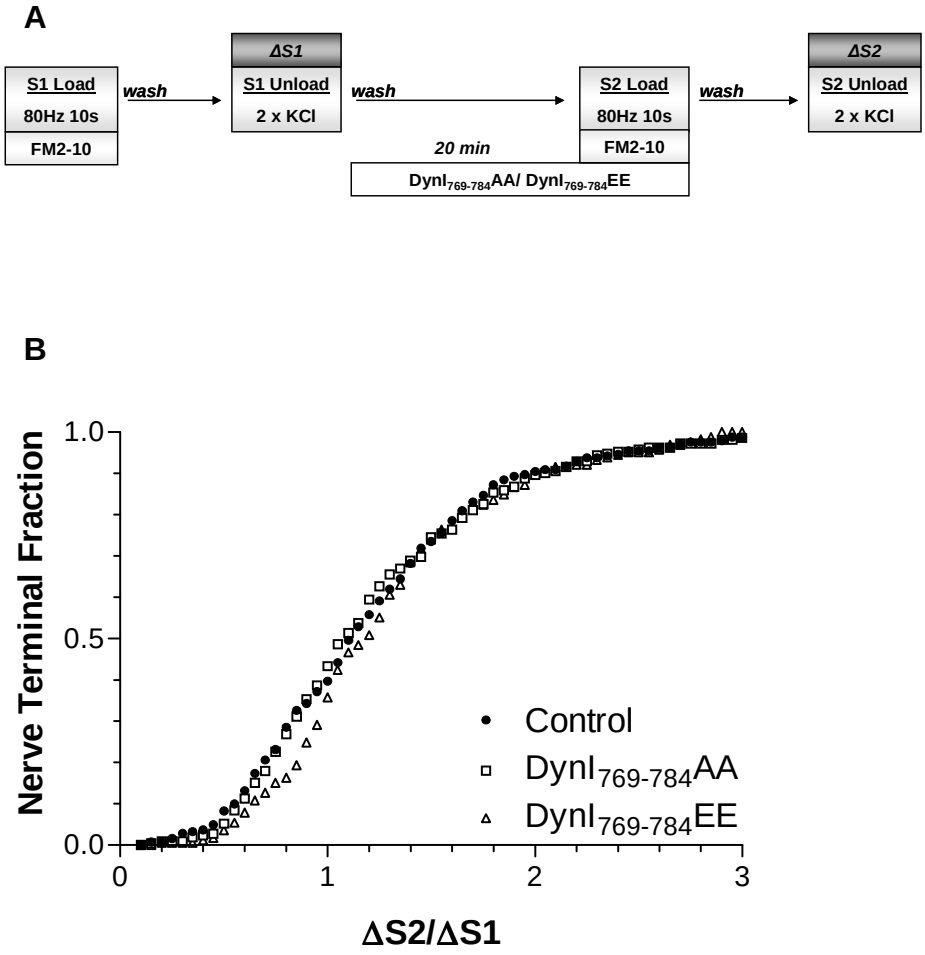

Figure 5.4 - Neither DynI$_{769-784}$AA nor DynI$_{769-784}$EE affect FM2-10 uptake during strong stimulation. **A,** CGNs were labelled with FM2-10 during stimulation with 800 APs (at 80 Hz) at S1 and S2. Cultures were incubated with 30 μM DynI$_{769-784}$AA or DynI$_{769-784}$EE for 20 minutes prior to and during the S2 load. Cells were unloaded with 2 sequential 30 s perfusions of KCl. **B.** Cumulative histogram of the extent of FM dye unloading (ΔS2/ΔS1) in individual nerve terminals. Closed circles = control, N = 242, open squares = DynI$_{769-784}$AA, N = 167,open triangles = DynI$_{769-784}$EE, N = 165.

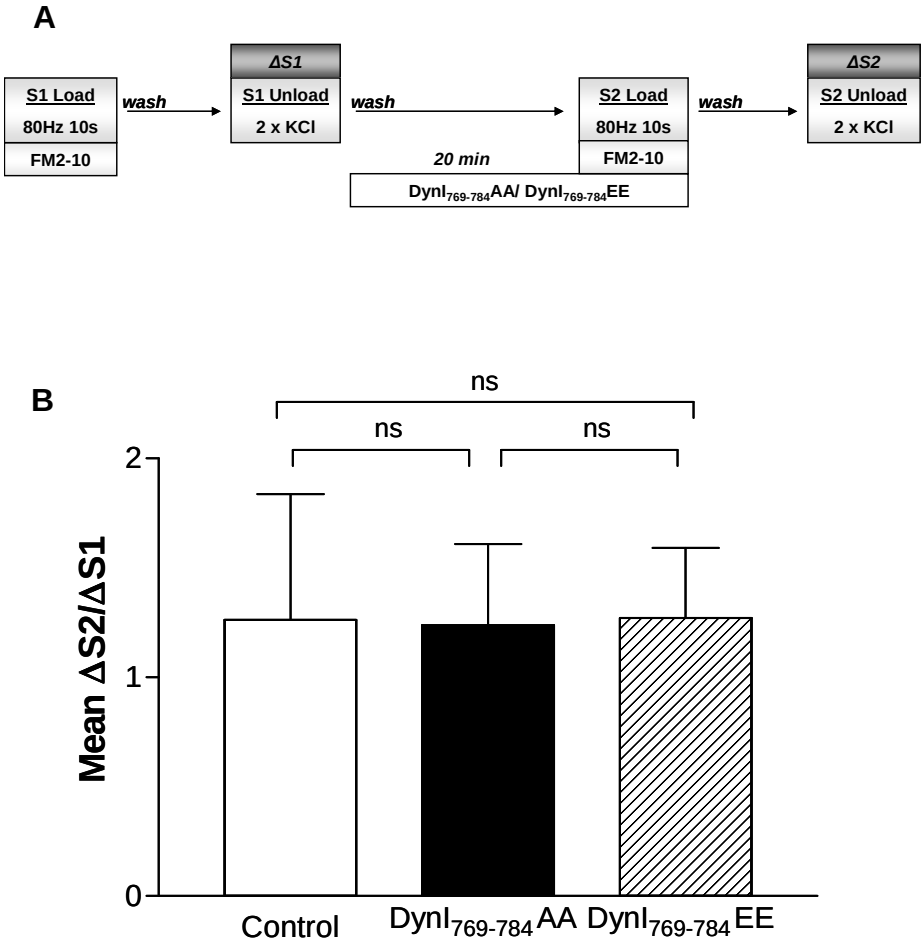

Figure 5.5 - Extent of FM2-10 dye unloading following incubation with DynI$_{769-784}$AA or DynI$_{769-784}$EE. . **A,** CGNs were labelled with FM2-10 during stimulation with 800 APs (at 80 Hz) at S1 and S2. Cultures were incubated with 30 μM DynI$_{769-784}$AA or DynI$_{769-784}$EE for 20 minutes prior to and during the S2 load. Cells were unloaded with 2 sequential 30 s perfusions of KCl. **B,** Bar chart of the extent of FM dye unloading (ΔS2/ΔS1). For all N=3 ± SEM, one-way ANOVA, ns = p>0.05.

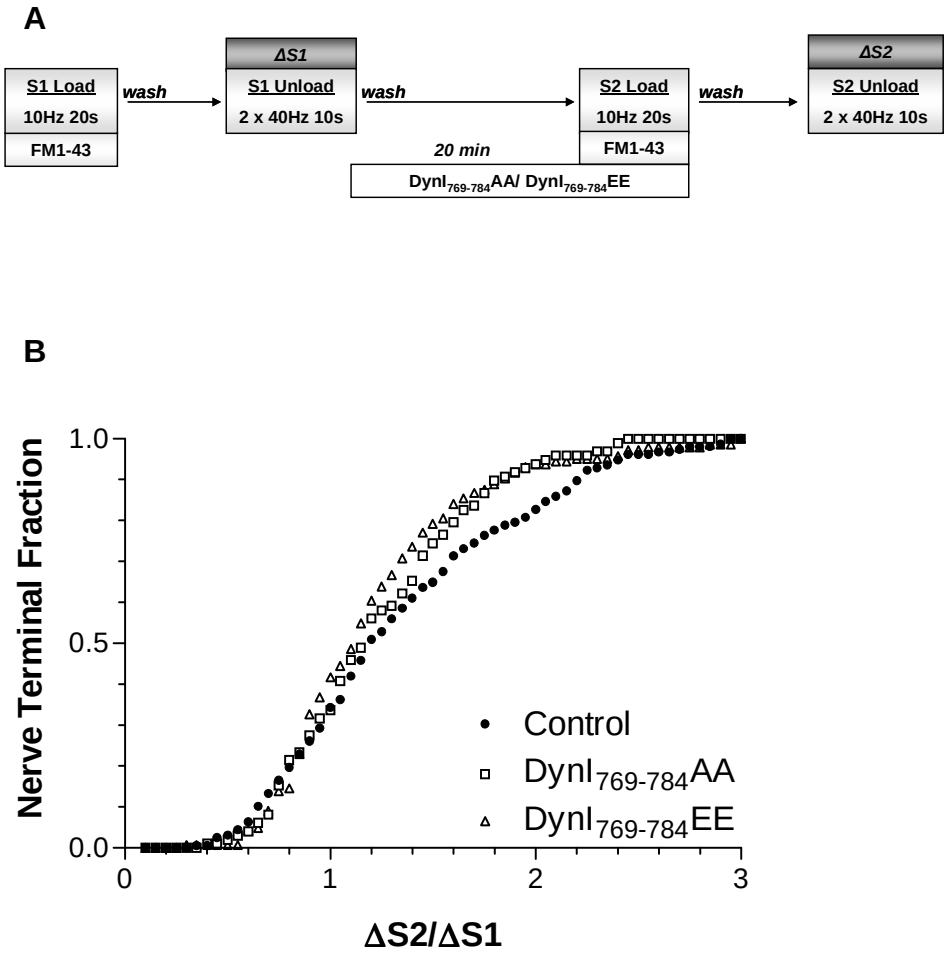

Figure 5.6 - Neither DynI$_{769-784}$AA nor DynI$_{769-784}$EE block FM1-43 uptake during mild stimulation. **A,** CGNs were labelled with FM1-43 during stimulation with 200 APs (at 10 Hz) at S1 and S2. Cultures were incubated with 30 μM DynI$_{769-784}$AA or DynI$_{769-784}$EE for 20 minutes prior to and during the S2 load. Cells were unloaded with 2 sequential 400 APs (at 40 Hz) stimulation. **B.** Cumulative histogram of the extent of FM dye unloading (ΔS2/ΔS1) in individual nerve terminals. Closed circles = control, N = 157, open squares = DynI$_{769-784}$AA, N = 98, open triangles = DynI$_{769-784}$EE, N = 144.

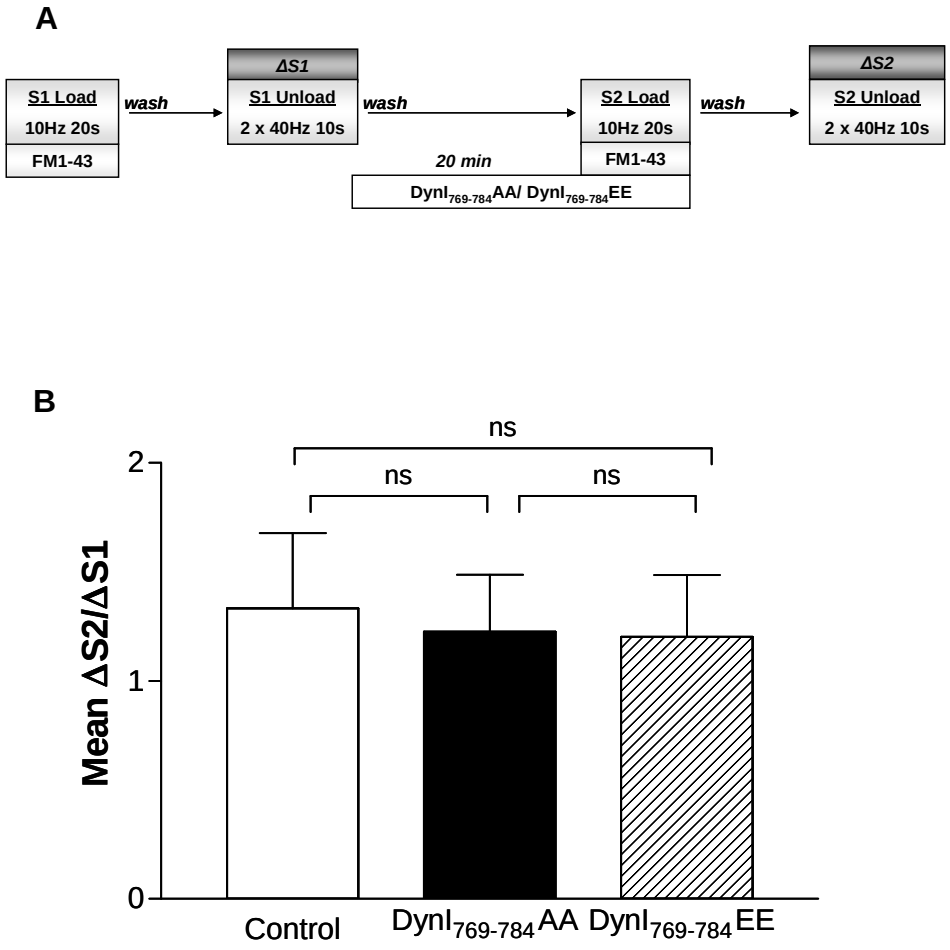

Figure 5.7 - Extent of FM1-43 dye unloading following incubation with DynI$_{769-784}$AA or DynI$_{769-784}$EE. **A,** CGNs were labelled with FM1-43 during stimulation with 200 APs (at 10 Hz) at S1 and S2. Cultures were incubated with 30 μM DynI$_{769-784}$AA or DynI$_{769-784}$EE for 20 minutes prior to and during the S2 load. Cells were unloaded with 2 sequential 400 APs (at 40 Hz) stimulation. **B.** Bar chart of the extent of FM dye unloading (ΔS2/ΔS1). For all N=3 ± SEM, one-way ANOVA, ns = p>0.05

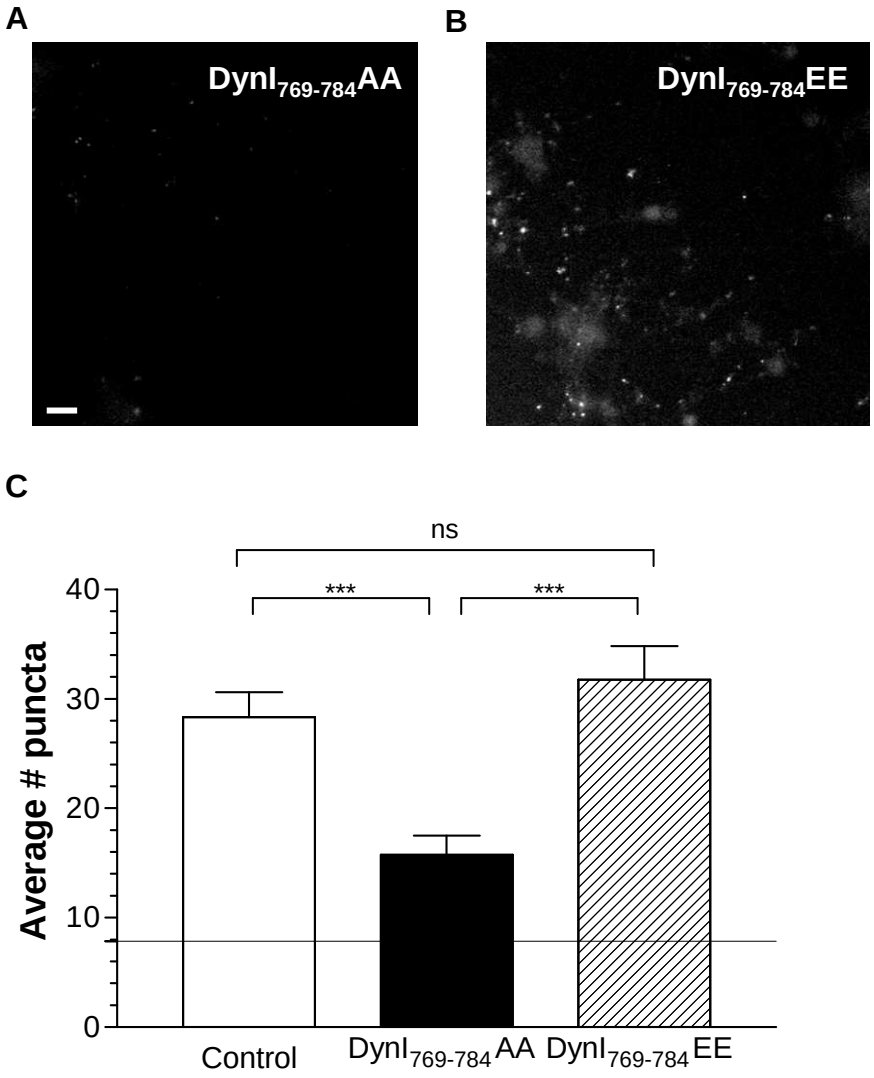

Figure 5.8 - DynI$_{769-784}$AA, but not DynI$_{769-784}$EE, blocks 40 kDa dextran uptake during strong stimulation. CGNs were incubated with 30 µM peptide for 20 minutes before and during 2 min KCl loading of 50 µM 40 kDa dextran. Representative images of (**A**) DynI$_{769-784}$AA and (**B**) DynI$_{769-784}$EE dextran loading, scale bar 20 µm. **C**, Bar chart of the extent of dextran internalisation expressed as the average number of puncta per field of view. For all N=3 ± SEM, one-way ANOVA, ns = $p>0.05$, *** = $p<0.001$.

A more direct assay of the effects of dynamin peptides on SV endocytosis is to look at the uptake of the fluid phase marker horseradish peroxidase (HRP) with electron microscopy (EM). Strong KCl stimulation activates both CME and ADBE in CGN cultures. CGN cultures were preincubated with both dynI$_{769\text{-}784}$AA and dynI$_{769\text{-}784}$EE, and then loaded with HRP during a 2 minute 50 mM KCl stimulation (Fig 5.9 **B** & **C**). Pre-incubation with dynI$_{769\text{-}784}$EE or dynI$_{769\text{-}784}$AA had no effect on the number of HRP labelled SVs visible (Fig 5.9 **E**). However incubation with the dynI$_{769\text{-}784}$EE resulted in a reduction in the number of resulting HRP labelled endosomes, whilst dynI$_{769\text{-}784}$AA did not alter the number of HRP labelled endosomes (Fig 5.9 **D**). Thus EM analysis of central nerve terminals confirms that disruption of the dynamin I –syndapin I interaction blocks ADBE.

5.2.2 Effects of GSK3β Inhibition on SVE.

Following de-phosphorylation by the calcium dependent protein calcineurin in response to stimuli, dynamin I must be re-phosphorylated to enable further rounds of endocytosis. GSK3β is a kinase which has been implicated in a number of signalling pathways, and phosphorylates the phospho-primed sequence –SXXXS(P), which corresponds to the phospho-box sequence of dynamin I. The effects of GSK3β inhibition on SV turnover in neurons was investigated, to see if this kinase could be playing a role in the re-phosphorylation of proteins essential for SVE.

Initially the effect of the GSK3β inhibitor CT99021 on SV turnover during strong stimulation was investigated. 800 APs were used to stimulate SV turnover (at 80 Hz), which activates both CME as well as the ADBE pathway. Addition of 2 μM CT99021 for 15 minutes prior to and during the S2 load has no effect on SV turnover

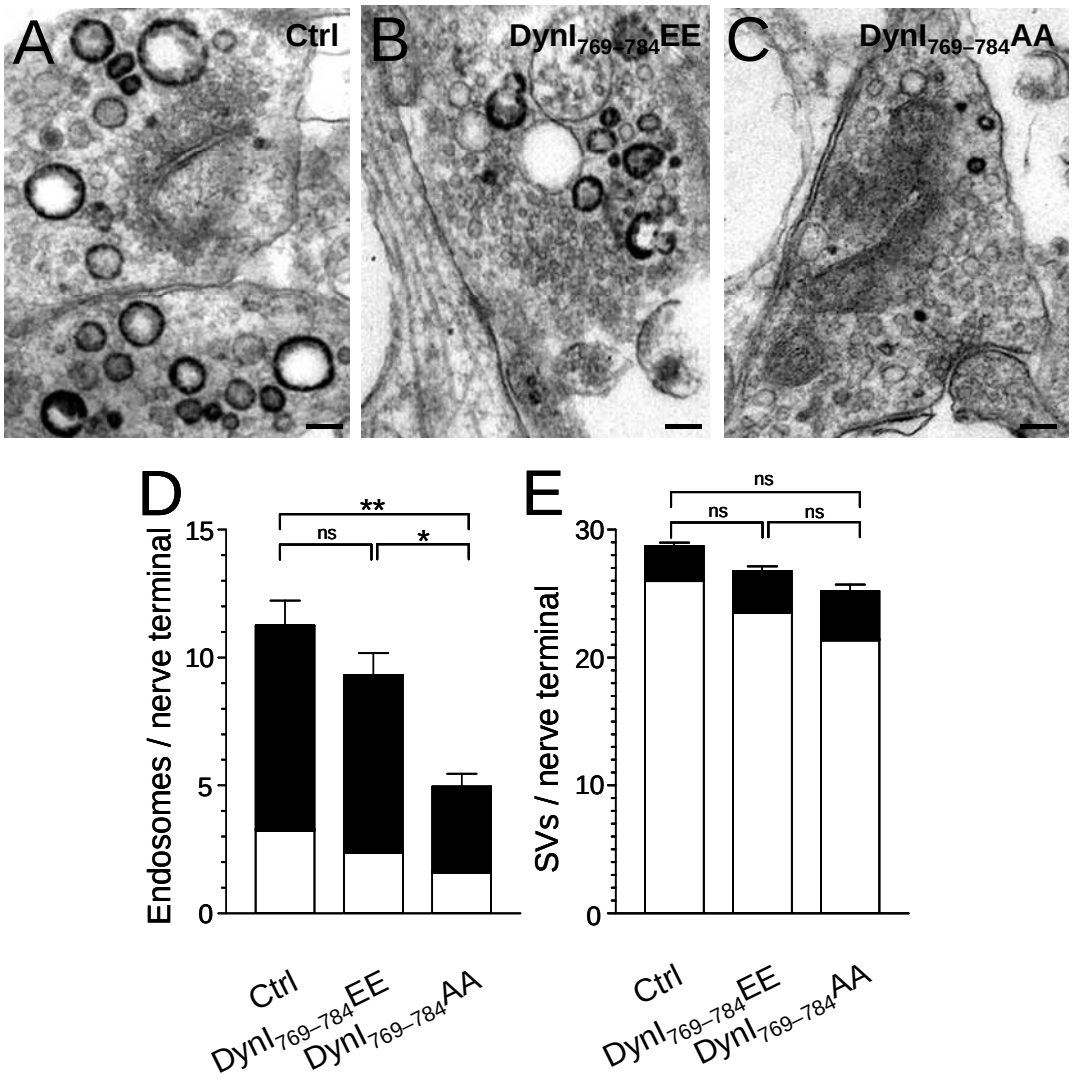

Figure 5.9 - Dynamin I null phospho-peptides lock HRP uptake into endosomes but not SVs. Granule neuron cultures were incubated with HRP and its loading was stimulated by a 2 min stimulus of 50 mM KCl. Where indicated cultures were incubated with 30 µM dynamin I peptides 15 min before and during stimulation (either $DynI_{769-784}AA$ or $DynI_{769-784}EE$). Panels show HRP-labelled structures in typical fields of view either in the absence of peptide (**A**) or in the presence of either $DynI_{769-784}EE$ (**B**) or $DynI_{769-784}AA$ (**C**). Scale bar represents 150 nm in all images. Mean number of either HRP-labelled (solid bars) or clear (open bars) endosomes (**D**) or SVs (**E**) per nerve terminal is displayed either in the absence (Ctrl) or presence of peptides (Ctrl, n = 44 nerve terminals; $DynI_{769-784}EE$, n = 31; $DynI_{769-784}AA$ n = 23; all ± SEM ** = $p < 0.01$, * = $p < 0.05$, one-way ANOVA).

during incubation (Fig 5.10 **B**), indicating that GSK3β has no role in SVE during stimulation. However when CT99021 is present in the experiment from the initial re-polarisation through to the end of the S2 load, a substantial block in the amount of SV turnover occurs (Fig 5.11 **B**). This can be explained by the nature of the calcineurin mediated dephosphorylation of the dephosphins, which occurs in response to stimulation. The subsequent re-phosphorylation of these proteins is necessary to facilitate further rounds of SV turnover. Addition of CT99021 to the cultures during the S1 load and unload ensures that dephosphorylation has occurred, and the block in SV turnover seen at S2 indicates that GSK3β inhibition has prevented the rephosphorylation of at least one of the dephosphins which is essential for further cycles of neurotransmission.

The same experiment was conducted using FM2-10 to label the cells, again with CT99021 present through from re-polarisation to the S2 load (Fig 5.12 **A**). In this instance, CT99021 had no effect on the amount of FM2-10 turned over at strong stimulation (Fig 5.12 **B**). As FM2-10 does not label membrane retrieved by bulk endocytosis, this indicates that ADBE is the retrieval pathway which is affected by GSK3β inhibition.

SV retrieval following mild stimulation occurs via the clathrin-mediated single SV pathway. Incubating with CT99021 from re-polarisation through to the end of the S2 load has no effect on the turnover of SVs labelled with FM1-43 during mild stimulation (Fig 15.13 **B**). This indicates that GSK3β inhibition has no effect on the retrieval of synaptic vesicles at this strength of stimulation, which occurs by CME.

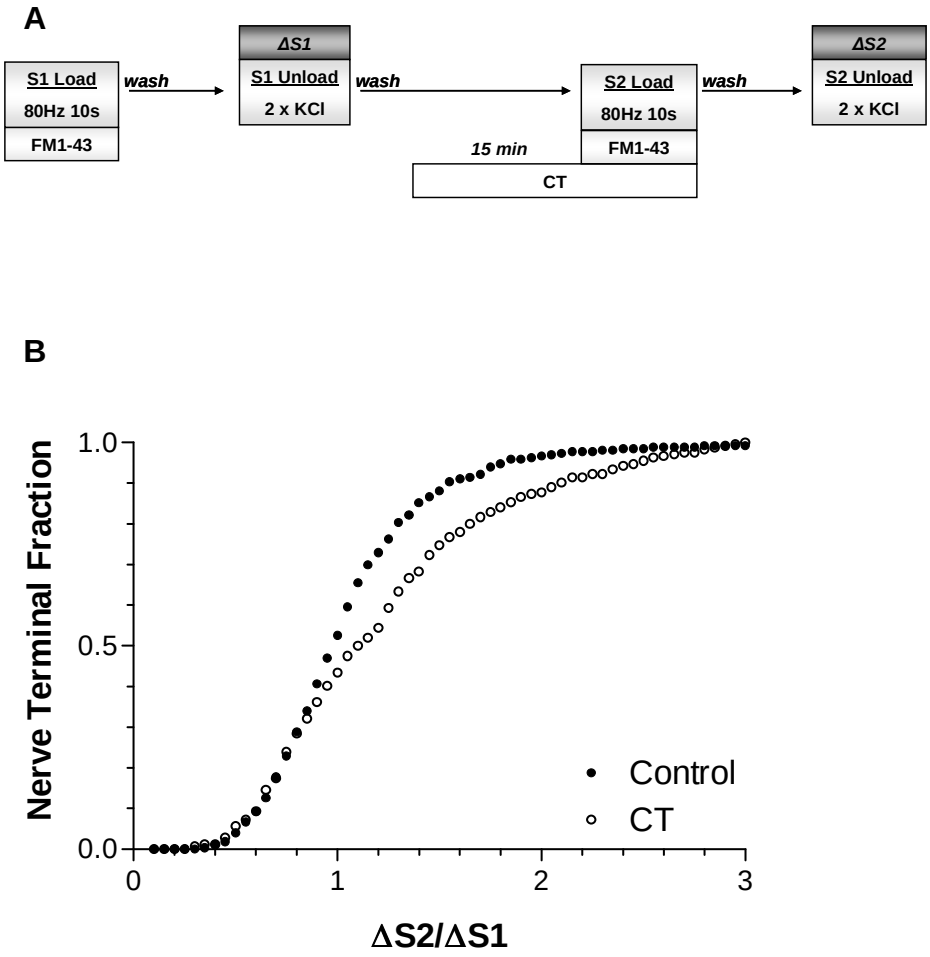

Figure 5.10 - CT99021 has no effect on FM1-43 loading during strong stimulation. **A,** CGNs were labelled with FM1-43 during stimulation with 800 APs (at 80 Hz) at S1 and S2. Cultures were incubated with 2 µM CT99021 for 15 minutes prior to and during the S2 load. Cells were unloaded by stimulation with 2 sequential 30 s 50 mM KCl stimulation. **B.** Cumulative histogram of the extent of FM dye unloading (ΔS2/ΔS1) in individual nerve terminals. Closed circles = control, N = 270, open circles = CT99021, N = 246.

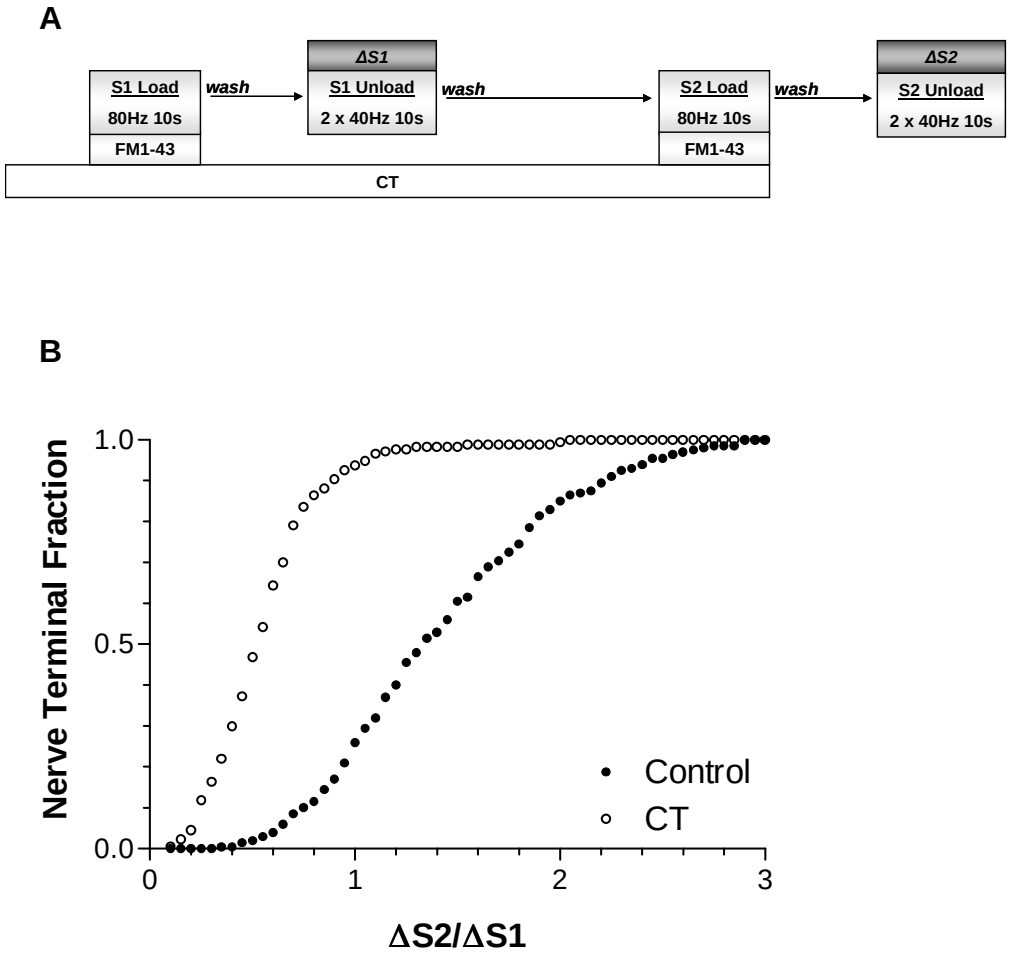

Figure 5.11 - Preincubation with CT99021 blocks FM1-43 uptake during strong stimulation. **A,** CGNs were labelled with FM1-43 during stimulation with 800 APs (at 80 Hz) at S1 and S2. Cultures were incubated with 2 μM CT99021 from 10 minutes prior to the S1 load through to the end of the S2 load. Cells were unloaded by stimulation with 2 sequential stimulations with 400 APs (at 40 Hz). **B.** Cumulative histogram of the extent of FM dye unloading (ΔS2/ΔS1) in individual nerve terminals. Closed circles = control, N = 209, open circles = CT99021, N = 177.

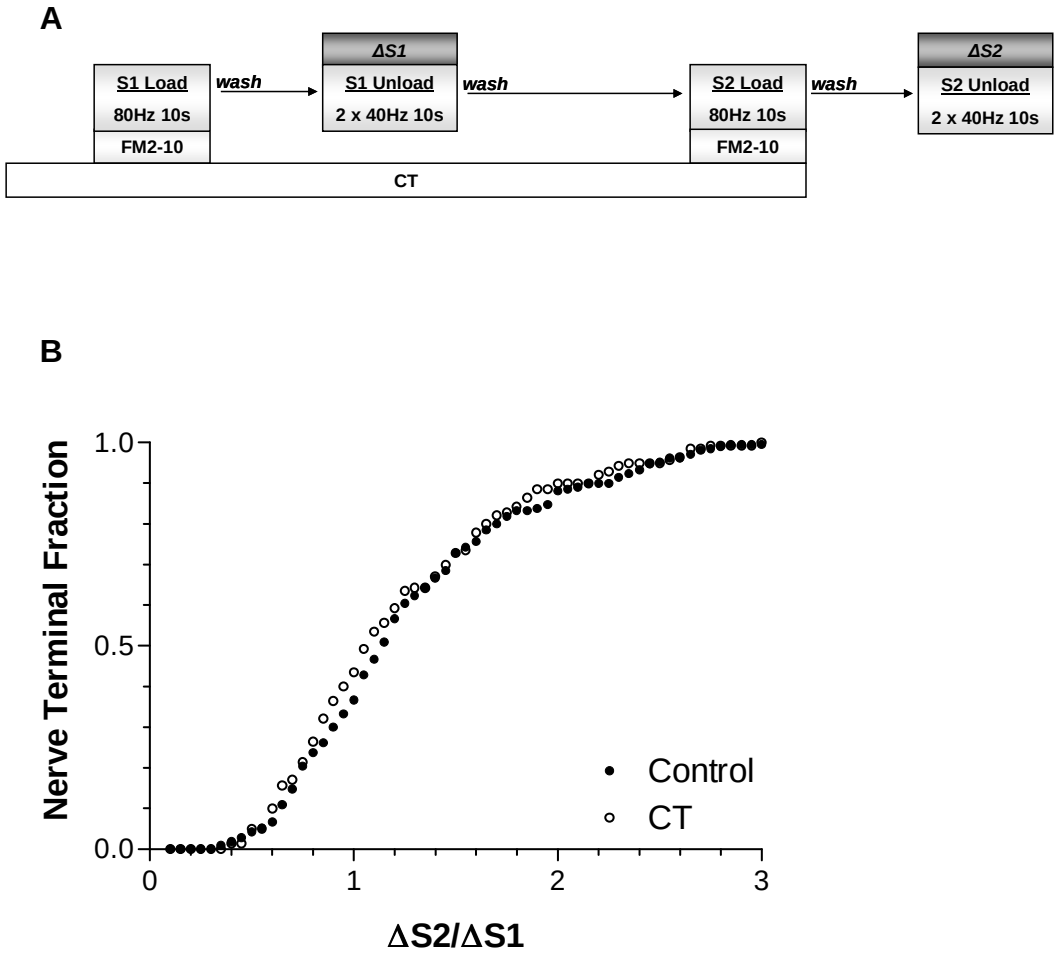

Figure 5.12 - Preincubation with CT has no effect on FM2-10 uptake during strong stimulation. **A,** CGNs were labelled with FM1-43 during stimulation with 800 APs (at 80 Hz) at S1 and S2. Cultures were incubated with 2 μM CT99021 from 10 minutes prior to the S1 load through to the end of the S2 load. Cells were unloaded by stimulation with 2 sequential 30 s KCl stimulation. **B,** Cumulative histogram of the extent of FM dye unloading (ΔS2/ΔS1) in individual nerve terminals. Closed circles = control, N = 210, open circles = CT99021, N = 140.

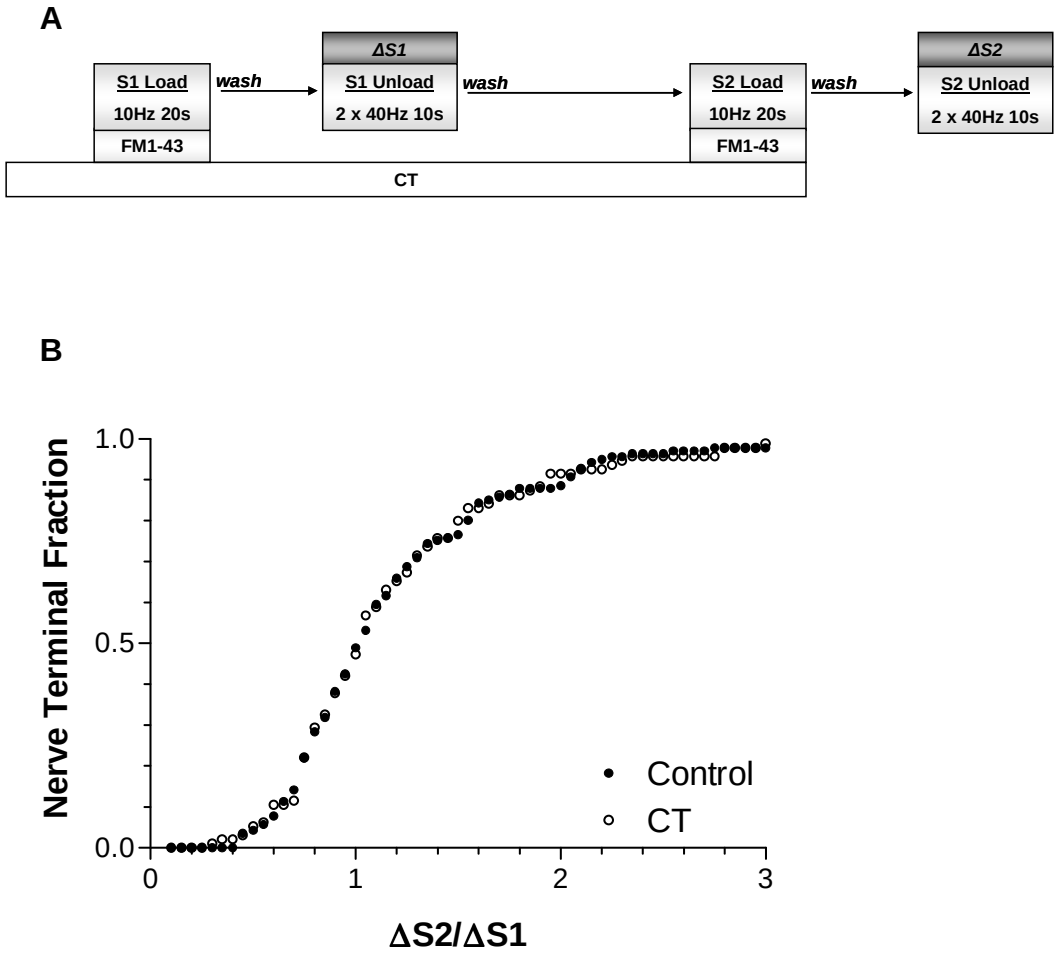

Figure 5.13 - Preincubation with CT has no effect on FM1-43 uptake during mild stimulation. **A,** CGNs were labelled with FM1-43 during stimulation with 200 APs (at 10 Hz) at S1 and S2. Cultures were incubated with 2 μM CT99021 from 10 minutes prior to the S1 load through to the end of the S2 load. Cells were unloaded by stimulation with 2 sequential stimulations with 400 APs (at 40 Hz). **B.** Cumulative histogram of the extent of FM dye unloading (ΔS2/ΔS1) in individual nerve terminals. Closed circles = control, N = 141, open circles = CT99021, N = 95.

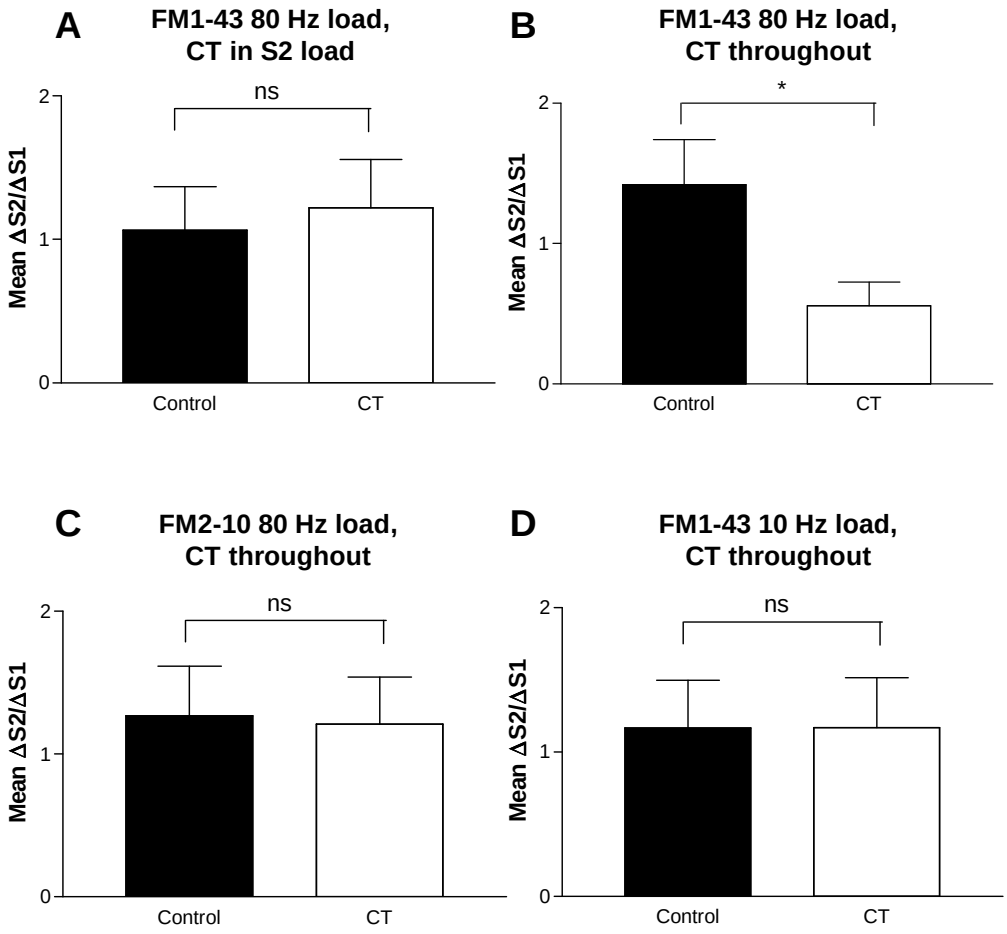

Figure 5.14 - Proportion of FM dye turnover with CT99021 incubation. Bar charts representing the mean proportion of SV turnover (mean ΔS2/ΔS1 ± SEM) for all CT99021 treated FM dye experiments. All experiments were analysed with unpaired t tests, N = 3 for all, ns = p>0.05, *** =** p< 0.05

To confirm a role for GSK3β -dependent protein rephosphorylation in ADBE, dextran uptake was examined in CT 99021 incubated cultures. CT99021 (2 μM) was added directly to the culture medium for 15 minutes before the cells were re-polarized in basic buffer also containing CT99021. Cultures were then loaded with 40 kDa dextran, in the presence of CT99021, during stimulation with 800 APs (Fig 5.15 **A)**. The average number of dextran loaded puncta was significantly decreased in cultures pre-incubated with CT99021 (Fig 5.15 **C**). Thus GSK3β -dependent rephosphorylation is essential for ADBE.

Another GSK3B inhibitor was investigated to confirm that the inhibitory effects detected in CT99021 treated cultures were due to the inhibition of GSK3β and not due to any other off-target effects. The procedure followed was identical, with the GSK3β inhibitor AR-AO14418 (5 μM) added to the culture medium for 15 minutes, and also during re-polarization and loading (Fig 5.15 **B**). Again, a significant decrease in number of internalised dextran puncta was observed, with AR-AO14418 incubated cultures three fold fewer puncta then control cultures (Fig 5.15 **C**). This confirms that the inhibition of GSK3β blocks the internalisation of 40 kDa dextrans in CGNs, and therefore GSK3β functions as a kinase whose ability to rephosphorylate substrates is important for ADBE.

5.2.3 Effects of Dynamin I GTPase Inhibition on SVE.

Inhibition of SVE by incubation with the small molecule cell permeable dynamin inhibitor dynasore (Macia *et al.*, 2006) has been reported in a number of systems (Newton *et al.*, 2006; Kirchhausen *et al.*, 2008; Lu *et al.*, 2009). Dyngo-4a is

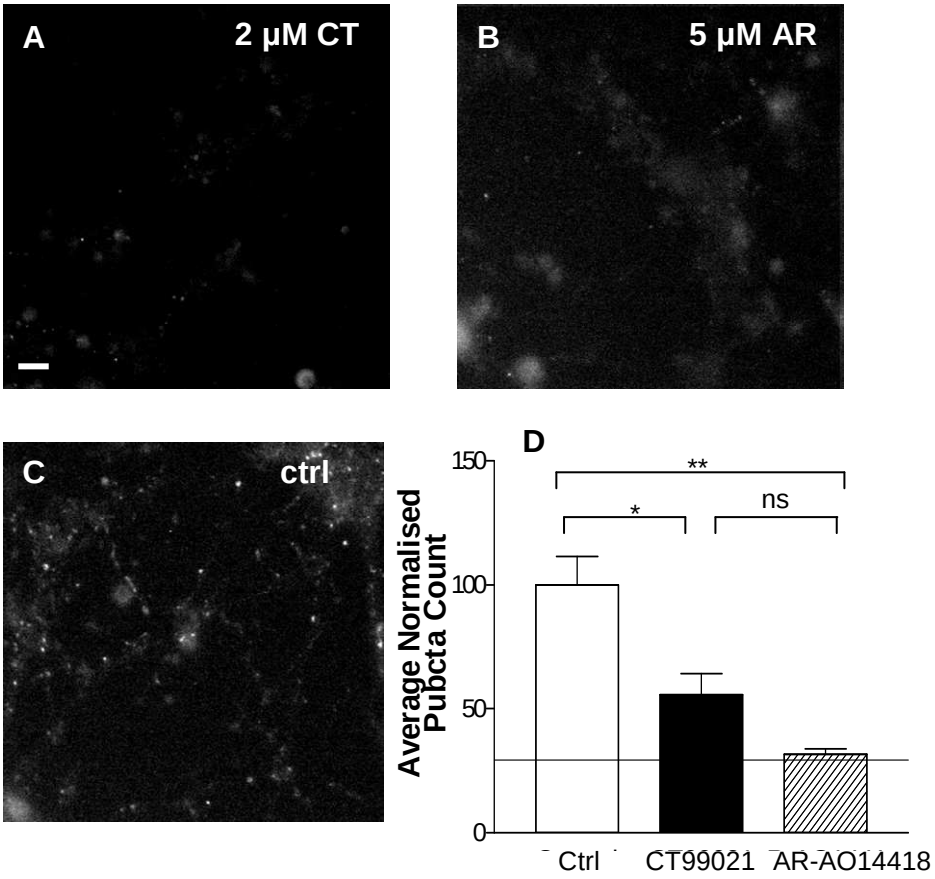

Figure 5.15 - Preincubation with CT99021 or AR-AO14418 blocks dextran uptake during strong stimulation. **A,** CGNs were labelled with 50 µM 40 kDa dextran during stimulation with 800 APs (at 80 Hz). 2 µM CT99021 (**B**) or 5 µM AR-AO14418 (**C**) was present in the cell culture medium for 15 minutes before repolarization, during re-polarization and during stimulation, scale bar 20 µm. **D,** Bar chart of the average number of internalised dextran puncta per field. For all N=3 ± SEM. Hatched line represents the average puncta count in unstimulated cultures. One way ANOVA, ns = $p>0.05$, * = $p<0.05$, ** = $p<0.01$

an analogue of dynasore, created by hydroxyl substitution. The effectiveness of dyngo4-a as a dynamin inhibitor was assessed by looking at the effects of the drug on SV turnover in the FM assay system. Incubation of cultures with dyngo4-a (30 μM) prior to and during the S2 load (Fig 5.16 **A**) resulted in a large block in SV turnover (Fig 5.16 **B)**. In order to asses whether this is caused by a block in endocytosis or exocytosis, dyngo was added to cultures prior to and during the S2 unload (Fig 5.16 **A**). Dyngo mildly inhibited the exocytosis of SVs, however the majority of its effects are mediated through the endocytosis pathway (Fig 5.16 **B,** Fig 5.17 **B**).

In order to compare the requirement for dynamin I GTPase activity in ADBE, the effects of both dyngo4-a and dynasore incubation on dextran internalisation were examined. At 30 μM, dyngo4-a robustly inhibited dextran internalisation, confirming that dynamin I GTPase activity is essential for ADBE (Fig 5.18 **D**). However the same concentration of dynasore has no effect on dextran internalisation (Fig 5.18 **D**). When cultures were incubated with 100 μM dynasore, a robust inhibition of dextran internalisation was then seen (Fig 5.18 **D**). This suggests that; 1, dynamin I GTPase activity is essential for ADBE and 2, dyngo4-a is a more potent dynamin inhibitor than dynasore.

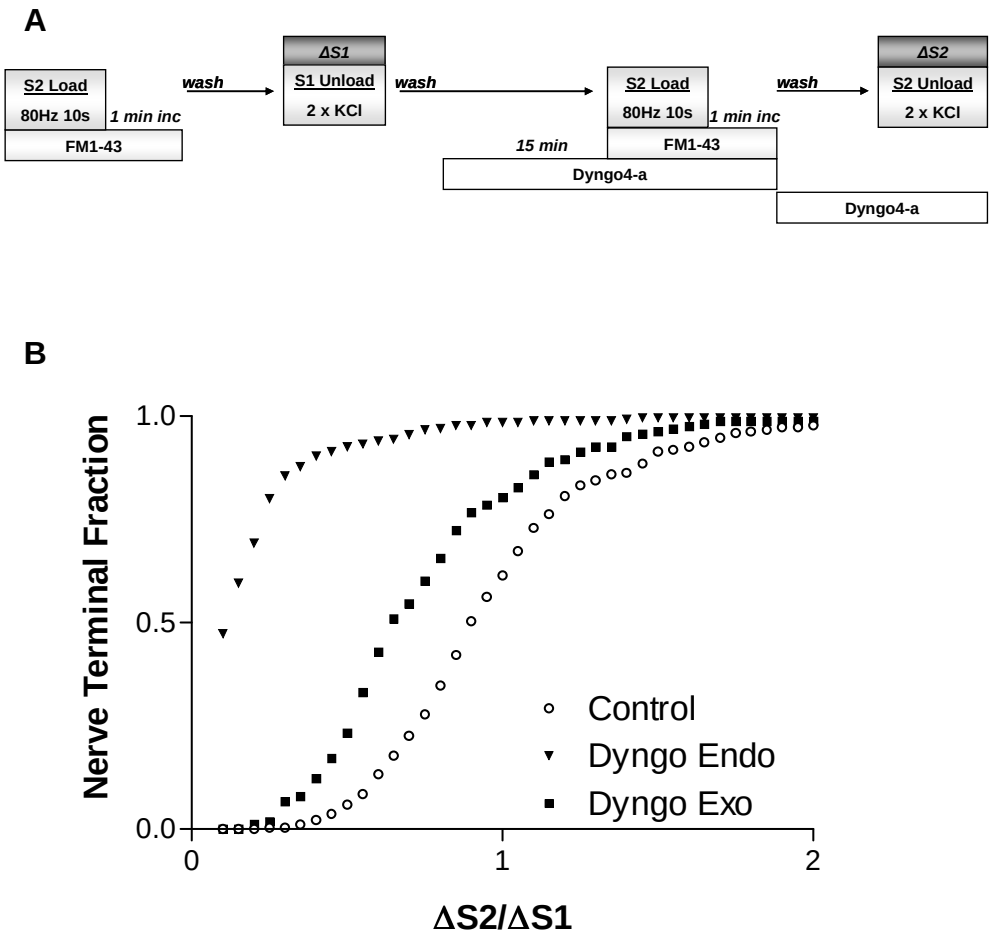

Figure 5.16 - Incubation with dyngo4-a pre-S2 load blocks SV turnover. **A**, CGNs were labelled with FM1-43 during stimulation with 800 APs (at 80 Hz) at S1 and S2. Cultures were incubated with 30 μM Dyngo for 10 minutes prior to and during the S2 load, or for 10 minutes prior to and during the S2 unload. Cells were unloaded with 2 sequential 30 s perfusions of KCl. **B,** Cumulative histogram of the extent of FM dye unloading (ΔS2/ΔS1) in individual nerve terminals. Open circles = control, N = 270, closed triangles = dyngo4-a in S2 load, N = 270, closed squares = dyngo4-a in S2 unload, N = 163.

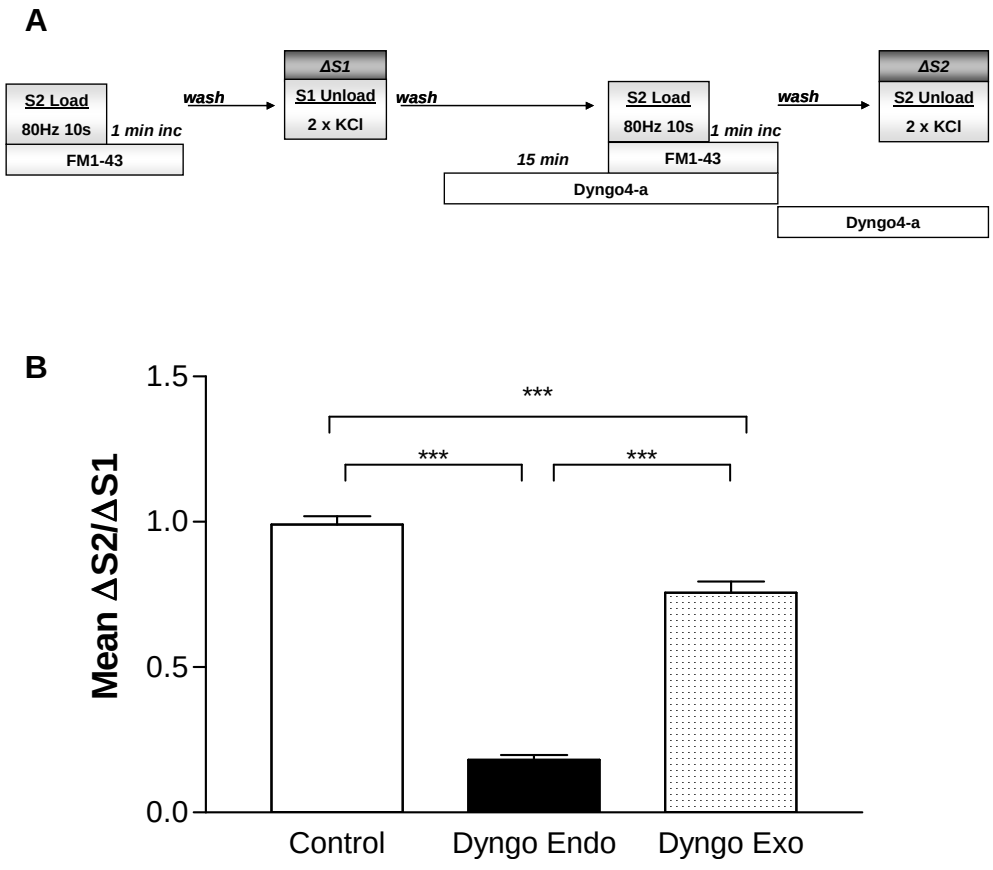

Figure 5.17 - Effect of dyngo on SV turnover. **A**, CGNs were labelled with FM1-43 during stimulation with 800 APs (at 80 Hz) at S1 and S2. Cultures were incubated with 30 μM Dyngo for 10 minutes prior to and during the S2 load, or for 10 minutes prior to and during the S2 unload. Cells were unloaded with 2 sequential 30 s perfusions of KCl **B,** Bar charts of the mean proportion of FM dye unloading (ΔS2/ΔS2) ± SEM for dyngo experiments. For all N = 3. One way ANOVA, ns = $p>0.05$ *** = $p<0.001$

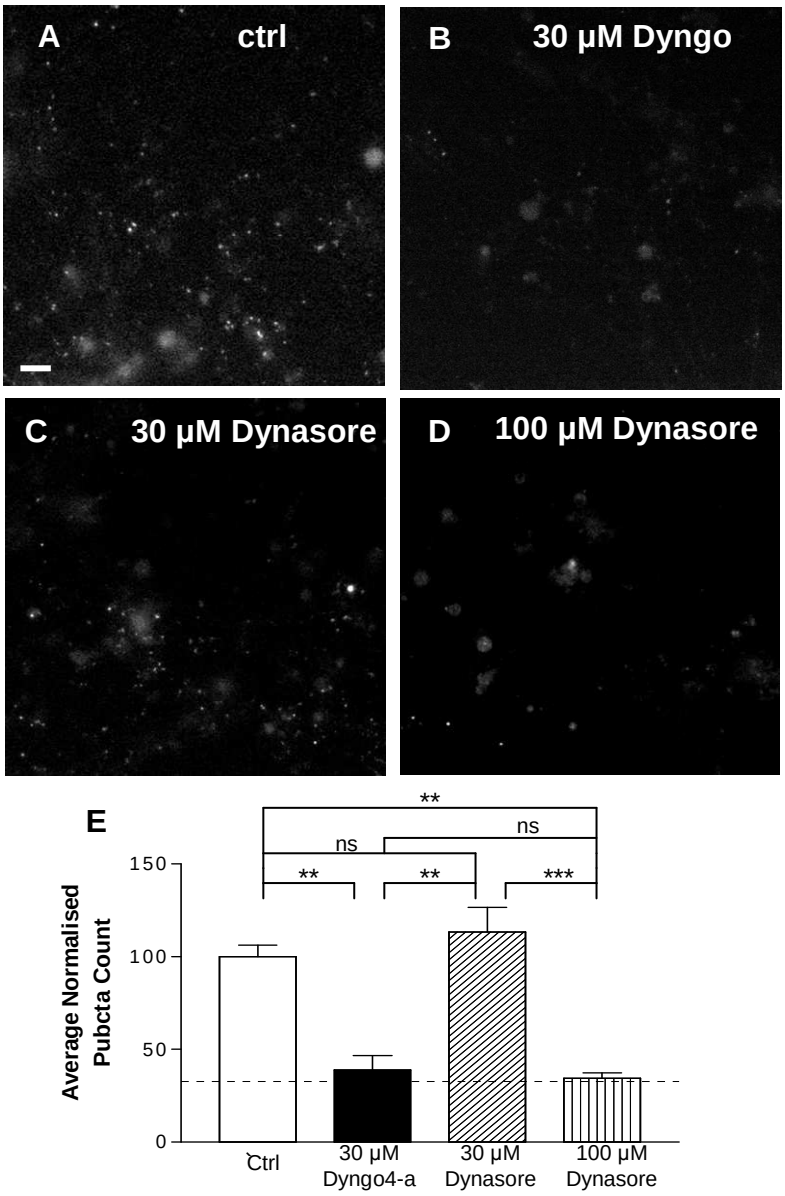

Figure 5.18 - Effects of dyngo and dynasore on ADBE. Representative images of dextran internalisation at 800 APs (80 Hz for 10 s) stimulation; control (**A),** following preincubation with 30 µM dyngo (**B**), 30 µM dynasore (**C**) and 100 µM dynasore (**D**), scale bar 20 µm. **E,** Average puncta % per field ± SEM, normalized to control. Hatched line represents average background fluorescence. One-way ANOVA, ns = p>0.05, ** = p < 0.01, *** = p< 0.001

5.3 Discussion

5.3.1 ADBE is dependent on the interaction between dephosphorylated dynamin I and syndapin I.

In order to elucidate the identity of the important molecular players in the activation of ADBE, we sought to look at the effects of interference with and inhibition of dynamin I on different forms of endocytosis in our central nerve terminal model system. Little is known about the regulatory players involved in this form of endocytosis, other than the implication of AP3 in a role in budding of SVs from endosomal intermediates in PC12 cells (Faúndez *et al.*, 1998). Dynamin I mediates several endocytosis pathways, but whether a separate pathway is controlled by dynamin dephosphorylation is unknown. Here we have shown that the dephosphorylation of dynamin I (and its subsequent interaction with syndapin I) do not play a role in CME, but are instead important in ADBE. Perturbation of the dynamin I-syndapin I interaction through introduction of competitive phospho-box peptides blocks ADBE as assayed by FM dye imaging and dextran uptake analysis. The implication that dynamin I dephosphorylation is essential for this form of endocytosis indicates that the dynamin I-syndapin I interaction may function as part of the molecular determinants that govern the switch between ADBE and CME.

ADBE occurs in response to increased neuronal activity (Chapter 4). As bulk endocytosis has been found to be activity dependent, the strength of stimulation at which dynamin I dephosphorylation occurs would also give an indication of the importance of the dynamin I-syndapin I interaction during increased neuronal activity. Unpublished observations from the lab show that dynamin I is

dephosphorylated in an activity-dependent manner, and the strength of stimulation at which dynamin is dephosphorylated corresponds to that at which ADBE is activated. Of interest would also be to investigate whether the other dephosphins are dephosphorylated in an activity dependent manner, and to see what effect perturbation of the interactions of these dephosphins would have on ADBE. As bulk endocytosis occurs in response to elevated activity levels, Ca^{2+} influx is likely to be the trigger for activation of the bulk endocytosis pathway. Calcineurin has been shown to be important for endocytosis during elevated stimulation (Chan & Smith, 2001; Kumashiro *et al.*, 2005), and is a likely candidate for detection of elevated Ca^{2+}.

The peptide to cell ratio has been proposed to be the regulating factor in the uptake of cell penetrating peptides, and not the concentration of peptide used (Hällbrink *et al.*, 2004). This will not have affected our results however, as although the cell density in the primary prep can vary very slightly between preps, all peptide experiments were conducted on cells from at least 2 different preparations. As the results were compiled from at least 2 different preps, any small effects of peptide-to-cell ratio dependent peptide uptake will have been compensated for. The use of fluorescently tagged dynamin I mutants, corresponding to the phospho-box domain region targeted by the cell penetrating peptides, could be used to confirm the importance of this dynamin I-syndapin I interaction. Work from our lab has shown that phospho-site specific mutations of dynamin I inhibit the uptake of FM1-43 but not FM2-10, indicating that the phospho-box is specifically involved in ADBE.

Syndapin I, amphiphysin I and endophilin I are the three major SH3 domain containing binding partners of the dynamin PRD. Syndapin I contains an F-bar

domain at its N terminus (Itoh *et al.*, 2005), whilst amphiphysin I and endophilin I both contain N-bar domains (Peter *et al.*, 2004). F-bar domains facilitate interactions with membranes of shallower curvature (Henne *et al.*, 2007; Shimada *et al.*, 2007), which would be consistent with the curvature of the membrane of bulk endosomes. N-bar domains are implicated in interaction with membranes of tighter curvature (Peter *et al.*, 2004), as would occur in the considerably smaller and more tightly curved synaptic vesicles. Several lines of evidence support this theory that dynamin I dephosphorylation controls distinct forms of endocytosis. Binding of dynamin I to amphiphysin I is unaffected by the phosphorylation state of dynamin (Tan *et al.*, 2003, Anggono *et al.*, 2006). Both endophilin I and syndapin I bind the same region of the dynamin PRD, but do so in a mutually exclusive manner, indicating that the function of these proteins in SVE may differ (Anggono & Robinson, 2007).

5.3.2 A REQUIREMENT FOR GSK3 DURING ADBE.

As inhibition of GSK3β resulted in a block in endocytosis, it can be inferred that the kinase is involved at some point in signalling in the endocytosis pathway. This block in endocytosis is only visible when FM1-43 is used to label the cells and not FM2-10, indicating that the bulk endocytosis pathway is affected by inhibition of GSK3β. Inhibition of dextran uptake, a measure of bulk endocytosis, confirmed that ADBE is inhibited in the presence of GSK3β inhibitors.

As the effects of GSK3β on endocytosis can only be seen following an initial round of stimulation, the kinase is affecting one/some of the proteins which need to be re-phosphorylated in order to function for subsequent rounds of endocytosis. Dynamin I is a likely substrate for re-phosphorylation by GSK3β activity, as it

contains the consensus sequence recognised by GSK3β -SXXXS(P). All the other dephosphins contain the sequence SXXXS at least once, however the key criteria is the phosphorylation-priming of the second serine, and dynamin is currently the only dephosphin where the 2 serines of the SXXXS consensus sequence are known to be phosphorylated.

Non-specific effects of the CT drug can be ruled out as the same effects are achieved by using the GSK3β inhibitor AR, supporting the idea that the effects are mediated via inhibition of GSK3β. Ideally the effect of these antagonists would have been corroborated via the overexpression of a dominant negative mutant of the enzyme. However there is currently no identified dominant negative GSK3β mutant; constitutively active GSK3β mutants have been identified (MacAulay *et al.*, 2005), but since dephosphorylation of serine 774 is the key event in ADBE this is not predicted to be dominant negative.

Cdk5 is known to rephosphorylate dynamin I at sites 774 and 778 both *in vitro* and *in vivo*, (Tan *et al.*, 2003); however it may be that the affinity of GSK3β is greater then that of cdk5, once cdk5 has pre-primed the downstream serine. It would be interesting to look at the effects of GSK3β versus cdk5 on pseudo pre-primed dynamin sequences, pre-primed at both S774 and S778. Further work would need to focus on the kinetics of cdk5 versus GSK3β for dynamin I phosphorylation. Of interest would also be the study of the dynamin isoform specificity of the kinase activity, as dynamin III contains similar phosphorylation sites to dynamin I (Graham *et al.*, 2007).

A number of experiments are necessary to further investigate the mechanism of action of GSK3β during SVE, in order to highlight the importance of this kinase at the pre-synaptic level.

5.3.3 Inhibition of the GTPase activity of Dynamin I

An obligate role for dynamin I in ADBE has been questioned by studies in the dynamin I KO mouse (Hayashi *et al.*, 2008; Lou *et al.*, 2008). Studies of the dynamin I KO mouse have allowed the study of the influence of the dynamin isoforms on endocytosis. These nerve terminals are capable of sustaining neurotransmission during mild stimulation, and impairment of SV recycling becomes evident in response to stronger stimulation (Ferguson et al, 2007, Hayashi et al, 2008). Although the dynamin I KO mouse only shows impairment under elevated stimulus, it is not possible to rule out a compensatory effect during mild stimulation of the other 2 isoforms of dynamin still present in these KO animals. Dynamin III is known to be phosphorylated at similar residues to dynamin I (Graham *et al.*, 2007). Further studies in the dynamin I KO mouse calyx of held show a specific effect on the slow phase of endocytosis, and not on the large downward capacitance shifts that correspond to the retrieval of large amounts of membrane (Lou *et al.*, 2008). Conditional dynamin II knockouts reveal that dynamin II is specifically required for CME, whilst both dynamin I and II isoforms can rescue marcopinocytosis in non-neuronal cells (Liu *et al.*, 2008). This suggests that dynamin isoforms and splice variants may be involved in mechanistically different forms of endocytosis.

In order to address this issue, we chose to investigate the effect of inhibition of the GTPase activity of dynamin I using two dynamin GTPase inhibitors; dyngo4-a

and dynasore. This negates the question of functional redundancy between the different isoforms of dynamin.

Dyngo4-a robustly inhibits the endocytosis of SV, as measured by FM dye turnover, indicating that all forms of SVE were abolished by incubation with this dynamin GTPase inhibitor. The direct role of dynamin I in ADBE was determined by monitoring dextran uptake during elevated neuronal activity (800 APs) in the presence of dyngo4-a or dynasore. Dyngo-4a inhibited dextran internalisation at much lower concentrations than dynasore, indicating it may be a more potent inhibitor of dynamin I GTPase activity. Unpublished observations from our lab indicate that dynasore blocks both CME and bulk endocytosis as detected by HRP uptake in EM samples. Therefore both CME and ADBE have an essential requirement for dynamin GTPase activity, whereas the dephosphorylation of dynamin I is specifically required for ADBE and not CME.

These studies have highlighted several possible interactions and modifications which may influence the pathway of endocytosis which occurs in response to stimuli. The interaction of dephosphorylated dynamin I with syndapin is essential for ADBE. The rephosphorylation of dynamin I by the kinase GSK3β is also essential for subsequent rounds of ADBE.

6. Effects of Antiepileptic Drugs on the Synaptic Vesicle Cycle

6.1 Introduction

Excessive excitability should cause an increase in synaptic vesicle (SV) recycling, but do defects in SV recycling cause the excitability seen in epilepsy?

6.1.1 Synaptic Vesicle Cycle Defects and Epilepsy.

A number of different lines of evidence implicate defects in the synaptic SV cycle as important contributing factors in some forms of epilepsy.

Several knockout (KO) mice generated by ablation of genes encoding SV proteins have shown abnormal neurotransmission and phenotypes consistent with epileptic type disorders. Synapsin I deficient mice showed marked impairment in the organisation of vesicles at the presynaptic terminal, and enhanced stimulation-evoked epileptic seizures (Li *et al.*, 1995). Generation of amphiphysin I KO mice produces a model suffering rare irreversible seizures, with defects in multiple stages of the vesicle cycle (Di Paolo *et al.*, 2002). Delivering high frequency stimulation can be used to mimic epilepsy in cell cultures, and double KOs of synaptogyrin I and synaptophysin I mice were found to take a longer time to recover from synaptic depression after such high frequency stimulation (Janz *et al.*, 1999). Mice lacking synaptojanin I displayed ataxia and general convulsions, with approximately 85% dead by 24 hours after birth. Electron microscopy (EM) revealed an increased number of clathrin coated vesicles (CCVs) in the synapses of cortical neuronal cultures of mutant mice and, similar to the synaptogyrin/synaptophysin double KOs, enhanced synaptic depression was observed (Cremona et al, 1999).

Human genetic analyses have also revealed mutations in synaptic vesicle proteins as the cause for a number of epilepsy type disorders. A nonsense mutation in

the gene for synapsin I was determined by linkage and microsatellite analysis as the likely cause of the epilepsy phenotype in a four generation family studied (Garcia *et al.*, 2004). In addition heterozygous missense mutations in MUNC18-1 have been detected in 4 unrelated individuals with early infantile epileptic encephalopathy (Saitsu *et al.*, 2008).

Further evidence of a link between SV recycling and epilepsy comes from studies which show that anticonvulsant and antiepileptic drugs (AEDs) alter neurotransmitter release. Riluzole, an anticonvulsant neuroprotective compound, depresses glutamate excitatory postsynaptic currents but has no effect on GABA mediated inhibitory postsynaptic currents (Prakriya & Mennerick, 2000). Several AEDs (oxcarbazepine, lamotrigine and felbamate) inhibit voltage-gated calcium currents in cortical and striatal neurons (Stefani *et al.*, 1997). As Ca^{2+} influx is the trigger for neurotransmitter release, this shows a link between AEDs and the SV cycle

Thus SV recycling and epilepsy have been linked through studies using KO mice, genetic analysis and synaptic transmission. One of the most direct lines of evidence linking epilepsy and the synaptic vesicle cycle was the identification of the synaptic vesicle protein, SV2A, as the binding site for the antiepileptic drug Levetiracetam (trade name Keppra) (Lynch *et al.*, 2004).

6.1.2 Synaptic Vesicle Protein 2

Synaptic vesicle protein 2 (SV2) was originally discovered by screening a library of monoclonal antibodies to identify novel proteins involved in regulated secretion of secretory vesicles (Buckley & Kelly, 1985). SV2 is present on all SVs

(Bajjalieh *et al.*, 1994) and because of this property it is commonly used as a SV marker.

6.1.2.1 ISOFORMS OF SV2

There are 3 isoforms of SV2; SV2A, SV2B and SV2C. Each isoform has a different expression profile in the brain. There is a high degree of conservation between all 3 isoforms, each of which contains 12 transmembrane domains, and is glycosylated at the N terminus (Buckley & Kelly 1985; Bajjalieh *et al.*, 1993; Janz & Südhof, 1999).

SV2A is ubiquitously expressed in the brain, with highest expression levels in subcortical regions (Bajjalieh *et al.*, 1993). SV2B shares 57% identity with SV2A (Janz & Sudhof, 1999). SV2B expression is found to have a broader distribution during development, with expression at P16 observed in the globus pallidus, colliculi and dentate gyrus of the hippocampus which is not seen in the adult (Bajjalieh *et al.*, 1994). Some neurons express both the SV2A and SV2B isoforms (for example almost all neurons in the CA2 region of the hippocampus), and both isoforms may even be present on the same vesicle (Bajjalieh *et al.*, 1994).

The third isoform, SV2C, shares 62% identity with SV2A (Janz & Sudhof, 1999), but has a much more restricted distribution pattern. It is found primarily in the basal forebrain, midbrain and brainstem, with low levels found in the cerebellar cortex (Janz & Südhof, 1999).

6.1.3 FUNCTION OF SV2 PROTEINS

The SV2 proteins have no yeast homologues, and are unique to vertebrates, suggesting their function may have developed as part of evolving complexity of the synaptic signalling system. SV2 has a number of possible functions, based both on inferences from the structure, and from reported protein-protein interactions.

Sequence homology to known transmembrane transporters suggests the SV2 proteins may function as transporters (Bajjalieh *et al.*, 1992; Feany *et al.*, 1992). However SV2A and SV2B expression patterns are not consistent with the theory that the different isoforms could serve as different neurotransmitter transporters, as SV2A is expressed in both GABAergic and glutamatergic neurons of the cerebellum (Bajjalieh *et al.*, 1994).

A number of observations infer SV2 has a modulatory role in SV traffic. For example both Ca^{2+} and phosphorylation regulated interactions of SV2 with synaptotagmin have been recorded. The cytoplasmic amino terminus of SV2A interacts directly with the C_2B domain of synaptotagmin in a calcium dependent manner (Schivell *et al.*, 1996). It was subsequently shown that this interaction is modulated by amino terminal phosphorylation of SV2A, with an increase in binding affinity of the phosphorylated SV2A (Pyle *et al.*, 2000).

More recently SV2 has been shown to bind adenine nucleotides, providing further evidence of a function of SV2 in modulation of secretion. SV2A has 2 ATP binding sites in the cytoplasmic domain, suggesting a link between energy levels and SV2 function (Yao & Bajjalieh, 2008).

6.1.4 SV2 KNOCKOUT MICE

Although the exact function (or functions) of SV2 are still unclear, studies of SV2A KO mice demonstrate that it is essential for normal neurotransmission and survival (Crowder *et al.*, 1999), despite not being essential for either exocytosis or endocytosis (Janz *et al.*, 1999). There is no alteration in gross brain morphology of SV2A KO mice (Crowder *et al.*, 1999) nor is there any difference in the size, number or location of SVs (Janz *et al.*, 1999). Synapses lacking SV2 package and release neurotransmitter, indicating that SV2s are not responsible for this function (Janz et al, 1999). However SV2A is found to be important in Ca^{2+}-dependent regulation of neurotransmitter release during repetitive stimulation (Janz *et al.*, 1999). As repetitive stimulation is a model used for induction of epilepsy, this showed that SV2A could be implicated in a role in epilepsy. SV2A was identified as the necessary and sufficient binding partner for the AED Levetiracetam in 2004 (Lynch *et al.*, 2004).

6.1.5 LEVETIRACETAM

Levetiracetam was already known to have a mechanism of action distinct from other AEDs. It had no effect on acute seizure models (maximal electroshock seizure test and maximal pentylenetetrazol seizure test), but has a potent effect on generalized seizures in chronically kindled models of epilepsy (both electrically and pentylenetetrazol-kindled models) (Klitgaard *et al.*, 1998).

Kindling is a model of epileptogenesis where animals are subjected to repeated subconvulsive stimuli, which ultimately results in generalized seizures of the animals; with several specific electrographic and behavioural stages. This

paradigm was found to be associated with an accumulation of 7S SNARE complexes in the ipsilateral hippocampus (Matveeva *et al.*, 2003). This kindling-induced accumulation of SNARE complexes was prevented by Levetiracetam (Matveeva *et al.*, 2008), suggesting a possible mechanism of action of its interaction with SV2A.

The effects of Levetiracetam on SV2A and SNARE complexes suggest a possible effect on the regulation of neurotransmitter release. In agreement, exposure of rat hippocampal slices to 100 μM Levetiracetam for 3 hours led to inhibition of subsequent synaptic potentials during a train of stimuli, and also led to a reduction in vesicle fusion as determined by quantification of FM1-43 destaining (Yang *et al.*, 2007). This evidence implicates Levetiracetam as a modulator of the synaptic vesicle cycle.

As the binding partner for Levetiracetam is a protein implicated in the synaptic vesicle cycle, and as Levetiracetam has been shown to be a modulator of neurotransmitter release, then Levetiracetam could potentially work through influencing the exocytosis or endocytosis of synaptic vesicles. To investigate this possibility, the standard S1 S2 FM dye assay, and electron microscopy was used to assess the effect of Levetiracetam, UCB-22060and UCB106758-1 on our neuronal cell model systems. 22060, UCB 060, is an inactive enantiomer of Levetiracetam, which lacks the antiepileptic properties of Levetiracetam, and fails to bind to the same site on SV2A (Lynch *et al.*, 2004). UCB 106758-1 is a novel AED.

6.2 RESULTS

To investigate the effects of Levetiracetam on SV turnover in cerebellar granule neurons (CGNs), the S1 S2 FM dye assay was used, with drug incubations prior to and during S2 loading. This should reveal the effects on either exocytosis or endocytosis, since FM dye uptake is dependent on both processes.

For all experiments cells were loaded at S1 with FM1-43 as described in the figure legends (using either high K^+ or electrical stimulation). After a 10 minute rest, cells were unloaded using 2 brief sequential stimuli. Following S1 unloading cells were incubated with the relevant drug for 15 minutes, with the drug also included in the S2 load. S2 loading and unloading were otherwise identical to the S1 loading conditions.

6.2.1 LEVETIRACETAM OR ANALOGUES HAVE NO EFFECT ON SYNAPTIC VESICLE TURNOVER EVOKED BY A MAXIMAL STIMULUS.

We first looked at the effect of Levetiracetam and its analogues on SV turnover using a protocol that evokes maximal SV turnover. This will indicate an effect on either exocytosis or endocytosis, since a change in the amount of dye unloaded could be due to an alteration in either the exocytosis or endocytosis of vesicles. KCl (50 mM) was used to stimulate the cells for dye loading (Fig. 6.1 **A**). This stimulus turns over all available SVs, by activating both the bulk and the single-vesicle retrieval pathway (chapter 3).

With KCl stimulation, no difference was seen between the control conditions and the cultures which were incubated with 100 μM Levetiracetam for 20 minutes prior to and during the S2 load of FM dye (Fig 6.1 **B**). When the cultures were

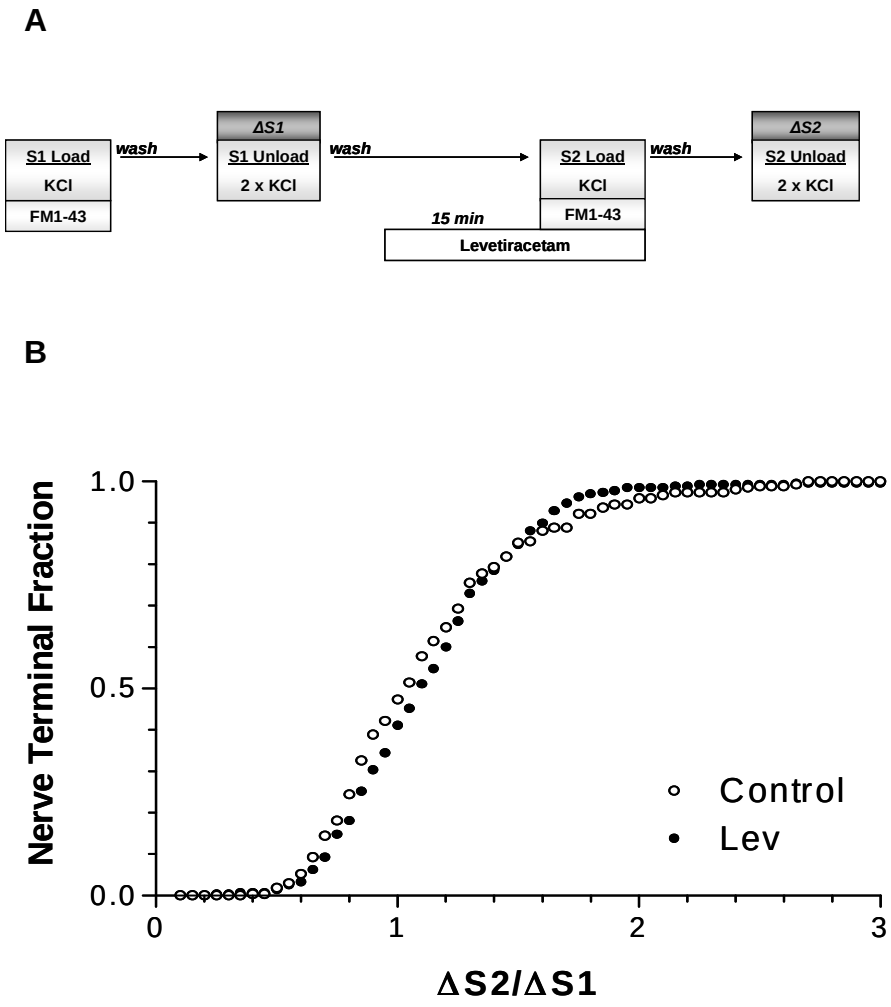

Figure 6.1 - Levetiracetam has no effect on synaptic vesicle turnover at maximal loading stimulation. **A**, Granule neuron cultures were loaded with 10 μM FM1-43 using stimulation with 50 mM KCl. Dye was washed immediately from the cultures after stimulation. Dye was then unloaded using 2 sequential 30 s stimuli of 50 mM KCl. This protocol was repeated at S2. Cultures were incubated with 100 μM Levetiracetam for 15 min prior to and including S2 loading. **B**, Cumulative histogram of the effect of Levetiracetam on SV turnover in individual nerve terminals (ΔS2/ΔS1, control N=270, Lev N=270). Open symbols = control, solid = Lev.

pre-incubated with either 22060 (Fig 6.2 **B**), or 106758-1 (Fig 6.3 **B**), again no difference was observed in vesicle turnover.

This indicates that neither Levetiracetam nor its analogues have any effect on SV turnover evoked by prolonged exposure to elevated KCl.

6.2.2 Levetiracetam and its analogues have no effect on SV turnover at 80 Hz stimulation.

KCl stimulation, whilst being the strongest stimulation available for induction of SV turnover, is not a physiologically relevant stimulus. To mimic strong physiological stimulation, such as that observed in epilepsy, 800 action potentials (APs) were delivered at a frequency of 80 Hz, with the FM dye washed from the cultures directly after cessation of stimulation (Fig. 6.4 **A**). This strength of stimulation activates both bulk endocytosis and the single synaptic vesicle pathway (chapter 3). Dye was washed immediately after termination of stimulation to specifically label the pathway of recycling that occurs during stimulation.

When cultures were incubated with 100 μM Levetiracetam, no effect of the drug on turnover of SVs was observed (Fig. 6.4 **B**) with this stimulation protocol. Neither 22060 (Fig. 6.5 **B**) nor 106758-1 have an inhibition of SV turnover with this maximal stimulus (Fig 6.6 **B**). Thus Levetiracetam and its analogues have no effect on SV turnover during strong prolonged stimulation.

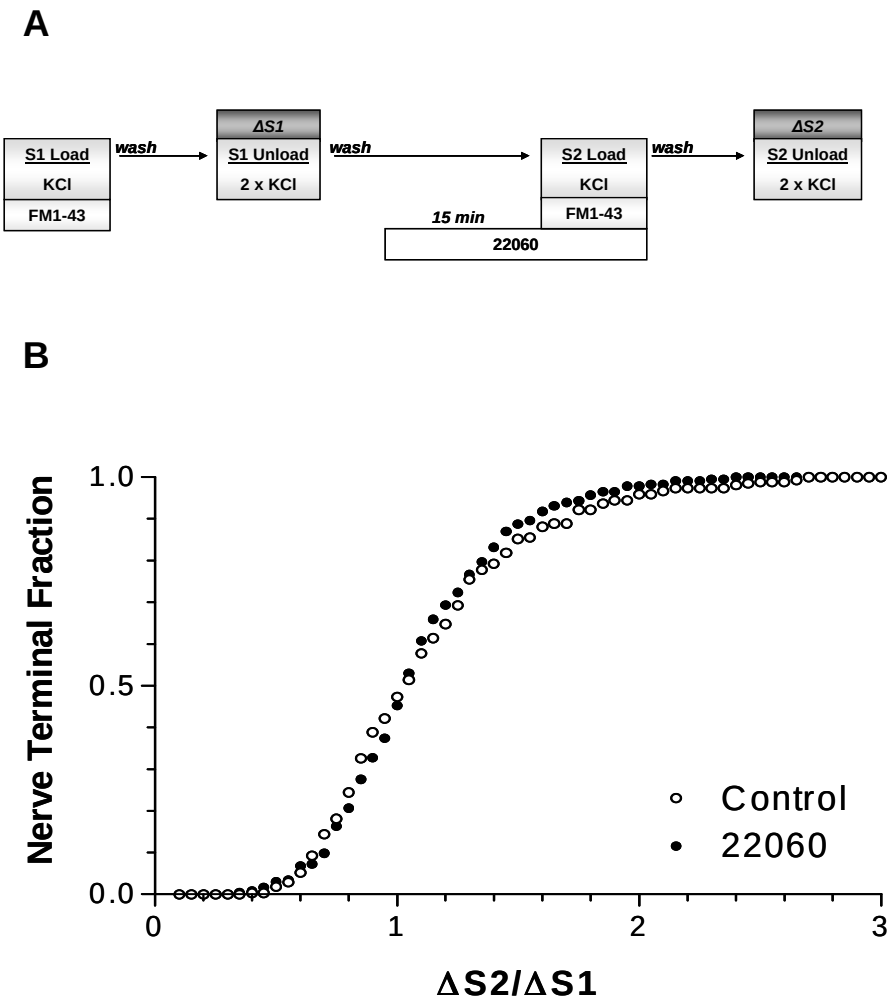

Figure 6.2 - 22060 has no effect on synaptic vesicle turnover at maximal loading stimulation. **A**, Granule neuron cultures were loaded with 10 μM FM1-43 using stimulation with 50 mM KCl. Dye was washed immediately from the cultures after stimulation. Dye was then unloaded using 2 sequential stimuli of 800 action potentials (80 Hz for 10 s). This protocol was repeated at S2. Cultures were incubated with 100 μM 22060 for 15 min prior to and including S2 loading. **B**, Cumulative histogram of the effect of 22060 on SV turnover in individual nerve terminals (ΔS2/ΔS1, control N=270, 22060 N=232). Open symbols = control, solid = 22060.

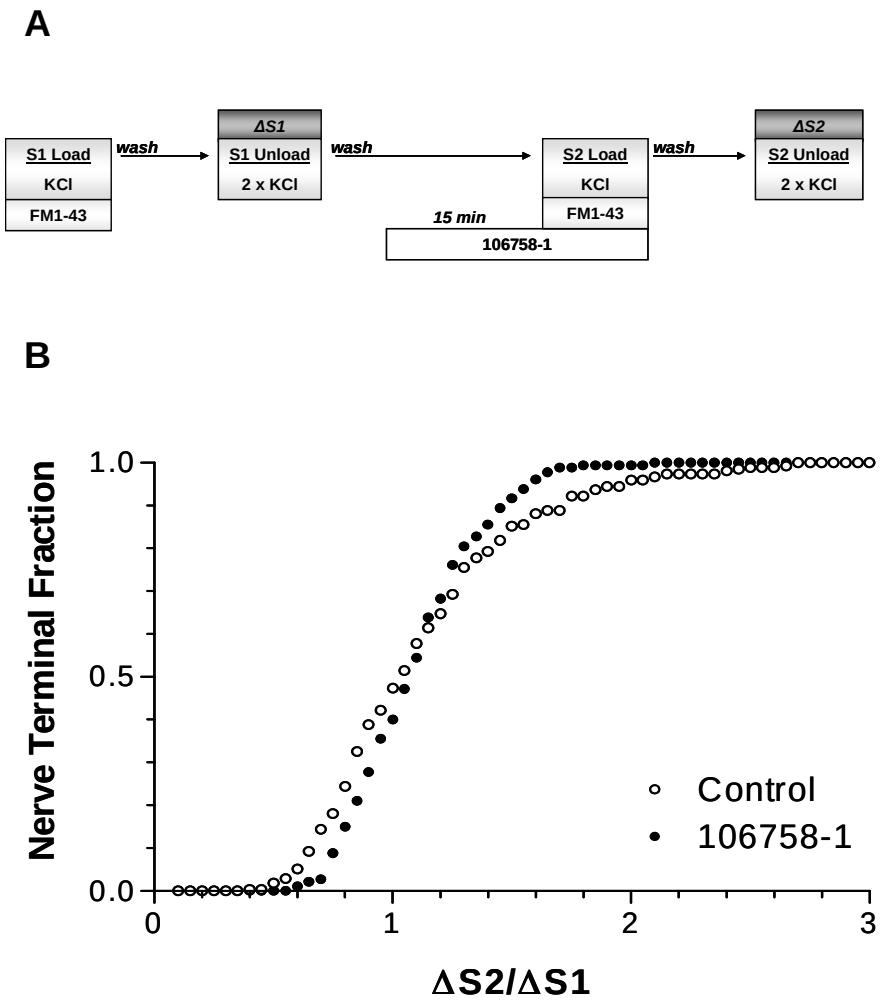

Figure 6.3 - 106758-1 has no effect on synaptic vesicle turnover at maximal loading stimulation. **A**, Granule neuron cultures were loaded with 10 μM FM1-43 using stimulation with 50 mM KCl. Dye was washed immediately from the cultures after stimulation. Dye was then unloaded using 2 sequential 30 s stimuli of 50 mM KCl. This protocol was repeated at S2. Cultures were incubated with 20 μM 106758-1 for 15 min prior to and including S2 loading. **B**, Cumulative histogram of the effect of 106758-1 on SV turnover in individual nerve terminals (ΔS2/ΔS1, control N=270, 106758-1 N=180). Open symbols = control, solid = 106758-1.

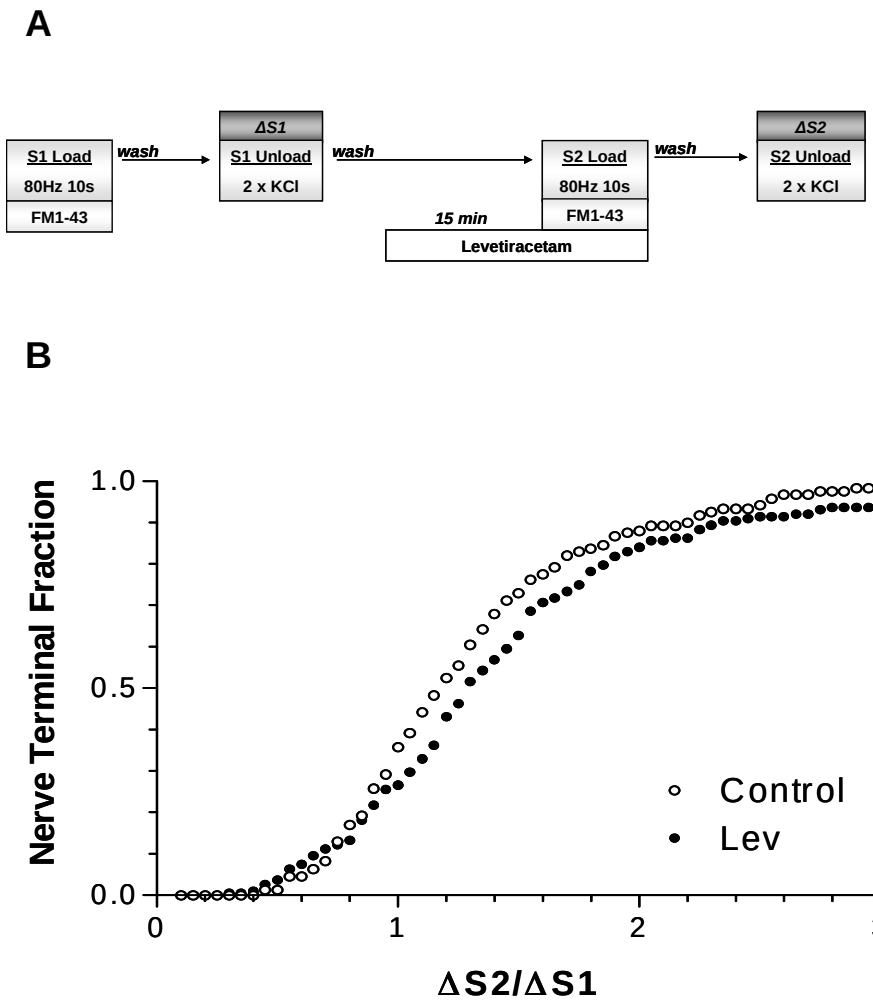

Figure 6.4 - Levetiracetam has no effect on synaptic vesicle turnover at maximal physiological loading stimulation. **A**, Granule neuron cultures were loaded with 10 μM FM1-43 using stimulation with 800 action potentials (80 Hz for 10 s). Dye was washed immediately from the cultures after stimulation. Dye was then unloaded using 2 sequential 30 s stimuli of 50 mM KCl. This protocol was repeated at S2. Cultures were incubated with 100 μM Levetiracetam for 15 min prior to and including S2 loading. **B**, Cumulative histogram of the effect of Levetiracetam on SV turnover in individual nerve terminals (ΔS2/ΔS1, control N=240, Lev N=188). Open symbols = control, solid = Lev.

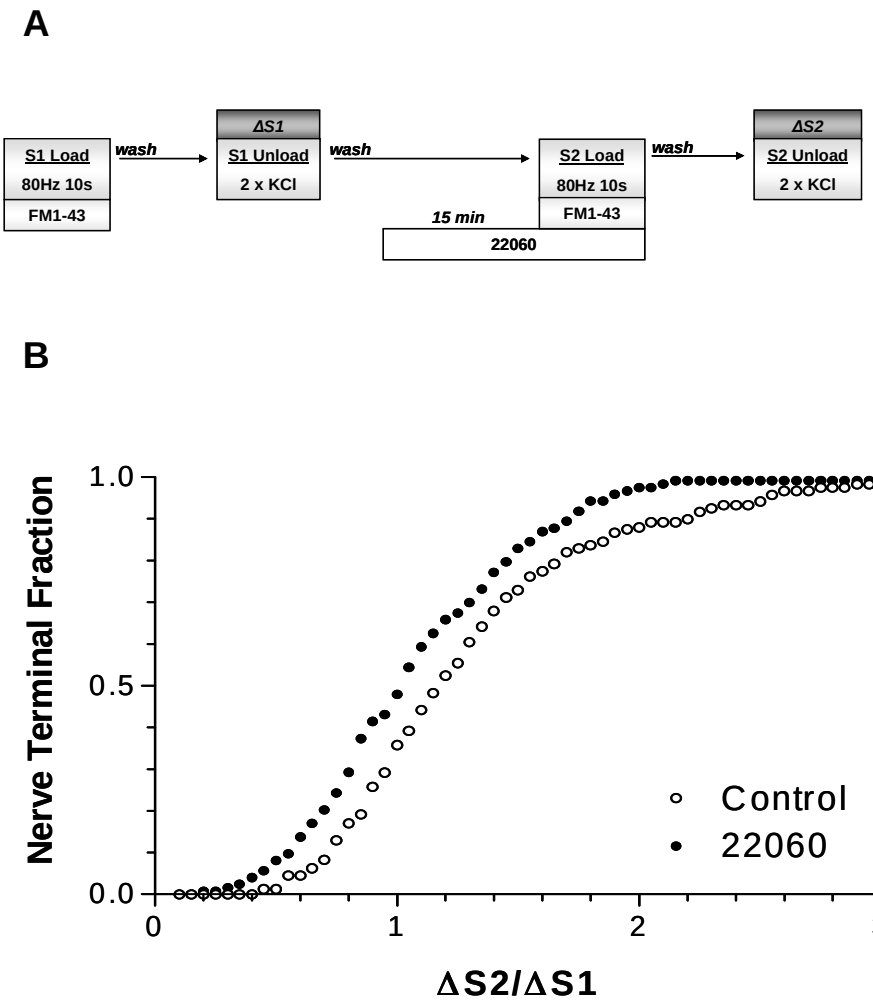

Figure 6.5 - 22060 has a small effect on synaptic vesicle turnover at maximal physiological loading stimulation. **A**, Granule neuron cultures were loaded with 10 μM FM1-43 using stimulation with 800 action potentials (80 Hz for 10 s). Dye was washed immediately from the cultures after stimulation. Dye was then unloaded using 2 sequential 30 s stimuli of 50 mM KCl. This protocol was repeated at S2. Cultures were incubated with 100 μM 22060 for 15 min prior to and including S2 loading. **B**, Cumulative histogram of the effect of 22060 on SV turnover in individual nerve terminals (ΔS2/ΔS1, control N=240, 22060 N=258). Open symbols = control, solid = 22060.

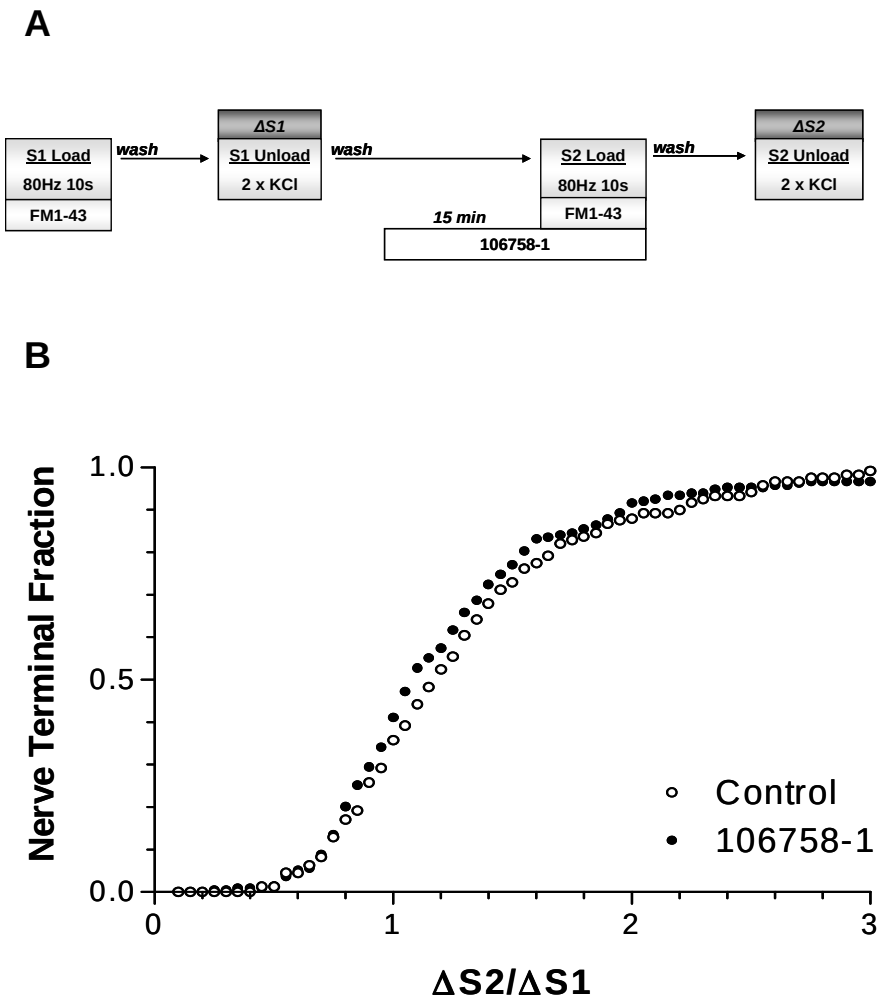

Figure 6.6 - 106758-1 has no effect on synaptic vesicle turnover at maximal physiological loading stimulation. **A**, Granule neuron cultures were loaded with 10 μM FM1-43 using stimulation with 800 action potentials (80 Hz for 10 s). Dye was washed immediately from the cultures after stimulation. Dye was then unloaded using 2 sequential 30 s stimuli of 50 mM KCl. This protocol was repeated at S2. Cultures were incubated with 20 μM 106758-1 for 15 min prior to and including S2 loading. **B,** Cumulative histogram of the effect of 106758-1 on SV turnover in individual nerve terminals (ΔS2/ΔS1, control N=240, 106758-1 N=214). Open symbols = control, solid = 106758-1.

6.2.3 Levetiracetam and its analogues have no effect on slow endocytosis.

Stimulation with 800 APs results in a large retrieval of SVs after termination of the stimulus, predominantly via the single SV route. Therefore to reveal any effects which may be occurring during the slow phase of endocytosis (which persists after termination of stimulation), FM dye was left on the cultures for one minute following 800 APs stimulation (Fig. 6.7 **A**).

Pre-incubation with Levetiracetam again had no effect on the turnover of SVs during slow endocytosis (Fig. 6.7 **B**).even when extra time was allowed for labelling of the slow endocytosis pathway. There was a small decrease observed in SV turnover with 22060 incubation (Fig 6.8 **B**), but no effect of 106758-1 on SV turnover when extra time is allowed to label the slow pathway of endocytosis (Fig 6.9 **B**). Thus Levetiracetam and its analogues have no effect on SV turnover evoked by strong prolonged stimulus regardless of whether fast or slow pathways retrieval pathways are investigated.

6.2.4 Levetiracetam and its analogues have no effect on SV turnover at mild stimulation.

Mild stimulation of cerebellar granule cells is known to only activate the single vesicle pathway of clathrin-mediated endocytosis, and not bulk endocytosis (Evans & Cousin, 2007). To see if incubation with Levetiracetam could be affecting this pathway of SV retrieval, cells were stimulated with 300 APs at 10 Hz, with the FM dye washout delayed for 1 minute (Fig. 6.10 **A**). This is to allow sufficient time for labelling of the single vesicle retrieval pathway.

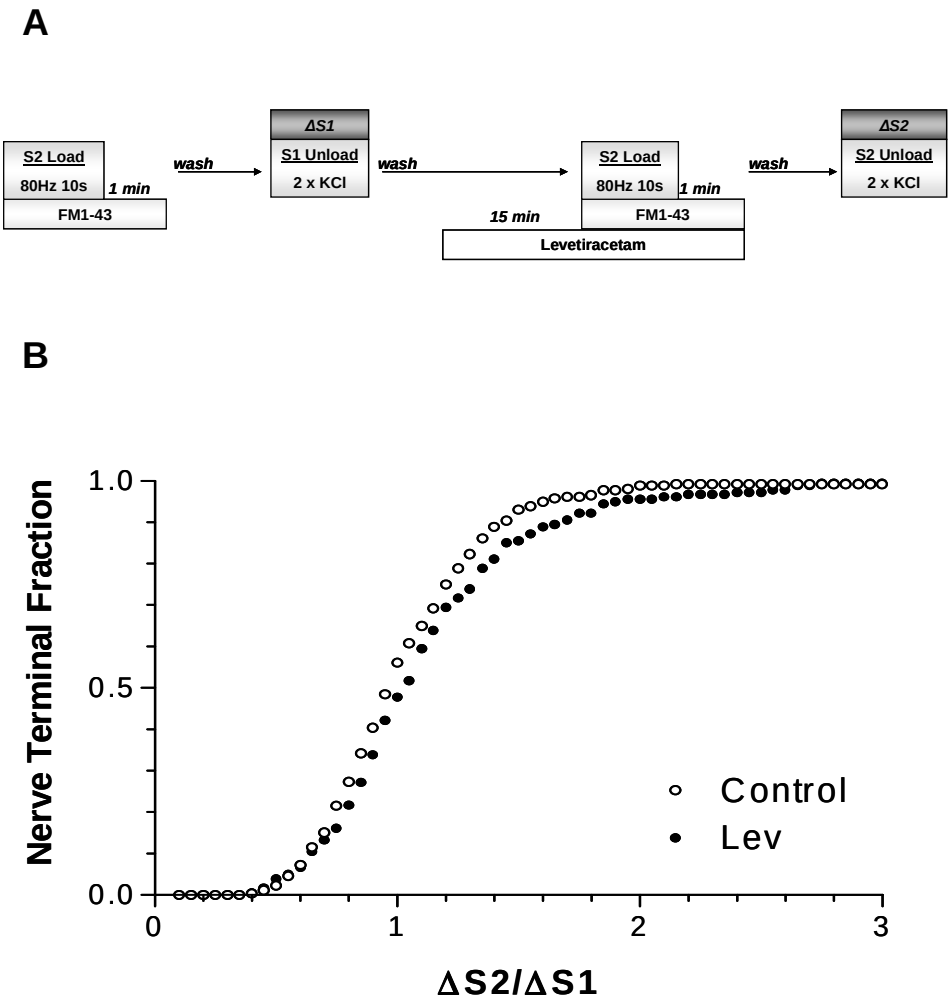

Figure 6.7 - Levetiracetam has no effect on slow endocytosis at maximal physiological loading stimulation. **A**, Granule neuron cultures were loaded with 10 µM FM1-43 using stimulation with 800 action potentials (80 Hz for 10 s). Dye washout was delayed for 1 minute. Dye was then unloaded using 2 sequential 30 s stimuli of 50 mM KCl. This protocol was repeated at S2. Cultures were incubated with 100 µM Levetiracetam for 15 min prior to and including S2 loading. **B**, Cumulative histogram of the effect of Levetiracetam on SV turnover in individual nerve terminals (ΔS2/ΔS1, control N=260, Lev N=180). Open symbols = control, solid = Lev.

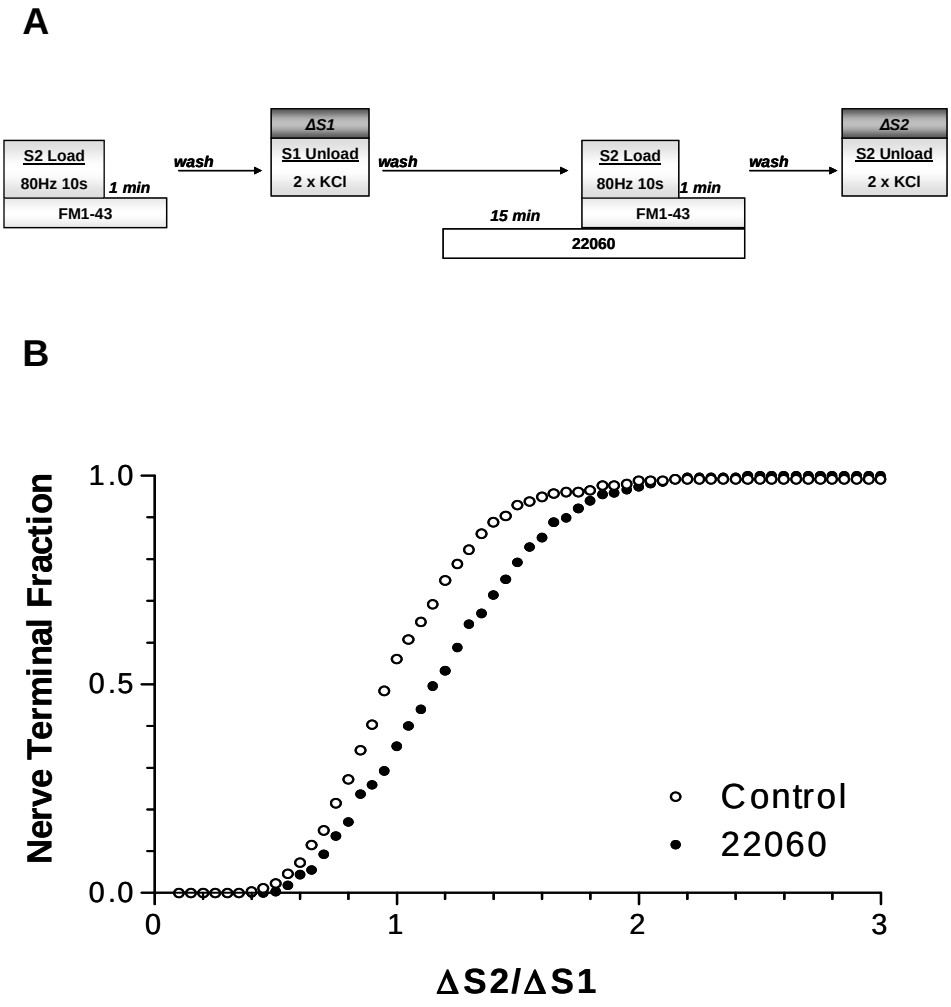

Figure 6.8 - 22060 has a small effect on slow endocytosis at maximal physiological loading stimulation. **A**, Granule neuron cultures were loaded with 10 μM FM1-43 using stimulation with 800 action potentials (80 Hz for 10 s). Dye washout was delayed for 1 minute. Dye was then unloaded using 2 sequential 30 s stimuli of 50 mM KCl. This protocol was repeated at S2. Cultures were incubated with 100 μM 22060 for 15 min prior to and including S2 loading. **B**, Cumulative histogram of the effect of 22060 on SV turnover in individual nerve terminals (ΔS2/ΔS1, control N=260, 22060 N=123). Open symbols = control, solid = 22060.

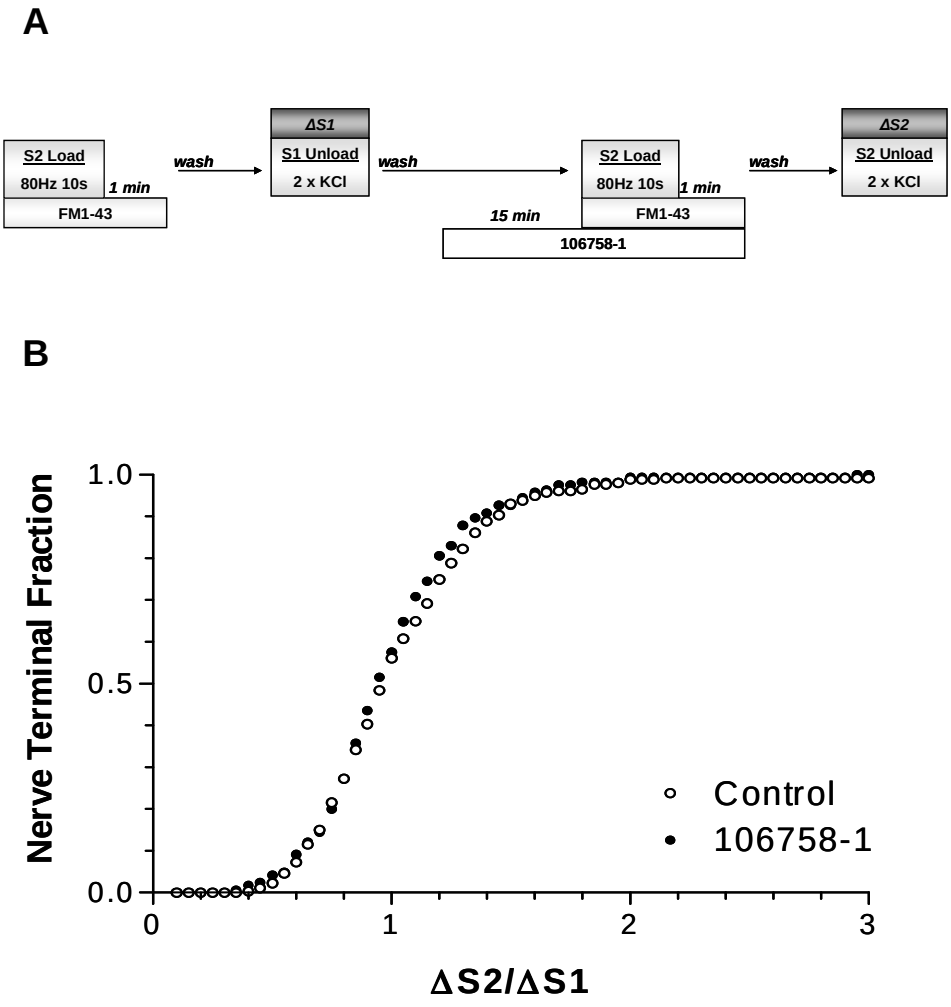

Figure 6.9 - 106758-1 has no effect on slow endocytosis at maximal physiological loading stimulation. **A**, Granule neuron cultures were loaded with 10 μM FM1-43 using stimulation with 800 action potentials (80 Hz for 10 s). Dye washout was delayed for 1 minute. Dye was then unloaded using 2 sequential 30 s stimuli of 50 mM KCl. This protocol was repeated at S2. Cultures were incubated with 20 μM 106758-1 for 15 min prior to and including S2 loading. **B**, Cumulative histogram of the effect of 106758-1 on SV turnover in individual nerve terminals (ΔS2/ΔS1, control N=260, 22060 N=165). Open symbols=control, solid=106758-1.

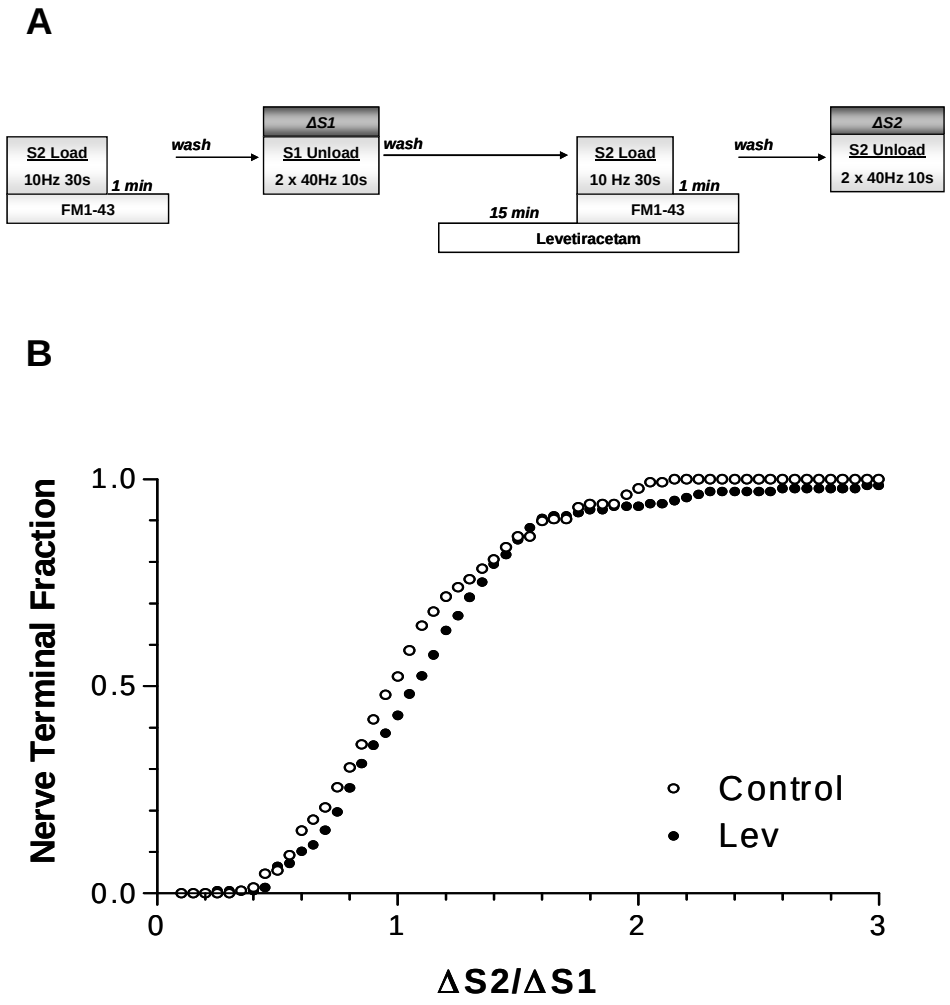

Figure 6.10 - Levetiracetam has no effect on synaptic vesicle turnover during mild stimulation. **A**, Granule neuron cultures were loaded with 10 μM FM1-43 using stimulation with 300 action potentials (10 Hz for 30 s). Dye washout was delayed for 1 minute. Dye was then unloaded using 2 sequential stimuli of 400 action potentials (40 Hz for 10 s). This protocol was repeated at S2. Cultures were incubated with 100 μM Levetiracetam for 15 min prior to and including S2 loading. **B**, Cumulative histogram of the effect of Levetiracetam on SV turnover in individual nerve terminals (ΔS2/ΔS1, control N=269, Lev N=137) Open symbols = control, solid = Lev.

Pre S2 incubation with Levetiracetam has no effect on synaptic vesicle turnover via the single vesicle clathrin-mediated route (Fig. 6.10 **B**). At this mild stimulation, neither 22060 (Fig 6.11 **B**) nor 106758-1 (Fig 6.12 **B**) have any effect on the turnover of SVs either. Thus drug incubation with strong or mild stimulation has no obvious effects on SV exocytosis or endocytosis (Fig 6.13)

6.2.5 Visualisation of different SV endocytosis routes in cultures incubated with Levetiracetam.

The experiments with FM dye uptake indicate a lack of effect of any of the drugs on SV turnover evoked by different stimulation paradigms. Electron microscopy (EM) was performed to confirm this observation. This is a more direct way of looking at SV turnover, as changes can be detected at the level of the individual synapse. To observe any subtle changes were occurring that had been indistinguishable with FM imaging, horseradish peroxidase (HRP) was used as a fluid phase marker of endocytic events in EM samples of cerebellar granule neurons.

Several different loading paradigms were investigated in cultures pre-incubated with Levetiracetam. Firstly the effect of Levetiracetam on spontaneous vesicle turnover was investigated by HRP labelling of resting cells. Very few HRP labelled SVs are present, consistent with previous observations of CGNs in studies on resting cultures. Very few HRP labelled SVs are present. An average of only approximately 1.0 ± 0.41 clear endosomes and 0.3 ± 0.26 HRP labelled endosomes per control nerve terminal are evident. In the cultures incubated with Levetiracetam, 1.5 ± 0.29 clear endosomes and 0.03 ± 0.03 HRP labelled endosomes were observed. Also very few HRP labelled SVs are present (0.67 ± 0.37 for control, 0.39 ± 0.17 for

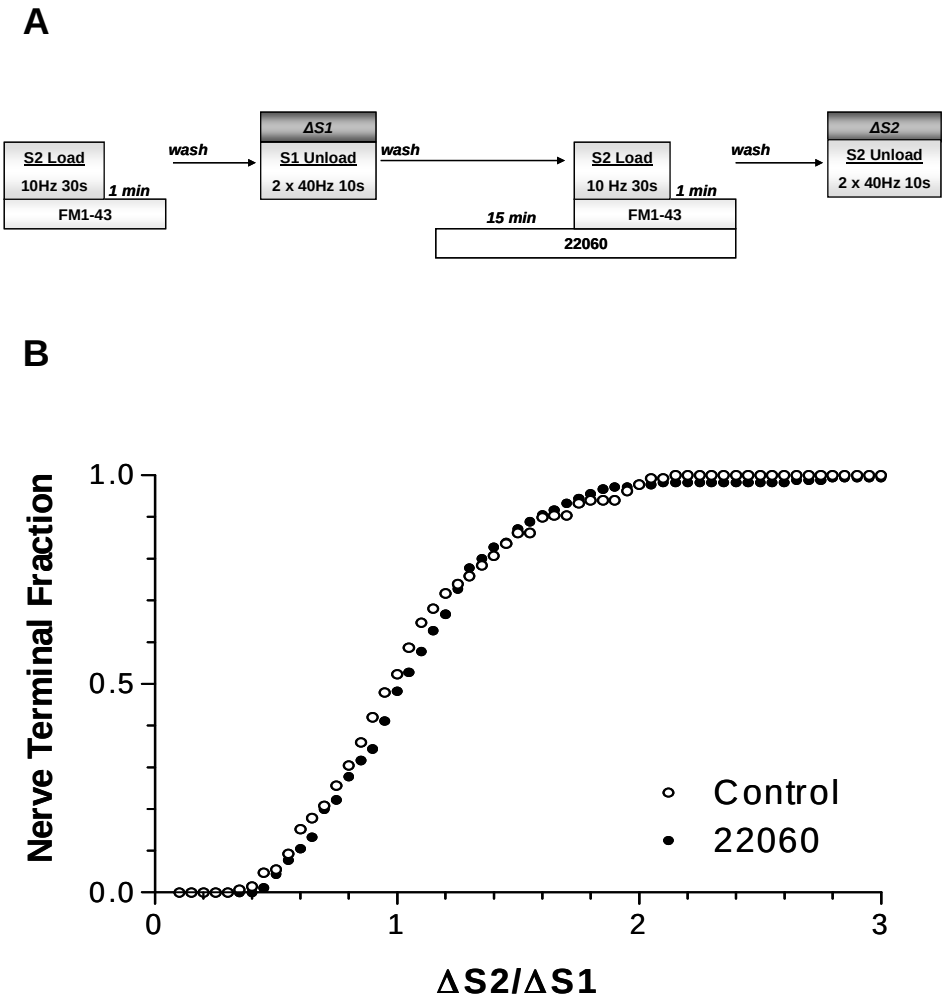

Figure 6.11 - 22060 has no effect on synaptic vesicle turnover during mild stimulation. **A**, Granule neuron cultures were loaded with 10 μM FM1-43 using stimulation with 300 action potentials (10 Hz for 30 s). Dye washout was delayed for 1 minute. Dye was then unloaded using 2 sequential stimuli of 400 action potentials (40 Hz for 10 s). This protocol was repeated at S2. Cultures were incubated with 100 μM 22060 for 15 min prior to and including S2 loading. **B**, Cumulative histogram of the effect of 22060 on SV turnover in individual nerve terminals (ΔS2/ΔS1, control N=269, 22060 N=180). Open symbols = control, solid = 22060.

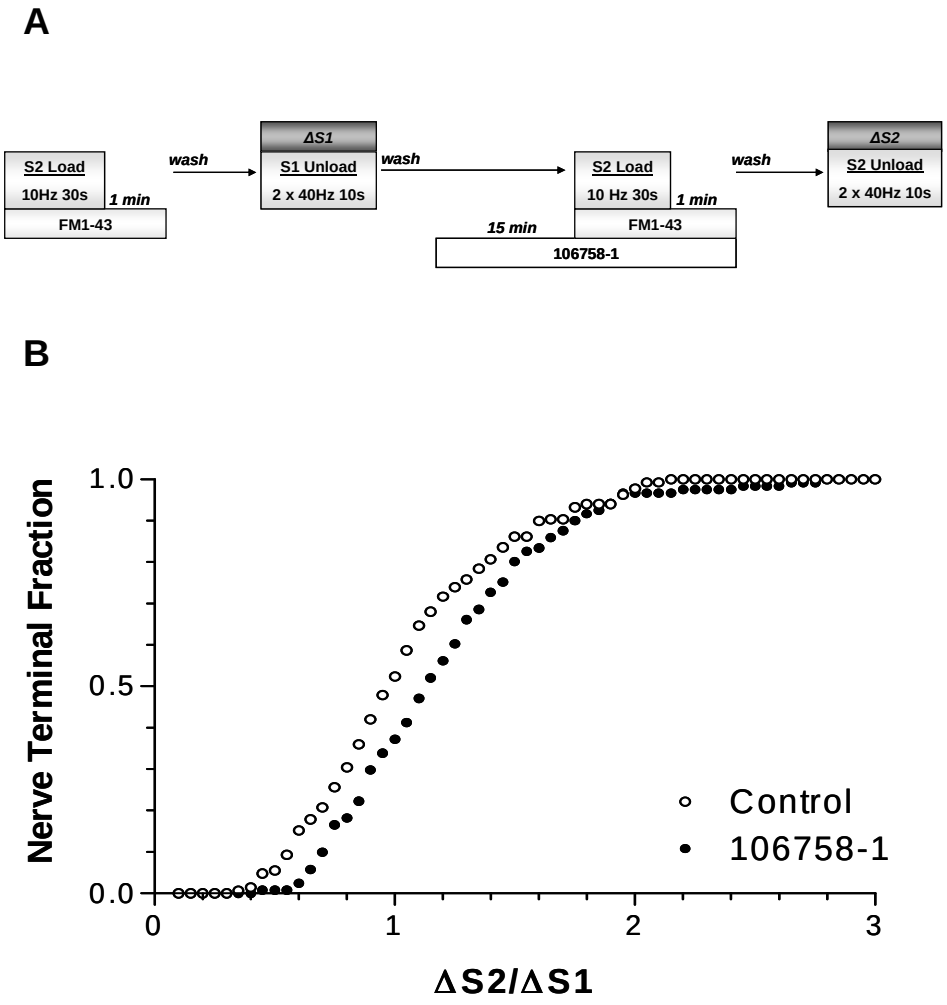

Figure 6.12 - 106758-1 has no effect on synaptic vesicle turnover during mild stimulation. A, Granule neuron cultures were loaded with 10 μM FM1-43 using stimulation with 300 action potentials (10 Hz for 30 s). Dye washout was delayed for 1 minute. Dye was then unloaded using 2 sequential stimuli of 400 action potentials (40 Hz for 10 s).This protocol was repeated at S2. Cultures were incubated with 20 μM 106758-1 for 15 min prior to and including S2 loading. B, Cumulative histogram of the effect of 106758-1 on SV turnover in individual nerve terminals (ΔS2/ΔS1, control N=269, 106758-1 N=121). Open symbols = control, solid = 106758-1.

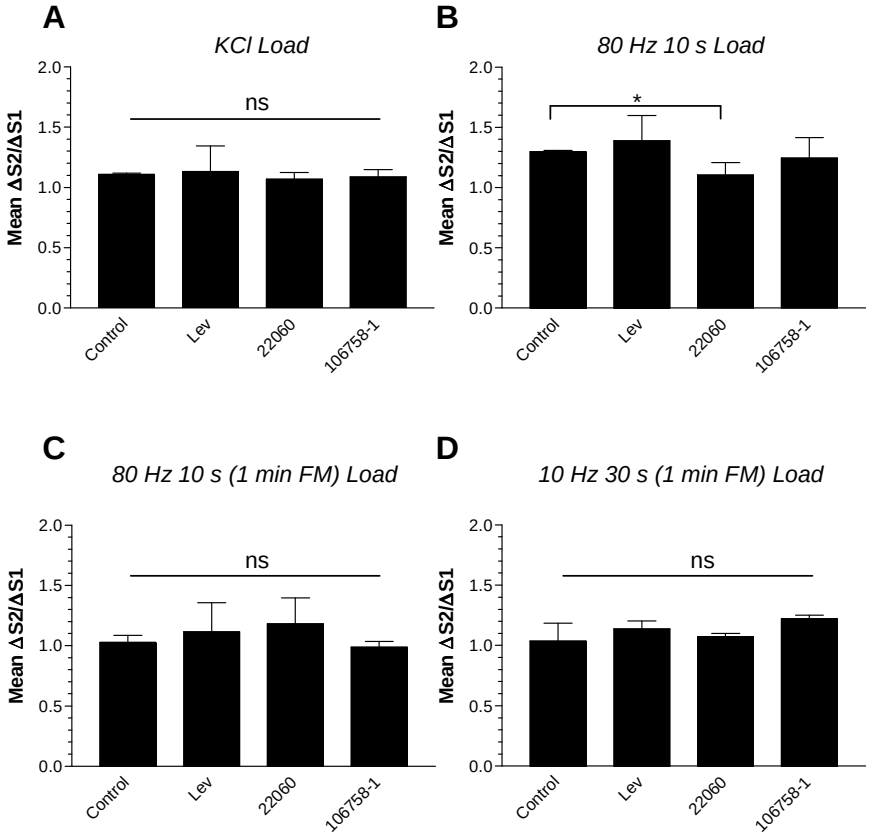

Figure 6.13 - Drug treatment has no effect on SV turnover with any stimulation protocol. Bar charts represent the mean proportion of SV turnover (mean ΔS2/ΔS1 ± SD) for control, Levetiracetam, 22060 and 106758-1 incubated cultures. For all graphs data was collated from the experiments described in previous figures. **A**, KCl loaded cultures. (Control N=3, Lev N=3, 22060 N=3, 106758-1 N=2). **B**, 80 Hz 10 s loaded cultures. (Control N=3, Lev N=3, 22060 N=2, 106758-1 N=3). **C**, 80 Hz 10 s loaded (1 minute FM) cultures. (Control N=3, Lev N=2, 22060 N=3, 106758-1 N=2). **D**, 10 Hz 30 s loaded (1 minute FM) cultures. (Control N=3, Lev N=2, 22060 N=2, 106758-1 N=2.). Unpaired t-test, * = $p < 0.05$

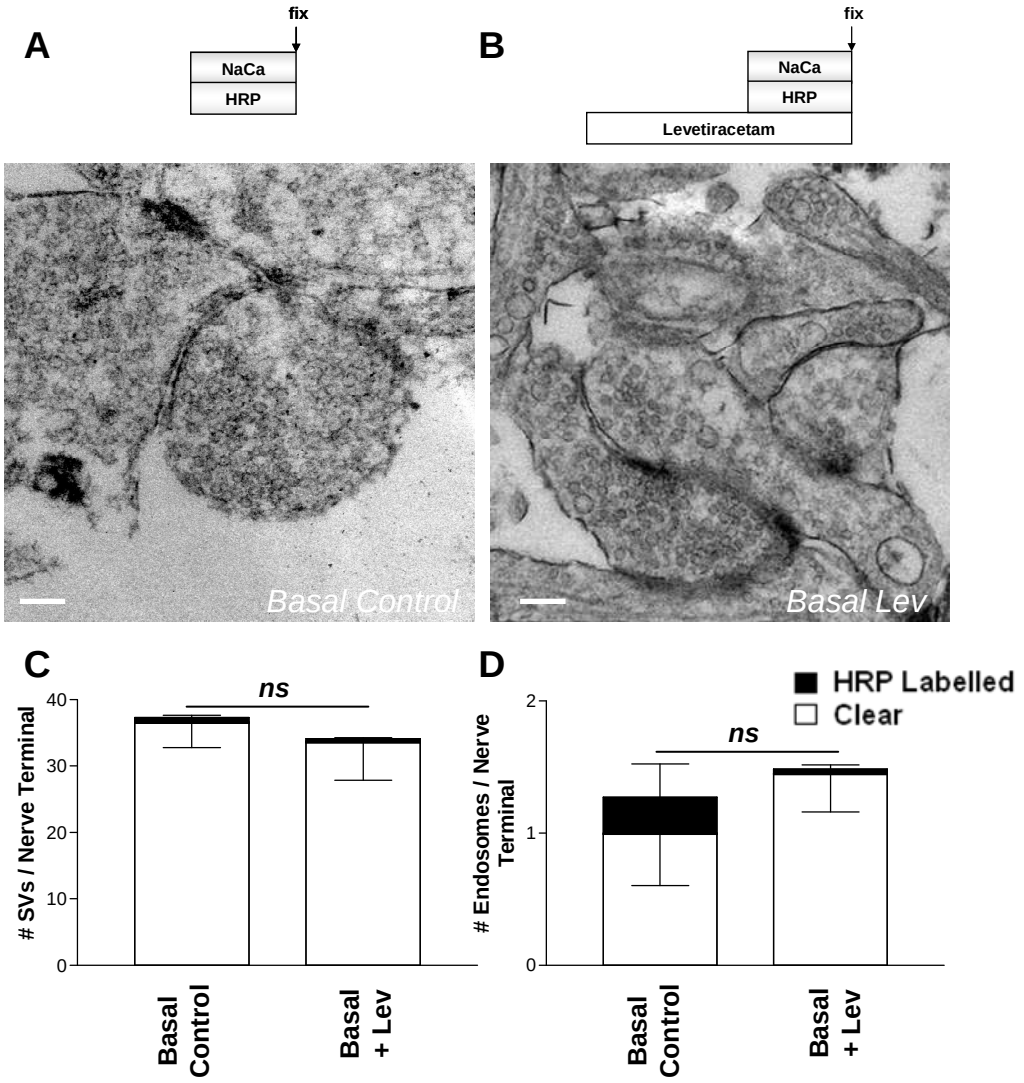

Figure 6.14 - Levetiracetam has no effect on the number of HRP-labelled synaptic vesicles or HRP-labelled endosomes in cultures at rest. Granule neuron cultures were incubated with HRP in the absence (**A**) and presence (**B**) of 100 µM Levetiracetam without any external simulation. Representative EMs for each condition are shown, scale bar 200 nm. The mean number of HRP-labelled (filled bars) and clear (open bars) synaptic vesicles (**C**) and endosomes (**D**) per nerve terminal (± SEM) in the presence and absence of Levetiracetam is shown. (Basal Ctrl N=12 nerve terminals, basal Lev N=33. Two-tailed t-test.).

Levetiracetam). Levetiracetam had no significant effect on the number of either clear or HRP-labelled SVs or endosomes in cultures at rest (Fig. 6.14).

HRP loading during KCl stimulation was used to investigate the effects of Levetiracetam on synaptic vesicle turnover at maximal stimulation. KCl stimulation was chosen as it activates both the bulk and the single vesicle retrieval pathways, so will allow the effects of Levetiracetam on either of these pathways to be visualised. A large increase in the number of HRP labelled SVs (6.3 ± 0.53) and endosomes (2.1 ± 0.25) was observed, confirming activation of both pathways.

Levetiracetam had no significant effect on the number of either clear or HRP-labelled SVs or endosomes stimulated by this protocol (Fig. 6.15). Thus Levetiracetam has no effect on SV endocytosis processes that are active during strong stimulation.

Addition of the fluid phase marker post-stimulation allows visualisation of the single vesicle retrieval pathway, which predominates following termination of stimulation. Therefore HRP labelling of cells directly following cessation of KCl stimulation was used to investigate the effect of Levetiracetam on the slow endocytosis pathway. In agreement, control cultures showed a decrease in the number of HRP labelled endosomes (0.3 ± 0.09) when HRP is applied following stimulation (Fig 6.16 D) than during stimulation (Fig 6.15 D), showing the predominant recycling pathway after stimulation to be the single vesicle retrieval pathway. Levetiracetam had no significant effect on the number of either clear or HRP-labelled SVs or endosomes when cultures were labelled directly after KCl stimulation (Fig. 6.16). Thus Levetiracetam has no effect on SV endocytosis retrieval following strong stimulation.

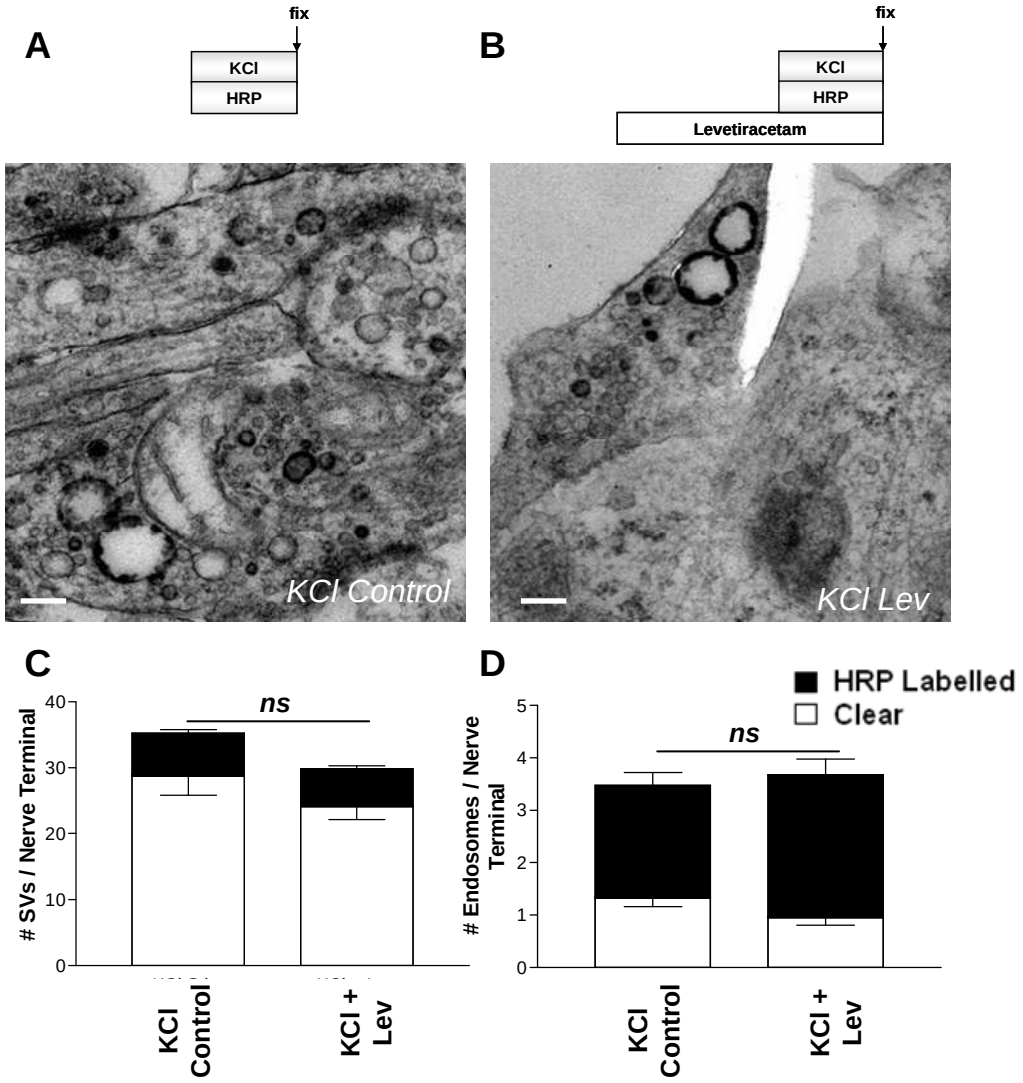

Figure 6.15 - Levetiracetam has no effect on the number of HRP-labelled synaptic vesicles or HRP-labelled endosomes in strongly stimulated cultures. **A**, Granule neuron cultures were loaded with HRP by stimulation for 2 minutes with 50 mM KCl. Loading occurred in the absence (**A**) and presence (**B**) of 100 µM Levetiracetam. Representative EMs for each condition are shown, scale bar 200 nm. The mean number of HRP-labelled (filled bars) and clear (open bars) synaptic vesicles (**C**) and endosomes (**D**) per nerve terminal (± SEM) in the presence and absence of Levetiracetam is shown. (KCl Ctrl N=63 nerve terminals, KCl Lev N=80 Two-tailed t-test).

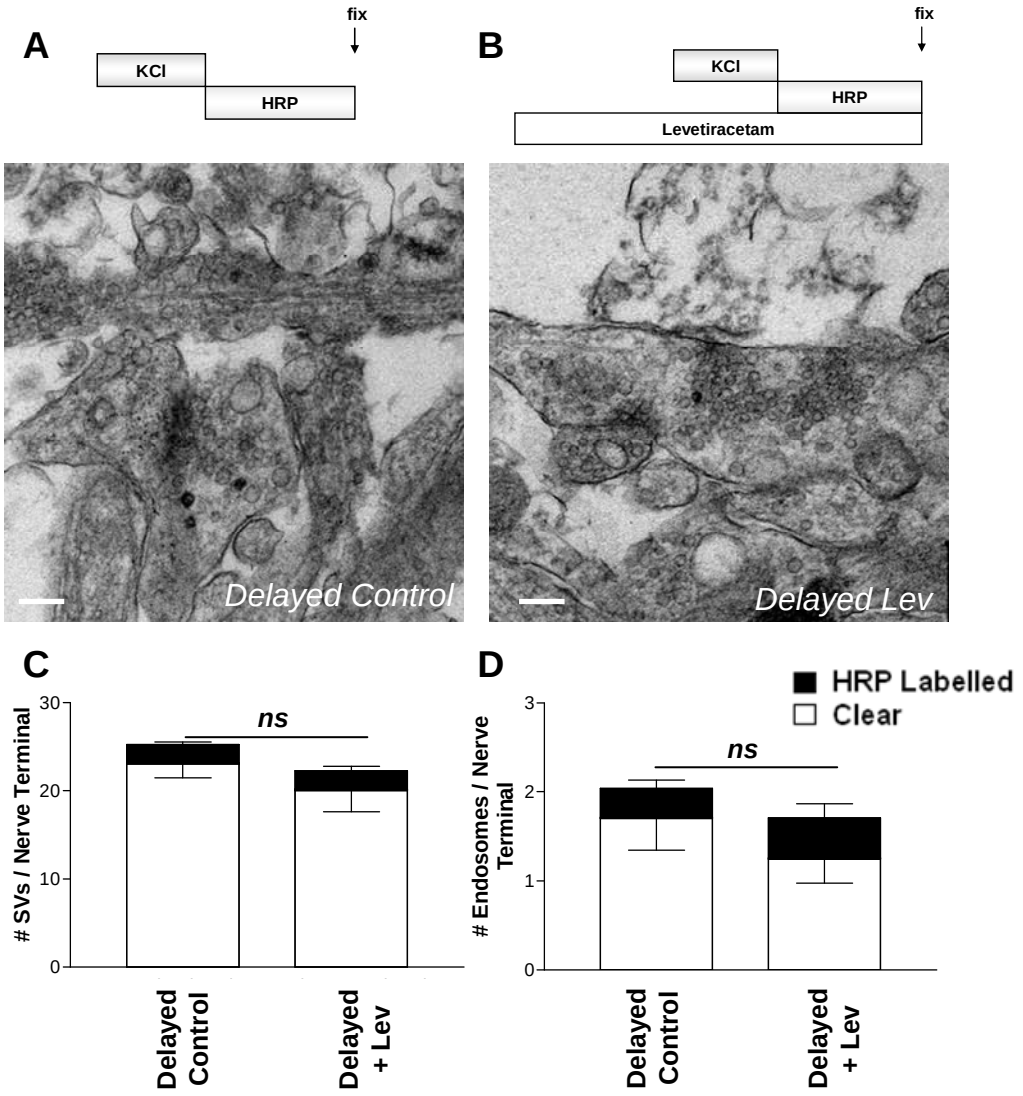

Figure 6.16 - Levetiracetam has no effect on the number of HRP-labelled synaptic vesicles or HRP-labelled endosomes in cultures labelled post-stimulation. **A**, Granule neuron cultures were loaded by incubation with HRP for 5 minutes immediately after 2 minutes of 50 mM KCl stimulation. Loading occurred in the absence (**A)** and presence (**B**) of 100 µM Levetiracetam. Representative EMs for each condition are shown, scale bar 200 nm. The mean number of HRP-labelled (filled bars) and clear (open bars) synaptic vesicles (**C**) and endosomes (**D**) per nerve terminal (± SEM) in the presence and absence of Levetiracetam is shown. (Delayed Ctrl N=49 nerve terminals, delayed Lev N=31 Two-tailed t-test).

6.3 Discussion

The identification of the synaptic vesicle protein SV2A as the necessary and sufficient binding partner for Levetiracetam indicates that Levetiracetam may mediate its anti-epileptic effects pre-synaptically. To investigate this possibility, its effect on the SV life cycle was examined in a central nerve terminal culture system.

6.3.1 Experimental conditions for studying the effects of Levetiracetam and its analogues on SV turnover.

In order to see the effect of Levetiracetam, 22060 and 106758-1 on synaptic vesicle turnover we used both strong and mild stimuli to challenge our cell cultures. We did this in order to determine the effects of the drug treatments on different forms of exocytosis or endocytosis. Maximal stimulation with KCl immediately activates the fusion of the readily releasable pool (RRP) and the reserve pool (RP), as well as activating both clathrin-mediated and bulk endocytosis (Royle & Lagnado, 2003). Mild stimulation with action potentials is known to activate only the fusion of the RRP, and the clathrin-mediated single vesicle pathway (Granseth *et al.*, 2006; Evans & Cousin, 2007). Addition of labelling dyes for the period immediately following stimulation allows labelling of the slow phase of endocytosis, which is known to be predominantly the single vesicle retrieval pathway. Through using various strengths of stimulation and delayed addition of dyes, it was hoped that any effect of Levetiracetam on SV exocytosis or endocytosis would be revealed.

6.3.2 Choice of fluorescent dyes for pharmacological analysis.

FM dye assays were performed at these differing stimulation frequencies for each of the drugs. It was necessary to utilize an assay which would allow the labelling and investigation of all retrieval pathways. FM1-43 was chosen as it labels all endocytic structures, whereas FM2-10 does not label bulk endosomes and only labels the single vesicle pathway (Richards *et al.*, 2000). In addition FM1-43 also labels both the RRP and RP when loaded during maximal stimulation (Evans & Cousin 2007), ensuring all aspects of both endocytosis and exocytosis were examined.

6.3.3 No significant effect of Levetiracetam or its analogues on SV turnover at any strength of stimulation

In general the FM dye assays showed no change in the amount of dye unloaded between S1 and S2, indicating no effect of any of the drugs on synaptic vesicle turnover of either mild or strong stimulation.

This suggests Levetiracetam does not modulate its effects via SV recycling. Is it possible that any effects have been missed? Although the use of different stimulation protocols in the FM dye assays allows the study of a number of different endocytosis pathways, it neglects the study of the most controversial form of endocytosis; kiss-and-run. This is because FM1-43 is thought to be too hydrophobic to be released during the fusion pore open time, and it is therefore possible that effects due to Levetiracetam could be missed. There are a couple of techniques which could rule out any effects on this form of endocytosis. FM1-43 can be used in combination with quenching agents such as bromophenol blue (Harata *et al.*, 2006),

or tracking of full fusion events with quantum dots (Zhang *et al.*, 2007; Zhang *et al.*, 2009). Alternatively FM analysis could be combined with whole-cell patch clamp capacitance measurements in a model system of a larger synapse (e.g. goldfish retinal bipolar cells).

Kiss-and-run is most prevalent at mild stimulation frequencies (Aravanis *et al.*, 2003), and it is therefore unlikely that Levetiracetam mediates its effects via kiss-and-run. The mild stimulation frequencies at which kiss-and-run is prevalent would not be a major component of the SV turnover that operates during excess neuronal activity in epilepsy.

Analysis with FM dye loading only takes into account gross changes in amount of recycling membrane and may miss subtle defects in SV pool organisation or morphology. Therefore it was necessary to look in more detail at the level of the synapse to confirm a lack of effect of Levetiracetam on SV turnover in our culture system. We looked at the effects of Levetiracetam at the level of the individual synapse using EM, to get a better idea of any changes occurring in morphology which would be undetectable with FM dye assays. The FM data was supported by the EM data, which also showed no significant difference between SV turnover in control versus cultures incubated with Levetiracetam.

6.3.4 Levetiracetam has been shown to have a presynaptic effect on neurotransmission in hippocampal slices.

Our studies have not found any effect of Levetiracetam on SV turnover. However other groups have shown that a prolonged exposure to Levetiracetam can significantly reduce the rate of vesicle release during mild stimulation (Yang *et al.*,

2007). A number of similarities exist between the two different experimental approaches. The concentrations of Levetiracetam used were identical, and with acute exposure to Levetiracetam Yang *et al.* (2007) found no effect on synaptic vesicle transmission. However with prolonged exposure they detected a significant alteration in paired pulse response, and a reduction in the rate of vesicle release following a train of stimulation in hippocampal slices. The length of the incubation of Levetiracetam was proposed to be effective by allowing entry of the drug to the nerve terminals.

We also looked at prolonged exposure to Levetiracetam. In this instance we left our cultures incubating in Levetiracetam for 1 hour before the S2 load of FM dye. However this did not reveal any significant difference between control and drug treated cultures (data not shown).

Of interest is the fact that the total vesicle pool in the EM of the Levetiracetam treated cultures is consistently (though not significantly) lower than the control cultures (for example, KCl stimulated cultures control total synaptic vesicle pool ± SEM was 35.25 ± 3.1, KCl + Levetiracetam was 29.88 ±2.33). It would be interesting to see if this difference is perpetuated during long trains of stimuli, as was the protocol used by Yang *et al.* in hippocampal slices. The reduction in vesicle release could be due to there being progressively less vesicles formed after repeated stimulation (as was their method of stimulus delivery). We would not have detected this with our FM dye assays, with only 1 set of load and unload stimuli delivered after Levetiracetam incubation.

Treatment with Levetiracetam showed no effect on synaptic vesicle turnover at any of the stimulation frequencies in these studies. Therefore it is unlikely that whatever effect Levetiracetam has through its binding to SV2 is mediated via an immediate change in SV trafficking in our system. There are several possible alternate explanations for the mechanism of action of the Levetiracetam/SV2A interaction.

6.3.5 Alternative explanations for the mechanism of action of the Levetiracetam/SV2A interaction.

The function of SV2A is still unknown. SV2A deficient mice displayed no problems with exocytosis and endocytosis per se (Janz *et al.*, 1999), but rather displayed a dysfunction in Ca^{2+} regulated exocytosis after sustained stimulation (short term depression), which implicates a function of SV2A during epileptic discharges. This coupled with the observation that SV2 functions before fusion occurs (Xu & Bajjalieh, 2001) supports the idea that SV2A acts as a modulator of the cycle at a level distinct from the synaptic vesicle cycle. As the exact function of SV2A is still undetermined, it's possible that the nature of the Levetiracetam SV2A interaction has no bearing on actual vesicle turnover, but rather that the mechanism of action is at a modulatory level. This is supported by the lack of an effect on vesicle turnover in our Levetiracetam studies. Use of protein tomogragphy has shown no difference in protein conformations of SV2A between control and Levetiracetam treated samples (Lynch *et al.*, 2008). So although Levetiracetam is known to bind SV2A, it's not yet been shown to have any effect on the protein itself.

6.3.6 What other ways could Levetiracetam control SV2A function apart from direct effects on SV turnover?

The mechanism of action of the Levetiracetam SV2A interaction in epilepsy could possibly be via protection of the SV2A protein. SV2A expression levels in the hippocampus were found to be decreased both in patients that died from status epilepticus, and also in chronically epileptic rats (van Vliet *et al.*, 2008). Therefore Levetiracetam may mediate the protection of SV2A in the synapse during epileptic stimuli.

6.3.7 Region specific mechanism of action of Levetiracetam.

The study which showed that Levetiracetam decreases vesicle release after a train of stimuli was performed on slices from the hippocampus (Yang *et al.*, 2007), and expression levels of SV2A are found to be decreased in the hippocampus of chronically epileptic rats (van Vliet *et al.*, 2008). This evidence could suggest a region specific mechanism of action of the drug.

How could a region specific mechanism of action then be explained? When the relative distributions of the different SV2 isoforms were looked at more closely, it appears that their expression patterns could contribute to this lack of a difference. As the cerebellum is the source of the granule neurons used in our study, SV2 isoform expression patterns here were of particular interest. The SV2A isoform is found to express in all types of cerebellar neurons, whether GABAergic purkinje cells or glutamatergic granule cells. However the expression of SV2B is found only in the glutamatergic granule cells of the cerebellum (Bajjalieh *et al.*, 1994).

6.3.8 Functional redundancy of isoforms leading to compensation.

It has been observed that some functional redundancy exists between SV2A and SV2B (Janz *et al.*, 1999). It's possible in our system that this functional redundancy could mean SV2B, which is only expressed in granule cells in the cerebellum, is compensating for the effects of SV2A, and explaining the lack of any effect of Levetiracetam on the cell culture system.

6.3.9 Studies in KO mice

In order to further assess the interaction between Levetiracetam and SV2A, SV2A and B double KOs would be extremely useful. A more direct way of confirming whether Levetiracetam has an effect on SV turnover would be to conduct similar experiments on the SV2 double KO mice. This could confirm the specificity of the Levetiracetam/SV2A interaction mediating this effect.

The exact function of SV2 is still unknown, which hampers the attempts to elucidate the mechanism of the interaction between SV2A and Levetiracetam. Determining the function of SV2A will no doubt lead to better understanding of the exact nature of the Levetiracetam SV2A interaction.

7. Final Discussion

7. Final Discussion

Characterisation of bulk endocytosis through the development of tailored assay systems has revealed that bulk endocytosis is a fast event that is triggered during strong stimulation, and that this process is dependent on both the dephosphorylation specific interaction between dynamin I and syndapin I, and the subsequent rephosphorylation of dynamin I by GSK3.

7.1 Bulk Synaptic Vesicle Endocytosis is Rapidly Triggered During Strong Stimulation

During periods of low stimulatory input, neurons can sustain neurotransmitter release purely by cycling of the readily RRP, without any mobilization of vesicles from the RP (Richards *et al.*, 2003). However when the stimulus load is increased, single SV retrieval by CME can become saturated. This leaves the synapse in a position where the surface area of the pre-synaptic membrane is increasing due to the addition of a large amount of collapsed SV membrane. This increase in surface area translates to an increase in the volume of the synapse, which could compromise the integrity of such a complex structure. Therefore, when the exocytic load scales, a new mechanism of endocytosis which retrieves a greater amount of SV membrane would be an efficient mechanism to counter and correct for these potentially detrimental increases in synaptic surface area. We have shown that bulk endocytosis is immediately activated during strong stimulation, is completed rapidly, and that retrieval by bulk endocytosis terminates after cessation of stimulation

What is the signal that leads to this switch in endocytic retrieval? Calcineurin, a calcium-dependent protein phosphatase responsible for the dephosphorylation of

dynamin I, is a likely candidate for a role as this ADBE sensory trigger. Increased activity will lead to a larger influx of Ca^{2+} through VGCCs, which will increase the intracellular cytosolic Ca^{2+} concentration. The intracellular Ca^{2+} increase will reflect accurately the intensity of the activity, and could thus be an effective reporter for the need to activate the bulk retrieval pathway. Calcineurin has a low, micromolar affinity for Ca^{2+} (Klee & Crouch, 1979); this affinity is lower than the intracellular Ca^{2+} concentrations which occur in the cytosol during mild stimulation. However when activity increases a greater rise in intracellular Ca^{2+} concentration will occur, leading to activation of calcineurin resulting in dephosphorylation of the calcineurin substrates, the dephosphins. In agreement, a requirement for calcinuerin is seen in both hippocampal neurons and chromaffin cells, where inhibition of calcineurin decreases SV turnover during stronger stimulation, but no affect is seen during mild stimulation (Chan & Smith, 2001, Kumashiro *et al.*, 2005). This further supports the idea that the action of calcineurin is important during increased neuronal activity, highlighting calcineurin as the ideal sensor for the switch to activate retrieval by bulk endocytosis in response to increased activity.

7.2 The Phosphorylation-Dependent Dynamin I-Syndapin I Interaction Selectively Recruits an Activity-Dependent Synaptic Vesicle Endocytosis Pathway

Calcineurin is the protein phosphatase responsible for the dephosphorylation of dynamin I. We have shown that the dephosphorylation specific dynamin I-syndapin I interaction is essential for bulk endocytosis, through perturbation of the

interaction using inhibitory peptides and looking at the resultant differences in uptake of both FM dyes and large dextrans. The presence of the F-BAR domain in syndapin I can bind to and tubulate membrane of a shallower curvature than that tubulated by the N-BAR domains of either amphiphysin I or endophilin I. Thus it can be visualised that bulk endosomes, which have a larger diameter and thus are of shallower curvature could be produced by syndapin I interaction, whilst SVs which have a smaller diameter and are more tightly curved are bound by amphiphysin I and endophilin I. In agreement, injection of antibodies against syndapin in lamprey terminals results in an activity-dependent inhibition of endocytosis, an effect which is specific for bulk endocytosis, and not CME (Andersson *et al.*, 2008), whilst interference with amphiphysin inhibits SVE evoked by mild stimulation (Shupliakov *et al.*, 1997). Observations from our lab show that degree of dynamin I dephosphorylation parallels the increase of stimulation to a strength at which bulk endocytosis is activated (M. Cousin, personal communication), thus the recruitment of bulk endocytosis as a retrieval mechanism complements the change in phosphorylation status of dynamin I which results in enabling an interaction of dynamin I with syndapin I.

During mild stimulation the major membrane retrieval pathway is CME (Granseth *et al.*, 2006, Evans & Cousin 2007). Following stronger stimulation ADBE is recruited in conjunction with CME. The interaction of dynamin I with amphiphysin I is necessary for the progression of CME (Shupliakov *et al.*, 1997). This interaction is independent of the phosphorylation status of dynamin I (Tan *et al.*, 2003, Anggono *et al.*, 2006), and thus CME progresses during all stimulation strengths. Intense stimulation results in dephosphorylation of dynamin I by

calcineurin, enabling an interaction with syndapin I, and ADBE then progresses mediated by the F-BAR domain of syndapin I.

Further evidence to support this theory can be gathered from studies of the dynamin I KO mouse. The dynamin I KO mouse was originally perceived to manifest a defect in endocytosis following an increase in the strength of stimulation; this defect was only seen during the stronger stimulus, under conditions of mild stimulus the terminals do not show impairment in SV turnover (Ferguson *et al.*, 2007). This defect was only seen during stimulation and not after, fitting with a role for dynamin I dephosphorylation in fast bulk endocytosis. Conversely in the calyx of held dynamin I was proposed to mediate slow CME, which the authors say represents the major retrieval pathway (Lou *et al.*, 2008). However in this same synapse, also using capacitance measurements, bulk retrieval has been found to occur rapidly (Wu & Wu, 2007), and we have now shown that in small central synapses the mechanism which responds to elevations in stimulus strength is retrieval by bulk endocytosis. This indicates that it may in fact be the pathway of bulk retrieval which is affected by a loss of dynamin I function. Conversely, the majority of structures seen at the synapse of dynamin I KO neurons following acute stimulation are endosomal in structure, indicating that these endosomes have been generated by a dynamin I independent pathway. However this was observed primarily in inhibitory neurons; excitatory neurons were largely unaffected even under these increased stimulus conditions (Hayashi *et al.*, 2008). This indicates that there may in fact be differences between inhibitory and excitatory synapses in the contribution of dynamin I to SVE.

Unpublished observations from the lab indicate that dynasore, a selective inhibitor of the GTPase action of dynamin I and II, blocks both bulk endocytosis and CME in CGNs (M Cousin, personnel communication). This indicates that the GTPase activity of dynamin I is required for both CME and ADBE, whilst the phophorylation specific interaction of dynamin I and syndapin I is important in ADBE. Thus the role of dynamin I in endocytosis is still not entirely clear, and further studies are needed to conclusively show the mechanisms of action of dynamin I in SVE.

7.3 GSK3B IS ESSENTIAL FOR ACTIVITY-DEPENDENT BULK SYNAPTIC VESICLE ENDOCYTOSIS

Following dephosphorylation of dynamin I by calcineurin, dynamin I must then be re-phosphorylated. Cdk5 has been shown *in vitro* to facilitate the rephosphorylation of serines 774 and 778 of dynamin I, the major phosphorylation sites on dynamin I (Tan *et al.*, 2003). The action of cdk5 has been shown to be essential for bulk endocytosis, but not CME (Evans & Cousin, 2007). The presence of the consensus sequence for GSK3 at these dynamin I phosphorylation sites prompted the investigation of the effect of GSK3β activity on SV turnover. Selective GSK3β antagonists used in conjunction with FM dye and dextran assays showed that GSK3β activity is essential for ADBE, but not CME, in CGNs. This suggests that rephosphorylation of serine 774 by GSK3 is essential for bulk endocytosis. In agreement, GSK3 antagonists specifically block rephosphorylation of serine 774, but not serine 778 (M. Cousin, personal communication). As the rephosphorylation of dynamin I is essential to enable subsequent rounds of ADBE, the role of GSK3 β as a

kinase which phosphorylates dynamin I serine 774, following serine 778 phosphorylation-priming by cdk5, is essential for ADBE.

7.4 MODEL

The results accrued during the thesis work allow a model for the activation and progression of bulk endocytosis in a small central nerve terminal system.

Under mild stimulation conditions CME is sufficient to maintain neurotransmission. During periods of increased neuronal activity (for example epileptic firing) the capacity of CME is limited, and excess membrane is rapidly retrieved by a recruitment of bulk endocytosis. Increased Ca^{2+} influx is the key to this switch, which is mediated by calcineurin. Dynamin I is dephosphorylated by calcineurin, enabling the dephosphorylation-specific interaction of dynamin I with syndapin I, resulting in rapid retrieval of membrane by bulk endocytosis (Fig 7.1). Vesicles which bud from these bulk endosomes serve to repopulate the RP. In order to enable further rounds of ADBE, dynamin I must be rephosphorylated. Dynamin I rephosphorylation is mediated by cdk5 phospho-priming at serine 778, and subsequent GSK3β phosphorylation at serine 778 (Fig 7.2). Without this re-phosphorylation event no further rounds of bulk endocytosis can be sustained. Following termination of stimulation, ADBE ceases. Retrieval by CME persists for several minutes following strong stimulation.

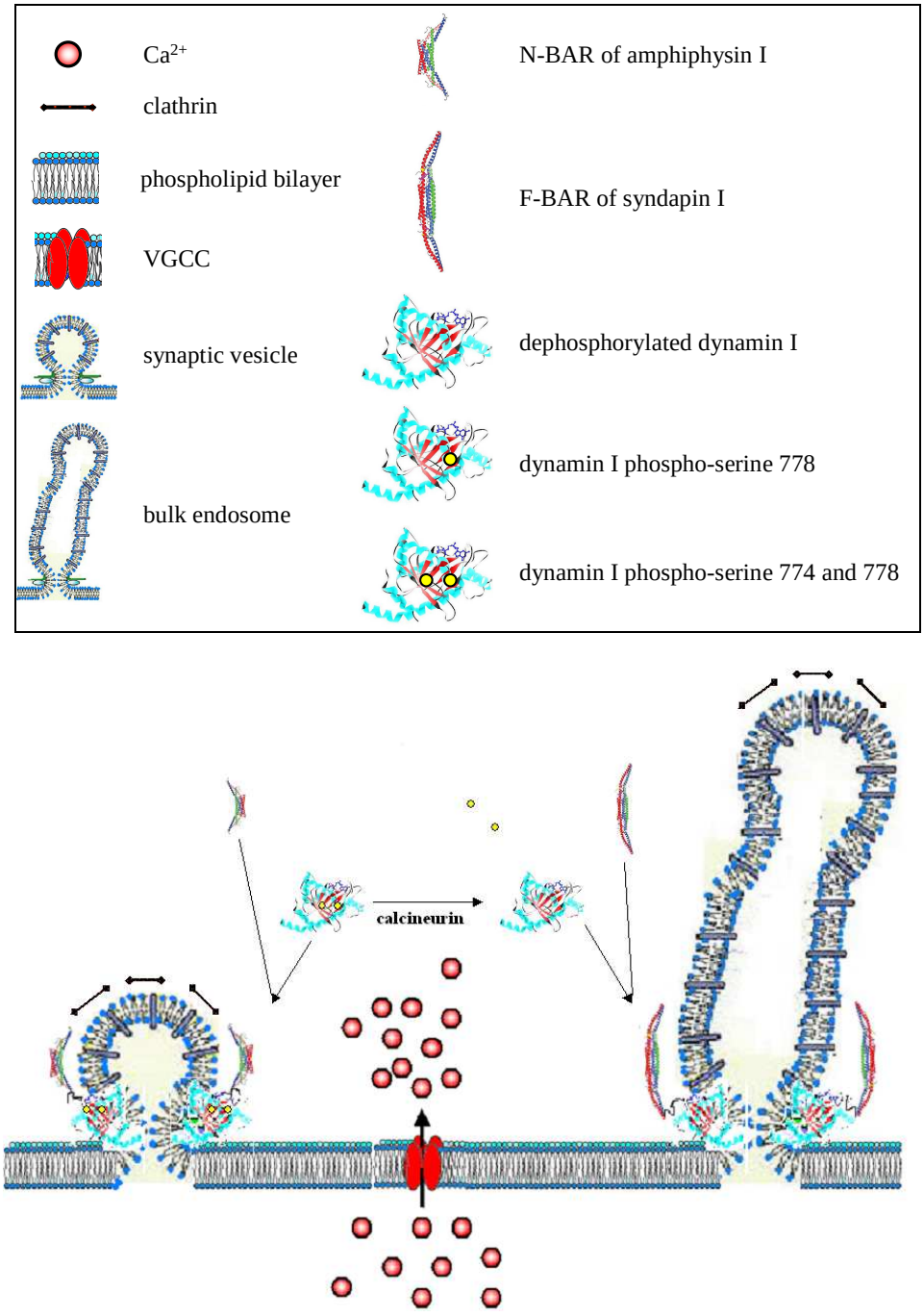

Figure 7.1 - Model of activation of bulk retrieval in cerebellar granule neurons.

Increased intracellular Ca^{2+} during strong stimulation induces dephosphorylation of dynamin I by calcineurin. Dephosphorylated dynamin I interacts specifically with syndapin I, mediating bulk retrieval of SV membrane. CME mediated by the interaction of amphiphysin I with dynamin progresses as normal.

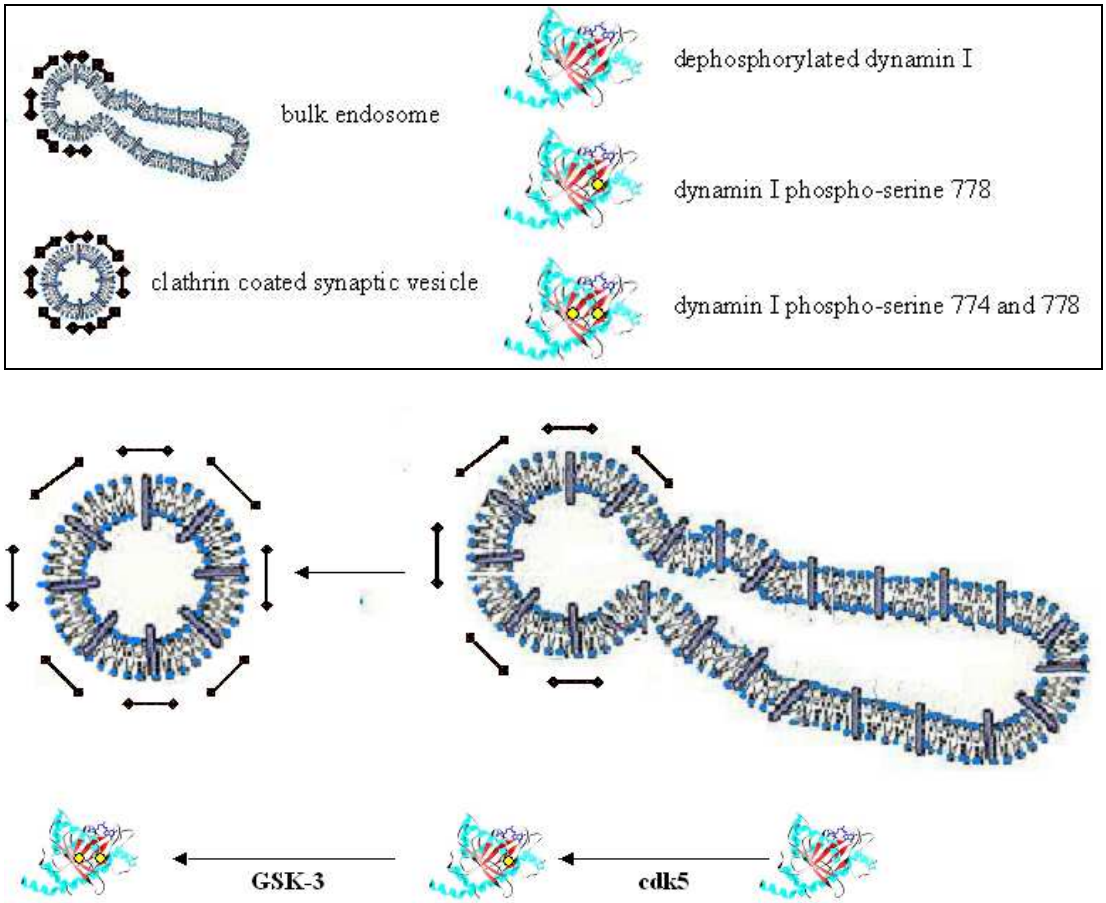

Figure 7.2 - Model for rephosphorylation of dynamin I necessary for bulk retrieval

Following bulk retrieval, dynamin I serine 778 is phosphorylated by cdk5, priming the consensus sequence for GSK-3 mediated phosphorylation of dynamin I 774. The rephosphorylation of GSK-3 is necessary to enable further rounds of bulk endocytosis.

7.5 Future Work

There are a number of future experiments which could be pursued in order to further elucidate the exact pathway which has been suggested by the work presented in this thesis.

7.5.1 The role of Dynamins III

The dynamin I KO mouse only showed defects in endocytosis when the stimulus load is increased, but not during mild stimulation (Ferguson *et al.*, 2007). As neither dynamin II nor dynamin III levels were affected in this model, there is a possibility that either one of these isoforms could be compensating for this lack of dynamin I. As the major phosphorylation sites of dynamin III so closely parallel those of dynamin I (Graham *et al.*, 2007), it would be interesting to see if dynamin III can itself mediate a specific form of SVE. As the dynamin I KO mice manifest defects under intensified stimulation, then it could be that dynamin III can either compensate for phosphorylated dynamin I due to its phosphoryaltion similarities, or it may be that dynamin III itself has a key role to play in SVE. The generation of a dynamin III KO, or a combinational double KO of dynamins I and III would enable investigation of these possibilities.

7.5.2 siRNAs

One problem with the GSK3 studies is that they have been done using pharmacological methods, and thus non-specific effects of these antagonists cannot be ruled out. A more direct method of targeting is necessary; shRNA against GSK3β

would circumnavigate the possibility of any non-specific pharmalogical effects. In order to further clarify the role of GSK3 in the ADBE pathway, the function of GSK3 could be abolished through delivery of shRNA. This raises problems as GSK3 is functional in a vast number of pathways, however it has been published that both GSK3α and GSK3β can be separately targeted by shRNA in mouse P19 cells (Yu *et al.*, 2003). Specific inhibition of GSK3β in CGNs could conclusively show that GSK3 is necessary for; 1) dynamin I phosphorylation (detected using immunofluorescence) and 2), the progression of bulk endocytosis (using the tailored bulk endocytosis assays previously described).

Similarly, the siRNA mediated inhibition of a number of other targets would lead to better understanding of the role of the dephosphins in regulation of different endocytic pathways. Disruption of syndapin has been shown to inhibit ADBE in the lamprey (Andersson *et al.*, 2008), and specific inhibition of the N-BAR proteins amphiphysin and endophilin might serve to elucidate if they have a specific role in different forms of SVE. Specifically a subsequent rescue of knocked down proteins, using mutants which abolish the interactions of the knocked down SVE proteins (for example specific interaction domains, or phosphorylation sites of the dephosphins) could be an extremely valuable tool in dissecting the importance of these interactions in specific forms of endocytosis. Thus the molecular switch which controls the modifications in types of endocytosis employed by a neuron could be investigated.

7.5.3 Further Characterisation of the Role of GSK3 in SVE.

Cdk5 is implicated in the rephosphorylation of dynamin I, PIPKIγ, and synaptojanin (Tan *et al.*, 2003, Lee *et al.*, 2004, Lee *et al.*, 2005), and serine 857 of

dynamin I has been shown to be phosphorylated by Mnb/Dyrk1A (Huang *et al.*, 2004). We have now implicated GSK3 as a kinase which can rephosphorylate at least one of these dephosphins, and this particular interaction has been shown to be specifically implicated in ADBE. The specific link between GSK3 phosphorylation of dynamin I hasn't been conclusively shown yet. Overexpression of S774A and S774E mutants (where the 778 site is unaltered) could be used to directly show this interaction through transfection and observation of the affect on FM dye loading and dextran uptake.

Abele, A. E., K. P. Scholz, et al. (1990). "Excitotoxicity induced by enhanced excitatory neurotransmission in cultured hippocampal pyramidal neurons." Neuron **4**(3): 413-9.

Ahle, S. and E. Ungewickell (1986). "Purification and properties of a new clathrin assembly protein." Embo J **5**(12): 3143-9.

Ales, E., L. Tabares, et al. (1999). "High calcium concentrations shift the mode of exocytosis to the kiss-and-run mechanism." Nat Cell Biol **1**(1): 40-4.

Alvarez de Toledo, G., R. Fernandez-Chacon, et al. (1993). "Release of secretory products during transient vesicle fusion." Nature **363**(6429): 554-8.

Andersson, F., J. Jakobsson, et al. (2008). "Perturbation of syndapin/PACSIN impairs synaptic vesicle recycling evoked by intense stimulation." J Neurosci **28**(15): 3925-33.

Anggono, V. and P. J. Robinson (2007). "Syndapin I and endophilin I bind overlapping proline-rich regions of dynamin I: role in synaptic vesicle endocytosis." J Neurochem **102**(3): 931-43.

Anggono, V., K. J. Smillie, et al. (2006). "Syndapin I is the phosphorylation-regulated dynamin I partner in synaptic vesicle endocytosis." Nat Neurosci **9**(6): 752-60.

Arac, D., X. Chen, et al. (2006). "Close membrane-membrane proximity induced by Ca(2+)-dependent multivalent binding of synaptotagmin-1 to phospholipids." Nat Struct Mol Biol **13**(3): 209-17.

Aravanis, A. M., J. L. Pyle, et al. (2003). "Imaging single synaptic vesicles undergoing repeated fusion events: kissing, running, and kissing again." Neuropharmacology **45**(6): 797-813.

Babity, J. M., J. N. Armstrong, et al. (1997). "A novel seizure-induced synaptotagmin gene identified by differential display." Proc Natl Acad Sci U S A **94**(6): 2638-41.

Bajjalieh, S. M., G. D. Frantz, et al. (1994). "Differential expression of synaptic vesicle protein 2 (SV2) isoforms." J Neurosci **14**(9): 5223-35.

Bajjalieh, S. M., K. Peterson, et al. (1993). "Brain contains two forms of synaptic vesicle protein 2." Proc Natl Acad Sci U S A **90**(6): 2150-4.

Bajjalieh, S. M., K. Peterson, et al. (1992). "SV2, a brain synaptic vesicle protein homologous to bacterial transporters." Science **257**(5074): 1271-3.

Balaji, J. and T. A. Ryan (2007). "Single-vesicle imaging reveals that synaptic vesicle exocytosis and endocytosis are coupled by a single stochastic mode." Proc Natl Acad Sci U S A **104**(51): 20576-81.

Bao, H., R. W. Daniels, et al. (2005). "AP180 maintains the distribution of synaptic and vesicle proteins in the nerve terminal and indirectly regulates the efficacy of Ca2+-triggered exocytosis." J Neurophysiol **94**(3): 1888-903.

Barouch, W., K. Prasad, et al. (1997). "Auxilin-induced interaction of the molecular chaperone Hsc70 with clathrin baskets." Biochemistry **36**(14): 4303-8.

Bauerfeind, R., K. Takei, et al. (1997). "Amphiphysin I is associated with coated endocytic intermediates and undergoes stimulation-dependent dephosphorylation in nerve terminals." J Biol Chem **272**(49): 30984-92.

Benmerah, A., M. Bayrou, et al. (1999). "Inhibition of clathrin-coated pit assembly by an Eps15 mutant." J Cell Sci **112 (Pt 9)**: 1303-11.

Benmerah, A., B. Begue, et al. (1996). "The ear of alpha-adaptin interacts with the COOH-terminal domain of the Eps 15 protein." J Biol Chem **271**(20): 12111-6.

Benmerah, A., J. Gagnon, et al. (1995). "The tyrosine kinase substrate eps15 is constitutively associated with the plasma membrane adaptor AP-2." J Cell Biol **131**(6 Pt 2): 1831-8.

Bennett, M. K., N. Calakos, et al. (1992). "Syntaxin: a synaptic protein implicated in docking of synaptic vesicles at presynaptic active zones." Science **257**(5067): 255-9.

Betz, W. J., F. Mao, et al. (1996). "Imaging exocytosis and endocytosis." Curr Opin Neurobiol **6**(3): 365-71.

Blair, R. E., S. Sombati, et al. (2004). "Epileptogenesis causes acute and chronic increases in GABAA receptor endocytosis that contributes to the induction and maintenance of seizures in the hippocampal culture model of acquired epilepsy." J Pharmacol Exp Ther **310**(3): 871-80.

Blasi, J., E. R. Chapman, et al. (1993). "Botulinum neurotoxin A selectively cleaves the synaptic protein SNAP-25." Nature **365**(6442): 160-3.

Blasi, J., E. R. Chapman, et al. (1993). "Botulinum neurotoxin C1 blocks neurotransmitter release by means of cleaving HPC-1/syntaxin." Embo J **12**(12): 4821-8.

Bonanomi, D., E. F. Fornasiero, et al. (2008). "Identification of a developmentally regulated pathway of membrane retrieval in neuronal growth cones." J Cell Sci **121**(Pt 22): 3757-69.

Bostik, P., P. Wu, et al. (2001). "Identification of protein kinases dysregulated in CD4(+) T cells in pathogenic versus apathogenic simian immunodeficiency virus infection." J Virol **75**(23): 11298-306.

Braun, A., R. Pinyol, et al. (2005). "EHD proteins associate with syndapin I and II and such interactions play a crucial role in endosomal recycling." Mol Biol Cell **16**(8): 3642-58.

Bronk, P., J. J. Wenniger, et al. (2001). "Drosophila Hsc70-4 is critical for neurotransmitter exocytosis in vivo." Neuron **30**(2): 475-88.

Buckley, K. and R. B. Kelly (1985). "Identification of a transmembrane glycoprotein specific for secretory vesicles of neural and endocrine cells." J Cell Biol **100**(4): 1284-94.

Burgoyne, R. D. and A. Morgan (2003). "Secretory granule exocytosis." Physiol Rev **83**(2): 581-632.

Cao, H., F. Garcia, et al. (1998). "Differential distribution of dynamin isoforms in mammalian cells." Mol Biol Cell **9**(9): 2595-609.

Cao, H., J. Chen, et al. (2007). "Dynamin 2 mediates fluid-phase micropinocytosis in epithelial cells." J Cell Sci **120**(Pt 23): 4167-77.

Carter, D. S., S. N. Haider, et al. (2006). "Altered calcium/calmodulin kinase II activity changes calcium homeostasis that underlies epileptiform activity in hippocampal neurons in culture." J Pharmacol Exp Ther **319**(3): 1021-31.

Ceccarelli, B., W. P. Hurlbut, et al. (1973). "Turnover of transmitter and synaptic vesicles at the frog neuromuscular junction." J Cell Biol **57**(2): 499-524.

Cestra, G., L. Castagnoli, et al. (1999). "The SH3 domains of endophilin and amphiphysin bind to the proline-rich region of synaptojanin 1 at distinct sites that display an unconventional binding specificity." J Biol Chem **274**(45): 32001-7.

Chan, S. A. and C. Smith (2001). "Physiological stimuli evoke two forms of endocytosis in bovine chromaffin cells." J Physiol **537**(Pt 3): 871-85.

Chappell, T. G., W. J. Welch, et al. (1986). "Uncoating ATPase is a member of the 70 kilodalton family of stress proteins." Cell **45**(1): 3-13.

Chen, H., S. Fre, et al. (1998). "Epsin is an EH-domain-binding protein implicated in clathrin-mediated endocytosis." Nature **394**(6695): 793-7.

Chen, X., S. Barg, et al. (2008). "Release of the styryl dyes from single synaptic vesicles in hippocampal neurons." J Neurosci **28**(8): 1894-903.

Chen, Y., L. Deng, et al. (2003). "Formation of an endophilin-Ca2+ channel complex is critical for clathrin-mediated synaptic vesicle endocytosis." Cell **115**(1): 37-48.

Chugh, J., A. Chatterjee, et al. (2006). "Structural characterization of the large soluble oligomers of the GTPase effector domain of dynamin." Febs J **273**(2): 388-97.

Clayton, E. L., G. J. Evans, et al. (2007). "Activity-dependent control of bulk endocytosis by protein dephosphorylation in central nerve terminals." J Physiol **585**(Pt 3): 687-91.

Coggins, M. R., C. P. Grabner, et al. (2007). "Stimulated exocytosis of endosomes in goldfish retinal bipolar neurons." J Physiol **584**(Pt 3): 853-65.

Cook, T. A., R. Urrutia, et al. (1994). "Identification of dynamin 2, an isoform ubiquitously expressed in rat tissues." Proc Natl Acad Sci U S A **91**(2): 644-8.

Cousin, M. A. (2000). "Synaptic vesicle endocytosis: calcium works overtime in the nerve terminal." Mol Neurobiol **22**(1-3): 115-28.

Cousin, M. A. and P. J. Robinson (1999). "Mechanisms of synaptic vesicle recycling illuminated by fluorescent dyes." J Neurochem **73**(6): 2227-39.

Cousin, M. A. and P. J. Robinson (2000). "Ca(2+) influx inhibits dynamin and arrests synaptic vesicle endocytosis at the active zone." J Neurosci **20**(3): 949-57.

Cousin, M. A. and P. J. Robinson (2001). "The dephosphins: dephosphorylation by calcineurin triggers synaptic vesicle endocytosis." Trends Neurosci **24**(11): 659-65.

Cousin, M. A., T. C. Tan, et al. (2001). "Protein phosphorylation is required for endocytosis in nerve terminals: potential role for the dephosphins dynamin I and synaptojanin, but not AP180 or amphiphysin." J Neurochem **76**(1): 105-16.

Cremona, O., G. Di Paolo, et al. (1999). "Essential role of phosphoinositide metabolism in synaptic vesicle recycling." Cell **99**(2): 179-88.

Crowder, K. M., J. M. Gunther, et al. (1999). "Abnormal neurotransmission in mice lacking synaptic vesicle protein 2A (SV2A)." Proc Natl Acad Sci U S A **96**(26): 15268-73.

David, C., P. S. McPherson, et al. (1996). "A role of amphiphysin in synaptic vesicle endocytosis suggested by its binding to dynamin in nerve terminals." Proc Natl Acad Sci U S A **93**(1): 331-5.

De Gois, S., E. Jeanclos, et al. (2006). "Identification of endophilins 1 and 3 as selective binding partners for VGLUT1 and their co-localization in neocortical glutamatergic synapses: implications for vesicular glutamate transporter trafficking and excitatory vesicle formation." Cell Mol Neurobiol **26**(4-6): 679-93.

de Heuvel, E., A. W. Bell, et al. (1997). "Identification of the major synaptojanin-binding proteins in brain." J Biol Chem **272**(13): 8710-6.

de Lange, R. P., A. D. de Roos, et al. (2003). "Two modes of vesicle recycling in the rat calyx of Held." J Neurosci **23**(31): 10164-73.

Derossi, D., A. H. Joliot, et al. (1994). "The third helix of the Antennapedia homeodomain translocates through biological membranes." J Biol Chem **269**(14): 10444-50.

Di Paolo, G., S. Sankaranarayanan, et al. (2002). "Decreased synaptic vesicle recycling efficiency and cognitive deficits in amphiphysin 1 knockout mice." Neuron **33**(5): 789-804.

Diatloff-Zito, C., A. J. Gordon, et al. (1995). "Isolation of an ubiquitously expressed cDNA encoding human dynamin II, a member of the large GTP-binding protein family." Gene **163**(2): 301-6.

Dickman, D. K., J. A. Horne, et al. (2005). "A slowed classical pathway rather than kiss-and-run mediates endocytosis at synapses lacking synaptojanin and endophilin." Cell **123**(3): 521-33.

Drake, M. T., M. A. Downs, et al. (2000). "Epsin binds to clathrin by associating directly with the clathrin-terminal domain. Evidence for cooperative binding through two discrete sites." J Biol Chem **275**(9): 6479-89.

Elefant, F. and K. B. Palter (1999). "Tissue-specific expression of dominant negative mutant Drosophila HSC70 causes developmental defects and lethality." Mol Biol Cell **10**(7): 2101-17.

Embi, N., D. B. Rylatt, et al. (1980). "Glycogen synthase kinase-3 from rabbit skeletal muscle. Separation from cyclic-AMP-dependent protein kinase and phosphorylase kinase." Eur J Biochem **107**(2): 519-27.

Evans, G. J. and M. A. Cousin (2007). "Activity-dependent control of slow synaptic vesicle endocytosis by cyclin-dependent kinase 5." J Neurosci **27**(2): 401-11.

Evergren, E., H. Gad, et al. (2007). "Intersectin is a negative regulator of dynamin recruitment to the synaptic endocytic zone in the central synapse." J Neurosci **27**(2): 379-90.

Evergren, E., M. Marcucci, et al. (2004). "Amphiphysin is a component of clathrin coats formed during synaptic vesicle recycling at the lamprey giant synapse." Traffic **5**(7): 514-28.

Farsad, K., N. Ringstad, et al. (2001). "Generation of high curvature membranes mediated by direct endophilin bilayer interactions." J Cell Biol **155**(2): 193-200.

Faundez, V., J. T. Horng, et al. (1998). "A function for the AP3 coat complex in synaptic vesicle formation from endosomes." Cell **93**(3): 423-32.

Fazioli, F., L. Minichiello, et al. (1993). "eps15, a novel tyrosine kinase substrate, exhibits transforming activity." Mol Cell Biol **13**(9): 5814-28.

Feany, M. B., S. Lee, et al. (1992). "The synaptic vesicle protein SV2 is a novel type of transmembrane transporter." Cell **70**(5): 861-7.

Ferguson, S. M., G. Brasnjo, et al. (2007). "A selective activity-dependent requirement for dynamin 1 in synaptic vesicle endocytosis." Science **316**(5824): 570-4.

Fernandez-Alfonso, T., R. Kwan, et al. (2006). "Synaptic vesicles interchange their membrane proteins with a large surface reservoir during recycling." Neuron **51**(2): 179-86.

Fernandez-Alfonso, T. and T. A. Ryan (2004). "The kinetics of synaptic vesicle pool depletion at CNS synaptic terminals." Neuron **41**(6): 943-53.

Fernandez, I., D. Arac, et al. (2001). "Three-dimensional structure of the synaptotagmin 1 C2B-domain: synaptotagmin 1 as a phospholipid binding machine." Neuron **32**(6): 1057-69.

Fesce, R., F. Grohovaz, et al. (1994). "Neurotransmitter release: fusion or 'kiss-and-run'?" Trends Cell Biol **4**(1): 1-4.

Fiol, C. J., A. M. Mahrenholz, et al. (1987). "Formation of protein kinase recognition sites by covalent modification of the substrate. Molecular mechanism for the synergistic action of casein kinase II and glycogen synthase kinase 3." J Biol Chem **262**(29): 14042-8.

Ford, M. G., I. G. Mills, et al. (2002). "Curvature of clathrin-coated pits driven by epsin." Nature **419**(6905): 361-6.

Ford, M. G., B. M. Pearse, et al. (2001). "Simultaneous binding of PtdIns(4,5)P2 and clathrin by AP180 in the nucleation of clathrin lattices on membranes." Science **291**(5506): 1051-5.

Forsythe, I. D. and G. L. Westbrook (1988). "Slow excitatory postsynaptic currents mediated by N-methyl-D-aspartate receptors on cultured mouse central neurones." J Physiol **396**: 515-33.

Fotin, A., Y. Cheng, et al. (2004). "Structure of an auxilin-bound clathrin coat and its implications for the mechanism of uncoating." Nature **432**(7017): 649-53.

Frost, A., P. De Camilli, et al. (2007). "F-BAR proteins join the BAR family fold." Structure **15**(7): 751-3.

Gad, H., P. Low, et al. (1998). "Dissociation between Ca2+-triggered synaptic vesicle exocytosis and clathrin-mediated endocytosis at a central synapse." Neuron **21**(3): 607-16.

Gad, H., N. Ringstad, et al. (2000). "Fission and uncoating of synaptic clathrin-coated vesicles are perturbed by disruption of interactions with the SH3 domain of endophilin." Neuron **27**(2): 301-12.

Gaidarov, I. and J. H. Keen (1999). "Phosphoinositide-AP-2 interactions required for targeting to plasma membrane clathrin-coated pits." J Cell Biol **146**(4): 755-64.

Gallop, J. L., C. C. Jao, et al. (2006). "Mechanism of endophilin N-BAR domain-mediated membrane curvature." Embo J **25**(12): 2898-910.

Gandhi, S. P. and C. F. Stevens (2003). "Three modes of synaptic vesicular recycling revealed by single-vesicle imaging." Nature **423**(6940): 607-13.

Garcia, C. C., H. J. Blair, et al. (2004). "Identification of a mutation in synapsin I, a synaptic vesicle protein, in a family with epilepsy." J Med Genet **41**(3): 183-6.

Geppert, M., Y. Goda, et al. (1994). "Synaptotagmin I: a major Ca2+ sensor for transmitter release at a central synapse." Cell **79**(4): 717-27.

Graham, M. E., V. Anggono, et al. (2007). "The in vivo phosphorylation sites of rat brain dynamin I." J Biol Chem **282**(20): 14695-707.

Granseth, B., B. Odermatt, et al. (2006). "Clathrin-mediated endocytosis is the dominant mechanism of vesicle retrieval at hippocampal synapses." Neuron **51**(6): 773-86.

Granseth, B., B. Odermatt, et al. (2007). "Clathrin-mediated endocytosis: the physiological mechanism of vesicle retrieval at hippocampal synapses." J Physiol **585**(Pt 3): 681-6.

Gray, N. W., L. Fourgeaud, et al. (2003). "Dynamin 3 is a component of the postsynapse, where it interacts with mGluR5 and Homer." Curr Biol **13**(6): 510-5.

Gray, N. W., A. E. Kruchten, et al. (2005). "A dynamin-3 spliced variant modulates the actin/cortactin-dependent morphogenesis of dendritic spines." J Cell Sci **118**(Pt 6): 1279-90.

Greener, T., B. Grant, et al. (2001). "Caenorhabditis elegans auxilin: a J-domain protein essential for clathrin-mediated endocytosis in vivo." Nat Cell Biol **3**(2): 215-9.

Groemer, T. W. and J. Klingauf (2007). "Synaptic vesicles recycling spontaneously and during activity belong to the same vesicle pool." Nat Neurosci **10**(2): 145-7.

Guichet, A., T. Wucherpfennig, et al. (2002). "Essential role of endophilin A in synaptic vesicle budding at the Drosophila neuromuscular junction." Embo J **21**(7): 1661-72.

Haffner, C., K. Takei, et al. (1997). "Synaptojanin 1: localization on coated endocytic intermediates in nerve terminals and interaction of its 170 kDa isoform with Eps15." FEBS Lett **419**(2-3): 175-80.

Halbach, A., M. Morgelin, et al. (2007). "PACSIN 1 forms tetramers via its N-terminal F-BAR domain." Febs J **274**(3): 773-82.

Hallbrink, M., J. Oehlke, et al. (2004). "Uptake of cell-penetrating peptides is dependent on peptide-to-cell ratio rather than on peptide concentration." Biochim Biophys Acta **1667**(2): 222-8.

Hanson, P. I., J. E. Heuser, et al. (1997). "Neurotransmitter release - four years of SNARE complexes." Curr Opin Neurobiol **7**(3): 310-5.

Hao, W., Z. Luo, et al. (1999). "AP180 and AP-2 interact directly in a complex that cooperatively assembles clathrin." J Biol Chem **274**(32): 22785-94.

Harata, N., T. A. Ryan, et al. (2001). "Visualizing recycling synaptic vesicles in hippocampal neurons by FM 1-43 photoconversion." Proc Natl Acad Sci U S A **98**(22): 12748-53.

Harata, N. C., S. Choi, et al. (2006). "Frequency-dependent kinetics and prevalence of kiss-and-run and reuse at hippocampal synapses studied with novel quenching methods." Neuron **49**(2): 243-56.

Harris, T. W., E. Hartwieg, et al. (2000). "Mutations in synaptojanin disrupt synaptic vesicle recycling." J Cell Biol **150**(3): 589-600.

Hata, Y., C. A. Slaughter, et al. (1993). "Synaptic vesicle fusion complex contains unc-18 homologue bound to syntaxin." Nature **366**(6453): 347-51.

Haucke, V. and P. De Camilli (1999). "AP-2 recruitment to synaptotagmin stimulated by tyrosine-based endocytic motifs." Science **285**(5431): 1268-71.

Hawryluk, M. J., P. A. Keyel, et al. (2006). "Epsin 1 is a polyubiquitin-selective clathrin-associated sorting protein." Traffic **7**(3): 262-81.

Hayashi, M., A. Raimondi, et al. (2008). "Cell- and stimulus-dependent heterogeneity of synaptic vesicle endocytic recycling mechanisms revealed by studies of dynamin 1-null neurons." Proc Natl Acad Sci U S A **105**(6): 2175-80.

Heerssen, H., R. D. Fetter, et al. (2008). "Clathrin dependence of synaptic-vesicle formation at the Drosophila neuromuscular junction." Curr Biol **18**(6): 401-9.

Henne, W. M., H. M. Kent, et al. (2007). "Structure and analysis of FCHo2 F-BAR domain: a dimerizing and membrane recruitment module that effects membrane curvature." Structure **15**(7): 839-52.

Heuser, J. (1980). "Three-dimensional visualization of coated vesicle formation in fibroblasts." J Cell Biol **84**(3): 560-83.

Heuser, J. E. and T. S. Reese (1973). "Evidence for recycling of synaptic vesicle membrane during transmitter release at the frog neuromuscular junction." J Cell Biol **57**(2): 315-44.

Heuser, J. E. and T. S. Reese (1981). "Structural changes after transmitter release at the frog neuromuscular junction." J Cell Biol **88**(3): 564-80.

Holt, M., A. Cooke, et al. (2004). "High mobility of vesicles supports continuous exocytosis at a ribbon synapse." Curr Biol **14**(3): 173-83.

Holt, M., A. Cooke, et al. (2003). "Bulk membrane retrieval in the synaptic terminal of retinal bipolar cells." J Neurosci **23**(4): 1329-39.

Hooper, C., V. Markevich, et al. (2007). "Glycogen synthase kinase-3 inhibition is integral to long-term potentiation." Eur J Neurosci **25**(1): 81-6.

Huang, Y., M. C. Chen-Hwang, et al. (2004). "Mnb/Dyrk1A phosphorylation regulates the interaction of dynamin 1 with SH3 domain-containing proteins." Biochemistry **43**(31): 10173-85.

Hussain, N. K., S. Jenna, et al. (2001). "Endocytic protein intersectin-l regulates actin assembly via Cdc42 and N-WASP." Nat Cell Biol **3**(10): 927-32.

Hussain, N. K., M. Yamabhai, et al. (2003). "A role for epsin N-terminal homology/AP180 N-terminal homology (ENTH/ANTH) domains in tubulin binding." J Biol Chem **278**(31): 28823-30.

Hussain, N. K., M. Yamabhai, et al. (1999). "Splice variants of intersectin are components of the endocytic machinery in neurons and nonneuronal cells." J Biol Chem **274**(22): 15671-7.

Itoh, T., K. S. Erdmann, et al. (2005). "Dynamin and the actin cytoskeleton cooperatively regulate plasma membrane invagination by BAR and F-BAR proteins." Dev Cell **9**(6): 791-804.

Jakobsson, J., H. Gad, et al. (2008). "Role of epsin 1 in synaptic vesicle endocytosis." Proc Natl Acad Sci U S A **105**(17): 6445-50.

Janz, R., Y. Goda, et al. (1999). "SV2A and SV2B function as redundant Ca2+ regulators in neurotransmitter release." Neuron **24**(4): 1003-16.

Janz, R. and T. C. Sudhof (1999). "SV2C is a synaptic vesicle protein with an unusually restricted localization: anatomy of a synaptic vesicle protein family." Neuroscience **94**(4): 1279-90.

Janz, R., T. C. Sudhof, et al. (1999). "Essential roles in synaptic plasticity for synaptogyrin I and synaptophysin I." Neuron **24**(3): 687-700.

Jiang, R. F., T. Greener, et al. (1997). "Interaction of auxilin with the molecular chaperone, Hsc70." J Biol Chem **272**(10): 6141-5.

Jockusch, W. J., G. J. Praefcke, et al. (2005). "Clathrin-dependent and clathrin-independent retrieval of synaptic vesicles in retinal bipolar cells." Neuron **46**(6): 869-78.

Johansson, J. U., J. Ericsson, et al. (2008). "An ancient duplication of exon 5 in the Snap25 gene is required for complex neuronal development/function." PLoS Genet **4**(11): e1000278.

Johnson, J. M. and W. J. Betz (2008). "The color of lactotroph secretory granules stained with FM1-43 depends on dye concentration." Biophys J **94**(8): 3167-77.

Johnson, J. W. and P. Ascher (1987). "Glycine potentiates the NMDA response in cultured mouse brain neurons." Nature **325**(6104): 529-31.

Jolivalt, C. G., C. A. Lee, et al. (2008). "Defective insulin signaling pathway and increased glycogen synthase kinase-3 activity in the brain of diabetic mice: parallels with Alzheimer's disease and correction by insulin." J Neurosci Res **86**(15): 3265-74.

Jope, R. S. and M. S. Roh (2006). "Glycogen synthase kinase-3 (GSK3) in psychiatric diseases and therapeutic interventions." Curr Drug Targets **7**(11): 1421-34.

Jope, R. S., C. J. Yuskaitis, et al. (2007). "Glycogen synthase kinase-3 (GSK3): inflammation, diseases, and therapeutics." Neurochem Res **32**(4-5): 577-95.

Jorgensen, E. M., E. Hartwieg, et al. (1995). "Defective recycling of synaptic vesicles in synaptotagmin mutants of Caenorhabditis elegans." Nature **378**(6553): 196-9.

Kasprowicz, J., S. Kuenen, et al. (2008). "Inactivation of clathrin heavy chain inhibits synaptic recycling but allows bulk membrane uptake." J Cell Biol **182**(5): 1007-16.

Kessels, M. M. and B. Qualmann (2002). "Syndapins integrate N-WASP in receptor-mediated endocytosis." Embo J **21**(22): 6083-94.

Kessels, M. M. and B. Qualmann (2006). "Syndapin oligomers interconnect the machineries for endocytic vesicle formation and actin polymerization." J Biol Chem **281**(19): 13285-99.

Khvotchev, M. and T. C. Sudhof (1998). "Developmentally regulated alternative splicing in a novel synaptojanin." J Biol Chem **273**(4): 2306-11.

Kim, W. T., S. Chang, et al. (2002). "Delayed reentry of recycling vesicles into the fusion-competent synaptic vesicle pool in synaptojanin 1 knockout mice." Proc Natl Acad Sci U S A **99**(26): 17143-8.

Kirchhausen, T. and S. C. Harrison (1981). "Protein organization in clathrin trimers." Cell **23**(3): 755-61.

Kirchhausen, T., E. Macia, et al. (2008). "Use of dynasore, the small molecule inhibitor of dynamin, in the regulation of endocytosis." Methods Enzymol **438**: 77-93.

Klee, C. B., T. H. Crouch, et al. (1979). "Calcineurin: a calcium- and calmodulin-binding protein of the nervous system." Proc Natl Acad Sci U S A **76**(12): 6270-3.

Klein, D. E., A. Lee, et al. (1998). "The pleckstrin homology domains of dynamin isoforms require oligomerization for high affinity phosphoinositide binding." J Biol Chem **273**(42): 27725-33.

Klingauf, J., E. T. Kavalali, et al. (1998). "Kinetics and regulation of fast endocytosis at hippocampal synapses." Nature **394**(6693): 581-5.

Klitgaard, H., A. Matagne, et al. (1998). "Evidence for a unique profile of levetiracetam in rodent models of seizures and epilepsy." Eur J Pharmacol **353**(2-3): 191-206.

Koenig, J. H. and K. Ikeda (1989). "Disappearance and reformation of synaptic vesicle membrane upon transmitter release observed under reversible blockage of membrane retrieval." J Neurosci **9**(11): 3844-60.

Koenig, J. H. and K. Ikeda (1996). "Synaptic vesicles have two distinct recycling pathways." J Cell Biol **135**(3): 797-808.

Koh, T. W., V. I. Korolchuk, et al. (2007). "Eps15 and Dap160 control synaptic vesicle membrane retrieval and synapse development." J Cell Biol **178**(2): 309-22.

Koh, T. W., P. Verstreken, et al. (2004). "Dap160/intersectin acts as a stabilizing scaffold required for synaptic development and vesicle endocytosis." Neuron **43**(2): 193-205.

Kumar, V., S. R. Alla, et al. (2009). "Syndapin is dispensable for synaptic vesicle endocytosis at the Drosophila larval neuromuscular junction." Mol Cell Neurosci **40**(2): 234-41.

Kumashiro, S., Y. F. Lu, et al. (2005). "Regulation of synaptic vesicle recycling by calcineurin in different vesicle pools." Neurosci Res **51**(4): 435-43.

Kuromi, H. and Y. Kidokoro (1998). "Two distinct pools of synaptic vesicles in single presynaptic boutons in a temperature-sensitive Drosophila mutant, shibire." Neuron **20**(5): 917-25.

Lamaziere, A., C. Wolf, et al. (2008). "The homeodomain derived peptide Penetratin induces curvature of fluid membrane domains." PLoS ONE **3**(4): e1938.

Lawrie, A. M., M. E. Graham, et al. (1993). "Synchronous calcium oscillations in cerebellar granule cells in culture mediated by NMDA receptors." Neuroreport **4**(5): 539-42.

Lee, S. Y., S. Voronov, et al. (2005). "Regulation of the interaction between PIPKI gamma and talin by proline-directed protein kinases." J Cell Biol **168**(5): 789-99.

Lee, S. Y., M. R. Wenk, et al. (2004). "Regulation of synaptojanin 1 by cyclin-dependent kinase 5 at synapses." Proc Natl Acad Sci U S A **101**(2): 546-51.

Leenders, A. G., G. Scholten, et al. (2002). "Sequential changes in synaptic vesicle pools and endosome-like organelles during depolarization near the active zone of central nerve terminals." Neuroscience **109**(1): 195-206.

Lemmon, S. K., A. Pellicena-Palle, et al. (1991). "Sequence of the clathrin heavy chain from Saccharomyces cerevisiae and requirement of the COOH terminus for clathrin function." J Cell Biol **112**(1): 65-80.

Leroy, K. and J. P. Brion (1999). "Developmental expression and localization of glycogen synthase kinase-3beta in rat brain." J Chem Neuroanat **16**(4): 279-93.

Leszczyszyn, D. J., J. A. Jankowski, et al. (1991). "Secretion of catecholamines from individual adrenal medullary chromaffin cells." J Neurochem **56**(6): 1855-63.

Li, L., L. S. Chin, et al. (1995). "Impairment of synaptic vesicle clustering and of synaptic transmission, and increased seizure propensity, in synapsin I-deficient mice." Proc Natl Acad Sci U S A **92**(20): 9235-9.

Lichte, B., R. W. Veh, et al. (1992). "Amphiphysin, a novel protein associated with synaptic vesicles." Embo J **11**(7): 2521-30.

Lindner, R. and E. Ungewickell (1991). "Light-chain-independent binding of adaptors, AP180, and auxilin to clathrin." Biochemistry **30**(37): 9097-101.

Liu, J. P., K. A. Powell, et al. (1994). "Dynamin I is a Ca(2+)-sensitive phospholipid-binding protein with very high affinity for protein kinase C." J Biol Chem **269**(33): 21043-50.

Liu, J. P., A. T. Sim, et al. (1994). "Calcineurin inhibition of dynamin I GTPase activity coupled to nerve terminal depolarization." Science **265**(5174): 970-3.

Liu, Y. W., M. C. Surka, et al. (2008). "Isoform and splice-variant specific functions of dynamin-2 revealed by analysis of conditional knock-out cells." Mol Biol Cell **19**(12): 5347-59.

Lou, X., S. Paradise, et al. (2008). "Selective saturation of slow endocytosis at a giant glutamatergic central synapse lacking dynamin 1." Proc Natl Acad Sci U S A **105**(45): 17555-60.

Lu, W., H. Ma, et al. (2009). "Dynamin and activity regulate synaptic vesicle recycling in sympathetic neurons." J Biol Chem **284**(3): 1930-7.

Lundin, P., H. Johansson, et al. (2008). "Distinct uptake routes of cell-penetrating peptide conjugates." Bioconjug Chem **19**(12): 2535-42.

Lynch, B. A., N. Lambeng, et al. (2004). "The synaptic vesicle protein SV2A is the binding site for the antiepileptic drug levetiracetam." Proc Natl Acad Sci U S A **101**(26): 9861-6.

Lynch, B. A., A. Matagne, et al. (2008). "Visualization of SV2A conformations in situ by the use of Protein Tomography." Biochem Biophys Res Commun.

MacAulay, K., A. S. Blair, et al. (2005). "Constitutive activation of GSK3 down-regulates glycogen synthase abundance and glycogen deposition in rat skeletal muscle cells." J Biol Chem **280**(10): 9509-18.

Macia, E., M. Ehrlich, et al. (2006). "Dynasore, a cell-permeable inhibitor of dynamin." Dev Cell **10**(6): 839-50.

Majumdar, A., S. Ramagiri, et al. (2006). "Drosophila homologue of Eps15 is essential for synaptic vesicle recycling." Exp Cell Res **312**(12): 2288-98.

Mani, M., S. Y. Lee, et al. (2007). "The dual phosphatase activity of synaptojanin1 is required for both efficient synaptic vesicle endocytosis and reavailability at nerve terminals." Neuron **56**(6): 1004-18.

Marie, B., S. T. Sweeney, et al. (2004). "Dap160/intersectin scaffolds the periactive zone to achieve high-fidelity endocytosis and normal synaptic growth." Neuron **43**(2): 207-19.

Marks, B. and H. T. McMahon (1998). "Calcium triggers calcineurin-dependent synaptic vesicle recycling in mammalian nerve terminals." Curr Biol **8**(13): 740-9.

Martens, S., M. M. Kozlov, et al. (2007). "How synaptotagmin promotes membrane fusion." Science **316**(5828): 1205-8.

Marxen, M., W. Volknandt, et al. (1999). "Endocytic vacuoles formed following a short pulse of K+ -stimulation contain a plethora of presynaptic membrane proteins." Neuroscience **94**(3): 985-96.

Masuda, M., S. Takeda, et al. (2006). "Endophilin BAR domain drives membrane curvature by two newly identified structure-based mechanisms." Embo J **25**(12): 2889-97.

Matveeva, E. A., T. C. Vanaman, et al. (2008). "Levetiracetam prevents kindling-induced asymmetric accumulation of hippocampal 7S SNARE complexes." Epilepsia.

Matveeva, E. A., S. W. Whiteheart, et al. (2003). "Accumulation of 7S SNARE complexes in hippocampal synaptosomes from chronically kindled rats." J Neurochem **84**(3): 621-4.

Mayer, A., W. Wickner, et al. (1996). "Sec18p (NSF)-driven release of Sec17p (alpha-SNAP) can precede docking and fusion of yeast vacuoles." Cell **85**(1): 83-94.

McLeod, J. R., Jr., M. Shen, et al. (1998). "Neurotoxicity mediated by aberrant patterns of synaptic activity between rat hippocampal neurons in culture." J Neurophysiol **80**(5): 2688-98.

McNiven, M. A. (1998). "Dynamin: a molecular motor with pinchase action." Cell **94**(2): 151-4.

McPherson, P. S., A. J. Czernik, et al. (1994). "Interaction of Grb2 via its Src homology 3 domains with synaptic proteins including synapsin I." Proc Natl Acad Sci U S A **91**(14): 6486-90.

McPherson, P. S., E. P. Garcia, et al. (1996). "A presynaptic inositol-5-phosphatase." Nature **379**(6563): 353-7.

McPherson, P. S., K. Takei, et al. (1994). "p145, a major Grb2-binding protein in brain, is co-localized with dynamin in nerve terminals where it undergoes activity-dependent dephosphorylation." J Biol Chem **269**(48): 30132-9.

Mears, J. A., P. Ray, et al. (2007). "A corkscrew model for dynamin constriction." Structure **15**(10): 1190-202.

Medine, C. N., C. Rickman, et al. (2007). "Munc18-1 prevents the formation of ectopic SNARE complexes in living cells." J Cell Sci **120**(Pt 24): 4407-15.

Micheva, K. D., B. K. Kay, et al. (1997). "Synaptojanin forms two separate complexes in the nerve terminal. Interactions with endophilin and amphiphysin." J Biol Chem **272**(43): 27239-45.

Micheva, K. D., A. R. Ramjaun, et al. (1997). "SH3 domain-dependent interactions of endophilin with amphiphysin." FEBS Lett **414**(2): 308-12.

Miesenbock, G., D. A. De Angelis, et al. (1998). "Visualizing secretion and synaptic transmission with pH-sensitive green fluorescent proteins." Nature **394**(6689): 192-5.

Miller, T. M. and J. E. Heuser (1984). "Endocytosis of synaptic vesicle membrane at the frog neuromuscular junction." J Cell Biol **98**(2): 685-98.

Morgan, J. R., K. Prasad, et al. (2001). "Uncoating of clathrin-coated vesicles in presynaptic terminals: roles for Hsc70 and auxilin." Neuron **32**(2): 289-300.

Morgan, J. R., K. Prasad, et al. (2003). "Eps15 homology domain-NPF motif interactions regulate clathrin coat assembly during synaptic vesicle recycling." J Biol Chem **278**(35): 33583-92.

Morgan, J. R., X. Zhao, et al. (1999). "A role for the clathrin assembly domain of AP180 in synaptic vesicle endocytosis." J Neurosci **19**(23): 10201-12.

Morris, S. A., S. Schroder, et al. (1993). "Clathrin assembly protein AP180: primary structure, domain organization and identification of a clathrin binding site." Embo J **12**(2): 667-75.

Muller, A. J., J. F. Baker, et al. (2003). "Targeted disruption of the murine Bin1/Amphiphysin II gene does not disable endocytosis but results in embryonic cardiomyopathy with aberrant myofibril formation." Mol Cell Biol **23**(12): 4295-306.

Murphy, T. H., L. A. Blatter, et al. (1992). "Spontaneous synchronous synaptic calcium transients in cultured cortical neurons." J Neurosci **12**(12): 4834-45.

Neher, E. and A. Marty (1982). "Discrete changes of cell membrane capacitance observed under conditions of enhanced secretion in bovine adrenal chromaffin cells." Proc Natl Acad Sci U S A **79**(21): 6712-6.

Neves, G., A. Gomis, et al. (2001). "Calcium influx selects the fast mode of endocytosis in the synaptic terminal of retinal bipolar cells." Proc Natl Acad Sci U S A **98**(26): 15282-7.

Neves, G. and L. Lagnado (1999). "The kinetics of exocytosis and endocytosis in the synaptic terminal of goldfish retinal bipolar cells." J Physiol **515 (Pt 1)**: 181-202.

Newton, A. J., T. Kirchhausen, et al. (2006). "Inhibition of dynamin completely blocks compensatory synaptic vesicle endocytosis." Proc Natl Acad Sci U S A **103**(47): 17955-60.

Nonet, M. L., O. Saifee, et al. (1998). "Synaptic transmission deficits in Caenorhabditis elegans synaptobrevin mutants." J Neurosci **18**(1): 70-80.

Okamoto, M., S. Schoch, et al. (1999). "EHSH1/intersectin, a protein that contains EH and SH3 domains and binds to dynamin and SNAP-25. A protein

connection between exocytosis and endocytosis?" J Biol Chem **274**(26): 18446-54.

Owen, D. J., P. Wigge, et al. (1998). "Crystal structure of the amphiphysin-2 SH3 domain and its role in the prevention of dynamin ring formation." Embo J **17**(18): 5273-85.

Paillart, C., J. Li, et al. (2003). "Endocytosis and vesicle recycling at a ribbon synapse." J Neurosci **23**(10): 4092-9.

Perera, R. M., R. Zoncu, et al. (2006). "Two synaptojanin 1 isoforms are recruited to clathrin-coated pits at different stages." Proc Natl Acad Sci U S A **103**(51): 19332-7.

Perez-Otano, I., R. Lujan, et al. (2006). "Endocytosis and synaptic removal of NR3A-containing NMDA receptors by PACSIN1/syndapin1." Nat Neurosci **9**(5): 611-21.

Perin, M. S., N. Brose, et al. (1991). "Domain structure of synaptotagmin (p65)." J Biol Chem **266**(1): 623-9.

Peter, B. J., H. M. Kent, et al. (2004). "BAR domains as sensors of membrane curvature: the amphiphysin BAR structure." Science **303**(5657): 495-9.

Pevsner, J., S. C. Hsu, et al. (1994). "Specificity and regulation of a synaptic vesicle docking complex." Neuron **13**(2): 353-61.

Pishvaee, B., G. Costaguta, et al. (2000). "A yeast DNA J protein required for uncoating of clathrin-coated vesicles in vivo." Nat Cell Biol **2**(12): 958-63.

Prakriya, M. and S. Mennerick (2000). "Selective depression of low-release probability excitatory synapses by sodium channel blockers." Neuron **26**(3): 671-82.

Prasad, K., J. Heuser, et al. (1994). "Complex formation between clathrin and uncoating ATPase." J Biol Chem **269**(9): 6931-9.

Prasad, K. and R. E. Lippoldt (1988). "Molecular characterization of the AP180 coated vesicle assembly protein." Biochemistry **27**(16): 6098-104.

Pucadyil, T. J. and S. L. Schmid (2008). "Real-time visualization of dynamin-catalyzed membrane fission and vesicle release." Cell **135**(7): 1263-75.

Pyle, J. L., E. T. Kavalali, et al. (2000). "Rapid reuse of readily releasable pool vesicles at hippocampal synapses." Neuron **28**(1): 221-31.

Pyle, R. A., A. E. Schivell, et al. (2000). "Phosphorylation of synaptic vesicle protein 2 modulates binding to synaptotagmin." J Biol Chem **275**(22): 17195-200.

Qualmann, B. and R. B. Kelly (2000). "Syndapin isoforms participate in receptor-mediated endocytosis and actin organization." J Cell Biol **148**(5): 1047-62.

Qualmann, B., J. Roos, et al. (1999). "Syndapin I, a synaptic dynamin-binding protein that associates with the neural Wiskott-Aldrich syndrome protein." Mol Biol Cell **10**(2): 501-13.

Raible, D. W. and J. S. Eisen (1994). "Restriction of neural crest cell fate in the trunk of the embryonic zebrafish." Development **120**(3): 495-503.

Ramjaun, A. R. and P. S. McPherson (1996). "Tissue-specific alternative splicing generates two synaptojanin isoforms with differential membrane binding properties." J Biol Chem **271**(40): 24856-61.

Ramjaun, A. R. and P. S. McPherson (1998). "Multiple amphiphysin II splice variants display differential clathrin binding: identification of two distinct clathrin-binding sites." J Neurochem **70**(6): 2369-76.

Ramjaun, A. R., K. D. Micheva, et al. (1997). "Identification and characterization of a nerve terminal-enriched amphiphysin isoform." J Biol Chem **272**(26): 16700-6.

Ramjaun, A. R., J. Philie, et al. (1999). "The N terminus of amphiphysin II mediates dimerization and plasma membrane targeting." J Biol Chem **274**(28): 19785-91.

Razzaq, A., I. M. Robinson, et al. (2001). "Amphiphysin is necessary for organization of the excitation-contraction coupling machinery of muscles, but not for synaptic vesicle endocytosis in Drosophila." Genes Dev **15**(22): 2967-79.

Richards, D. A., C. Guatimosim, et al. (2000). "Two endocytic recycling routes selectively fill two vesicle pools in frog motor nerve terminals." Neuron **27**(3): 551-9.

Richards, D. A., C. Guatimosim, et al. (2003). "Synaptic vesicle pools at the frog neuromuscular junction." Neuron **39**(3): 529-41.

Richards, D. A., S. O. Rizzoli, et al. (2004). "Effects of wortmannin and latrunculin A on slow endocytosis at the frog neuromuscular junction." J Physiol **557**(Pt 1): 77-91.

Rickman, C., C. N. Medine, et al. (2007). "Functionally and spatially distinct modes of munc18-syntaxin 1 interaction." J Biol Chem **282**(16): 12097-103.

Ringstad, N., H. Gad, et al. (1999). "Endophilin/SH3p4 is required for the transition from early to late stages in clathrin-mediated synaptic vesicle endocytosis." Neuron **24**(1): 143-54.

Ringstad, N., Y. Nemoto, et al. (2001). "Differential expression of endophilin 1 and 2 dimers at central nervous system synapses." J Biol Chem **276**(44): 40424-30.

Rizzoli, S. O. and W. J. Betz (2004). "The structural organization of the readily releasable pool of synaptic vesicles." Science **303**(5666): 2037-9.

Rizzoli, S. O. and W. J. Betz (2005). "Synaptic vesicle pools." Nat Rev Neurosci **6**(1): 57-69.

Robinson, P. J., J. P. Liu, et al. (1994). "Phosphorylation of dynamin I and synaptic-vesicle recycling." Trends Neurosci **17**(8): 348-53.

Rosenthal, J. A., H. Chen, et al. (1999). "The epsins define a family of proteins that interact with components of the clathrin coat and contain a new protein module." J Biol Chem **274**(48): 33959-65.

Roux, A., K. Uyhazi, et al. (2006). "GTP-dependent twisting of dynamin implicates constriction and tension in membrane fission." Nature **441**(7092): 528-31.

Royle, S. J. and L. Lagnado (2003). "Endocytosis at the synaptic terminal." J Physiol **553**(Pt 2): 345-55.

Ryan, T. A. (2001). "Presynaptic imaging techniques." Curr Opin Neurobiol **11**(5): 544-9.

Saitsu, H., M. Kato, et al. (2008). "De novo mutations in the gene encoding STXBP1 (MUNC18-1) cause early infantile epileptic encephalopathy." Nat Genet **40**(6): 782-8.

Salcini, A. E., S. Confalonieri, et al. (1997). "Binding specificity and in vivo targets of the EH domain, a novel protein-protein interaction module." Genes Dev **11**(17): 2239-49.

Salcini, A. E., M. A. Hilliard, et al. (2001). "The Eps15 C. elegans homologue EHS-1 is implicated in synaptic vesicle recycling." Nat Cell Biol **3**(8): 755-60.

Salim, K., M. J. Bottomley, et al. (1996). "Distinct specificity in the recognition of phosphoinositides by the pleckstrin homology domains of dynamin and Bruton's tyrosine kinase." Embo J **15**(22): 6241-50.

Sankaranarayanan, S., D. De Angelis, et al. (2000). "The use of pHluorins for optical measurements of presynaptic activity." Biophys J **79**(4): 2199-208.

Sankaranarayanan, S. and T. A. Ryan (2000). "Real-time measurements of vesicle-SNARE recycling in synapses of the central nervous system." Nat Cell Biol **2**(4): 197-204.

Sano, K., Y. Takai, et al. (1983). "A role of calcium-activated phospholipid-dependent protein kinase in human platelet activation. Comparison of thrombin and collagen actions." J Biol Chem **258**(3): 2010-3.

Sara, Y., T. Virmani, et al. (2005). "An isolated pool of vesicles recycles at rest and drives spontaneous neurotransmission." Neuron **45**(4): 563-73.

Schiavo, G., F. Benfenati, et al. (1992). "Tetanus and botulinum-B neurotoxins block neurotransmitter release by proteolytic cleavage of synaptobrevin." Nature **359**(6398): 832-5.

Schivell, A. E., R. H. Batchelor, et al. (1996). "Isoform-specific, calcium-regulated interaction of the synaptic vesicle proteins SV2 and synaptotagmin." J Biol Chem **271**(44): 27770-5.

Schmid, S. L., A. K. Matsumoto, et al. (1982). "A domain of clathrin that forms coats." Proc Natl Acad Sci U S A **79**(1): 91-5.

Schoch, S., F. Deak, et al. (2001). "SNARE function analyzed in synaptobrevin/VAMP knockout mice." Science **294**(5544): 1117-22.

Schroder, S. and E. Ungewickell (1991). "Subunit interaction and function of clathrin-coated vesicle adaptors from the Golgi and the plasma membrane." J Biol Chem **266**(12): 7910-8.

Schulze, K. L., K. Broadie, et al. (1995). "Genetic and electrophysiological studies of Drosophila syntaxin-1A demonstrate its role in nonneuronal secretion and neurotransmission." Cell **80**(2): 311-20.

Schuske, K. R., J. E. Richmond, et al. (2003). "Endophilin is required for synaptic vesicle endocytosis by localizing synaptojanin." Neuron **40**(4): 749-62.

Seal, R. P., O. Akil, et al. (2008). "Sensorineural deafness and seizures in mice lacking vesicular glutamate transporter 3." Neuron **57**(2): 263-75.

Shanley, L. J., D. O'Malley, et al. (2002). "Leptin inhibits epileptiform-like activity in rat hippocampal neurones via PI 3-kinase-driven activation of BK channels." J Physiol **545**(Pt 3): 933-44.

Shih, W., A. Gallusser, et al. (1995). "A clathrin-binding site in the hinge of the beta 2 chain of mammalian AP-2 complexes." J Biol Chem **270**(52): 31083-90.

Shimada, A., H. Niwa, et al. (2007). "Curved EFC/F-BAR-domain dimers are joined end to end into a filament for membrane invagination in endocytosis." Cell **129**(4): 761-72.

Shupliakov, O., P. Low, et al. (1997). "Synaptic vesicle endocytosis impaired by disruption of dynamin-SH3 domain interactions." Science **276**(5310): 259-63.

Slepnev, V. I. and P. De Camilli (2000). "Accessory factors in clathrin-dependent synaptic vesicle endocytosis." Nat Rev Neurosci **1**(3): 161-72.

Smith, C. J., N. Grigorieff, et al. (1998). "Clathrin coats at 21 A resolution: a cellular assembly designed to recycle multiple membrane receptors." Embo J **17**(17): 4943-53.

Sollner, T., M. K. Bennett, et al. (1993). "A protein assembly-disassembly pathway in vitro that may correspond to sequential steps of synaptic vesicle docking, activation, and fusion." Cell **75**(3): 409-18.

Sombati, S. and R. J. Delorenzo (1995). "Recurrent spontaneous seizure activity in hippocampal neuronal networks in culture." J Neurophysiol **73**(4): 1706-11.

Spruce, A. E., L. J. Breckenridge, et al. (1990). "Properties of the fusion pore that forms during exocytosis of a mast cell secretory vesicle." Neuron **4**(5): 643-54.

Staal, R. G., E. V. Mosharov, et al. (2004). "Dopamine neurons release transmitter via a flickering fusion pore." Nat Neurosci **7**(4): 341-6.

Stefani, A., F. Spadoni, et al. (1997). "Voltage-activated calcium channels: targets of antiepileptic drug therapy?" Epilepsia **38**(9): 959-65.

Stevens, C. F. and J. H. Williams (2000). ""Kiss and run" exocytosis at hippocampal synapses." Proc Natl Acad Sci U S A **97**(23): 12828-33.

Stowell, M. H., B. Marks, et al. (1999). "Nucleotide-dependent conformational changes in dynamin: evidence for a mechanochemical molecular spring." Nat Cell Biol **1**(1): 27-32.

Sudhof, T. C. (2002). "Synaptotagmins: why so many?" J Biol Chem **277**(10): 7629-32.

Sutton, R. B., D. Fasshauer, et al. (1998). "Crystal structure of a SNARE complex involved in synaptic exocytosis at 2.4 A resolution." Nature **395**(6700): 347-53.

Sweitzer, S. M. and J. E. Hinshaw (1998). "Dynamin undergoes a GTP-dependent conformational change causing vesiculation." Cell **93**(6): 1021-9.

Takei, K., O. Mundigl, et al. (1996). "The synaptic vesicle cycle: a single vesicle budding step involving clathrin and dynamin." J Cell Biol **133**(6): 1237-50.

Takei, K., V. I. Slepnev, et al. (1999). "Functional partnership between amphiphysin and dynamin in clathrin-mediated endocytosis." Nat Cell Biol **1**(1): 33-9.

Tan, T. C., V. A. Valova, et al. (2003). "Cdk5 is essential for synaptic vesicle endocytosis." Nat Cell Biol **5**(8): 701-10.

Tebar, F., S. Confalonieri, et al. (1997). "Eps15 is constitutively oligomerized due to homophilic interaction of its coiled-coil region." J Biol Chem **272**(24): 15413-8.

Tebar, F., T. Sorkina, et al. (1996). "Eps15 is a component of clathrin-coated pits and vesicles and is located at the rim of coated pits." J Biol Chem **271**(46): 28727-30.

Teng, H., M. Y. Lin, et al. (2007). "Macroendocytosis and endosome processing in snake motor boutons." J Physiol **582**(Pt 1): 243-62.

Tsuboi, T. and G. A. Rutter (2003). "Insulin secretion by 'kiss-and-run' exocytosis in clonal pancreatic islet beta-cells." Biochem Soc Trans **31**(Pt 4): 833-6.

Ubach, J., X. Zhang, et al. (1998). "Ca2+ binding to synaptotagmin: how many Ca2+ ions bind to the tip of a C2-domain?" Embo J **17**(14): 3921-30.

Ullrich, B., C. Li, et al. (1994). "Functional properties of multiple synaptotagmins in brain." Neuron **13**(6): 1281-91.

Ungewickell, E. (1985). "The 70-kd mammalian heat shock proteins are structurally and functionally related to the uncoating protein that releases clathrin triskelia from coated vesicles." Embo J **4**(13A): 3385-91.

Ungewickell, E., H. Ungewickell, et al. (1995). "Role of auxilin in uncoating clathrin-coated vesicles." Nature **378**(6557): 632-5.

van der Bliek, A. M. and E. M. Meyerowitz (1991). "Dynamin-like protein encoded by the Drosophila shibire gene associated with vesicular traffic." Nature **351**(6325): 411-4.

van Vliet, E. A., E. Aronica, et al. (2008). "Decreased expression of synaptic vesicle protein 2A, the binding site for levetiracetam, during epileptogenesis and chronic epilepsy." Epilepsia.

Vercelli, A., M. Repici, et al. (2000). "Recent techniques for tracing pathways in the central nervous system of developing and adult mammals." Brain Res Bull **51**(1): 11-28.

Verstreken, P., O. Kjaerulff, et al. (2002). "Endophilin mutations block clathrin-mediated endocytosis but not neurotransmitter release." Cell **109**(1): 101-12.

Verstreken, P., T. W. Koh, et al. (2003). "Synaptojanin is recruited by endophilin to promote synaptic vesicle uncoating." Neuron **40**(4): 733-48.

Vijayakrishnan, N., E. A. Woodruff, 3rd, et al. (2009). "Rolling blackout is required for bulk endocytosis in non-neuronal cells and neuronal synapses." J Cell Sci **122**(Pt 1): 114-25.

Vinatier, J., E. Herzog, et al. (2006). "Interaction between the vesicular glutamate transporter type 1 and endophilin A1, a protein essential for endocytosis." J Neurochem **97**(4): 1111-25.

Virmani, T., W. Han, et al. (2003). "Synaptotagmin 7 splice variants differentially regulate synaptic vesicle recycling." Embo J **22**(20): 5347-57.

Voglmaier, S. M., K. Kam, et al. (2006). "Distinct endocytic pathways control the rate and extent of synaptic vesicle protein recycling." Neuron **51**(1): 71-84.

Wang, C. T., J. C. Lu, et al. (2003). "Different domains of synaptotagmin control the choice between kiss-and-run and full fusion." Nature **424**(6951): 943-7.

Washbourne, P., P. M. Thompson, et al. (2002). "Genetic ablation of the t-SNARE SNAP-25 distinguishes mechanisms of neuroexocytosis." Nat Neurosci **5**(1): 19-26.

Waters, J. and S. J. Smith (2002). "Vesicle pool partitioning influences presynaptic diversity and weighting in rat hippocampal synapses." J Physiol **541**(Pt 3): 811-23.

Wendland, B., K. E. Steece, et al. (1999). "Yeast epsins contain an essential N-terminal ENTH domain, bind clathrin and are required for endocytosis." Embo J **18**(16): 4383-93.

Wienisch, M. and J. Klingauf (2006). "Vesicular proteins exocytosed and subsequently retrieved by compensatory endocytosis are nonidentical." Nat Neurosci **9**(8): 1019-27.

Wilkinson, R. S. and H. Teng (2003). "The nerve-muscle synapse of the garter snake." J Neurocytol **32**(5-8): 523-38.

Wong, W. T., C. Schumacher, et al. (1995). "A protein-binding domain, EH, identified in the receptor tyrosine kinase substrate Eps15 and conserved in evolution." Proc Natl Acad Sci U S A **92**(21): 9530-4.

Woodgett, J. R. (1990). "Molecular cloning and expression of glycogen synthase kinase-3/factor A." Embo J **9**(8): 2431-8.

Wu, W. and L. G. Wu (2007). "Rapid bulk endocytosis and its kinetics of fission pore closure at a central synapse." Proc Natl Acad Sci U S A **104**(24): 10234-9.

Wu, W., J. Xu, et al. (2005). "Activity-dependent acceleration of endocytosis at a central synapse." J Neurosci **25**(50): 11676-83.

Xu, T. and S. M. Bajjalieh (2001). "SV2 modulates the size of the readily releasable pool of secretory vesicles." Nat Cell Biol **3**(8): 691-8.

Yamabhai, M., N. G. Hoffman, et al. (1998). "Intersectin, a novel adaptor protein with two Eps15 homology and five Src homology 3 domains." J Biol Chem **273**(47): 31401-7.

Yang, X. F., A. Weisenfeld, et al. (2007). "Prolonged exposure to levetiracetam reveals a presynaptic effect on neurotransmission." Epilepsia **48**(10): 1861-9.

Yang, Z., H. Li, et al. (2001). "Dynamin II regulates hormone secretion in neuroendocrine cells." J Biol Chem **276**(6): 4251-60.

Yao, J. and S. M. Bajjalieh (2008). "Synaptic vesicle protein 2 binds adenine nucleotides." J Biol Chem **283**(30): 20628-34.

Yu, J. Y., J. Taylor, et al. (2003). "Simultaneous inhibition of GSK3alpha and GSK3beta using hairpin siRNA expression vectors." Mol Ther **7**(2): 228-36.

Zelhof, A. C., H. Bao, et al. (2001). "Drosophila Amphiphysin is implicated in protein localization and membrane morphogenesis but not in synaptic vesicle endocytosis." Development **128**(24): 5005-15.

Zeng, K., X. Wang, et al. (2008). "Enhanced Synaptic Vesicle Traffic in Hippocampus of Phenytoin-Resistant Kindled Rats." Neurochem Res.

Zhang, B., Y. H. Koh, et al. (1998). "Synaptic vesicle size and number are regulated by a clathrin adaptor protein required for endocytosis." Neuron **21**(6): 1465-75.

Zhang, Q., Y. Q. Cao, et al. (2007). "Quantum dots provide an optical signal specific to full collapse fusion of synaptic vesicles." Proc Natl Acad Sci U S A **104**(45): 17843-8.

Zhang, Q., Y. Li, et al. (2009). "The Dynamic Control of Kiss-And-Run and Vesicular Reuse Probed with Single Nanoparticles." Science.

Zoncu, R., R. M. Perera, et al. (2007). "Loss of endocytic clathrin-coated pits upon acute depletion of phosphatidylinositol 4,5-bisphosphate." Proc Natl Acad Sci U S A **104**(10): 3793-8.